SEDIMENTARY LITHOFACIES, PETROGRAPHY AND DIAGENESIS OF THE KAPUNI GROUP IN THE KAPUNI FIELD, TARANAKI BASIN, NEW ZEALAND

BRENT JOHN COOPER
(2004)

SEDIMENTARY LITHOFACIES, PETROGRAPHY AND DIAGENESIS OF THE KAPUNI GROUP IN THE KAPUNI FIELD, TARANAKI BASIN, NEW ZEALAND

A thesis presented in partial fulfilment of the requirements for the degree of Master of Science with Honours in Earth Science at Massey University, Palmerston North, New Zealand

Brent John Cooper
(2004)

ABSTRACT

The reservoir architecture and quality of the Kapuni Group sandstones in seven wells (Kapuni-1, -3, -8, -12, Deep-1, 14 and -15) in the Kapuni Field are characterised using available core and digital geophysical log data. The study focused primarily on the Eocene Mangahewa Formation, but where limited core permits the older Kaimiro and Farewell formations are also examined.

Eleven lithofacies in the Kapuni Group, identified and defined in core on the basis of colour, lithology, bedding, texture and sedimentary structures, are interpreted to represent tidal sand bar, tidal-inlet channel, fluvial-tidal channel, spit platform, sand flat, shallow marine, tidal channel, meandering tidal channel, mud flat, swamp and marsh environments. Correlation of core lithofacies with geophysical log motifs enabled lithofacies identification where core data are not available. Log motifs representing each of the lithofacies were then extrapolated to uncored sections of the Mangahewa Formation in the Kapuni Field wells.

Interpretation of lithofacies in core and geophysical log motifs indicate that the Mangahewa Formation was deposited in an estuarine setting. During initial deposition of the Mangahewa Formation tide-dominated estuarine lithofacies were deposited. A major coal horizon, the K20 coal, in the field represents a period of maximum infilling. Above this coal core and log data indicate a wave-dominated estuary exhibiting a clearly-defined, "tripartite" (coarse-fine-coarse) distribution of lithofacies.

Provenance studies suggest that low-grade metamorphic and granitic rocks are the dominant source for the Kapuni Group sandstones. Minor input from sedimentary and acid volcanic source rocks are also identified. A volcanic source, however, is more important in sandstones from the Farewell Formation, than in the younger Kapuni Group formations. Probable sources include the low-grade metamorphic rocks of Lower Cambrian to Permian age, Permian to Carboniferous Karamea Granite, Triassic and Jurassic greywacke-argillite sediments, Upper Cretaceous Pakawau Group sediments and Pre Cambrian to Upper Cretaceous acid volcanics.

Reservoir quality variations in the Kapuni Group sandstones are directly related to environmental and diagenetic processes that have controlled porosity reduction and enhancement. Porosity has been reduced mainly by mechanical and chemical compaction, clay formation (predominantly kaolinite and illite in the Mangahewa and Kaimiro formations and smectite in the Farewell Formation), carbonate precipitation

(primarily siderite and calcite), quartz and feldspar overgrowths and pyrite precipitation. While, porosity has been enhanced primarily by carbonate dissolution and subordinately by grain and clay dissolution and minor grain fracturing.

The Mangahewa Formation sandstone lithofacies of tidal sand bar and tidal channel environments exhibit the best reservoir characteristics. Future reservoir development in the Kapuni Field and exploration in the Kapuni Field should focus on identifying and exploiting these lithofacies.

ACKNOWLEDGMENTS

In undertaking this study a number of people deserve recognition for their assistance and input into this thesis. First and foremost I would like to thank my supervisor Julie Palmer whose helpful guidance on all aspects of this study has been more than appreciated. Thanks also to Clel Wallace for help with preparing thin-sections and taking photomicrographs and Bob Stewart for advice on aspects relating to mineralogy.

Thanks to Peter King, Institute of Geological and Nuclear Sciences, Lower Hutt, for identifying and suggesting the topic. I would also like to thank Peter Webb from Shell-Todd Oil Services Limited for his help in providing information on previous studies that have been completed in the Kapuni Field.

I am particularly grateful to Joe Whitton and Michele D'Ath, Landcare Research, Palmerston North for their help with x-ray diffraction, differential thermal analysis and infra-red analysis studies. Thanks also to Doug Hopcroft and Raymond Bennett at Hort Research for help with scanning electron microscopy. I would also like to thank several people at the Institute of Geological and Nuclear Sciences, Lower Hutt; Sarah Thornton for providing geophysical data and Neville Orr for advice on preparing thin sections.

Thanks go to several people at Crown Minerals for their help. In particular, a special thanks to Bill King for opening the core library at Gracefield, often at late notice, and for providing keys so that I could have access after hours. Also thanks to Sam Bowler for his help at the resource library.

Financial support was provided by the New Zealand Petroleum Exploration Association Scholarship (PEANZ). I would like to thank PEANZ and its members for providing funding for this topic and for selection as the first recipient of this award.

Lastly, I would like to thank my parents Ashley and Judith Cooper for their moral and financial support throughout the duration of my studies.

TABLE OF CONTENTS

LIST OF FIGURES

LIST OF PLATES

LIST OF TABLES

INTRODUCTION

1.1 BACKGROUND

The Kapuni Field is New Zealand's largest onshore gas/condensate field, located approximately 40 km south of New Plymouth in the southeastern part of the Taranaki Peninsula (Figure 1.1). Discovered in 1959 by Shell BP Todd Oil Services Limited (SBPT)[1], the field was brought into production in 1970. A total of 15 wells (Kapuni-1 to -15) and two side-tracks (Kapuni-3A and 15A) have been drilled[2]. Currently 11 production wells in the field produce gas and condensate from multiple sandstone reservoirs of the Eocene Kapuni Group. At 1 July 2001 total reserve estimates for the field stand at 62 million barrels (mmbbls) of condensate and 1322 billion cubic feet (bcf) of gas, with remaining reserves of 3.5 mmbbls of condensate and 421.4 bcf of gas (Crown Minerals, 2002).

1.2 PURPOSE AND SCOPE OF STUDY

The aim of this study is to characterise the reservoir architecture and reservoir quality of the Eocene Mangahewa Formation in the Kapuni Field. The older Kaimiro and Farewell formations, which along with the Mangahewa Formation complete the Paleocene to Eocene Kapuni Group succession, are also examined. Although, hydrocarbons are not produced from either of these deeper formations in the field, they do provide important reservoirs elsewhere in the Taranaki Basin[3]. This study is based only on those Kapuni Field wells where both core and digital geophysical logs are available for the Kapuni Group; namely: Kapuni-1, Kapuni-3, Kapuni-8, Kapuni-12, Kapuni Deep-1, Kapuni-14 and Kapuni-15.

Specific objectives of this study are to:

- Identify sedimentary lithofacies in core from the Kapuni Group and interpret their environments of deposition
- Relate sedimentary lithofacies in the Mangahewa Formation to their corresponding geophysical log patterns (log motifs) and then extrapolate to uncored sections in the wells

[1] BP terminated its upstream activities in New Zealand in January 1991 as a result Shell BP Todd Oil Services (SPBT) changed to Shell Todd Oil Services (STOS).
[2] The Kapuni-13 well was named Kapuni Deep-1.
[3] The Kaimiro Formation provides the main producing reservoir sandstones 'D sands' in the Maui Field, whist the Kupe Field produces from sandstones of the Farewell Formation.

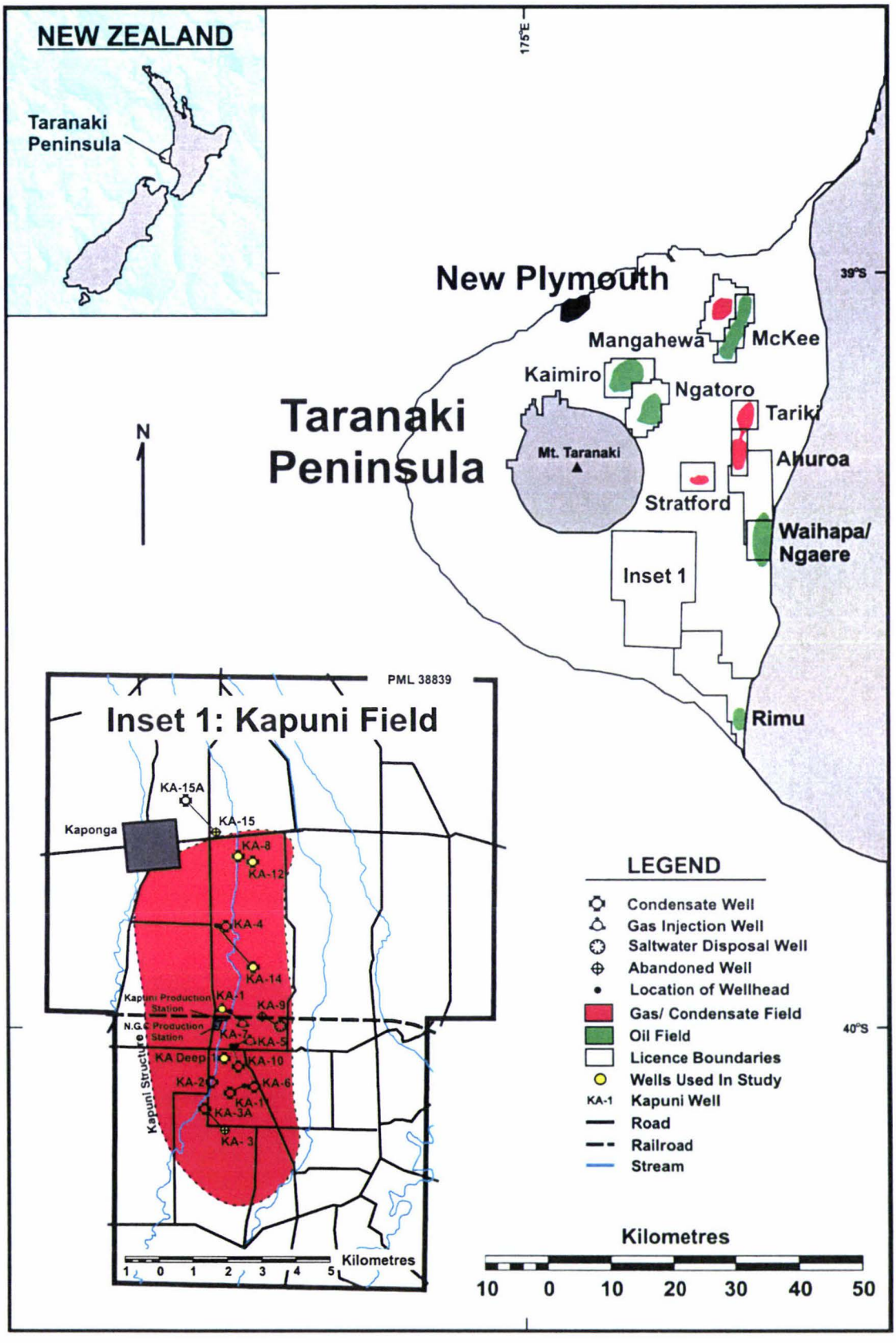

Figure 1.1: Location map of the Kapuni Field and wells

- Develop an environment of deposition model for the Mangahewa Formation based on lithofacies from core and log motifs
- Identify the composition, porosity, texture and classify sandstones in the Kapuni Group
- Elucidate the provenance for the Kapuni Group sandstones
- Identify the diagenetic processes in the Kapuni Group sandstones and determine how they have modified the original sandstone
- Establish the sequence and timing of diagenesis in the Kapuni Group sandstones.

1.3 PREVIOUS WORK

Previous studies in the Kapuni Field have addressed various aspects of the stratigraphy, sedimentology, provenance, petrography and diagenesis of the Kapuni Group. Although, these studies have afforded a better understanding of the depositional and post-depositional process in the field most have focused on a limited number of wells and samples from the best producing reservoir intervals in the Mangahewa Formation. A discussion of previous work in the Kapuni Field is limited to published and unpublished reports, unpublished university theses and reports held on open file at the Ministry of Economic Development.

1.3.1 Stratigraphy and Sedimentology

Seismic surveys undertaken in onshore Taranaki from 1956 to 1957, led to the discovery of the Kapuni Field. The first stratigraphy and lithological descriptions of the Kapuni Group in the Kapuni Field were carried out by van der Klugt *et al.* (1959) following the drilling of the Kapuni-1 well. A glauconitic sandstone overlying a sequence of sandstones and coal beds with intercalations of calcareous siltstones and carbonaceous shales were identified. These strata were correlated with the thin sequence of similar sediments in North Taranaki recognised as the Mangaotaki Formation, first described by Glennie and Jaeckli (1956). In the Kapuni Field van der Klugt *et al.* (1959) informally subdivided the coal measure sequence into a sandstone-siltstone upper part, a middle interval of carbonaceous shales and a mostly sandstone dominated sequence in the lower part. Deposition of sediment in an overall fresh to brackish water environment was attributed to the formation.

After reviewing subsurface data from wells in the Kapuni Field and elsewhere in the Taranaki Basin Short (1962) recognised that the lithology, thickness and age of the Kapuni-1 coal measures were different from those described in the type section for the Mangaotaki Formation; and renamed the sequence the Kapuni Coal Measure Formation. He also suggested that during the Middle to Upper Eocene deltaic-lagoonal conditions prevailed across the Taranaki Basin and proposed that sediment was predominantly

derived by one large river that drained into the basin from the north and east via a saddle in the Patea-Tongaporutu High.

Hicks (1962) and van Wijlen (1963) interpreted the seismic data along with data from logs, cores and cuttings from the first four wells (Kapuni-1 to -4) drilled. Hicks recognised major marker horizons based on 'microlog porosities' and named these the upper member comprising alternating shale, sandstone and coal, the "Main Sand" member composed of mainly sandstone with minor siltstone, shale and coal and the lower member composed predominantly of sandstone. The study by van Wijlen identifies and extensively describes the key marker beds in the Kapuni Formation. Further seismic surveys were carried out in 1971 and 1973 as 7 additional wells (Kapuni-5 to -11) and one appraisal outstep well (Kapuni-3A) were drilled. An interpretation of this seismic data was carried out by de Boer (1973).

A paleoecological study of the Eocene Mangaotaki Formation succession was carried out by Lutz (1964). The analysis focused on cores collected from the Kapuni-3 well in the Kapuni Field. Lutz assigned an Oligocene to Eocene age and interpreted the sequence penetrated as being deposited in a lower coastal plain environment.

To provide a geological basis for reservoir simulation studies Haskell (1975) undertook a geological review of the Kapuni Field, re-evaluating the seismic data and information available from the Kapuni-5 to -11 and Kapuni-3A outstep wells. Three major intervals were correlated between these wells and described as the K3, K2 and K1 intervals; revising the members previously described by Hicks (1962). The K3 interval extended from the base of the Mangahewa Formation to the K2 interval and was divided into the K3E, K3D, K3C and K3A sandstones. The K3E "Main Sands" occur at the base of the K3 interval and consist of a sequence of sandstone beds with overlying thin interbedded carbonaceous shales and coal (braided or meandering channel systems with surrounding mud flat and salt marsh environments). Above the "Main Sands" the K3C sandstone (channel system) and K3D sandstone (regressive beach) occur. The K3A "Upper Sands" occur at the top of the K3 interval comprising dominantly sandstone (redeposited from an emergent sandbar). The K2 interval comprising interbedded mudstones, shales and coals with localised silty sandstone beds (tidally exposed mud-flat and salt marsh environments) was recognised from the top of the K3 interval to the base of the Kap-20 coal (a thick coal that formed a prominent marker in each well, representing a period of widespread supralittoral swamp development). The K1 interval was reported to extend from the top of the Kap-20 coal to the top of the Kapuni Formation. The interval was subdivided into the K1C sandstone (channel system) and K1A sandstone (regressive beach deposit), while the remainder of the K1 interval was described as comprising shale and coal interbeds (tidally exposed mud-flat and salt marsh environments). In general the

sequence penetrated in the Kapuni Field wells was interpreted by Haskell as lower coastal plain deposits comprising tidal channel, mud flat and salt marsh derived coals.

In a regional study of wells in the Taranaki Basin Harrison (1979) developed coal percentage and sandstone-shale ratio maps based mainly on gamma-ray, electric, induction-electric and sonic wireline logs. Five Kapuni Field wells (Kapuni-1, -2, -3, -4 and -8) were used in the study to examine the Upper Member of the Kapuni Formation in the Taranaki Basin. The highest percentage of coal in the basin was identified in the Kapuni Field wells, decreasing north and westward in the basin. On the basis of contour shape around the Kapuni Field and westward Harrison maintained that deposition of the Kapuni Formation occurred as part of a large delta complex prograding westward in the Taranaki Basin.

In a detailed study Hogan (1979) examined the stratigraphy and sedimentology of the Kapuni Formation from core obtained from eight onshore Taranaki wells, including two from the Kapuni Field (Kapuni-1 and -3). Hogan defined the type section of the Kapuni Formation in the Kapuni-1 well between 3245m and 3976m and divided the formation informally into four members (upper sandstone member, middle sandstone member, coal member and lower sandstone member) in which sandstone, shale and coal-bearing lithofacies were recognised. The subdivision varied slightly from those originally devised by Hicks (1962) and later redefined by Haskell (1975) as they were based on lithological variation, and spontaneous potential and resistivity logs. Hogan attributed marine to lagoonal or terrestrial environments of deposition to the Kapuni Formation.

Palmer (1980) provided a detailed description of core material from the Mangahewa Formation in eight onshore Taranaki wells. Two of these wells (Kapuni-1 and -3) were from the Kapuni Field. In the study stratigraphic columns were drawn for each core identifying colour, lithology, estimated grain size, siderite and level of bioturbation. A summary of the general lithology for each well was also given.

In 1983 the deepest well in the Southern Hemisphere Kapuni Deep-1 was drilled in the Kapuni Field to a depth of 5660.20 mahbdf[4]. Shell BP Todd Oil Services Limited (1984) presented a geological summary from the well based on information obtained from drill cuttings, sidewall cores, conventional cores and wireline logs. The Kapuni Formation was described as incorporating four regressive cycles defined as Cycles D, C, B and A. In reference to the reservoir intervals defined by Haskell (1975) Cycle D incorporated the K3A reservoir, Kap-20 coal and K1C sandstones; whilst Cycle C comprised the K3E reservoir. Cycle B represented the interval between seismic horizons A and B, incorporating the coastal sandstones which pass up into poorly developed coal measures

[4] mahbdf (metres along hole below derrick floor)

(Kaimiro Formation). While Cycle A was defined to include a thick sequence of massive coastal sandstones (Farewell Formation), although drilling did not reach the base of this sequence.

In a later study, Palmer (1985) reviewed the stratigraphy and sedimentology of pre-Miocene sedimentary sequences in the Taranaki Basin. In the study the Kapuni Coal Measure Formation of Short (1962) was upgraded to the Kapuni Group to formalise the grouping of Paleocene to Eocene sandstone-coal measure sequence first encountered in the Kapuni-1 well. The Kapuni Group was subdivided into four formations by Palmer; from oldest to youngest they are the Kaimiro Formation, Omata Formation, Mangahewa Formation and McKee Formation.

In an attempt to standardise the nomenclature and dating of lithologic units King (1988a; 1988b) revised the stratigraphy in the Taranaki Basin. An investigation of key wells in offshore Taranaki lead King (1988a) to expand the Kapuni Group to incorporate the Farewell Formation of Paleocene age, which was originally assigned by Suggate (1956) to the Pakawau Group. This reassignment, however, created difficulties in subdividing similar coarse-grained rocks outcropping in northwest Nelson. Nevertheless, the subsequent identification of marine sediments in the Pakawau Group, reclassification of the late Cretaceous interval by Thrasher (1992) and discovery by Bal (1994) of an unconformity at the top of this interval added further support for inclusion of the Farewell Formation into the Kapuni Group.

Shell BP Todd Oil Services Limited (1988) undertook a geological and petrophysical analysis of core from the Kapuni-14 well. The study was based on 89m of core cut through the Mangahewa Formation K3E reservoir with the main objective to provide detailed lithological descriptions, a sedimentological model and petrophysical analyses to supplement K3E core from the Kapuni-3 well. In the study 5 lithological facies and 11 subfacies were distinguished on the basis of sedimentary structures and grain size. Subfacies were interpreted to represent tidal channel, tidally influenced distributary channel, mouth bar, lagoonal and/or tidal flat and floating peat swamp environments. The overall depositional environment was considered to be an upper deltaic plain to lower deltaic plain setting.

Structural influences on sandstone depositional systems and hydrocarbon accumulations in the Kapuni Field were investigated by Haskell (1989). The Kapuni Group sequence was interpreted to be deposited under regional lower coastal plain conditions. In particular Haskell elucidates to lacustrine, lagoonal and estuarine settings with fluvial to tidally influenced fluvial channels, tidal channels, sand and mud flat and swamp environments. He also noted that it was not possible to provide bed by bed correlation

across the field, but refers to the sequence of units previously identified by Haskell (1975) comprising the K3, K2 and K1 reservoir intervals.

A major review of the Kapuni Field was initiated in 1989 with the acquisition of 3D seismic data covering the entire petroleum mining licence. Voggenreiter (1991) provided an interpretation of the data, and asserted that amplitude patterns of the K1 interval near the top of the Kapuni Group reflected lithologic changes diagnostic of fluviatile meandering channel features. Along with well data the work by Voggenreiter formed the basis for reservoir simulation studies of the Mangahewa Formation by Bryant and Bartlett (1992). Bryant and Bartlett developed a 3D reservoir model based on correlatable coals and associated mudstones across the field, subdividing the stratigraphic succession into nine layers. These layers, their boundaries and incumbent geology are examined in more detail later as they form the basis for current reservoir understanding in the Kapuni Field.

Shell Todd Oil Services Limited (1992) provided a lithological description and sedimentological interpretation of 18.60m of core cut from the K1A reservoir interval in the Kapuni-15 well. The K1A sandstones were originally interpreted as deposits of a low sinuosity distributary channel, although on the basis of tidal cross-bedding and *Ophiomorpha* trace fossils the interval was refined by Brekelmans *et al.* (1991) and Bryant and Bartlett (1992) to represent vertically stacked tidally-influenced channels. Sandstones in the K1A reservoir were also recognised as similar to those identified in core from the Kapuni-12 well, which form part of a coarsening upward shoreface body.

Flores *et al.* (1993) studied the sedimentology of the Kapuni Group reservoir system using almost 1,000m of core from nine wells in the Taranaki Basin. In the Kapuni Field, reservoir sandstones in the Mangahewa Formation were described in general as stacked fluviotidal facies, bounded by major truncations. These facies were interpreted to be deposited in predominantly tidal-creek and fluviotidal channels and subordinate tidal-inlet channel environments.

In the most comprehensive study of the Taranaki Basin to-date, King and Thrasher (1996) examined the Cretaceous-Cenozoic geology and petroleum systems of the Taranaki Basin. In this study the Paleocene to Eocene Kapuni Group was subdivided into the Farewell, Kaimiro, Mangahewa and McKee formations. This reclassification also lead King and Thrasher to redefine the Kaimiro Formation which was originally assigned by Palmer (1985) to predominantly sandy, unfossiliferous strata encountered beneath early to middle Eocene marine mudstones of the Omata Member in the Taranaki Peninsula; to include all strata of Early Eocene age throughout the basin.

1.3.2 Geophysical Log Signatures (Log Motifs)

Log signatures have been used extensively used in the Kapuni Field wells to define cyclothems and reservoir intervals, however, limited work has been done on identifying individual units or lithofacies. The only analysis of log signature response at this scale was completed by Shell BP Todd Oil Services Limited (1988) on core from the Kapuni-14 well. The study found that when correlating the gamma-ray log to core, a cut off value of 60 API units separated the cross-bedded sandstones from the heterogeneous sandstones. The lithodensity/compensated neutron logs (LDL/CNL) was found to display good separation in the cross-bedded sandstones in the gas zone, heterolithic lithofacies demonstrated negative separation in the gas bearing section and positive separation in the lower water bearing zones. Whilst pronounced positive separation occurred in the mudstones and extreme positive separation coincided with sideritic intervals. The photoelectric factor log (PEF) was used to define the cross-bedded sandstones at 1.8 to 2.2 PEF units, heterogeneous sandstones at 2.1 to 2.5 PEF units, heterolithic at 2.0 to 2.7 PEF units and mudstones at 2.5 to 3.0 PEF units. PEF values over 2.6 units corresponded to intervals in which plant debris and/or pyrite were volumetrically important. The resistivity logs generally demonstrated a marked separation between MSFL and LL in the cross-bedded, heterolithic and heterogeneous lithofacies. On the raw resistivity curves, the heterogeneous sandstones were described as exhibiting a typically smooth trace for the heterolithic sandstones and cross-bedded sandstones; while the mudstones were considered easily identifiable by their uniform profile. Sonic transit times for the sonic (long spaced) log (SLS) were defined for the cross-bedded sandstones from 79 to 93 microseconds/ft, heterogeneous sandstones from 74 to 85 microseconds/ft, heterolithic from 64 to 87 microseconds/ft and mudstones from 63 to 82 microseconds/ft.

1.3.3 Provenance

Provenance in the Kapuni Field was first investigated by Hogan (1979). Modal analysis studies, particularly with respect to the undulose extinction and polycrystallinity of quartz grains lead Hogan to maintain that sandstones of the Kapuni Formation were predominantly derived from a low-grade metamorphic source, with sediment input also from plutonic and reworked sedimentary rocks. These findings along with sedimentological and stratigraphic evidence led Hogan to propose that that the formation was sourced from the Triassic and Jurassic greywacke-argillite metasediments, Pakawau Group sediments and Tasman Intrusives.

In studying the petrography of sandstones from the K1A reservoir interval in the Kapuni-12 well Challis and Mildenhall (1986) concluded on the basis of rock fragments, pebbles and detrital minerals, that the sandstones were derived almost entirely from a granitic source. Based on the identification of microcline, perthite and oligoclase feldspars, and the abundance of muscovite and biotite they suggested derivation from a two-mica

granite. A change from muscovite to biotite or its alteration products in the well was thought to indicate a slight change in the composition of the source rocks. In reference to earlier studies, Challis and Mildenhall noted that most New Zealand granites contain shear zones in which undulatory quartz is abundant and considered the strain of quartz grains not to be an important provenance indicator. Instead, the apparent scarcity of sphene, epidote, and magnetite and abundance of microcline and oligoclase was used as evidence to suggest the Karamea Granite as the probable source.

Shell BP Todd Oil Services Limited (1988) investigated the provenance of sandstones from the Mangahewa Formation K3E reservoir interval primarily in the Kapuni-14 well, but also included samples from the Kapuni-3 well. On the basis of abundant quartz, scarcity or unstable minerals and rock fragments, and moderate grain rounding they suggested that sandstones were at least partly derived from a sedimentary source, and named the quartzose sediments of the Late Cretaceous Pakawau Group as a likely candidate. However, the dominant source rocks for the Kapuni Formation were considered to be granitic. Due to the absence of sphene and epidote, scarcity of magnetite and presence of K-feldspar the granitic source was identified as the Karamea Granite. They also suggested that a difference in the percentage of undulose and polycrystalline quartz and clay type and abundance between the Kapuni-3 and Kapuni-14 wells may indicate a slightly different source for the sediments.

In a petrographic summary of Taranaki petroleum reports Smale (1996) noted in the Taranaki Basin that the composition of the Kapuni Group was mainly granitic, with minor schist and altered acid volcanic rocks. Karamea type granite was identified as a provenance for the Kapuni Group in the Kapuni Field. Although volcanic rock fragments were noted to exceed granitic, the granitic provenance was still considered dominant.

1.3.4 Petrography and Diagenesis

The petrography and diagenesis of the Kapuni Formation in the Kapuni Field was first described by Hogan (1979). Petrographic microscopy, cathodoluminescence, infra-red spectrometry, x-ray diffractometry and scanning electron microscopy studies were conducted. Hogan concluded that the Kapuni Group sediments had been considerably modified by post-depositional processes. Quartz cementation and dissolution, formation of styolites, feldspar alteration, clay precipitation, carbonate cementation, pyrite precipitation and coalification of organic matter were identified as important diagenetic processes. Quartz cementation, feldspar alteration and kaolinite formation were deemed early diagenetic features, while quartz solution, illite formation, carbonate cementation (mainly siderite with some calcite) and pyrite precipitation were considered late diagenetic features.

Challis and Mildenhall (1986) conducted an investigation into the petrography and diagenesis of sandstones in the Kapuni-12 well. The sandstones were described as moderately to poorly sorted, fine- to medium-grained feldsarenites and subfeldsarenites. Compaction and the formation of authigenic kaolinite, illite, glauconite and carbonates (mainly dolomite, with less common calcite and siderite) and pyrite were identified as diagenetic processes reducing reservoir quality. In particular an increase in the proportion of mica and the transition from muscovite to biotite were considered to attribute to low porosity in the upper part of the K1 sequence in the Kapuni-12 well. Secondary quartz overgrowths were identified as the first stage in the diagenetic history of the sediments. Detrital kaolinite was considered to form the early cement, whilst carbonate was generally considered to be a late diagenetic mineral.

Shell BP Todd Oil Services Limited (1988) examined core from the K3E reservoir interval from the Kapuni-14 and -3 wells. The sandstones were described as fine- to medium-grained, moderately- to well-sorted subfeldsarenites. Kaolinite was identified as the main clay mineral with minor illite and mixed-layer illite-smectite. Petrographic studies indicated that syntaxial quartz overgrowths were not common, while the identification of carbonates included ankerite and siderite. The diagenetic history was considered to firstly involve the recrystallisation of original sedimentary clays to form well-crystallised kaolinite and mixed-layer illite/smectite. Next the dissolution of original calcite or dolomite cements occurred by organic acids creating considerable secondary porosity. Finally, late precipitation of ankerite and siderite reduced porosity in some sandstones.

A study by van der Lingen *et al.* (1988) provided the first comprehensive overview of diagenetic features in the Kapuni Group sandstones in the Taranaki Basin. Diagenetic processes adversely affecting reservoir quality of the sandstones in the Kapuni Field were namely; compaction, pressure solution, clay neoformation, quartz overgrowth formation and carbonate neoformation. Secondary porosity development was considered to enhance reservoir quality; through the dissolution of earlier (corroding) carbonate cements, dissolution of calcic plagioclase, quartz dissolution and grain fracturing. Progressive diagenetic stages in the Kapuni Group were identified. Early diagenetic features were recognised as plagioclase corrosion and kaolinite neoformation. Pressure solution and compaction were also recognised as early diagenetic processes, but thought not to be important until after carbonate cement dissolution. Carbonate cementation and dissolution were interpreted to occur at any depth. Whilst, dissolution of staurolite, garnets and quartz overgrowths were interpreted as late diagenetic processes.

Diagenetic controls on the porosity and permeability of the Kapuni Group sandstones in the Taranaki Basin were investigated by Collen (1988). In the study which concerned

sandstones from two wells (Kapuni-1 and -3) in the Kapuni Field and the Ingleweood-1 well; mechanical compaction and the precipitation of silica, carbonate cements (predominantly calcite, less common siderite and rare dolomite and ankerite) and authigenic clays (kaolinite, illite and chlorite) were identified as the most important factors reducing reservoir quality. The dissolution of carbonate (particularly calcite) was considered the most important process for creating secondary porosity. Other less important processes in secondary porosity development were the dissolution of detrital grains and authigenic cements and the fracturing of rock and grains. Precipitation of silica was identified as an early cement which accompanied or closely followed precipitation of kaolinite and the dissolution of feldspar and other detrital grains. The crystallisation of illite and chlorite and successive deposition of cementing and replacive carbonates (mainly calcite, but also siderite, dolomite and ankerite) occurred next. The latest diagenetic processes included the dissolution of carbonates and feldspar, precipitation of kaolinite and the emplacement of hydrocarbons.

Smale (1996) provided a review on sandstone diagenesis in the Taranaki Basin summarising petroleum reports and the literature, in an attempt to unravel diagenetic sequences in the Maui, Kupe South and Kapuni Fields. Two main diagenetic sequences were distinguished in the basin. They were the 'Maui sequence' incorporating the Western Platform and adjacent areas and 'Kupe South sequence' representing onshore Taranaki. The Maui sequence was found to contain both late and early carbonate deposition around the middle of the sequence, while the Kupe South sequence (incorporating the Kapuni Field) was characterised by late quartz overgrowth development followed by carbonate dissolution.

The most extensive petrographic study in the Kapuni Field was conducted by Yunalis and Izhan (1995) primarily to assess potential reservoir problems related to sandstone mineralogy. The study involved a petrographic analysis of samples from the K1A, K3A, and K3E reservoirs in the Kapuni-3, -12, -14 and -15 wells. The mineralogical components (framework grains, clay matrix, and cements), texture and porosity of the samples, sequence and timing of diagenetic events and controls on the development of porosity and permeability were identified. The Mangahewa Formation sandstones were described as mostly quartz-rich with small but variable percentages of feldspar and lithics. Quartzarenite, subarkose and arkose sandstone were identified. Intragranular dissolution pores were recognised as the main porosity type with total visible porosity ranging from negligible (<0.4%) to good (19.6%). Of the diagenetic processes compaction, precipitation of pyrite and siderite, quartz overgrowth development, precipitation of ankerite, dissolution of feldspar/unstable grains and cements, and the formation of kaolinite represented the paragenetic sequence of diagenetic events and were considered the most important in determining sandstone reservoir quality.

The latest work on diagenesis in the Taranaki Basin is that of Smale *et al.* (1999) who studied the sandstone diagenesis of the Kapuni Group in the Kapuni Field and other onshore Taranaki wells. All three Kapuni Group formations (Farewell, Kaimiro and Mangahewa) were examined. The Farewell Formation comprised mainly feldsarenite sandstones. In the Kaimiro Formation feldsarenites and lithic feldsarenites predominated. While, the Mangahewa Formation sandstones are mainly feldspathic litharenites. In the study sandstones from the Farewell Formation were found to be more feldspathic than the younger Kapuni Group sandstones. Porosity was identified as variable (1.9% - 12.3%) in the Mangahewa and Kaimiro Formations and negligible (<1.9%) in the Farewell Formation. The diagenetic processes and sequence was largely consistent with the study by Collen (1988), although no evidence for early quartz cementation was found in the Kapuni Field. Kaolinite development was considered to be early; occurring before or during feldspar dissolution, whilst illite and chlorite were considered to form instead of kaolinite as a result of deeper burial. The main phase of quartz and feldspar overgrowth development occurred after clay mineral deposition. Carbonates (dolomite, ankerite, siderite and calcite) were thought to be late diagenetic features.

1.3.5 General Studies

Not withstanding the studies previously mentioned, a number of authors have provided either a general overview of the sedimentology, stratigraphy, provenance, petrography or diagenesis of the Kapuni Group in the Kapuni Field or make references in wider regional studies. McBeath (1976; 1977) was the first to provide a summary of the Kapuni Field, amongst other Taranaki Basin gas/condensate fields. Kear (1967) summarised the literature and presented a case study of the Kapuni Field. While more recently, Abbott (1990) presented an overview and classification of the Kapuni Field, mentioning the stratigraphy, trapping and reservoir systems.

A number of studies review or cite the Kapuni Group in the Kapuni Field as part of regional work on the Taranaki Basin. Some of the more important studies are summarised. The first notable studies of this type were provided by van der Sijp (1958a; 1958b; 1959) who described the Taranaki geology. Katz (1968; 1971; 1973; 1974; 1975a; 1975b; 1976a; 1976b) comprehensively discussed the oil potential in the Taranaki Basin focusing on the Kapuni Formation, which he described as being deposited in a lagoonal to deltaic environment. McLernon (1972; 1976; 1978) provided brief stratigraphic descriptions of the Kapuni Formation in Taranaki wells. Pilaar and Wakefield (1978) reviewed the stratigraphy of the Kapuni Formation in conjunction with the structural controls in the Taranaki Basin. A geological map of the Manaia area was published by Neall (1979). King and Cook (1987) presented a summary on the petroleum geology of onshore Taranaki. King and Robinson (1988) provided an overview of the Taranaki regional geology, while Robinson and King (1988) discussed hydrocarbon

reservoir potential in the Taranaki Basin. Later, King (1990; 1991; 1994) described the changes in sedimentary and structural style in the Taranaki Basin in a number of papers. King and Beggs (1991) detailed the geological controls on oil and gas occurrence in the Taranaki Basin. Geosearch (1991) presented a summary of the exploration development in the Taranaki Basin including a review of the Mangahewa Formation stratigraphy and reservoir intervals in the Kapuni Field. Palmer and Bulte (1991) discussed the stratigraphy of the Taranaki Basin in relation to its active margin setting. Smale (1992) examined the provenance of sediments in the Taranaki Basin based on heavy mineral assemblages. Robinson *et al.* (1986a; 1986b; 1986c) examined the depositional history of the Eocene to Oligocene sediments. Palmer and Andrews (1993) discussed the Cretaceous to Tertiary sedimentation and structural evolution in the Taranaki Basin. McAlpine and Bussell (1994) summarised the literature on the Kapuni Field along with other onshore Taranaki fields in a field guide on Taranaki's hydrocarbon accumulations and facilities. As previously mentioned, in the most detailed study of its kind, King and Thrasher (1996) compiled a monograph synthesising the Cretaceous to Cenozoic geology and petroleum systems of the Taranaki Basin from industry information along with other published and unpublished studies. Aside from redefining the Kapuni Group; they reviewed the distribution, deposition setting and provenance of the Kapuni Group, making reference to the Kapuni Field. They also discuss the reservoir system including porosity trends and diagenesis in the Taranaki Basin. More recently, Crown Minerals (2000; 2001; 2002; 2003) provide a geological overview of the Taranaki Basin in their annual petroleum publications.

1.4 GEOLOGICAL SETTING

1.4.1 Regional Geological Setting - Taranaki Basin

The Taranaki Basin, New Zealand's only commercial oil and gas producing region is located on the western coast of the North Island of New Zealand (Figure 1.2). This late-Cretaceous to Recent sedimentary basin comprises many interconnected sub-basins and depo-centres which collectively constitute an area of around 100,000 km^2 (King, 1994). The Taranaki Basin is primarily an offshore subsurface feature, but also includes the onshore areas of the Taranaki Peninsula and areas along the western margin of the North Island north of the peninsula and in the northwestern South Island (King and Thrasher, 1996).

All boundaries encompassing the Taranaki Basin are arbitrarily defined, due to the complex evolution of the basin (King and Thrasher, 1996). The eastern margin of the basin is defined by the north-south trending Taranaki Fault which bounds the subsurface Patea-Tongaporutu (basement) high and truncates the Cretaceous to mid-Tertiary

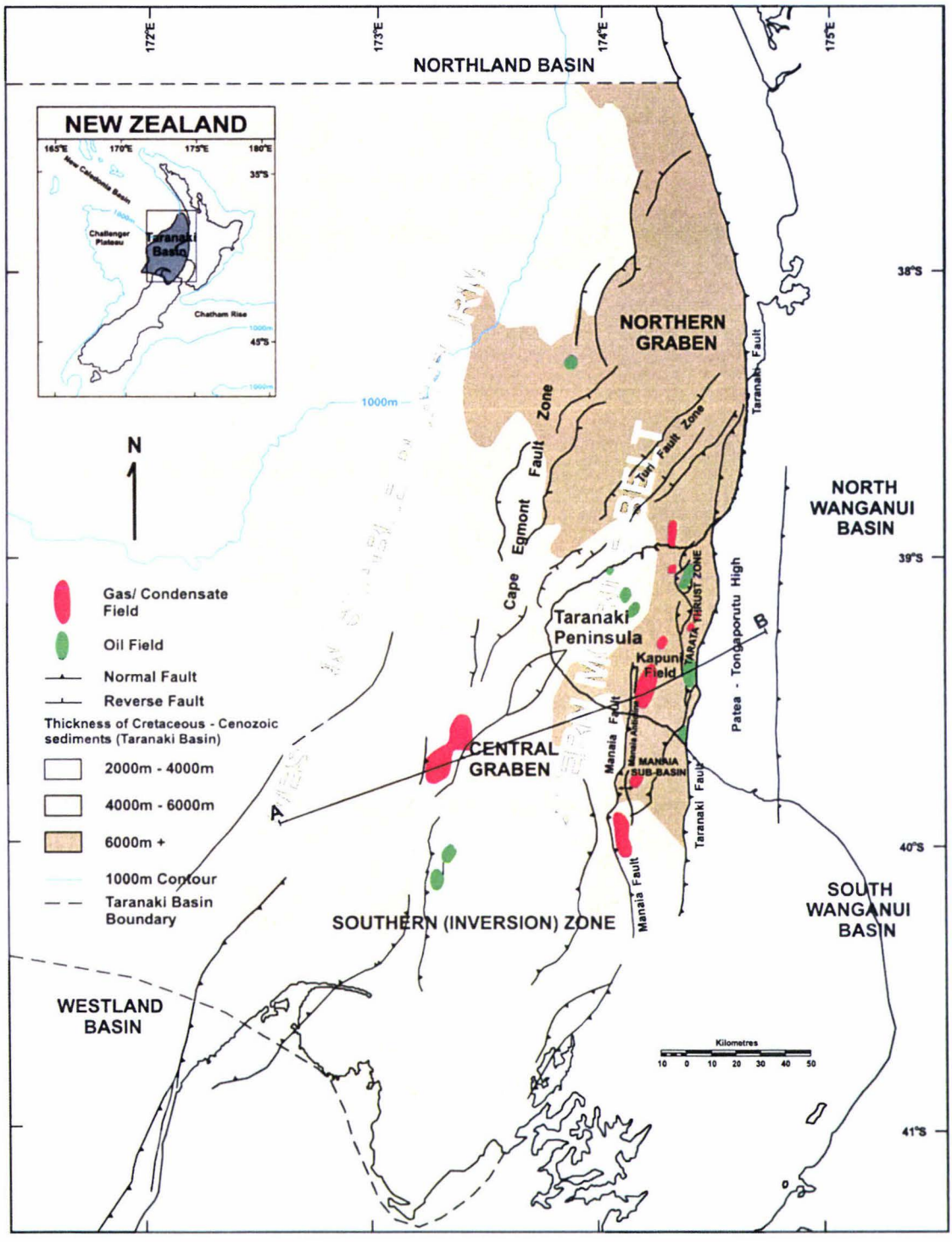

Figure 1.2: Taranaki Basin location map and main structural elements (Modified after King and Thrasher, 1996)

succession in the Taranaki Basin from the younger Neogene to Quaternary rocks in the adjacent north and south Wanganui Basins. Directly to the west the basin extends out beyond the present day continental shelf margin, in the southwest Neogene sediments onlap the Challenger Plateau, while in the northwest the seafloor descends into the New Caledonia Basin (King and Cook, 1987). In the south, the Taranaki Basin extends to onshore areas northwest of Nelson in the South Island (Palmer and Bulte, 1991). The northern limit of the basin has been defined as approximately the latitude of Auckland at 37°S where the Taranaki Basin adjoins the Northland Basin (Pilaar and Wakefield, 1978; Katz, 1976b; Isaac *et al.*, 1994). The boundary between the Taranaki Basin and Northland Basin is somewhat arbitrary and poorly defined offshore, and the two basins could in fact be contiguous (Palmer and Andrews, 1993; King, 1994; King and Thrasher 1996).

The Taranaki Basin comprises two main structural provinces; the Eastern Mobile Belt and the Western Stable Platform (Figures 1.2 and 1.3). The Eastern Mobile Belt, previously known as the Taranaki Graben, is composed of the Northern Graben and Central Graben in the northern sector and the Tarata Thrust Zone and Southern (Inversion) Zone in the southern sector of the basin. Collectively these sub-provinces represent a broad zone of deformation associated with progradation of the Australian-Pacific plate boundary through New Zealand that occurred in the Neogene (King and Thrasher, 1996). The western limit of this zone of deformation is delineated by the Cape Egmont Fault Zone. The Western Stable Platform extends from the upthrown side of the Cape Egmont Fault Zone to beyond the present day continental shelf, and in contrast to the Eastern Mobile Belt exhibits a relatively simple structure as the platform was largely unaffected by tectonic activity for much of the Cenozoic (Pilaar and Wakefield, 1978; Palmer and Bulte 1991; Palmer and Andrews, 1993).

1.4.2 Local Geological Setting - Kapuni Field

The Kapuni Field is situated along the productive Manaia Anticline which also contains the Kupe Field and Toru accumulations. The anticline is a significant inversion structure that strikes roughly north in the southeast of the basin (King and Thrasher, 1996). Structural contour maps generated by Haskell (1975) at the top of the Kapuni Group in the Kapuni Field indicate a c.18km long and 8km wide feature with four-way dip closure (pericline). The structure is bounded to the west by the Manaia Fault, a major east-heading, steeply dipping reverse fault in the basin. Along its length the anticline is truncated by a major angular unconformity (King and Thrasher, 1996). In the Kapuni Field, this unconformity is present just beneath the Miocene-Pliocene boundary.

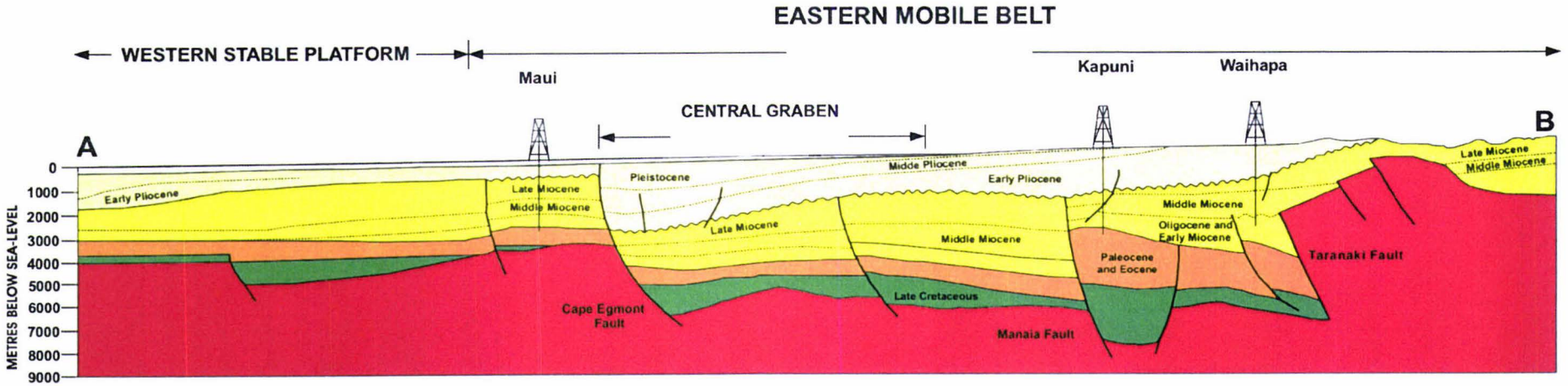

Figure 1.3: Cross-section through the Taranaki Basin showing the main structural elements (Modified after King and Thrasher, 1996)

Voggenreiter (1991; 1993) was the first to provide a detailed interpretation of faulting in the Kapuni Field from seismic data. In this study faults were interpreted as upward branching fault complexes attributed to wrench deformation. However, a review of the 3D seismic data by Holstege and Bishop (1998) reinterpreted the geometry and timing of faulting in the Kapuni Field (Figure 1.4). Planar normal faults, listric growth faults, thrust faults and reverse/reactivated faults were all recognised and three phases of faulting identified. Pre-late-Eocene extension and transtension resulted in listric and normal planar faults. Late-Eocene to Oligocene and mainly Miocene compression/inversion resulted in reactivation of the Manaia Fault. The final phase involved Plio-Pleistocene back-arc extension, manifested in small low angle thrust faults that accommodated crustal shortening.

1.5 STRATIGRAPHIC SUBDIVISION

1.5.1 Stratigraphic Subdivision in the Taranaki Basin

The Taranaki Basin contains a thick sequence (more than 7000m) of Late Cretaceous to Recent sedimentary rocks overlying varied Paleozoic and Mesozoic basement rocks (Figure 1.5). Stratigraphic subdivision in the basin is based on four 'megasequences' or groups, defined by seismic reflection character, age and lithology (King and Thrasher, 1996). They include the Late Cretaceous Pakawau Group, Paleocene-Eocene Kapuni Group and Moa Groups, Oligocene to Miocene Ngatoro and Wai-iti Groups and the Plio-Pleistocene Rotokare Group.

1.5.2 Stratigraphic subdivision of the Kapuni Group in the Kapuni Field

The Paleocene to Eocene Kapuni Group in the Taranaki Basin is distinguished by several marker horizons including major unconformities, marine flooding surfaces, and sequence boundaries, which are essentially time-line separating the Kapuni Group into formations (King and Thrasher, 1996). In the Kapuni Field the Kapuni Group comprises the Farewell, Kaimiro and Mangahewa formations.

i. Farewell Formation

The Farewell Formation, the basal formation of the Kapuni Group, is now considered to be Paleocene in age (Raine, 1984; King, 1988b). The Farewell Formation in the Kapuni Field is defined by the Cycle A seismic interval (Shell BP Todd Oil Services Limited, 1984). In Kapuni Deep-1, the only Kapuni well to penetrate the Farewell Formation, mainly coarse- to medium-grained sandstones and mudstones were identified. These were interpreted as deposits of coastal and lower coastal plain environments (Shell BP Todd Oil Services Limited, 1984). In the Kapuni Field and other wells in the Manaia

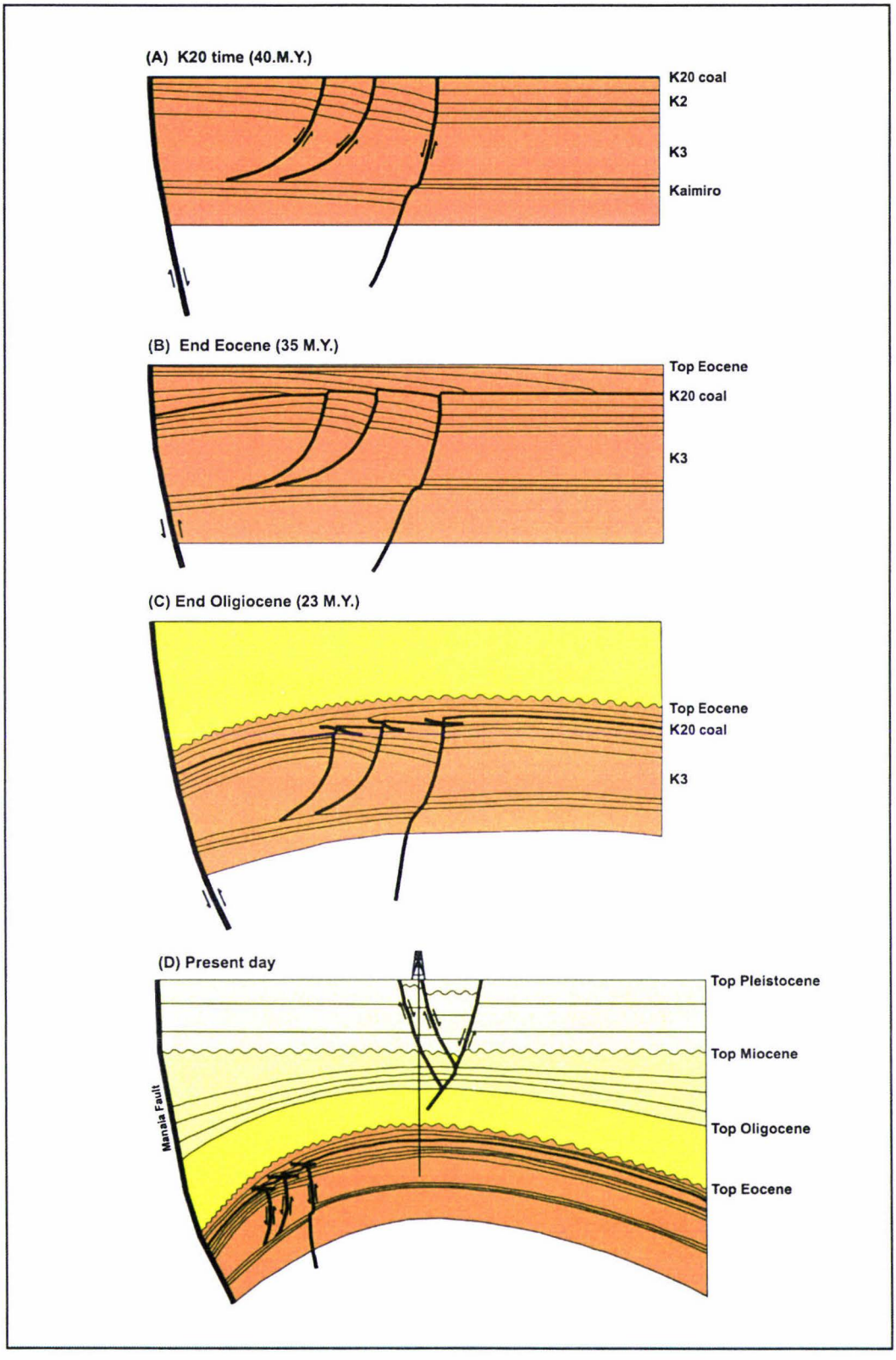

Figure 1.4: Idealised cross-sections showing the various stages in the evolution of the Kapuni anticline in the Kapuni Field. (A): basin transtension caused listric and planar normal faults – soft sediment deformation in coal/shale lithologies: (B): transition from transtension to compression (listric faults no longer active, Manaia transtensional fault beginning to reverse) with (C): main compressional/inversion phase (note thrust faults forming at pre-existing areas of weakness); (D): present situation with Plio-Pleistocene extension due to backarc extension/crustal downwarping (Modified after Holstege and Bishop, 1998).

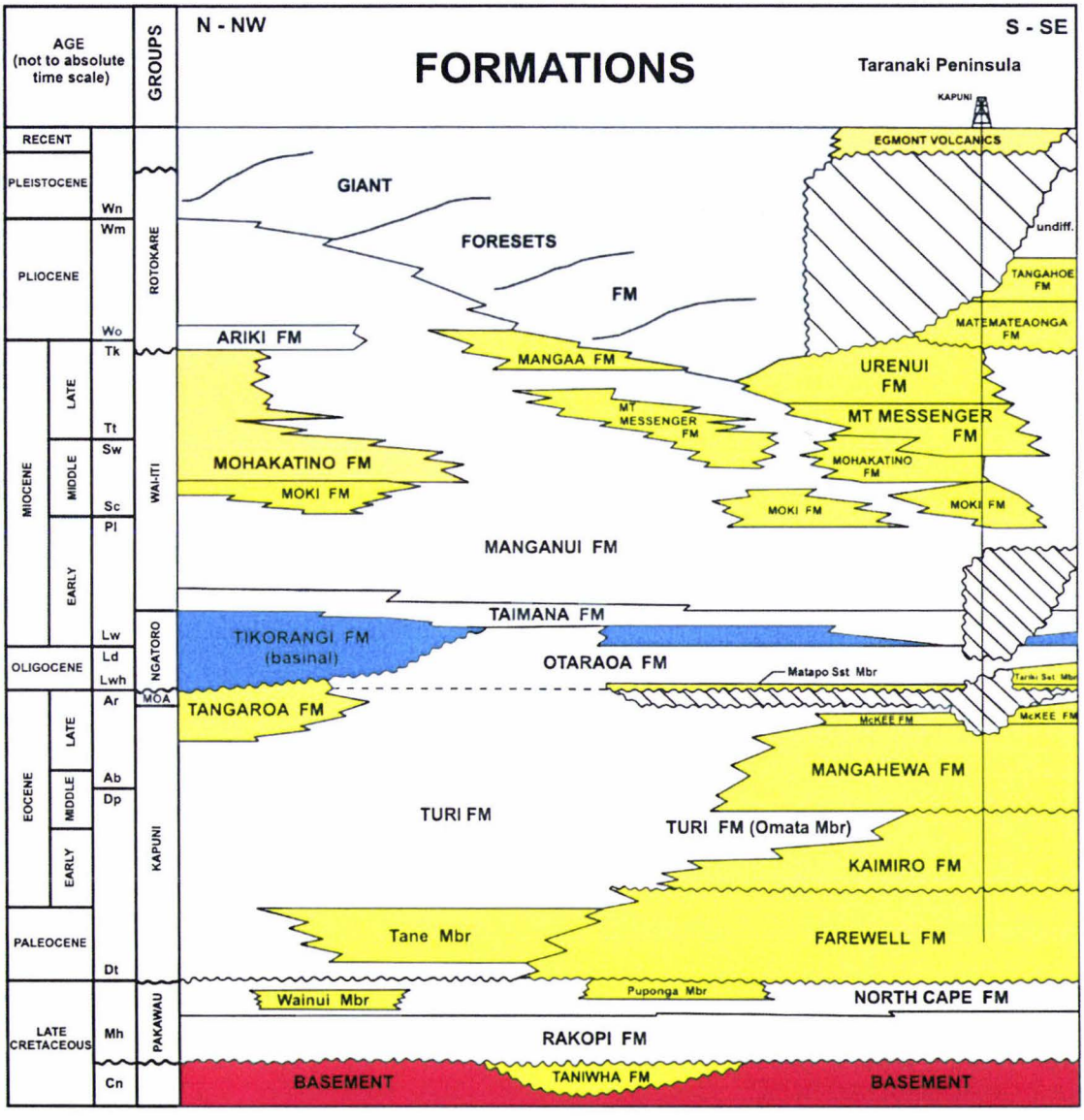

Figure 1.5: Cretaceous-Cenozoic stratigraphic framework for the Taranaki Basin (Modified after King and Thrasher, 1996)

sub-basin the top of the Farewell Formation is marked by an angular unconformity that relates to tilting in the Eocene (King and Thrasher, 1996).

ii Kaimiro Formation

The Kaimiro Formation in the Taranaki Basin corresponds to approximately the base of the Eocene (top Farewell Formation) up to the Omata Member, or where it is absent, such as in the Kapuni Field, an unconformity at the top of the Heretaungan stage - base Mangahewa Formation (King and Thrasher, 1996). In the Kapuni Field Shell BP Todd Oil Services Limited (1984) define the Kaimiro Formation as Cycle B, comprising primarily sandstone, siltstone, mudstone and less commonly coal deposited in terrestrial, upper coastal plain and swampy settings.

iii. Mangahewa Formation

The Mangahewa Formation includes all marginal marine and terrestrial lithofacies of middle to late Eocene age. Cycles C and D were defined by Shell BP Todd Oil Services Limited (1984) to characterise the Mangahewa Formation in the Kapuni Field. In the Kapuni wells the formation consists of alternating cycles of sandstones, capped by coals and mudstones that were deposited in fluvio-tidal environments (King and Thrasher, 1996). As previously mentioned the Mangahewa Formation has long been grouped informally into reservoir intervals for reservoir simulation studies. These subdivisions were originally based on major marker horizons identified through the Kapuni Field by Hicks (1962), van Wijlen (1963) and expanded on by Haskell (1975). A later study by Bryant and Bartlett (1992) supported these subdivisions but identified further correlatable coal and mudstone units across the field, allowing refinement of the subdivisions and the identification of nine reservoir layers (Figure 1.6). The following discussion reviews the reservoir layers defined by Bryant and Bartlett (1992), which they interpreted as characterising a tide-dominated estuarine environment.

The K3 interval comprises the main producing reservoir sandstones of the Mangahewa Formation in the Kapuni Field. At the base of the Mangahewa Formation the K3E3 and overlying K3E2 layers comprise estuarine sandstones with subordinate shale and coal. The K3E1 layer is composed of estuarine and fluvial channel sands with subordinate shales and thin coals. The K3U layer incorporates the interval between the 'Main Sands' and 'Upper Sands', comprising predominantly shales and coals with thin sheet and rare channel fill sands. The K3A layer 'Upper Sands' is composed of stacked channel-fill sands with subordinate shales and coals.

The K2 interval lies from the top of the K3 interval to the base of the K20 coal. The K2 interval lacks any significant sandstone units, and is primarily composed of shales, and coals with confined thin sheet and rare channel fill sands. The topmost part of the K2

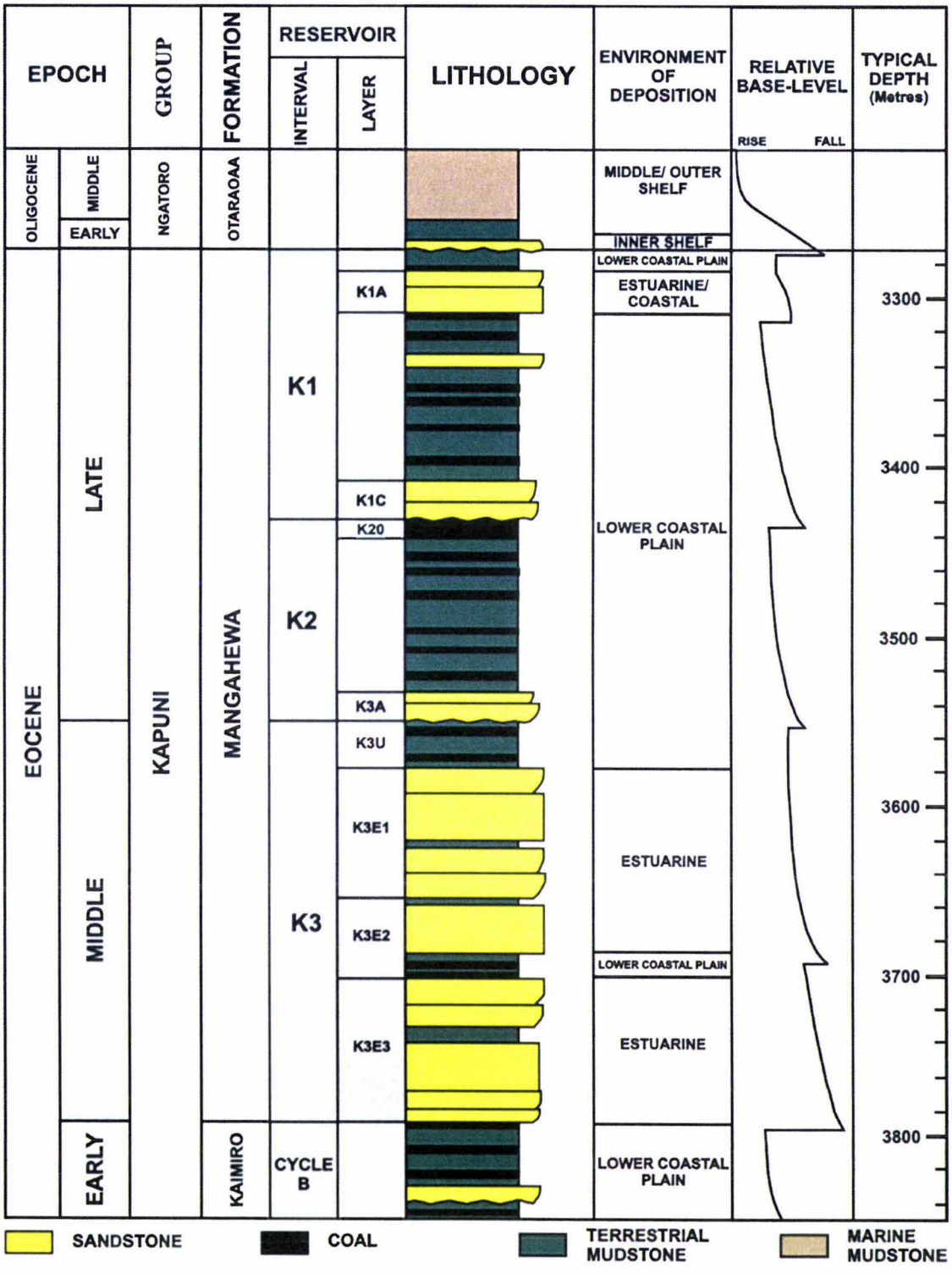

Figure 1.6: Schematic stratigraphy of the Mangahewa Formation in the Kapuni Field (Modified after Bryant and Bartlett, 1992)

interval is the K20 coal. The K20 coal is the only field wide marker bed that can be correlated with any certainty between the Kapuni wells, and represents a period of extensive swamp development in the Taranaki Basin[5] (Bryant and Bartlett, 1992).

The K1 interval extends from the top of the K20 coal to the top of the Mangahewa Formation. Overlying the K20 coal is the K1C sequence comprising stacked channel-fill sandstones with subordinate shales and coals. The K1 layer lies directly above the K1C sequence, consisting of laterally extensive coals and shales with thin sheet sandstones and rare channel-fill sandstones. The K1A layer, only present in the northern part of the field (Kapuni-8, -12 and -15 wells), comprises a wedge of paralic sandstones.

1.6 GEOHISTORY

The Taranaki Basin is a composite basin, exhibiting multiple phases of structural evolution and depositional fill (King and Thrasher, 1996). The geological history of the Taranaki Basin is reviewed in relation to structural, stratigraphic and paleogeographic developments that effected the Taranaki Basin throughout its development, with particular attention to events that occurred or impacted on the Manaia sub-basin where the Kapuni Field is located.

1.6.1 Late Cretaceous and Paleocene

Taranaki Basin development began in the late Cretaceous in response to the break-up of Gondwanaland and spreading in the Tasman Sea (Bulte, 1988). From the late Cretaceous to Paleocene the basin evolved as a series of rift grabens and normal faulted sub-basins; collectively constituting the Taranaki Rift (Thrasher, 1990; 1992). In the Manaia sub-basin rapid subsidence was controlled by the north- and northeast-striking Manaia Fault (King and Thrasher, 1996). Late Cretaceous paleogeographic reconstructions by King and Robinson (1988) indicate a block faulted subdued basin and range topography existed, where drainage systems flowed northwards off a southern hinterland. Terrestrial sediments of the Pakawau Group, comprising mostly conglomerate and sandstone lithofacies with subordinate carbonaceous mudstones were the main deposits (King and Thrasher, 1992). During the latest Cretaceous a widespread marine transgression inundated the Taranaki Basin from the north and west (Thrasher, 1992). Submergence of the former rift landscape resulted in the formation of complex tidal embayments.

[5] The K20 coal is also referred to as the Kap 20 coal in the Kapuni Field and recognized as the Toko Member (Palmer, 1985) in onshore wells in eastern parts of the Taranaki Basin

1.6.2 Paleocene to Early Oligocene

The Paleocene was a period of waning tectonic activity in the Taranaki Basin, as it became increasingly distal to the spreading centre and the rate of crustal cooling diminished (King, 1994). Only a few major late Cretaceous faults exhibited continued subsidence, most notably for this study the Manaia Fault (King and Thrasher, 1996). By the end of the Paleocene spreading in the Tasman Sea had ceased (Bulte, 1988), placing the Taranaki Basin in a passive margin during much of the Eocene. Repeated marine advances and retreats from the Paleocene to Eocene resulted in the paleoshoreline migrating back and forth across a low-lying coastal plain. Thick sequences of sandstones, mudstones and coals of the Kapuni Group were deposited in a coastal system generally aligned NW-SE through the middle of the basin. In the late Eocene the structural regime changed to compressional, in response to progressive convergence along the Australian Pacific plate boundary (Palmer and Andrews, 1993). The tectonic changes at this time manifested in the separate development of the Western Stable Platform and the Eastern Mobile Belt. Throughout the tectonic transition the marine transgression continued unabated; and by earliest Oligocene the basin was completely inundated. Shallow marine siltstones and mudstones of the Turi Formation were deposited during this time. The regional marine transgression reached a maximum in the mid to late Oligocene. Geohistory curves by Hayward (1987) and Hayward and Wood (1989) of the mid Oligocene indicate that the rate of subsidence significantly increased causing the whole basin to deepen. Subsidence and inundation of hinterland to the south and southeast reduced sediment supply and widespread bioclastic limestones of the Tikorangi Formation were variably deposited in what was predominantly a sediment starved deep-water basin. However, deposition of terrigenous mudstones and siltstones of the Otaraoa Formation, sourced from east of the Taranaki Fault dominated in proximal eastern and southern central areas (King, 1994).

1.6.3 Miocene

The earliest Miocene marked renewed tectonism as the full effect of a major reorganisation in the plate tectonic configuration of the Southwest Pacific impacted on the Taranaki Basin. Walcott (1987) contends that the instantaneous pole of rotation moved away from New Zealand causing accelerated plate convergence along the Australian-Pacific plate boundary. Convergence initiated a major phase of compression and tectonic uplift in the east and south of the basin. In the east overthrusting of the Taranaki Fault occurred and the associated Tarata Thrust Zone developed. The early Miocene also coincides with the onset of uplift and formation of the Southern Alps and modern Alpine Fault system in the South Island (Palmer and Andrews, 1993). The concurrence of increased convergence rates on both the Alpine Fault and Taranaki Fault lead Knox (1982) to propose that the Taranaki Fault was a splay off the Alpine Fault.

However, King and Thrasher (1996) challenged this assumption contesting that although the Taranaki Fault may have been an integral part of an early transform system, it was probably never physically connected to the Alpine Fault *per se*. In the late Miocene - Pliocene a broad region of contraction occurred in the southern Taranaki Basin (Southern Inversion Zone). In the Manaia sub-basin east-west directed compression resulted in reverse movement on the Manaia Fault and growth of the Manaia Anticline (Pilaar and Wakefield, 1978; Knox, 1982; Schmidt and Robinson, 1990). Most of the basin remained at bathyal depth until the early Miocene. In the mid Miocene increasing uplift in the hinterland to the south and east resulted in sediment supply exceeding subsidence in the basin. This influx of terrigenous sediment marked the onset of a major regressive sedimentary phase in the mid to late Miocene as mud dominated turbidite deposits of the Wai-iti Group denote the beginning of the modern continental shelf.

1.6.4 Plio-Pleistocene

Plate boundary deformation continued to impinge on the eastern margin of the Taranaki Basin throughout the Plio-Pleistocene. Compression persisted in the south while extension influenced the northern regions of the basin; meanwhile the Western Stable Platform remained quiescent. Plio-Pleistocene uplift in the southern hinterland and possibly inversion structures in the basin provided vast amounts of terrigenous material to the basin (King and Thrasher, 1996). Several kilometres of Rotokare Group fine-grained sediment accumulated during this time, overfilling tectonically controlled depocentres in the east and eventually spreading out as a northwestwardly prograding sedimentary wedge onto the Stable Western Platform (King and Thrasher, 1992). Latest Miocene and Pliocene sedimentation is represented by the Matemateaonga and Tangahoe formations in the south and east of the basin. The most Recent sediments in the basin include the andesitic Egmont Volcanics that have preserved the underlying sedimentary sequences from erosion.

SEDIMENTARY LITHOFACIES

2.1 INTRODUCTION

A sedimentary lithofacies is a body of rock with specific physical characteristics that differentiate it from those rocks above, below and immediately adjacent (Reading and Levell, 1996). In this study sedimentary lithofacies in core from the Kapuni Group are identified and their depositional environments interpreted. The main purpose of this work is to ascertain the depositional setting of the Kapuni Group where core material is available.

2.2 METHODOLOGY

2.2.1 Core Descriptions

Core from the Kapuni Group in the Kapuni-1, -3, -8, -12, -Deep-1, -14 and -15 wells was examined and described at the Ministry of Economic Development Core Library in Lower Hutt. In total 268.23m of core from the Kapuni Group in the Kapuni Field has been recovered and is available on open file for this study. Most of the core is from the Mangahewa Formation (226.32m), with 28.96m available from the Kaimiro Formation and 12.95m from the Farewell Formation. Core information is summarised in Appendix-1. Cores were logged in detail using standard sedimentological conventions (Appendix 2) and detailed descriptions of the cored intervals are available in Appendix 3. Both imperial and metric units were originally used to identify core depths on the wellsite. For consistency in this study all depths have been converted to metric, mahbdf (metres along hole below derrick floor) unless otherwise stated.

2.2.2 Lithofacies Classification

Lithofacies have been grouped on the basis of lithology into heterogenous sandstone (Ss), heterolithic sandstone/mudstone (SM), heterolithic mudstone/sandstone (MS), mudstone (M) and coal (C) categories. Eleven lithofacies in core from the Kapuni Group were identified and defined on the basis of observed colour, lithology, bedding, texture and sedimentary structures (Table 2.1). The heterogenous sandstone (Ss) lithofacies group comprises the coarse sandstone (Ss-c), pebbly sandstone (Ss-p), rafted coal sandstone (Ss-rc), cross-bedded sandstone (Ss-cb), massive bedded sandstone (Ss-mb) and speckled sandstone (Ss-s) lithofacies. The heterolithic sandstone dominated (SM) lithofacies group includes the coarse sandstone/mudstone (SM-c), and fine sandstone/mudstone (SM-f) lithofacies. The heterolithic mudstone dominated (MS)

RESERVOIR POTENTIAL	MAJOR LITHOLOGICAL GROUPS		LITHOLOGICAL FACIES DESCRIPTIVE TERMINOLOGY	LITHOFACIES GROUP	LITHOFACIES
Reservoir or Reservoir Potential	Sandstone	Heterogeneous	Coarse sandstone	Ss	Ss-c
			Pebbly sandstone		Ss-p
			Rafted coal sandstone		Ss-rc
	Heterolithic		Cross-bedded sandstone	Ss	Ss-cb
			Massive bedded sandstone		Ss-mb
			Speckled sandstone		Ss-s
		Sand-dom.	Fine sandstone/mudstone	SM	SM-f
			Coarse sandstone/mudstone		SM-c
Non-Reservoir		Mud-dom.	Lenticular bedded mudstone/sandstone	M	MS-lb
	Mudstone		Carbonacous mudstone		Mc
	Coal		Coal	C	C

Table 2.1: Lithofacies classification of the Kapuni Group in the Kapuni Field

lithofacies group comprises only the lenticular bedded mudstone/sandstone (MS-lb) lithofacies. Lastly, coals are characterised by the coal (C) lithofacies. Environmental interpretations were assigned on the basis of specific physical characteristics identified in each lithofacies. Figures 2.1 – 2.7 include stratigraphic columns, lithofacies classifications and environments of deposition for the Kapuni Group in the Kapuni Field wells studied. In addition, cored intervals have been correlated with the gamma-ray log, as recorded core depths in some wells did not correspond to geophysical log depths.

2.3 HETEROGENEOUS SANDSTONE LITHOFACIES GROUP

2.3.1 Coarse Sandstone Lithofacies (Ss-c)

i. Lithofacies Descriptions

The coarse sandstone (Ss-c) lithofacies is characterised in core from the Mangahewa Formation in the Kapuni-14 well between 4049.90m – 4059.00m, 4063.10 – 4078.15m and 4085.10m – 4092.50m and in the Kapuni-3 between 3641.14m – 3641.80m. The Ss-c lithofacies consist of light brownish-grey, light greyish-brown and light pinkish-grey, moderately- to well-sorted, sub-angular to sub-rounded, medium- to very coarse-grained sandstones.

The dominant sedimentary structures are planar cross-bedding (1cm to 10cm thick) and normal graded bedding (1cm – 20cm thick). Planar cross-bed surfaces are infrequently capped by mud-drapes or continuous and discontinuous fine silty wavy laminae which range in thickness from 1mm – 2.0cm (Plate 2.1). Subordinate massive bedding (<40cm thick) also occurs. Planar cross-beds, graded beds and massive beds occur as fining-upward or coarsening upward sequences, ranging from 66cm to 10.40m in thickness. Burrows and bioturbation are rare except at the top of a fining-upward sequence between 4049.90m - 4054.78m in Kapuni-14, where *Ophiomorpha* and *Teichichnus* type burrow systems have completely obliterated bedding structures. Palynology studies by Mildenhall (1998) identified the occurrence of *Spinizonocolpites prominatus* pollen in the Ss-c lithofacies.

The Ss-c lithofacies are commonly found in association with the coarse sandstone/mudstone (SM-c) lithofacies, occurring both stratigraphically above and below. Where the Ss-c lithofacies overlie the SM-c lithofacies, basal contacts are gradational. The Ss-c lithofacies exhibit sharp lower bedding contacts with the lenticular bedded mudstone/sandstone (MS-lb) and scoured lower bedding contacts with the massive bedded sandstone (Ss-mb) and coal (C) lithofacies.

LEGEND

Grain Size

C	Clay
S	Silt
VF	Very Fine Sand
F	Fine Sand
M	Medium Sand
C	Coarse Sand
VC	Very Coarse Sand
VFP	Very Fine Pebbles

Bedding/ Structures

	Planar Cross-bedding
	Herringbone Cross-bedding
	Planar Bedding
	Wavy Bedding
	Ripple Bedding
	Massive Bedding
	Normal Graded Bedding
	Lenticular Bedding
	Flaser Bedding
	Mud-Drapes
	Convolute Bedding
	Load Structures
	Bioturbation
	Intraclasts
	Plant Fragments
	Carbonaceous
	Coal Streaks
—c	Thin Coal Bed
	Coal
	Slickensided
	Fractures
	Core Missing

Trace Fossils

Ch	Chondrites
Op	Ophiomorpha
Sk	Skolithos
Te	Teichichnus
Th	Thalassinoides

Bedding Contacts

	Gradual Contact
	Sharp Contact
	Scoured Contact
	Contact Not Observed

Lithofacies Groups

Ss	Heterogeneous
SM	Heterolithic sandstone dominated
MS	Heterolithic mudstone dominated
M	Mudstone
C	Coal

Lithofacies

Ss-c	Coarse sandstone
Ss-p	Pebbly sandstone
Ss-rc	Rafted coal sandstone
Ss-cb	Cross-bedded sandstone
Ss-mb	Massive bedded sandstone
Ss-s	Speckled sandstone
SM-c	Coarse sandstone/mudstone
SM-f	Fine sandstone/mudstone
MS-lb	Lenticular bedded mudstone/sandstone
Mc	Carbonaceous mudstone
C	Coal

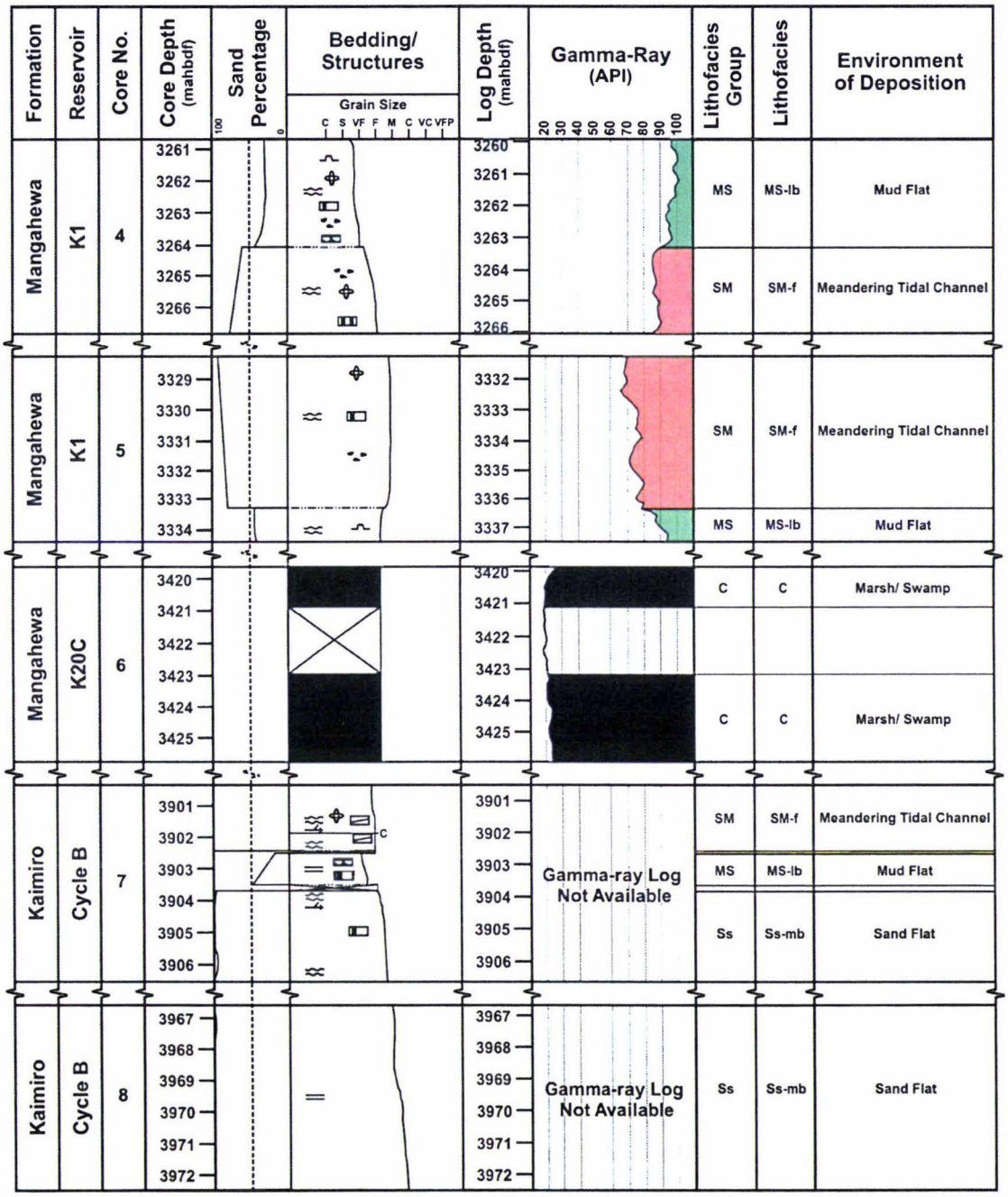

Figure 2.1: Stratigraphic column and lithofacies classification of core from the Mangahewa and Kaimiro formations in Kapuni-1 (Scale: 1:2)

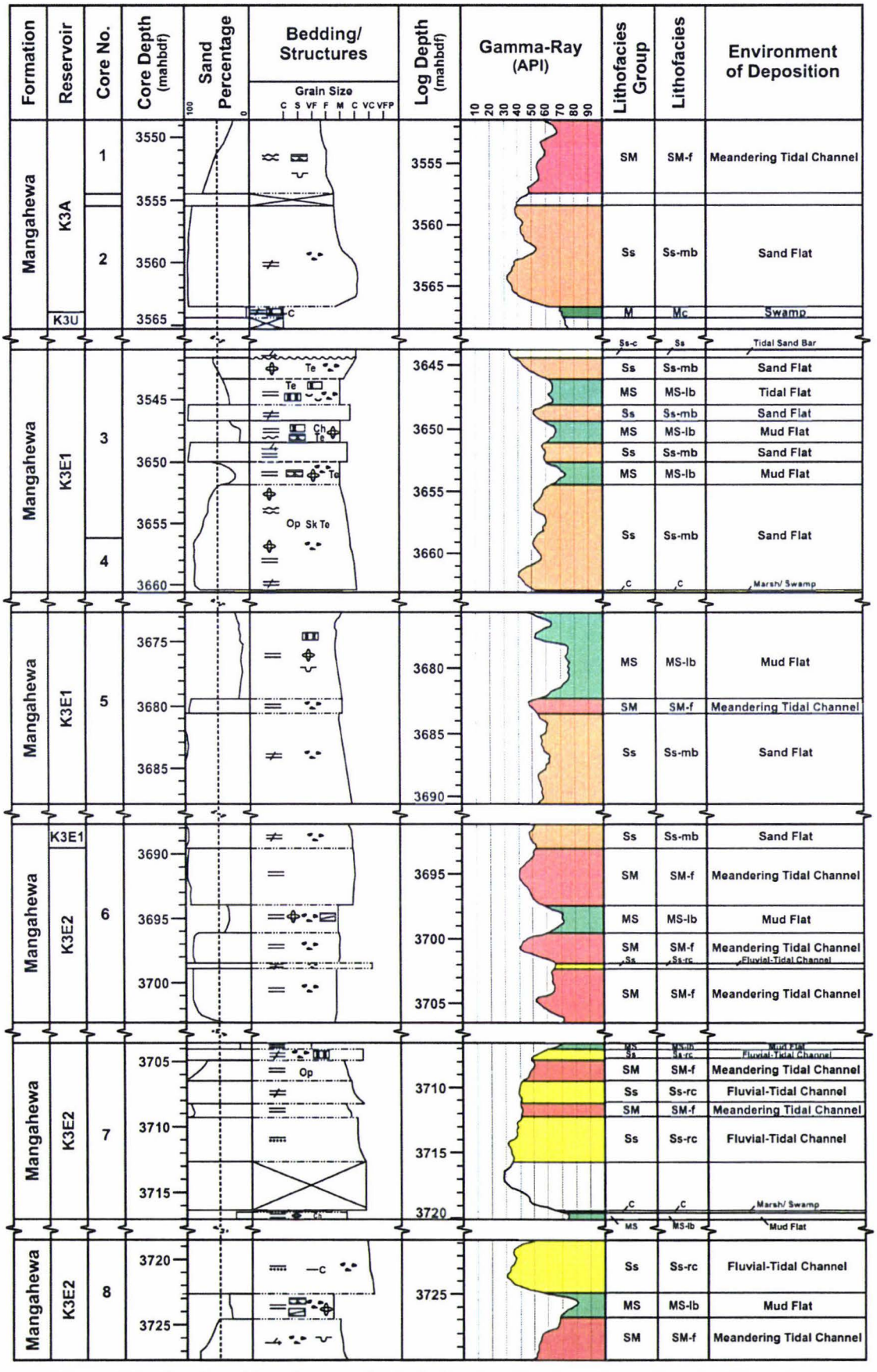

Figure 2.2: Stratigraphic column and lithofacies classification of core from the Mangahewa

Formation in Kapuni-3 (Scale: 1:4)

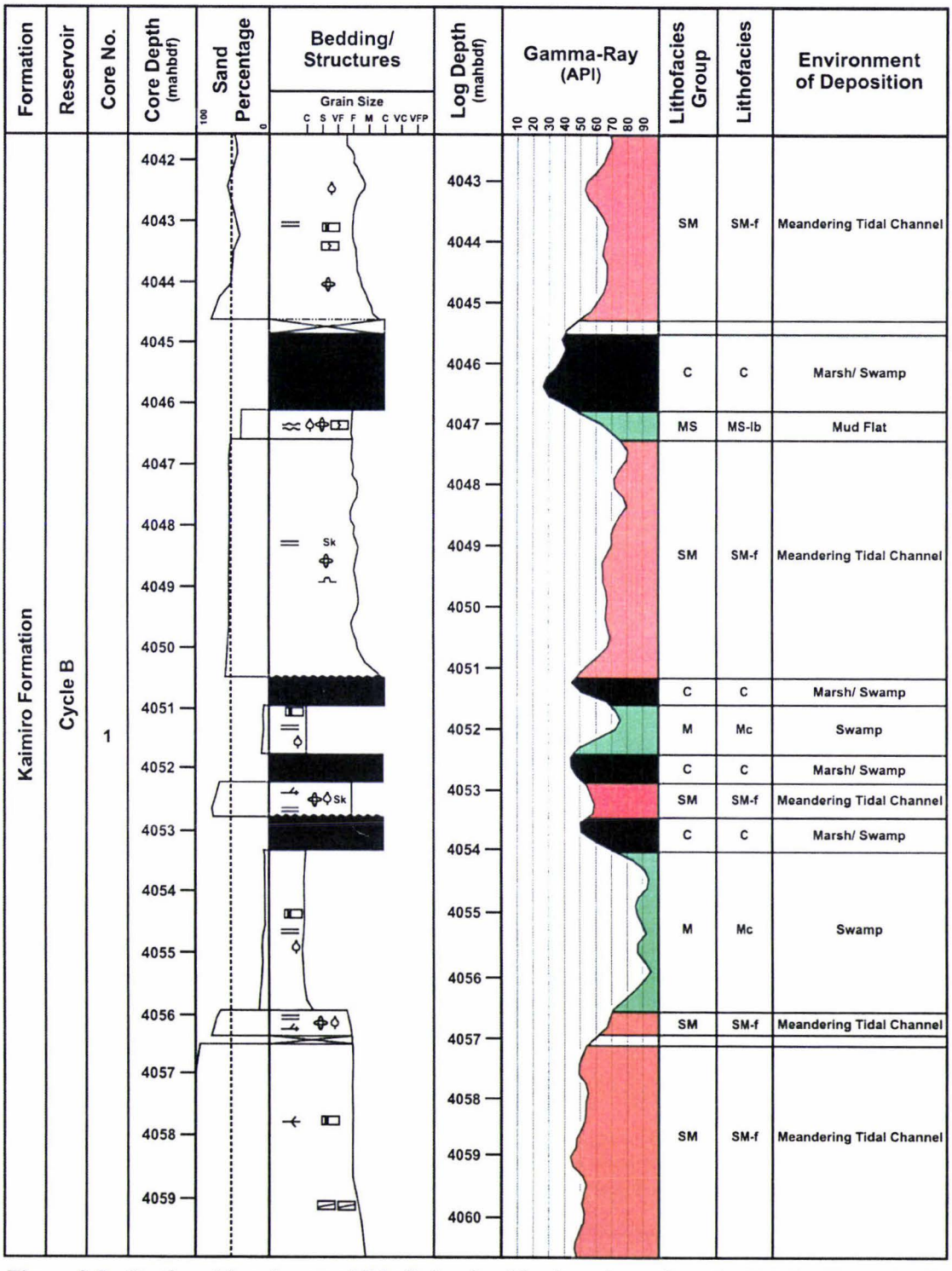

Figure 2.3: Stratigraphic column and lithofacies classification of core from the Kaimiro Formation in Kapuni-8 (Scale: 1:1)

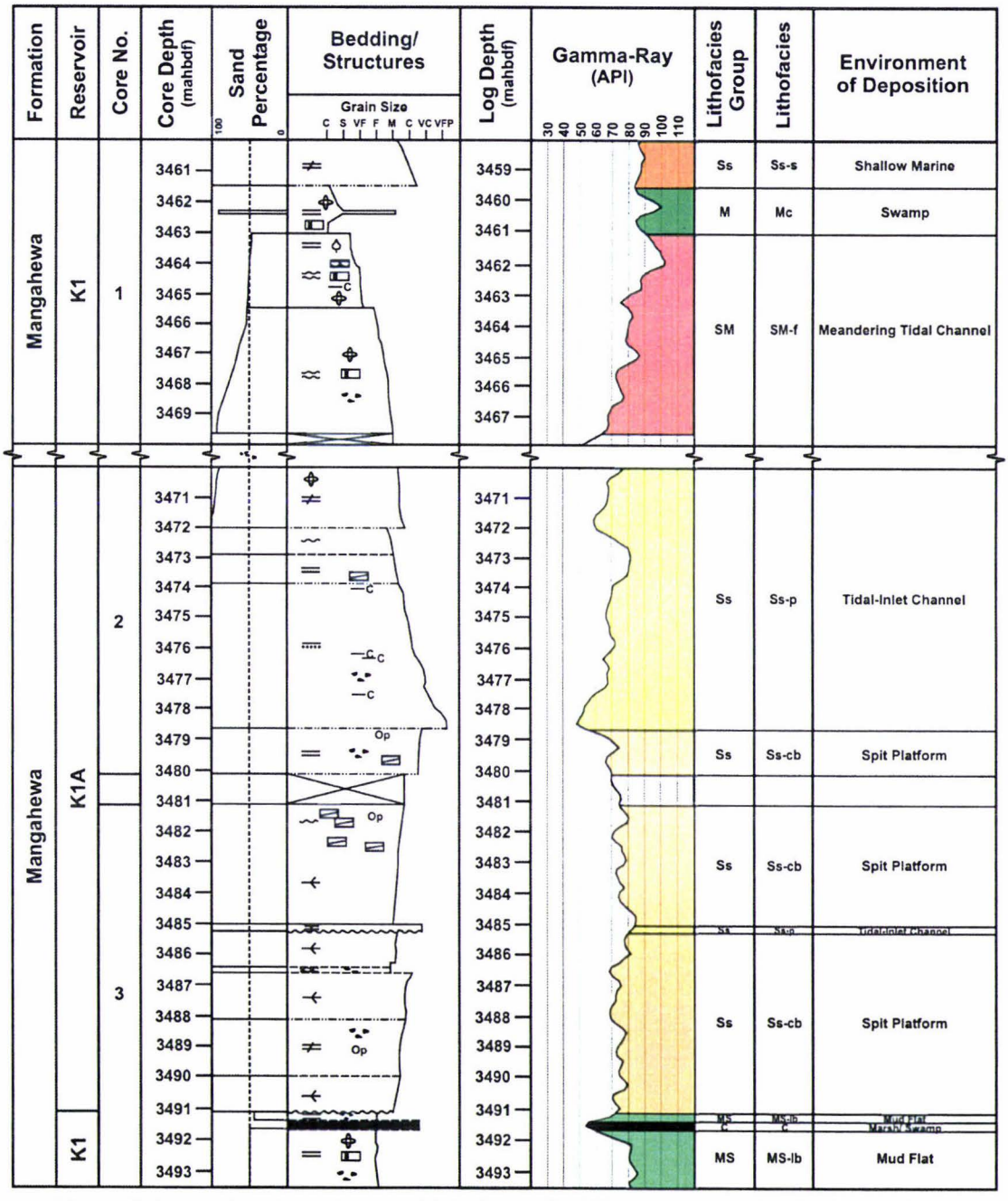

Figure 2.4: Stratigraphic column and lithofacies classification of core from the Mangahewa Formation in Kapuni-12 (Scale 1:2)

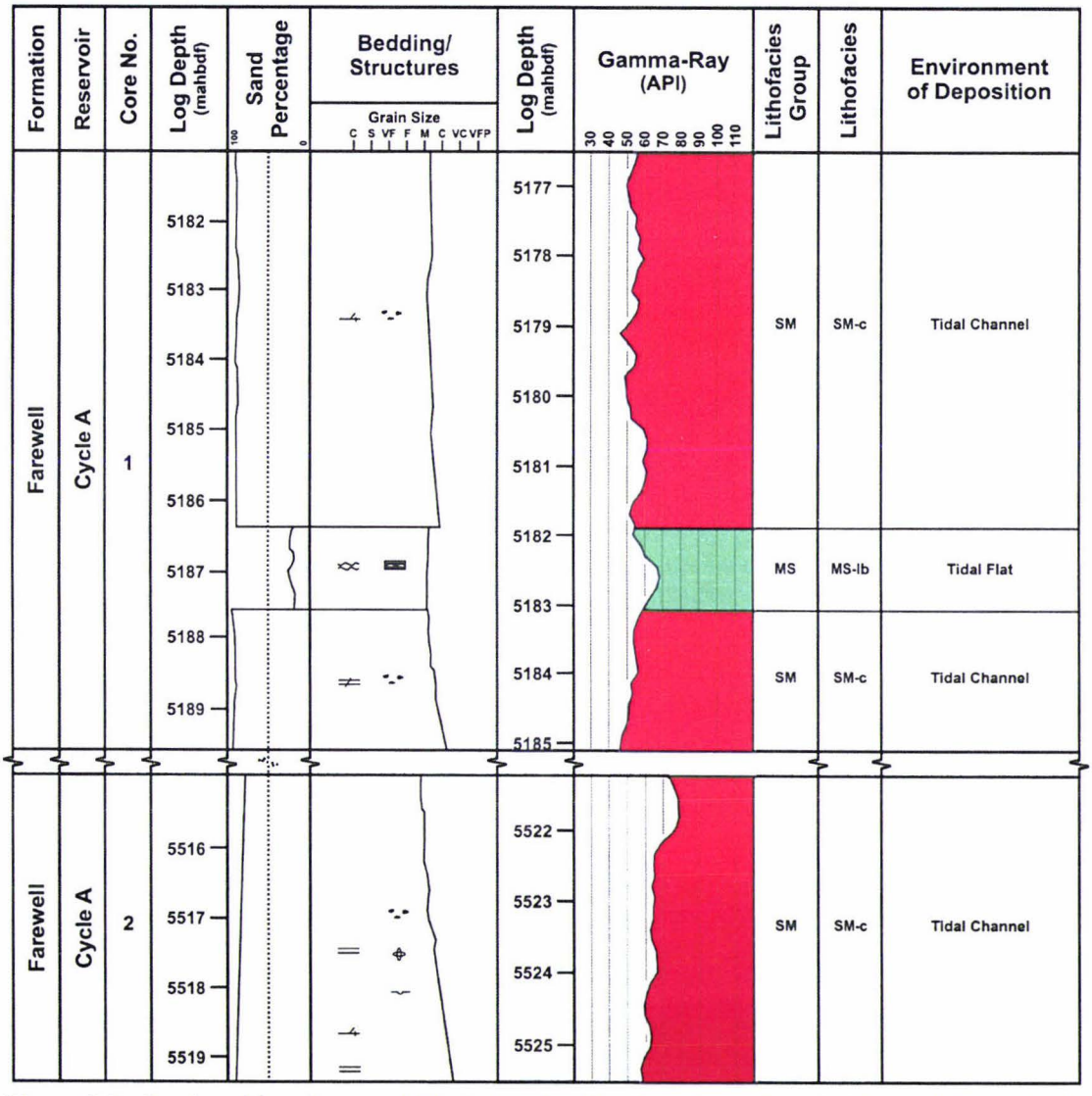

Figure 2.5: Stratigraphic column and lithofacies classification of core from the Farewell Formation in Kapuni Deep-1 (Scale 1:1)

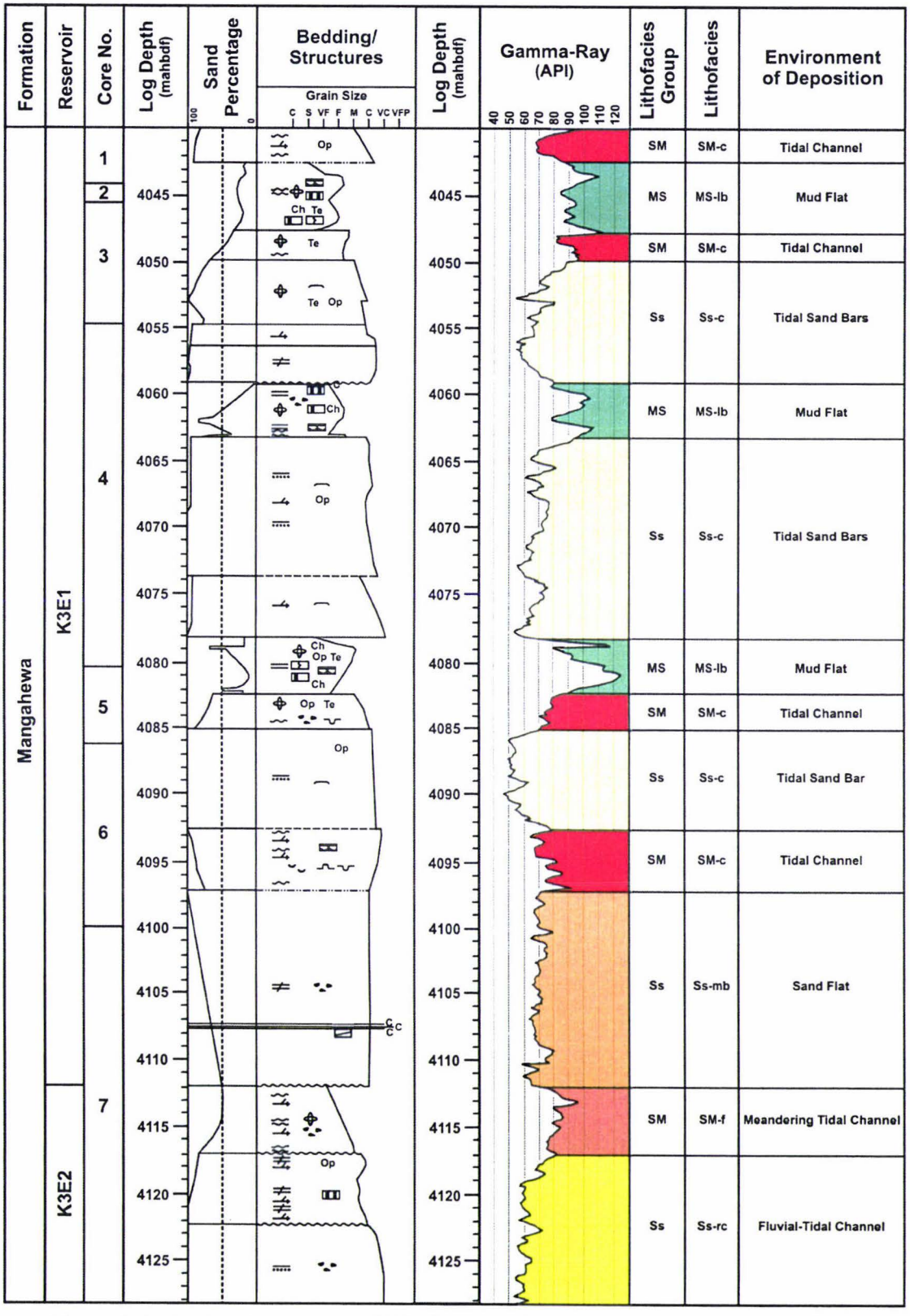

Figure 2.6: Stratigraphic column and lithofacies classification of core from the Mangahewa Formation in Kapuni-14 (Scale 1:4)

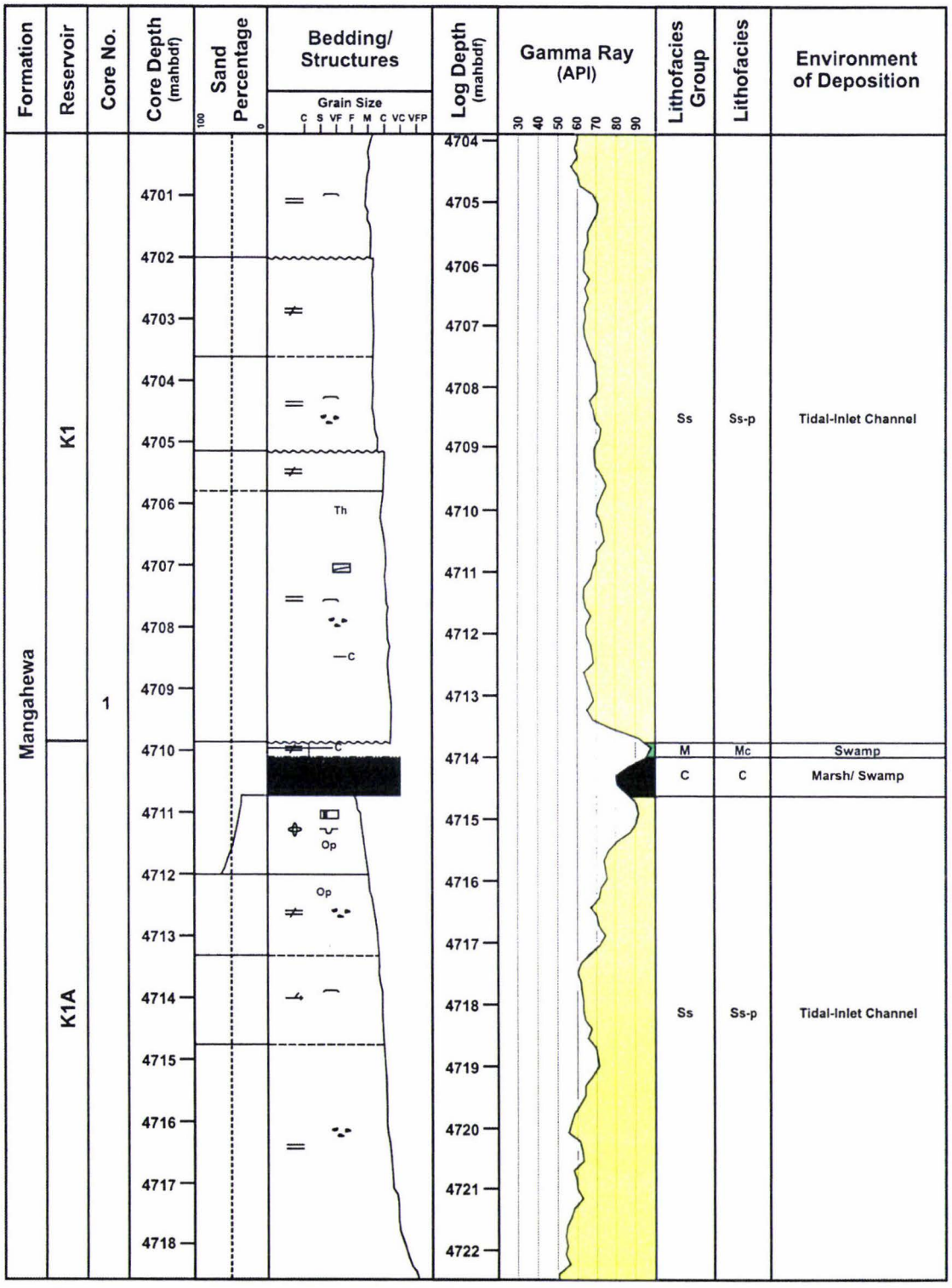

Figure 2.7: Stratigraphic column and lithofacies classification of core from the Mangahewa Formation in Kapuni-15 (Scale 1:1)

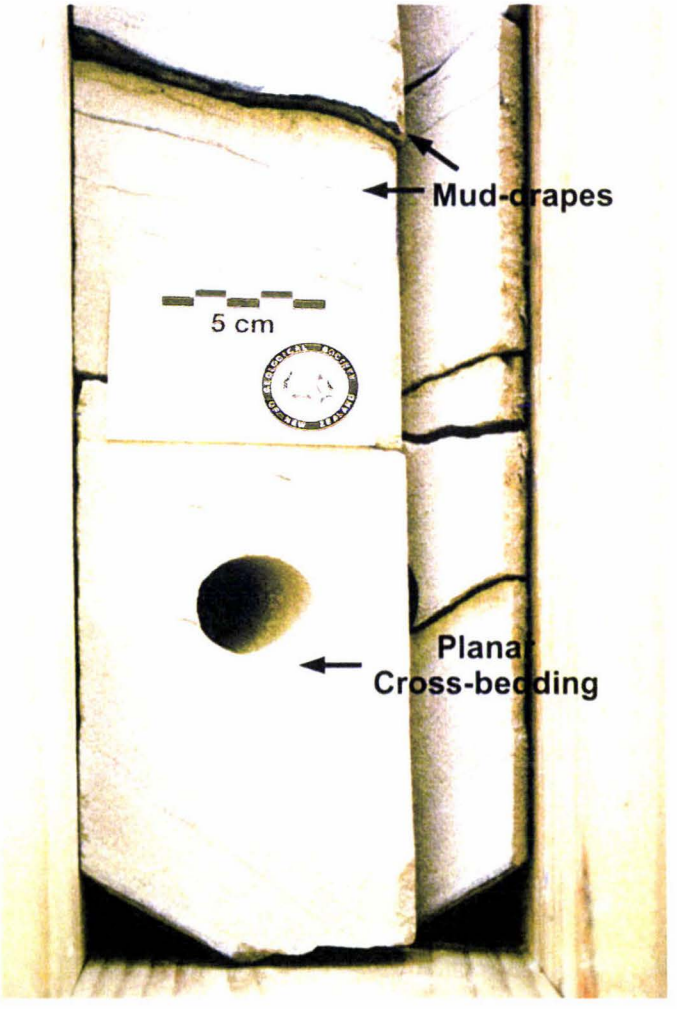

Plate 2.1: Planar cross-bedding in the coarse sandstone (Ss-c) lithofacies from the Mangahewa Formation with mud-drapes along some laminae in core from Kapuni-14 at c.4068.00m

ii. Environmental Interpretation

The coarse sandstone (Ss-c) lithofacies are characteristic of tidal sand bar deposits. Tidal sandbars are described by Dalrymple (1992) as predominantly medium- to coarse-grained cross-bedded sand bodies which develop in tide-dominated shallow marine settings, in the delta front region of tide-dominated deltas and in the mouth of tide-dominated estuaries. The planar cross-beds represent subaqueous dunes, while graded bedding and massive bedding are ascribed to times when sediment was deposited more rapidly, during storm or flood phases. The presence of mud-drapes and thin mudstone laminae, although not totally indicative, are most common in tidal environments (Collinson and Thompson, 1989). Reineck and Singh (1975) suggest that single mud-drapes are formed by slack-water periods of the dominant tide and if the subordinate currents are strong enough, a second mud-drape is deposited during the second slack water interval. In the Ss-c lithofacies, however, subordinate currents have generally been too weak to deposit sand, and the two mud-drapes have been amalgamated. The existence of both coarsening-upward and fining-upward sequences is attributed to changes in sea-level that occurred during deposition. Lateral shifting of sediment produces fining-upward sequences during transgression, whereas coarsening-upward sequences represent deposition during progradation when wave action is most intense on the crest of the bars (Dalrymple, 1992). Trace fossils including *Ophiomorpha* and *Teichichnus* type burrow systems are consistent with deposition in a subtidal environment. While *Spinizonocolpites prominatus* pollen supports a nearby coastal environment (Mildenhall, 1988).

2.3.2 Pebbly Sandstone Lithofacies (Ss-p)

i. Lithofacies Descriptions

The pebbly sandstone (Ss-p) lithofacies are represented in core from Mangahewa Formation in the Kapuni-12 well between 3470.00m – 3478.65m and 4085.00m – 4085.25m and in the Kapuni-15 well between 4700.00m – 4709.90m and 4710.70m – 4718.60m. The Ss-p lithofacies consist of light greyish-brown to dark grey and light greyish-white, sub-angular to sub-rounded, poorly- to well-sorted, medium-grained to very fine-pebbly sandstones. Massive beds (<2m thick), planar beds (2mm – 18cm thick) and normal graded beds (1cm.- 20cm thick) and are the dominant sedimentary structures with subordinate small-scale ripple laminae (2mm – 8mm thick) and rare planar cross-beds (3cm – 15cm thick) also present.

The Ss-p lithofacies comprise both fining-upward and coarsening-upward sequences. Two fining-upward sequences are identified. A complete 6.65m thick fining-upward cycle in Kapuni-12, comprises a normal graded bedded unit of coarse-pebbly sand at the base, which is overlain by a coarse to medium-grained planar bedded grading into small-scale ripple laminated sandstone at the top (Plates 2.2 and 2.3). In Kapuni-15 an

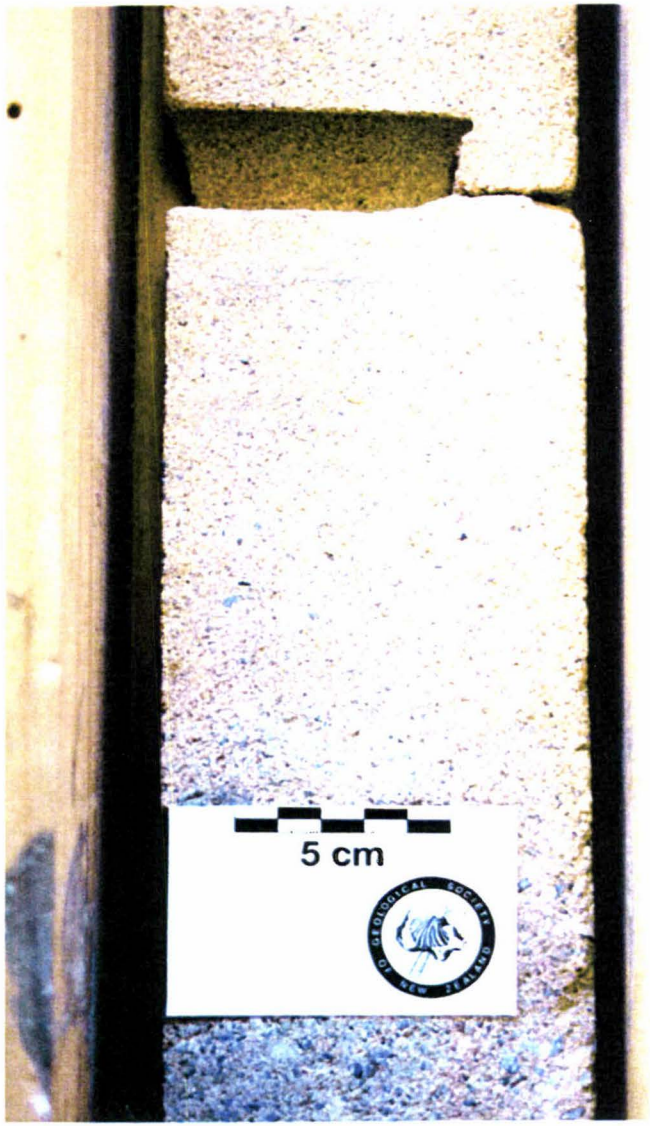

Plate 2.2: The basal graded bedded sandstone in the pebbly sandstone (Ss-p) lithofacies from the Mangahewa Formation in core from Kapuni-12 at c.3476.70m

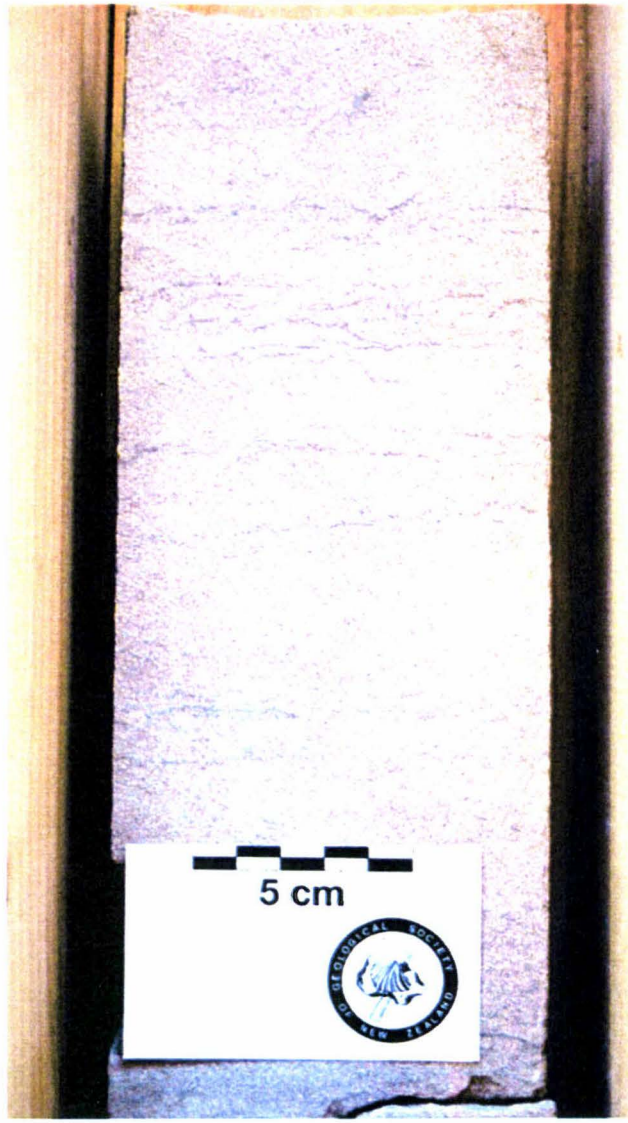

Plate 2.3: Small-scale ripple laminae in the pebbly sandstone (Ss-p) lithofacies from the Mangahewa Formation in core from Kapuni-12 at c.3472.50m

incomplete fining-upward sequence (7.90m thick) is composed of planar-bedded coarse- to medium-grained sandstone with occasional very fine pebbles at the base, overlain gradationally by medium-grained planar cross-bedded, then massive and finally bioturbated sandstones. The coarsening-upward sequence in Kapuni-15 comprises stacked cycles (<4.70m thick) of medium-grained planar bedded sandstones that grade upward into medium-grained massive sandstone beds.

Silty mud-drapes and paired mud-drapes cap the top of some planar bedded and planar cross-bedded surfaces. These mud-drapes are generally wavy, although some are rippled or convoluted. Wavy coal beds (<1cm thick) occur on the base of some foresets, while carbonaceous mudstone and coal intraclasts (<5mm to <3cm thick) are also common. Load cast structures and convolute bedding are prevalent in the bioturbated sandstone at the top of the fining-upward sequence in Kapuni-15. Clay-lined sub-vertical *Ophiomorpha* burrows infilled with clean coarse sand are common, while a single horizontal *Thalassinoides* type burrow occurs at c.4707.20m in Kapuni-15. A series of small fractures occur at c.3479.95 and at c.3473.70m (vertical offset = 3cm) in Kapuni-12 and c.4707.20m (vertical offset = 2cm) in Kapuni-15. The Ss-p lithofacies exhibit scoured lower bedding contacts with the underlying lenticular bedded mudstone/sandstone (MS-lb) and carbonaceous mudstone (Mc) lithofacies.

ii. Environmental Interpretation

The pebbly sandstone (Ss-p) lithofacies are characteristic of tidal-inlet channel sequences. Tidal-inlet channel deposits are formed by lateral migration, as they dissect barrier complexes (Reinson, 1992). Fining-upward sequences mark the waning of currents in the channel during transgression. The basal normal graded bedded coarse-pebbly sandstone unit in Kapuni-12 characterises a high energy lag deposit. Overlying the lag deposit the fining-upward trend and associated change from planar bedding to ripple laminae represent the deeper part of the channel and waning flow strengths during deposition. In core from Kapuni-15 the fining-upward trend represents a shallower part of the channel, indicated by the absence of the coarse-pebbly sandstone lag and presence of the bioturbated upper sandstone unit representing the final stages of channel abandonment. In contrast, coarsening-upward sequences represent deposition in the tidal-inlet channel during progradation. Mud-drapes support a tidal environment (Collinson and Thompson, 1989). Single mud-drapes have formed during slack-water periods of the dominant tide and a second mud-drape has been deposited where subordinate currents were strong enough (Reineck and Singh, 1975). Coal laminae and intraclasts together with carbonaceous mudstone intraclasts represent material derived from adjacent mud flat, swamp or marsh environments. Ichnofossils identified are consistent with tidal-inlet channel deposition as *Ophiomorpha* and *Thalassinoides* type burrows are typical of

subtidal and sandy shoreline environments respectively. Small fractures are interpreted as post-lithification tectonic features.

2.3.3 Rafted Coal Sandstone Lithofacies (Ss-rc)

i. Lithofacies Descriptions

The rafted coal sandstone (Ss-rc) lithofacies were identified in core from the Mangahewa Formation in the Kapuni-3 well between 3698.53m – 3698.93m, 3704.16m – 3704.97m, 3706.50m – 3708.20m, 3709.22m – 3712.72m, 3718.56m – 3722.73m and the Kapuni-14 well between 4116.95m – 4128.15m. The Ss-rc lithofacies consist of light brownish-grey to greyish-brown, moderately-sorted, sub-angular to sub-rounded, medium- to coarse-grained sandstones.

The Ss-rc lithofacies encompass fining-upward sandstone units (<11.20m) which decrease in grain-size and bed thickness upwards. The sandstones generally consist of massive beds (<81cm thick) and poorly- to well-defined normal graded beds (2cm - 25cm thick) that exhibit irregular bounding surfaces. Subordinate sedimentary structures include planar cross-bedding (5cm – 10cm thick). Graded beds, massive beds and planar cross-beds are generally characterised at their base by wavy carbonaceous mudstone or coal laminae that range from 1mm – 5mm in thickness (Plate 2.4). In the Kapuni-14 well between 4122.20m – 4128.15m there is a transition upwards from silty graded beds with carbonaceous laminae (<5mm thick) to planar cross-beds and massive beds with coal laminae (<1.5cm thick). Minor clay carbonaceous intraclasts (<2mm by <2 cm thick) are also common within the sandstones. Biogenic structures are almost absent except for a solitary vertical clay-lined *Ophiomorpha* type burrow observed in the Kapuni-14 well at 4117.80m. Lower bedding contacts of the Ss-rc lithofacies were not observed in core.

ii. Environmental Interpretation

The rafted coal sandstone (Ss-rc) lithofacies were deposited in tidally influenced fluvial channels. These low sinuosity distributary channels are common in delta and estuarine environments where they contain alternate bank attached bars and some mid-channel bars (Dalrymple *et al.*, 1992). An upward-fining trend and a general decrease in planar cross-bed, graded bed and massive bed set thickness upwards are indicative of a general decrease in the flow regime of the channel during transgression. The lower part of the sequence consists of normally graded beds with irregular lower bounding surfaces, which are interpreted as scour-and-fill structures. Collinson and Thompson (1989) suggest that scours are formed by vortex erosion in front of advancing dunes and are filled with sediment almost immediately. The planar cross-beds in the upper part of the sequence represent lateral and vertical accretion of sediment as bank attached bars along channel margins. Carbonaceous mudstone and coal at the base of the graded and massive beds

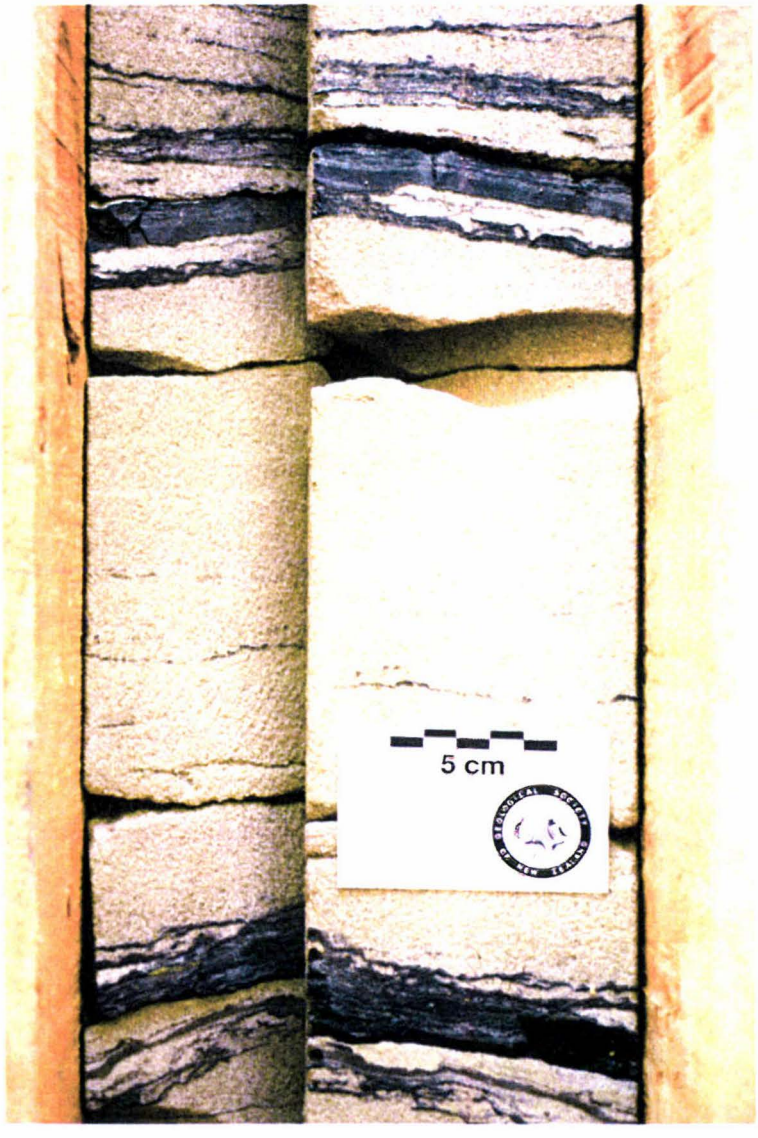

Plate 2.4: Massive sandstone with coal beds which have been rafted into place in the rafted coal sandstone (Ss-rc) lithofacies from the Mangahewa Formation in the Kapuni-14 well from c.4119.85m

and cross-bed foresets represent sediment rafted from marginal mud flat, swamp or marsh environments during channel migration. The presence of a single *Ophiomorpha* type burrow supports a subtidal influence, allowing discrimination from similar deposits of fluvial origin.

2.3.4 Cross-Bedded Sandstone Lithofacies (Ss-cb)

i. Lithofacies Descriptions

The cross-bedded sandstone (Ss-cb) lithofacies are identified in the Mangahewa Formation in the Kapuni-12 well between 3478.65m – 3485.00m and 3485.25m – 3491.10m. The Ss-cb lithofacies consist of grey and light greyish-brown, sub-angular to sub-rounded, moderately- to well-sorted, fine- to coarse-grained sandstones. The Ss-cb lithofacies comprise coarsening-upward sandstone sequences less than 6.35m in thickness. Herringbone cross-bedding (5mm – 6cm thick) and ripple bedding (5mm – 4cm thick) are the dominant sedimentary structures (Plate 2.5 and 2.6). Subordinate, massive bedding (<1.90m thick), planar bedding (2mm – 10cm thick) and wavy bedding (1cm – 10cm thick) also occur. Rare carbonaceous mudstone intraclasts (<1cm by <3cm) occur distributed throughout the sandstone. Clay-lined sub-vertical and vertical *Ophiomorpha* type burrows infilled with clean coarse sand are relatively common. Small fractures occur at c.3481.10m (vertical offset = 12mm), c.3481.75m (vertical offset = 2mm), c.3482.20m (vertical offset = 1cm) and c.3482.60m (vertical offset = 2mm) in the Kapuni-12 well. The Ss-cb lithofacies have scoured lower bedding contacts with the underlying lenticular bedded mudstone/sandstone (MS-lb) lithofacies.

ii. Environmental Interpretation

The cross-bedded sandstone (Ss-cb) lithofacies are interpreted as spit platform deposits. Spit platforms form part of a barrier complex, upon which a (spit) beach is built (Moslow and Tye, 1985). The coarsening-upward sequences are characteristic of transgressive deposits. At the base of the spit, herringbone cross-beds represent subaqueous dunes. Planar bedding characterises depositional periods in upper flow regime conditions. Ripple bedding near the top of the sequence represents the latter stages of spit platform accretion, and are comparable to "washed out" ripple laminae as described in tidal-inlet channel deposits by Kumar and Sanders (1974). Massive beds are likely to have been deposited rapidly during storm events. Rare carbonaceous intraclasts represent sediment eroded from nearby mud flat, swamp or marsh environments. Clay-lined *Ophiomorpha* type burrow systems are consistent with deposition in a sandy shoreline environment. The series of small fractures are interpreted as post-depositional tectonic structures.

Plate 2.5: Herringbone cross-bedding in the cross-bedded sandstone (Ss-cb) lithofacies from the Mangahewa Formation in core from Kapuni-12 at c3485.60m

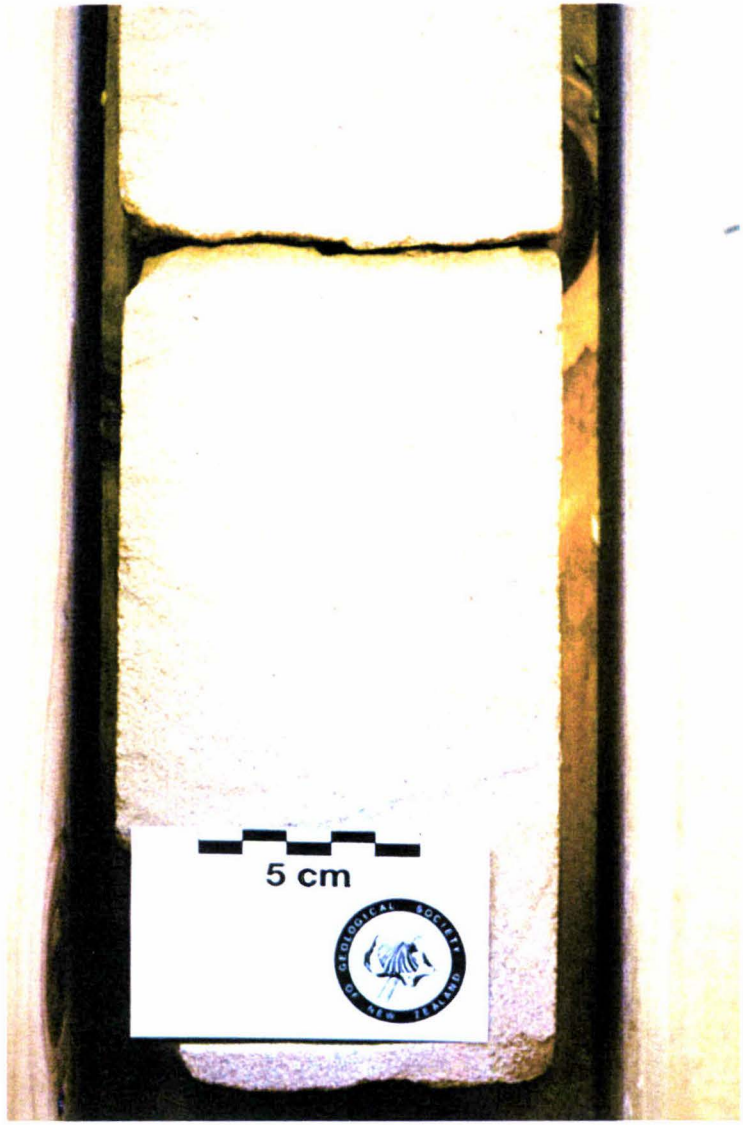

Plate 2.6: Ripple bedding in the cross-bedded sandstone (Ss-cb) lithofacies from the Mangahewa Formation in core from Kapuni-12 at c.3481.90m

2.3.5 Massive Bedded Sandstone Lithofacies (Ss-mb)

i. Lithofacies Descriptions

The massive bedded sandstone (Ss-mb) lithofacies are recognised in core from the Mangahewa Formation between 3555.49m – 3563.42m, 3641.80m – 3643.27m, 3645.30m – 3646.75m, 3648.30m – 3649.90m, 3651.80m – 3660.35m, 3680.51m – 3689.60m in the Kapuni-3 well and in the Kapuni-14 well between 4097.15m – 4111.96m. The Ss-mb lithofacies is also characterised in the Kaimiro Formation in the Kapuni-1 well between 3903.88m – 3906.63m and 3966.67m - 3972.46m. The Ss-mb lithofacies consist of light grey to light greyish-brown and light pinkish-grey, poorly- to moderately-sorted, sub-angular to sub-rounded, fine- to coarse-grained sandstones.

The massive bedded sandstone (Ss-mb) lithofacies comprise 1.45m – 10.04m thick units that either fine-upward or exhibit no discernable change in grain-size. In the Mangahewa Formation the Ss-mb lithofacies typically occur as massive units less than 10.04m in thickness (Plate 2.7). Although in the Kapuni-3 well, planar bedded (3mm – 7cm thick) and wavy bedded (5mm – 15cm thick) sandstones also occur with intermittent carbonaceous mudstone laminae. In some units where carbonaceous mudstones are present, bedding structures are often destroyed by bioturbation, such as between 3641.80m – 3643.27m in Kapuni-3. In the Kaimiro Formation wavy bedded (2mm – 3.5cm thick) and planar bedded (5mm – 3cm thick) sandstones predominate, with subordinate planar cross-bedding (2mm – 3cm thick) also present in Kapuni-1 between 3904.00m – 3904.45m.

Fine silty and carbonaceous mudstone or coaly intraclasts (<1mm by <3cm thick) are most abundant in the massive bedded sandstone (Ss-mb) lithofacies of all the Kapuni Group lithofacies. Well-cemented calcareous horizons are also common, particularly in the Kapuni-14 well, where vertical fractures infilled with carbonate were observed at c.4107.70m. In a paleoecological study Mildenhall (1988) identified *Spinizonocolpites prominatus* pollen in the Ss-mb lithofacies. The Ss-mb lithofacies exhibit sharp lower bedding contacts with the fine sandstone/mudstone (SM-f) and coal (C) lithofacies and gradational and sharp lower contacts with the lenticular bedded mudstone/sandstone (MS-lb) lithofacies.

ii. Environmental Interpretation

The massive bedded sandstone (Ss-mb) lithofacies are interpreted as sand flat deposits. These sand flats are characteristic of tidal-estuaries and occur where upper flow regime conditions predominate (Dalrymple *et al.*, 1992). Fining-upward sequences are restricted to deposition during transgressive episodes, however, where units exhibit no observable change in grain–size they may have been deposited in either transgressive or

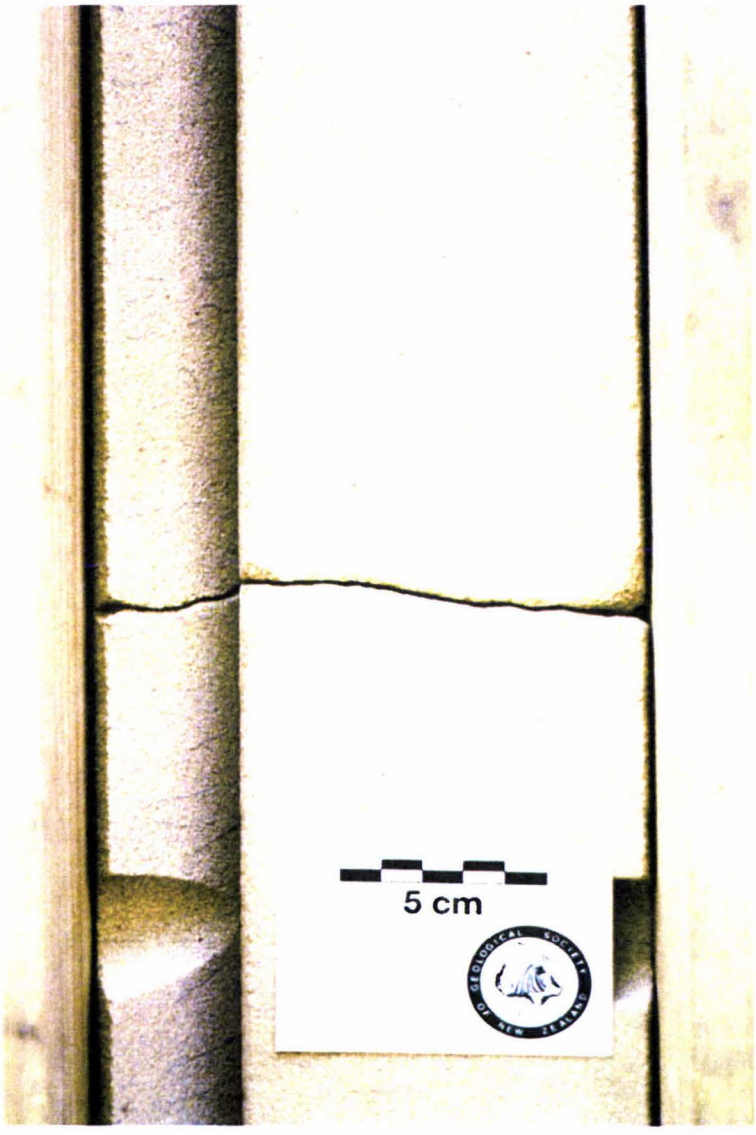

Plate 2.7: Massive sandstone with very fine carbonaceous intraclasts in the massive bedded sandstone (Ss-mb) lithofacies from the Mangahewa Formation in core from Kapuni-3 at c.3685.00m

progradational situations. The general lack of sedimentary structures other than intraclasts in the massive beds suggests reworking and rapid deposition of sediment, which is likely to occur in areas adjacent to the main channels. Carbonaceous mudstones and an increase in bioturbation in some units indicate deposition at greater distances from the main channels in mixed-flat areas. Planar bedding and wavy bedding represent depositional conditions that occur in the main channels. Hamilton (1979) suggests planar bedding and wavy bedding are dominant where the sand flats display a braided channel pattern where the estuary is broad. Whereas, planar cross-bedding occurs where sandflats are confined to a single channel further headward (Dalrymple, 1992). Carbonaceous and coaly intraclasts incorporated within the lithofacies indicate a high input of material eroded from nearby mud flat, swamp or marsh environments. The existence of *Spinizonocolpites prominatus* pollen supports a coastal environment for the sandstones (Mildenhall, 1988).

2.3.6 Speckled Sandstone Lithofacies (Ss-s)

i. Lithofacies Descriptions

The speckled sandstone (Ss-s) lithofacies consist of dark greenish-grey, well-sorted, sub-rounded, coarse-grained sandstone. The Ss-s lithofacies was only identified in core from the Mangahewa Formation in the Kapuni-12 well between 3460.00m – 3461.52m. The sandstone is typically homogeneous with no discernable changes in grain-size. Infact, massive bedding (1.52m) is the only observable sedimentary structure. The sandstone contains dark-green glauconite pellets, which in the upper part of the unit give it a distinctive speckled appearance (Plate 2.8). The lower bedding contact of the Ss-s sandstone lithofacies was not observed.

ii. Environmental Interpretation

The speckled sandstone (Ss-s) lithofacies was deposited in a shallow marine environment. Glauconite is an important index mineral, it forms *in situ* and does not transport or rework well because it is rapidly oxidised during weathering (Bell and Goodell, 1967). It is restricted to shallow marine environments (water depth 10 – 200m) that experience low rates of sedimentation and reducing conditions (Odin, 1988). Low rates of sedimentation suggest that massive bedding in the Ss-s lithofacies was generated by bioturbation from marine organisms completely obliterated bedding structures. No observable change in grain-size means that the sandstones could have been deposited in either transgressive or progradational situations.

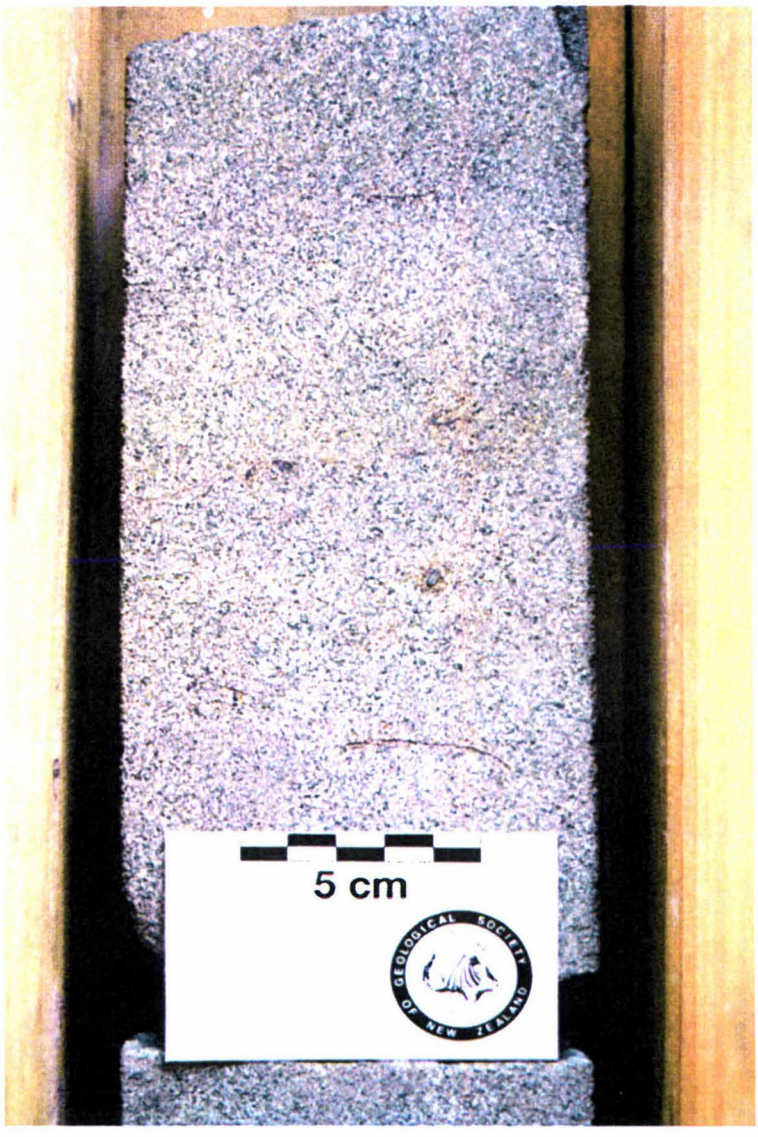

Plate 2.8: Glauconite pellets giving the massive sandstone a speckled appearance in the speckled sandstone (Ss-s) lithofacies from the Mangahewa Formation in the Kapuni-12 well at c3461.10m

2.4 SAND-DOMINATED HETEROLITHIC LITHOFACIES GROUP

2.4.1 Coarse Sandstone/Mudstone Lithofacies (SM-c)

i. Lithofacies Descriptions

The coarse sandstone/mudstone (SM-c) lithofacies occur in core from the Mangahewa Formation in the Kapuni-14 well between 4040.00m – 4042.47m, 4047.48m – 4049.90m, 4082.30m – 4085.10m and 4092.50m – 4097.15m. The SM-c lithofacies is also present in the Farewell Formation in the Kapuni Deep-1 well between 5181.00m – 5186.37m, 5187.98 – 5189.60m and 5515.00m – 5519.35m. The SM-c lithofacies are characterised by light greyish-brown, light pinkish-brown, light grey, moderate grey and grey, moderately- to moderately-well sorted, sub-angular to sub-rounded, medium- to very coarse-grained sandstones interbedded with silty or carbonaceous mudstones.

The SM-c lithofacies occur in association with the coarse sandstone (Ss-c) lithofacies. Analogous to the Ss-c lithofacies, the SM-c lithofacies comprise fining-upward and coarsening-upward sequences that range in thickness from 2.42m – 5.37m. Sandstones of the SM-c lithofacies are predominantly ripple bedded (5mm – 15cm thick) and planar cross-bedded (5mm – 25cm thick) (Plate 2.9). Subordinate massive bedding (<3.60m) and planar bedding (5cm – 15cm) also occur (Plate 2.10). The sandstones are interbedded with continuous and discontinuous planar bedded (2mm – 1cm thick) and wavy bedded (2mm – 9.5cm thick) silty and carbonaceous mudstones. Along bedding surfaces rare zones of flaser and lenticular bedding are observed e.g. in Kapuni-14 between 4092.50m - 4097.15m.

In the coarse sandstone/mudstone (SM-c) lithofacies soft sediment deformation occurs in the form of water escape and load cast structures. Biogenic structures include common *Ophiomorpha* and *Teichichnus* type burrows. In some units *Teichichnus* burrows have completely obliterated bedding structures, for example between 4047.48m - 4049.00m in Kapuni-14. Carbonaceous mudstone intraclasts (<2cm by <3cm) are common in the sandstones, particularly in the Farewell Formation. Mildenhall (1988) identified *Spinizonocolpites prominatus* pollen and dinoflagellates in samples from the SM-c lithofacies in Kapuni-14 well. Lower bedding contacts of the SM-c lithofacies are sharp with the underlying coarse sandstone (Ss-c) and lenticular bedded mudstone/sandstone (MS-lb) lithofacies, while lower contacts were not observed with the massive bedded sandstone (Ss-mb) lithofacies.

iv. Environmental Interpretation

The coarse sandstone/mudstone (SM-c) lithofacies are interpreted as being deposited in tidal channels that separate tidal sand bars, with fining-upward sequences indicative of waning flow conditions during transgression and coarsening-upward sequences deposited at times of progradation. Dalrymple *et al.* (1990) recognise these types of tidal channels

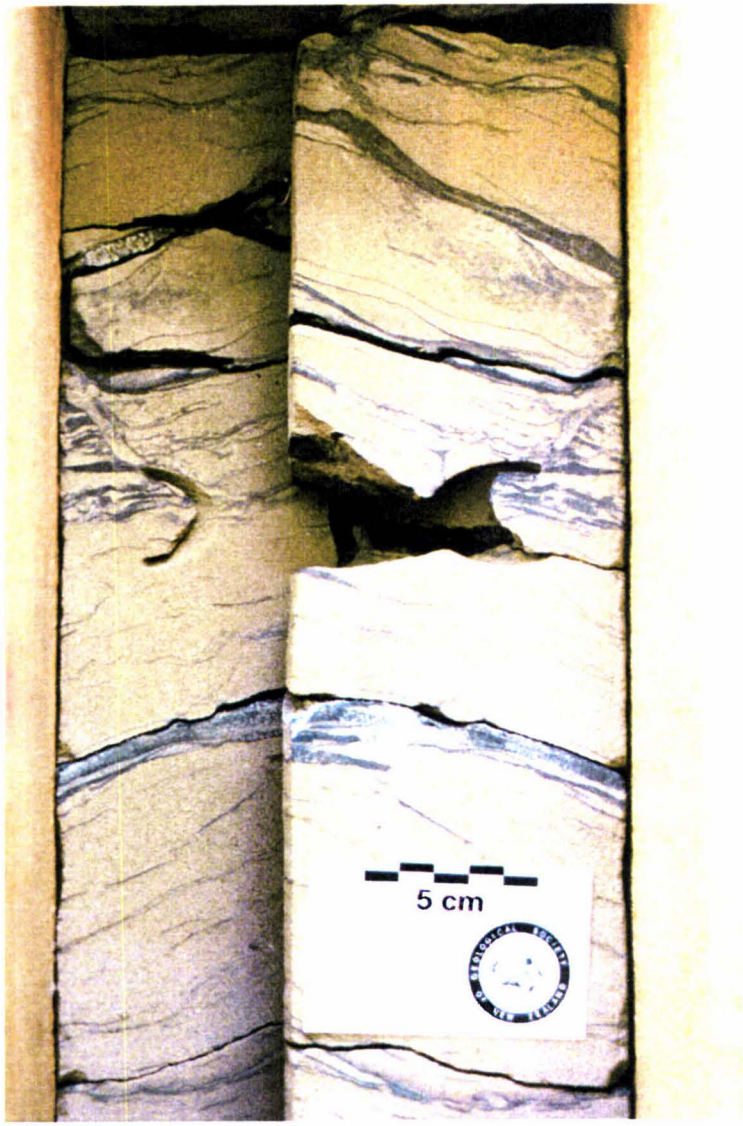

Plate 2.9: Ripple bedding in the coarse sandstone/mudstone (SM-c) lithofacies from the Mangahewa Formation in the Kapuni 14 well at c.4040.30m

Plate 2.10: Planar bedding in the coarse sandstone/mudstone (SM-c) lithofacies from the Mangahewa Formation in Kapuni-14 at c.4093.50m

in tide-dominated shallow marine settings, in the delta front region of tide-dominated deltas and in the mouth of tide-dominated estuaries. In these channels ripples are the stable bedform instead of dunes (Dalrymple, 1992). Thin mudstone beds in the SM-c lithofacies characterise deposition during periods of waning current strength of the subordinate current. Flaser and lenticular bedding are further evidence for fluctuating hydraulic conditions in subtidal environments, where periods of current activity are followed by periods of quiescence (Reineck and Singh, 1975). Potter (1967) suggests that water escape and load structures in sandstones are indicative of rapid sediment deposition in shallow but strongly fluctuating water currents. Carbonaceous intraclasts represent material ripped-up by tidal currents from nearby swamp and marsh environments. The identification of *Ophiomorpha* and *Teichichnus* type burrows, dinoflagellates and *Spinizonocolpites prominatus* pollen are consistent with deposition in a subtidal environment.

2.4.2 Fine Sandstone/Mudstone Lithofacies (SM-f)

i. Lithofacies Descriptions

The fine sandstone/mudstone (SM-f) lithofacies of the Mangahewa Formation were identified in the Kapuni-1 well between 3264.03m – 3266.85m, 3328.11 – 3333.15m, Kapuni-3 well between 3548.48m – 3554.58m, 3679.37m – 3680.51m, 3689.60m – 3694.00m, 3696.12m – 3698.53m, 3698.93m – 3703.02m, 3704.97m – 3706.50m, 3708.20m – 3709.22m and 3724.76m – 3727.70m in the Kapuni-12 well between 3463.02m – 3469.68m and Kapuni-14 well between 4111.96m – 4116.95m. The SM-f lithofacies were also recognised in the Kaimiro Formation in the Kapuni-1 well from 3900.53m – 3902.56m and Kapuni-8 well between 4041.65m – 4044.60m, 4046.63m – 4050.51m, 4052.21m – 4052.80m, 4055.95m – 4056.35m and 4056.47m – 4059.94m. The SM-f lithofacies comprise grey, dark grey, light grey, light greyish-brown, greyish-brown, light brownish-grey, greyish-white and light pinkish-grey, poorly- to moderately-sorted, very fine- to medium-grained sandstones interbedded with carbonaceous and silty mudstones.

The SM-f lithofacies consist of fining-upward interbedded sandstone and mudstone units (40cm to 6.66m thick) that decrease in grain-size and increase in mudstone bed thickness and frequency upwards. The sandstone and mudstone units are predominantly wavy laminated and bedded (Plate 2.11). Sandstones are planar laminated and bedded (2mm – 10cm thick), wavy laminated and bedded (1mm – 5cm thick), planar cross-bedded (5mm – 5cm thick), ripple laminated (2mm – 2cm thick), herringbone cross-bedded (5mm – 6cm thick) and lenticular bedded (2mm – 3cm thick). These sandstones are interbedded with continuous and discontinuous wavy laminated and bedded (1mm – 5cm thick), planar laminated and bedded (2mm – 18cm thick), planar cross-laminated (2mm – 1m thick) and small-scale ripple laminated (2mm – 2cm thick) carbonaceous and

Plate 2.11: Wavy bedding in the fine sandstone/mudstone (SM-f) lithofacies from the Mangahewa Formation in the Kapuni-14 well at c.3466.80m

argillaceous mudstones. Rare lenticular bedding also occurs eg. 3463.02 – 3465.47 in Kapuni-12. Soft sediment deformation includes common convolute bedding and load cast structures (<3cm by <5cm). Abundant carbonaceous mudstone intraclasts (<1cm by <1cm) occur in both sandstone and mudstone beds. Coal streaks (<3mm) occur, while carbonised plant fragments (<1cm by <3cm) are also common along bedding planes. Bioturbation is also frequent, and generally increases towards the top of the fining-upward units Although, in Kapuni-12 between 3465.47m – 3469.68m bioturbation is greatest in the basal sandier part of the sequence. Clay-lined vertical *Ophiomorpha* burrow structures are present in the Mangahewa Formation, while rare vertical *Skolithos* burrows structures occur in the Kaimiro Formation. Raine (1987) investigated the palynology of samples from the Kaimiro Formation in Kapuni-8 and Mildenhall (1988) studied samples from the Mangahewa Formation in Kapuni-14, both identified miospore assemblages that included *Spinizonocolpites prominatus* pollen, and dinoflagellate cysts. In the Kaimiro Formation small vertical fractures occur at c.3901.75m and c.3902.05m (vertical offsets = 3mm) and c.4016.50m (vertical offset = 1cm and 2cm) in the Kapuni-1 well and at c.4059.11m (vertical offset = 1cm and 2cm) in Kapuni-8. Slickensides were observed on some units. The SM-f lithofacies overlie the rafted coal sandstone (Ss-rc), massive bedded sandstone (Ss-mb) and lenticular bedded mudstone/sandstone (MS-lb) lithofacies where they exhibit scoured basal contacts.

iii. Environmental Interpretation

The fine sandstone/mudstone (SM-f) lithofacies are interpreted as meandering tidal channel deposits. Meandering tidal channels are common to both deltas (Donaldson *et al.*, 1970) and estuaries (Dalrymple *et al.*, 1992). The fine grain-size, fining-upward sequences, presence of *Ophiomorpha* and *Skolithos* type burrows and many highly scoured basal contacts with underlying lithofacies support transgressive meandering tidal channel environments. The sandier basal units characterise active channel deposits, while an increase in the carbonaceous mudstone in some upper units is indicative of meander tidal channel abandonment. Convolute bedding and load cast structures indicate that some units have been rapidly deposited during storm of flood episodes. Disseminated carbonaceous mudstone and coal intraclasts and carbonised plant fragments represent material derived from proximal swamp or marsh environments. *Spinizonocolpites prominatus* pollen is commonly associated with coastal paleoenvironments, while dinoflagellate cysts indicate connection to a marine environment (Raine, 1987). Slickensides and the series of small-scale fractures are interpreted as post-depositional tectonic structures.

2.5 MUD-DOMINATED HETEROLITHIC LITHOFACIES GROUP

2.5.1 Lenticular Bedded Mudstone/Sandstone Lithofacies (MS-lb)

i. Lithofacies Descriptions

The lenticular bedded mudstone/sandstone (MS-lb) lithofacies are identified in core throughout the Kapuni Group. The MS-lb lithofacies from the Mangahewa Formation are characterised in the Kapuni-1 well between 3260.75m – 3264.03m and 3333.15m – 3334.21m, Kapuni-3 well between 3643.27m – 3645.30m, 3646.75m – 3648.30m, 3649.90m – 3651.80m, 3672.84 – 3679.37m, 3694.00m – 3696.12m, 3703.62m – 3704.16m, 3716.56m – 3717.04m, 3722.73m – 3724.76m, Kapuni-12 well between 3491.10m – 3491.40m and 3491.70m – 3493.50m and Kapuni-14 well between 4042.47m – 4047.48m, 40459.16m – 4063.10m, 4078.15m – 4083.30m. In the Kaimiro Formation MS-lb lithofacies were identified in the Kapuni-1 well between 3902.66m – 3903.60m and Kapuni-8 well between 4046.12m – 4046.63m. While, the Farewell Formation MS-lb lithofacies occur in the Kapuni Deep-1 well between 5186.37m - 5187.58m. The MS-lb lithofacies consist of light grey, dark grey and brownish-black, carbonaceous to silty mudstones interlaminated with grey, light grey, moderate grey, greyish-brown, light brownish-grey, dark grey, poorly- to moderately well-sorted, very fine- to medium-grained sandstones.

The lenticular bedded mudstone/sandstone (MS-lb) lithofacies comprise fining-upward and coarsening-upward cycles which range in thickness from 48cm to 6.53m. An increase in mudstone content and bed thickness is evidenced where the lithofacies fine-upward, while the reverse occurs where sequences coarsen-upward. Where mudstone content and bed thickness increase upward, sequences are often capped by thin coal beds (<12cm thick). In contrast, where mudstone content and bed thickness decrease upward MS-lb sequences invariable grade into the massive bedded sandstone (Ss-mb) lithofacies.

The lenticular bedded mudstone/sandstone (MS-lb) lithofacies are characterised by common lenticular bedding, although it is generally not the dominant sedimentary structure. Sandstone and mudstone beds are typically planar laminated and bedded (1mm – 5cm thick) and wavy laminated and bedded (1mm – 5cm thick) (Plate 2.12). Rare small-scale ripple laminae (2mm – 1cm thick) also occur in the Mangahewa Formation at c.3647.90m in the Kapuni-3 well. In some MS-lb lithofacies frequent changes between planar, wavy and lenticular bedding occur with transition zones often indistinguishable due to bioturbation, good examples occur in the Kapuni-14 well between 4059.16m – 4061.65m and 4062.05m – 4063.10m.

Soft sediment deformation is rare in the MS-lb lithofacies, with load structures only observed in the Mangahewa Formation between 3672.84m – 3679.37m in the Kapuni-3

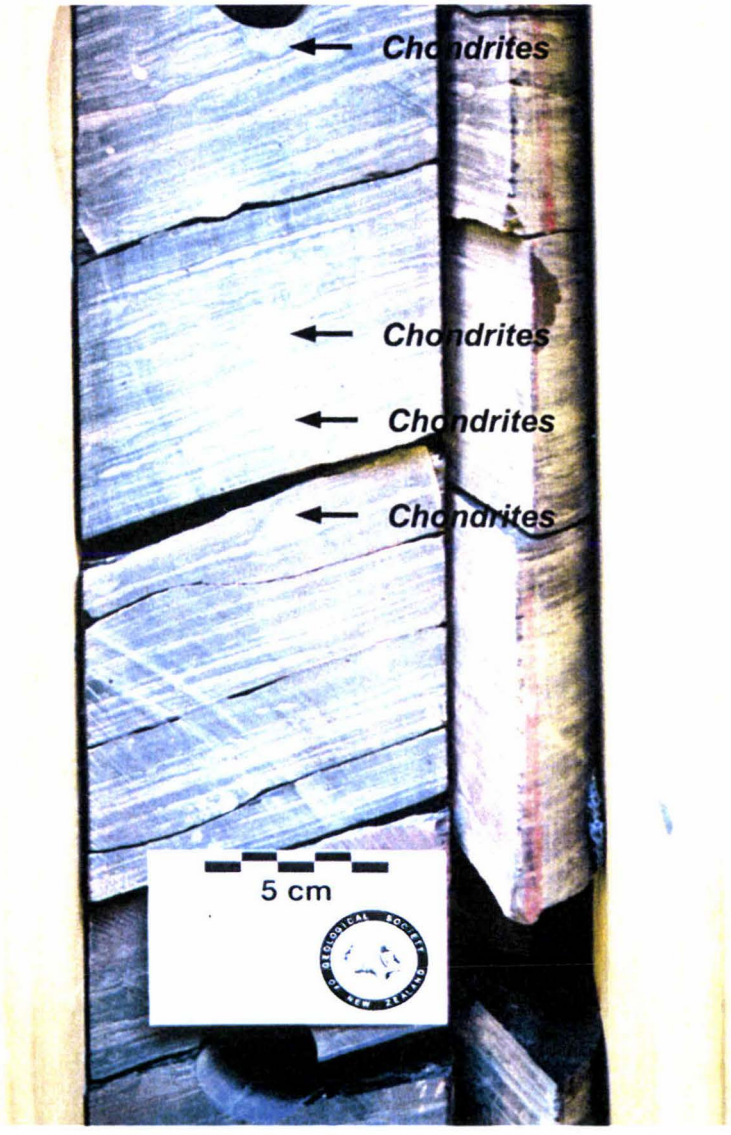

Plate 2.12: Planar laminae in the lenticular bedded mudstone/sandstone (MS-lb) lithofacies in Kapuni-14 well at 4081.60m – note the *Chondrites* type burrows

well. Mudstone beds regularly contain abundant coal streaks and laminae (<1cm) along with mudstone and coal intraclasts (<1cm by <3cm). In the Kaimiro Formation carbonised plant fragments (<1cm by <3cm) frequently occur along mudstone bedding surfaces. The MS-lb lithofacies generally exhibit some degree of bioturbation, with units ranging from moderately bioturbated to strongly bioturbated. Horizontal burrows are more common than vertical burrow structures and represent *Teichichnus* and *Chondrites* type burrow systems. In some sequences bedding structures have been completely obliterated by the activities of *Teichichnus*, for example between 4060.60m – 4061.15m in the Kapuni-14 well. Palynology studies of the MS-lb lithofacies record the dominance of *Haloragacidites harrisii* and *Myrtaceidites parvus* pollens (Challis and Mildenhall, 1986; Mildenhall, 1988), and the presence of *Spinizonocolpites prominatus* pollen and dinoflagellate cysts (Mildenhall, 1988). Slickensides are a common feature in the MS-lb lithofacies. The MS-lb lithofacies exhibit sharp lower bedding contacts with the massive bedded sandstone (Ss-mb) coarse sandstone/mudstone (SM-c) and fine sandstone/mudstone (SM-f) lithofacies.

iv. Environmental Interpretation

The lenticular bedded mudstone/sandstone (MS-lb) lithofacies are interpreted to represent mud flat deposits. Davis (1992) describes mud flats as low-relief environments that accumulate sediment within the intertidal range, including the supratidal zone, through the intertidal zone, and into the shallow portion of the subtidal zone. Mud flats are typical of estuaries, lagoons, bays, backshore of barrier-island complexes, deltas and along open coasts. The presence of lenticular bedding is indicative of subtidal environments, and is particularly abundant in mud flat sediments (Anderson *et al.*, 1981). Reineck and Singh (1975) note that transition from planar bedding to wavy to lenticular bedding in sedimentary sequences characterise a net decrease in current velocity and an increase in deposition and preservation of mud drapes.

Weimer *et al.* (1982) attributes the upward-fining trend of mud flat sequences to progradation. Whilst, an increase in sandstone bed thickness and an increase in sand content generally represents closer proximity to tidal channels (Terwindt, 1988). The common thin coal beds and streaks with in the MS-lb lithofacies are attributed to grasses and/or mangroves which temporarily colonized higher elevated parts of the tidal flats. Carbonaceous and coal intraclasts and carbonised plant fragments are further evidence for nearby vegetated swamp and marsh environments. Bioturbation of mudflat sequences is explained by Reineck and Singh (1975) who suggest that biogenic structures are prevalent in the muddy upper intertidal and supratidal zones and least abundant in sediment of the sandy lower intertidal zone and subtidal zone. Trace fossils including *Teichichnus* and *Chondrites* represent those associations typically found in subtidal environments. Dinoflagellate cysts support connection to a marine environment. While,

the identification of *Haloragacidites harrisii* and *Myrtaceidites parvus* pollens which are common to moist coastal forests and *Spinizonocolpites prominatus* pollen which is exclusive to coastal environments (Challis and Mildenhall, 1986; Mildenhall 1988), provide further evidence for a marginal marine depositional conditions. Slickensides indicate post-depositional tectonic movement.

2.6 MUDSTONE LITHOFACIES GROUP

2.6.1 Carbonaceous Mudstone Lithofacies (Mc)

i. Lithofacies Descriptions

The carbonaceous mudstone (Mc) lithofacies of the Mangahewa Formation were identified in core from the Kapuni-3 well between 3563.42m – 3564.33m, Kapuni-12 well between 3461.52m – 3463.02m and Kapuni-15 well between 4709.90m – 4710.10m. The Mc lithofacies were also present in the Kaimiro Formation between 4050.94m – 4051.76m and 4053.35m – 4055.95m in the Kapuni-8 well. The Mc lithofacies have a characteristic brownish-black, dark-grey to dark greyish brown colour and occur as massive (<91cm thick) and planar laminated (1mm – 1cm thick) units ranging from 20cm to 2.60m in thickness (Plate 2.13).

Common thin coal beds up to 3cm and rare sandstone beds less than 15cm thick are observed interbedded with in the mudstones. Carbonised plant fragments (<1cm by <4cm) are abundant along bedding surfaces in the Kaimiro Formation. The Mc lithofacies immediately overlie the fine sandstone/mudstone (SM-f), lenticular bedded mudstone/sandstone (MS-lb) and coal (C) lithofacies. Lower bedding contacts are sharp where the Mc lithofacies overlie the SM-f lithofacies, gradational with the MS-lb lithofacies and either sharp or gradational with coal (C) lithofacies.

iii. Environmental Interpretation

The carbonaceous mudstone (Mc) lithofacies were deposited in low-lying swamps. Swamps range from terrestrial to marine in character and are characterised by low relief, poor drainage, slow rates of accumulation and fine organic-rich sediment (Davis, 1992). Fine clastic sediment would have been supplied to the swamps from nearby tidal channels during flood events. Coal beds and carbonised plant fragments represent periods of established vegetation, while sandstone beds represent infrequent prolific flood events carrying coarser grain material in suspension. Planar bedding is typical of deposition in upper flow regime conditions during flood events, while massive bedding is most likely the result of bioturbation.

Plate 2.13: Massive carbonaceous mudstone in the mudstone (Mc) lithofacies from the Mangahewa Formation in the Kapuni-12 between c.3462.00m

2.7 COAL LITHOFACIES GROUP (C)

i. Lithofacies Descriptions

Coal (C) lithofacies are identified in core from the Mangahewa Formation in the Kapuni-1 well between 3419.86m – 3422.05m, 3423.10m – 3425.96m, Kapuni-3 well between 3660.35m – 3660.50m, Kapuni-12 well between 3716.38m – 3716.56m, 3491.40m – 3491.70m, Kapuni-14 well between 4059.00m - 4059.16m at c.4107.20m, c.4107.50m, c.4107.58 and c.4107.80m and Kapuni-15 well between 4710.10m – 4710.70m. In the Kaimiro Formation coals are recognised in the Kapuni-8 well between 4044.84m – 4046.12m, 4050.51m – 4050.94m, 4051.76m – 4052.21m and 4052.80m – 4053.35m. Coals are typically dark-brown to black in colour, contain inclusions of amberous material and are generally resinous (Plate 2.14). Although, in the Kapuni-15 well a 60cm dark-brown argillaceous coal occurs between 4710.10m – 4710.70m which does not contain amber or resin.

The coals typically occur as minor seams less than 1.28m in thickness. Although, in core from the Mangahewa Formation in the Kapuni-1 well, two coal intervals measuring 2.19m and 2.86m represent part of the K20 coal that forms a regional marker bed through the Kapuni Field. An analysis of this coal revealed that it has a low ash content of less than 2% (Bryant and Bartlett, 1992). Coal beds are commonly interbedded with planar bedded carbonaceous and argillaceous mudstone laminae and beds (1mm – 10cm thick), however, in the Kapuni-14 well between 4107.20m - 4107.80m four minor coal beds (2cm – 8cm) occur interbedded in the massive bedded sandstone (Ss-mb) lithofacies (Plate 2.15). The coal (C) lithofacies have gradational lower contacts with the carbonaceous mudstone (Mc) lithofacies, sharp or gradual basal contacts where they overlie the lenticular bedded mudstone/sandstone (MS-lb) lithofacies and contacts are distinctly sharp where they overlie or are interbedded with the massive bedded sandstone (Ss-mb) and fine sandstone/mudstone (SM-f) lithofacies.

ii. Environmental Interpretation

Coals are considered to have a floating swamp and/or marsh origin. Swamp environments have previously been discussed, nevertheless, Frey and Basan (1985) describe marsh's as vegetated intertidal areas that occur along the margins of estuaries, deltas, lagoons and in other protected strand environments. Established vegetation on the marsh ranges from grasses to mangroves, and for coals to be preserved the accumulation rate of organic matter must exceed the rate of decomposition by microbial and chemical processes (Davis, 1992). Thin interbedded mudstones in the coal units represent fine-grained clastic material derived from overbank flooding of tidal channels. A low ash content identified in the K20 coal indicates a rising water-table with limited clastic influx that existed for an extended period (Bryant and Bartlett, 1992). The presence of the K20 coal in all Kapuni Field wells and in other onshore wells in eastern parts of onshore

Plate 2.14: Coal with inclusions of amber from the Kaimiro Formation in the Kapuni-8 well at c.4056.00m

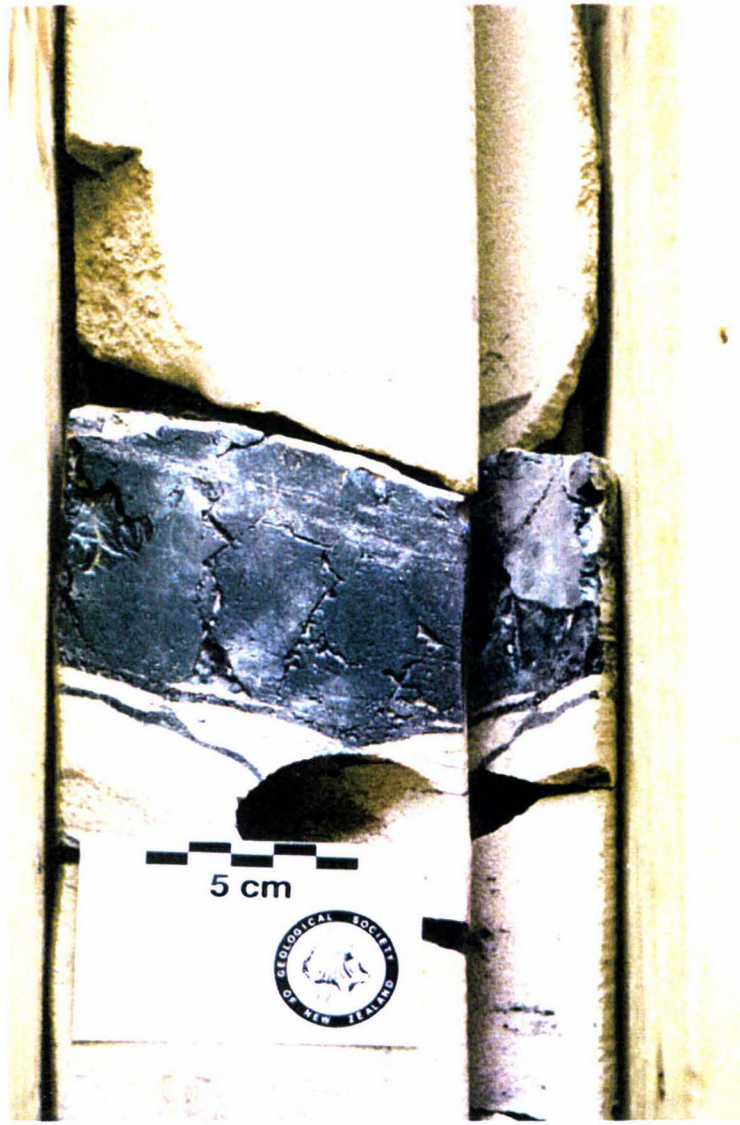

Plate 2.15: Coal interbedded in the massive bedded sandstone (Ss-mb) lithofacies from the Mangahewa Formation in the Kapuni-14 well at c.4107.95m

Taranaki where it is referred to as the Toko Member (Palmer, 1985), indicate that it is undeniably autochthonous. Other thinner coals identified in core from the Kapuni Group lack plant roots or subsoil, and although there no evidence suggesting they have formed *in situ*, this possibility cannot be ruled out. The exception occurs where coals with sharp basal contacts are interbedded in sandstone lithofacies e.g. the massive bedded sandstone (Ss-mb) lithofacies. In such cases coals have been transported from proximal swamp or marsh environments and are therefore allochthonous.

GEOPHYSICAL LOG ANALYSIS

3.1 INTRODUCTION

Geophysical logs record the properties of subsurface rocks in wells (Serra, 1985). In this study geophysical logs have been used to determine lithofacies in uncored sections of the Mangahewa Formation in each of the Kapuni wells. The study was constrained to those geophysical logs available in digital format. The gamma-ray log was the main log used as it is one of the most useful logs for; distinguishing lithology (shaliness), curve shape analysis (log motifs) and correlation between wells, but it was also the only common geophysical log to each well studied. Other logs used included the caliper, spontaneous potential, resistivity, sonic, neutron and density.

3.2 METHODOLOGY

To identify lithofacies in uncored sections of the Mangahewa Formation in the Kapuni wells, lithofacies in core were firstly correlated with and extrapolated onto the gamma-ray log by visual zoning of the lithofacies boundaries (see Figures 2.1 – 2.7). The gamma-ray logs were then extracted for comparisons at the same scale (Figure 3.1). Identification of lithofacies in uncored sections of the wells involved recognising cut-off values and characterising log motifs.

3.2.1 Cutoff Values

Cutoff values on the gamma-ray were identified by calibrating the log signatures of lithofacies to API (American Petroleum Institute) unit values. A shale line was identified to separate the sandstones (heterogeneous sandstone lithofacies and sand-dominated heterolithic lithofacies groups) from the mudstones (mudstone-dominated heterolithic lithofacies and mudstone lithofacies groups). This shale line was found to vary between the Kapuni wells, occurring consistently at 60 API units in the Kapuni-3, -8 and -Deep-1 wells and at 85 API units in the Kapuni-1, -12, -14 and -15 wells. The coincidence of two discrete 'shale line' values remains unclear in this study, but may relate to differences in calibration of the geophysical tools and/or to differential compaction of the sediments. For example, Cant (1992) explains that the concentration of radioactive elements in shale increase with compaction, so the shale line may need readjusting depending on the thickness being studied. Examination of the sandstone heterogeneous lithofacies group and sand dominated heterolithic lithofacies revealed another cutoff value in the wells which helped to distinguish the sandstone lithofacies. This boundary occurred at 20 API

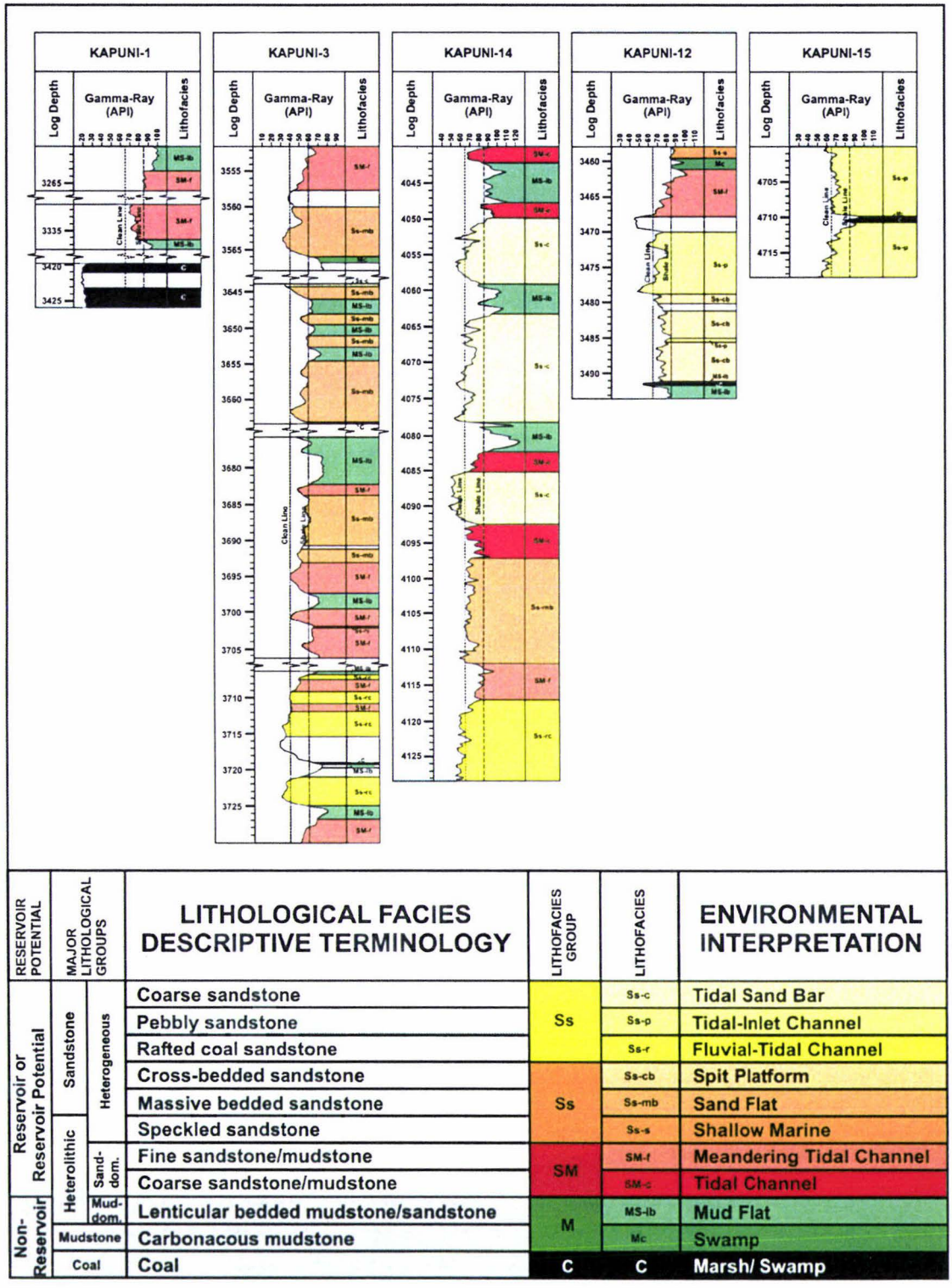

RESERVOIR POTENTIAL	MAJOR LITHOLOGICAL GROUPS		LITHOLOGICAL FACIES DESCRIPTIVE TERMINOLOGY	LITHOFACIES GROUP	LITHOFACIES	ENVIRONMENTAL INTERPRETATION
Reservoir or Reservoir Potential	Sandstone	Heterogeneous	Coarse sandstone	Ss	Ss-c	Tidal Sand Bar
			Pebbly sandstone		Ss-p	Tidal-Inlet Channel
			Rafted coal sandstone		Ss-r	Fluvial-Tidal Channel
			Cross-bedded sandstone	Ss	Ss-cb	Spit Platform
			Massive bedded sandstone		Ss-mb	Sand Flat
			Speckled sandstone		Ss-s	Shallow Marine
	Heterolithic	Sand-dom.	Fine sandstone/mudstone	SM	SM-f	Meandering Tidal Channel
			Coarse sandstone/mudstone		SM-c	Tidal Channel
Non-Reservoir		Mud-dom.	Lenticular bedded mudstone/sandstone	M	MS-lb	Mud Flat
	Mudstone		Carbonacous mudstone		Mc	Swamp
	Coal		Coal	C	C	Marsh/ Swamp

Figure 3.1: Log signatures of lithofacies from core in the Mangahewa Formation identified on the gamma-ray log

units from the shale line in each well. The line is defined here as the clean line, as an aid to characterise log motifs and describe the cleanness of the sandstone lithofacies.

3.2.2 Log Motif Characterisation

Log motifs in core were classified on the gamma-ray on the basis of curve shape and characteristics after the method described by Selley (1978), which recognises three general motifs based on log signatures (Figure 3.2). According to the method prescribed, log signature of the heterogeneous sandstone lithofacies and sand-dominated heterolithic lithofacies groups were classified as cylinder (sharp lower and sharp upper contacts), bell (sharp lower and gradational upper contacts) and funnel (gradational upper and sharp lower contacts) shaped motifs, while curve characteristics were recognised as smooth, serrated or complex in nature. The mudstone-dominated heterolithic lithofacies, mudstone lithofacies and coal lithofacies groups were also characterised on the basis of their log signatures. Figure 3.3 demonstrates the interpretation of log motifs on the gamma-ray from lithofacies identified in core.

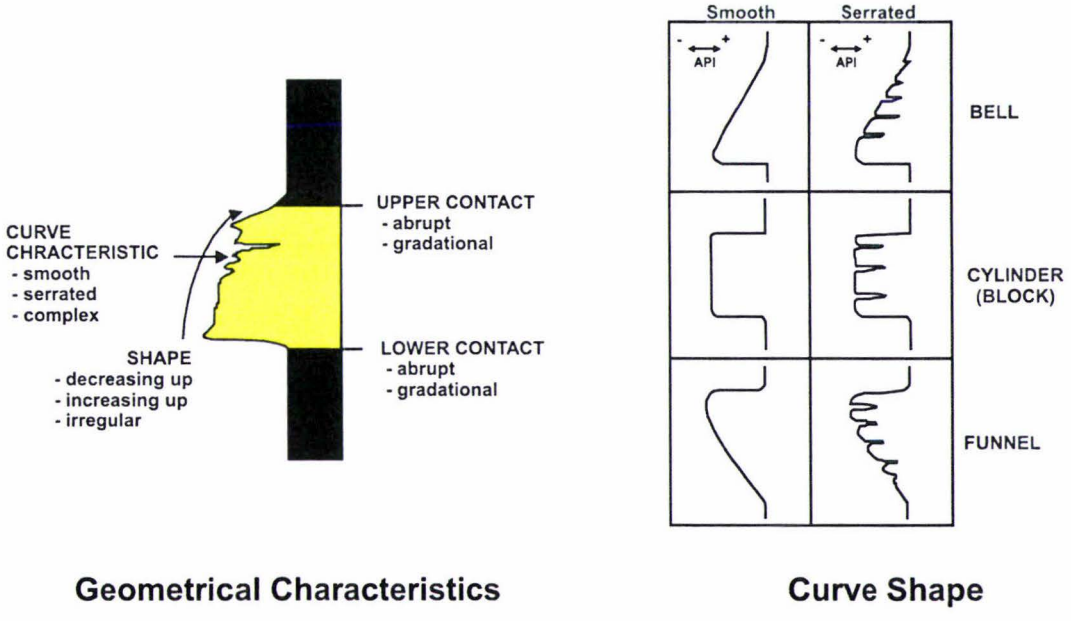

Figure 3.2: Classification of curve shape and characteristics based on the method by Selley (1978)

3.3 HETEROGENEOUS SANDSTONE LOG MOTIFS

3.3.1 Coarse Sandstone Log Motifs (Ss-c)

The coarse sandstone (Ss-c) lithofacies predominantly occur as stacked fining-upward bell motifs which exhibit smooth curve characteristics. Less common are coarsening-upward funnel motifs also with smooth curve characteristics. In the Kapuni-14 well between 4063.10m – 4078.15m funnel and bell shaped motifs have amalgamated to give the appearance of a cylinder motif. The Ss-c lithofacies typically exhibit clean log motifs

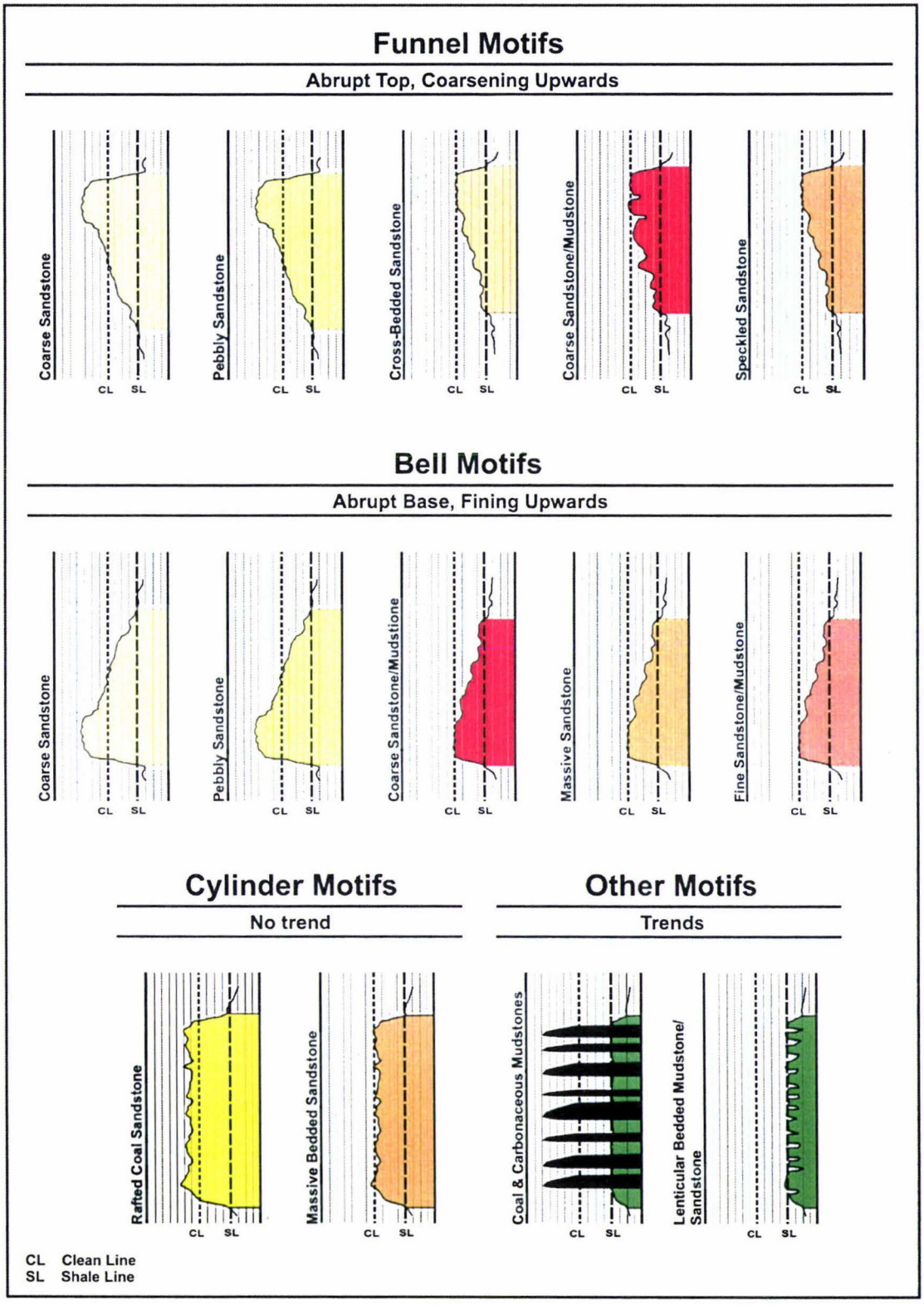

Figure 3.3: Classification of general log motifs on the gamma-ray identified from core in the Mangahewa Formation. The shale line (SL) separates the sandstones from the mudstones and the clean line (CL) distinguishes the cleaner sandstones

with log signatures greater than the clean line at their base (bell motifs) or greater than the clean line at their tops (funnel motifs). They are distinguished from similar log motifs of the pebbly sandstone (Ss-p) lithofacies by their association with coarse sandstone/mudstone (SM-c) log motifs.

3.3.2 Pebbly Sandstone Log Motifs (Ss-p)

The pebbly sandstone (Ss-p) lithofacies exhibit single and stacked bell and funnel shaped motifs. The motifs are generally clean with log signatures greater than the clean line at their base where they fine-upwards (bell motifs) or greater than the clean line at their top where they coarsen-upwards (funnel motifs). The Ss-p lithofacies are distinguished from similar coarse sandstone (Ss-c) log motifs by the presence of underlying planar cross-bedded sandstone (Ss-pc) log motifs.

3.3.3 Rafted Coal Sandstone Log Motifs (Ss-rc)

The rafted coal (Ss-rc) lithofacies exhibit cylinder motifs with smooth curve characteristics. In the Kapuni-3 well between 3706.66m – 3715.22m the Ss-rc log motifs in part fine-upwards due to being interbedded with fine sandstone/mudstone (SM-f) log motifs. The Ss-rc log motifs appear characteristically clean, however, lower gamma-ray API unit values in this lithofacies may be due inpart to the abundance of rafted coal laminae. The Ss-rc log motifs are the only lithofacies in the Mangahewa Formation demonstrating log signatures greater than the clean line for the entire motif. Ss-rc log motifs are most common stratigraphically beneath the fine sandstone/mudstone (SM-f) log motifs, although they also occur immediately above.

3.3.4 Cross-bedded Sandstone Log Motifs (Ss-cb)

The cross-bedded sandstone (Ss-cb) lithofacies display funnel motifs with smooth curve characteristics. Log signatures of the Ss-cb lithofacies occur between the clean line and the shale line. The Ss-cb log motifs are distinguished from the speckled sandstone (Ss-mb) log motifs by their association with the pebbly sandstone (Ss-p), which they overlie or underlie.

3.3.5 Massive Bedded Sandstone Log Motifs (Ss-mb)

The massive bedded sandstone (Ss-mb) lithofacies exhibit both cylinder and bell shaped motifs with smooth curves. The Ss-mb log signatures occur between the clean and shale lines. Log motifs are distinguished by their stratigraphic position underlying or overlying the coarse sandstone (Ss-c) or fine sandstone/mudstone (SM-f) log motifs, and frequent interbedding with lenticular bedded mudstone/sandstone (MS-lb) log motifs.

3.3.6 Speckled Sandstone Log Motifs (Ss-s)

Limited occurrence and thickness of the speckled sandstone lithofacies (Ss-s) limits an accurate log motif description. The Ss-s lithofacies are considered, however, to exhibit a smooth funnel shaped motif. Funnel shaped motifs are typical of shallow marine sandstones (Cant, 1992). Where observed the Ss-g log motif occurs between the clean and shale lines, however, the presence of glauconite in the Ss-s lithofacies may lead to misidentification as a mudstone, lying to the right of the shaleline. Checks on resistivity logs for higher ohmm values and sonic log for lower US/F values help to distinguish the Ss-s log motifs from the lenticular bedded mudstone/sandstone and carbonaceous mudstone log motifs.

3.4 SAND-DOMINATED HETEROLITHIC LOG MOTIFS

3.4.1 Coarse Sandstone/Mudstone Log Motifs (SM-c)

The coarse sandstone/mudstone lithofacies (SM-c) exhibit funnel and bell shaped motifs. The funnel shaped SM-c log motifs have serrated curve characteristics, while bell shaped log motifs exhibit smooth curve characteristics. Serrated curve characteristics are a reflection of greater mudstone bed thickness in the SM-c funnel shaped log motifs. The SM-c log signatures of both funnel and bell shaped log motifs occur between the clean and shale lines. Funnel and bell shaped SM-c log motifs are distinguished from massive bedded sandstone (Ss-mb), fine sandstone/mudstone (SM-f) and speckled sandstone (Ss-s) log motifs by their association with overlying or underlying coarse sandstone (Ss-c) log motifs.

3.4.2 Fine Sandstone/Mudstone Log Motifs (SM-f)

The fine sandstone/mudstone (SM-f) lithofacies demonstrate fining-upward bell shaped motifs with smooth curve characteristics. The SM-f log motifs have log signatures between the clean and the shale lines, although log signature may pass the shale line where interpretation of lithofacies in core indicate channel abandonment. The SM-f log motifs generally overlie the pebbly sandstone (Ss-p), rafted coal sandstone (Ss-rc) and lenticular bedded mudstone/sandstone (MS-lb) log motifs.

3.5 MUD-DOMINATED HETEROLITHIC LOG MOTIFS

3.5.1 Lenticular Bedded Mudstone/Sandstone Log Motifs (MS-lb)

Lenticular bedded mudstone/sandstone lithofacies are characterised by irregular shaped motifs with serrated curve characteristics. Log signatures on the gamma-ray generally do not pass the shale line. Differentiation of the MS-lb log motifs from the carbonaceous mudstone (Mc) log motifs is possible by their serrated curve characteristics and greater

thickness. The MS-lb log motifs occur interbedded with all other log motifs in the Mangahewa Formation.

3.6 MUDSTONE LOG MOTIFS

3.6.1 Carbonaceous Mudstone Log Motifs (Mc)

The carbonaceous mudstone (Mc) lithofacies generally comprise cylinder shaped log motifs with smooth curve characterises that do not pass the shale line. Carbonaceous mudstone (Mc) log motifs generally occur interbedded with coal (C) log motifs.

3.7 COAL LOG MOTIFS

Coals are characterised by low values on the gamma-ray (API) and density (gcm^3) logs and high values on the resistivity (ohmm) and sonic (US/F) logs. Gamma-ray log signatures of coal generally extent beyond the clean line for sandstones, however, if interbedded with carbonaceous mudstones they may only pass the shale line. Moreover, in the Kapuni-15 well a coal interval occurring between 4710.10m – 4710.70m exhibits a high API gamma-ray reading due to its argillaceous composition. Coal log motifs are generally characterised by their association with lenticular bedded mudstone/sandstone (MS-lb) and carbonaceous mudstones (Mc) log motifs, although, thin coals also occur with in some sandstone log motifs.

3.8 LOG MOTIF EXTRAPOLATION

Identification and characterisation of lithofacies on the gamma-ray allowed log motifs in the Mangahewa Formation to be extrapolated to uncored sections in the Kapuni wells (Figures 3.4 – 3.10). In each well comparisons with other available digital geophysical logs including; resistivity, sonic, density spontaneous potential and neutron logs were made to ensure that the practical limitations of the gamma-ray were reduced i.e. anomalies in radioactivity can lead to the misidentification of sandstones that are micaceous, feldspathic, glauconitic or those that contain uranium-rich pore waters. Further, where log signatures did not relate to log motifs identified in core, log curve shapes were related to common environmental interpretations such as those described by Pirson (1970), Serra and Sulpice (1975), Selley (1976) and Cant (1992). In the only occurrence, an unidentified funnel shaped log motif in the Kapuni-15 well at c.4069.50m was interpreted and defined as representing a flood-tidal delta log motif on the basis of stratigraphic position and log signature characteristics.

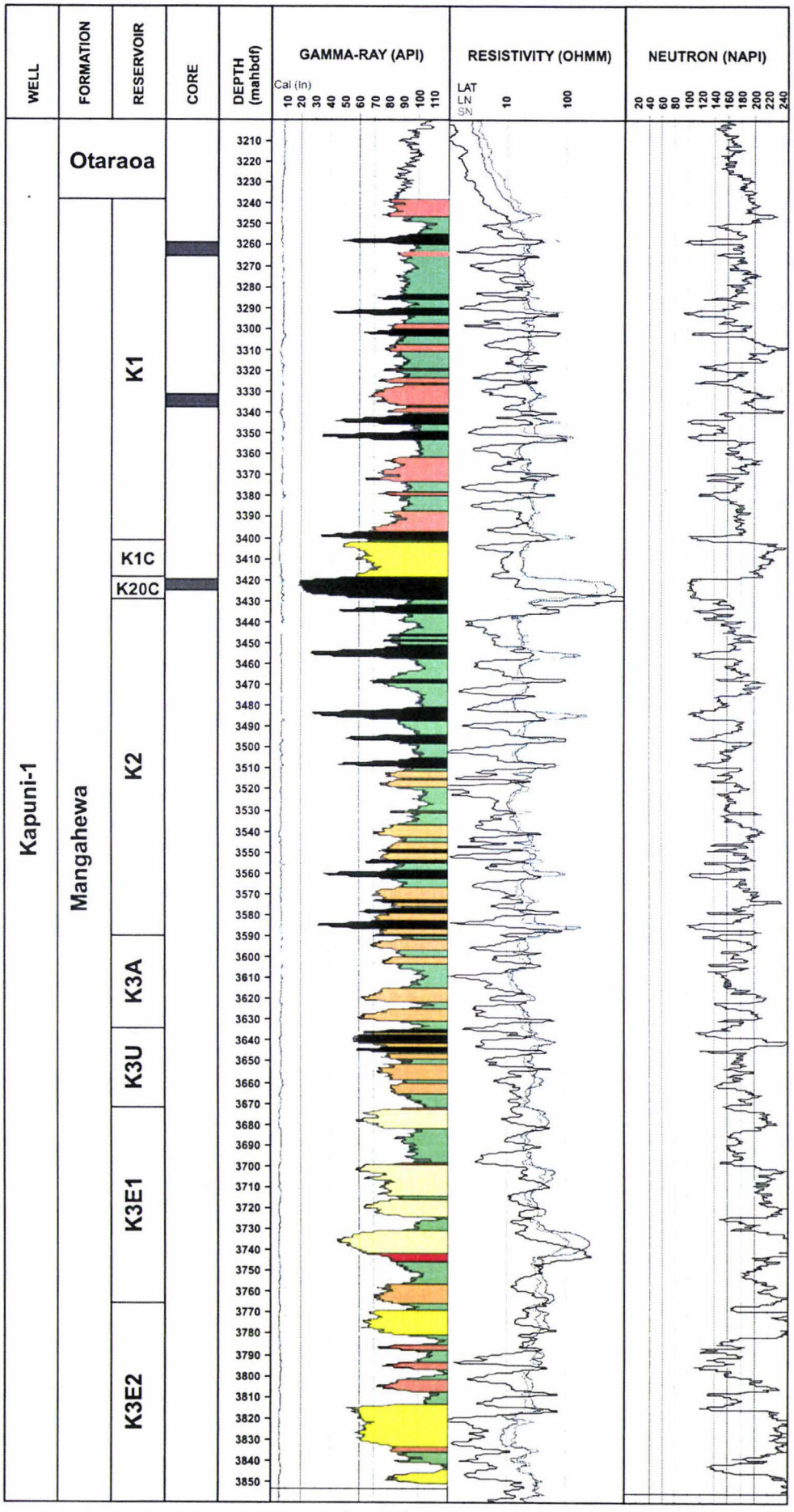

Figure 3.4: Log motifs identified in the Mangahewa Formation in Kapuni-1

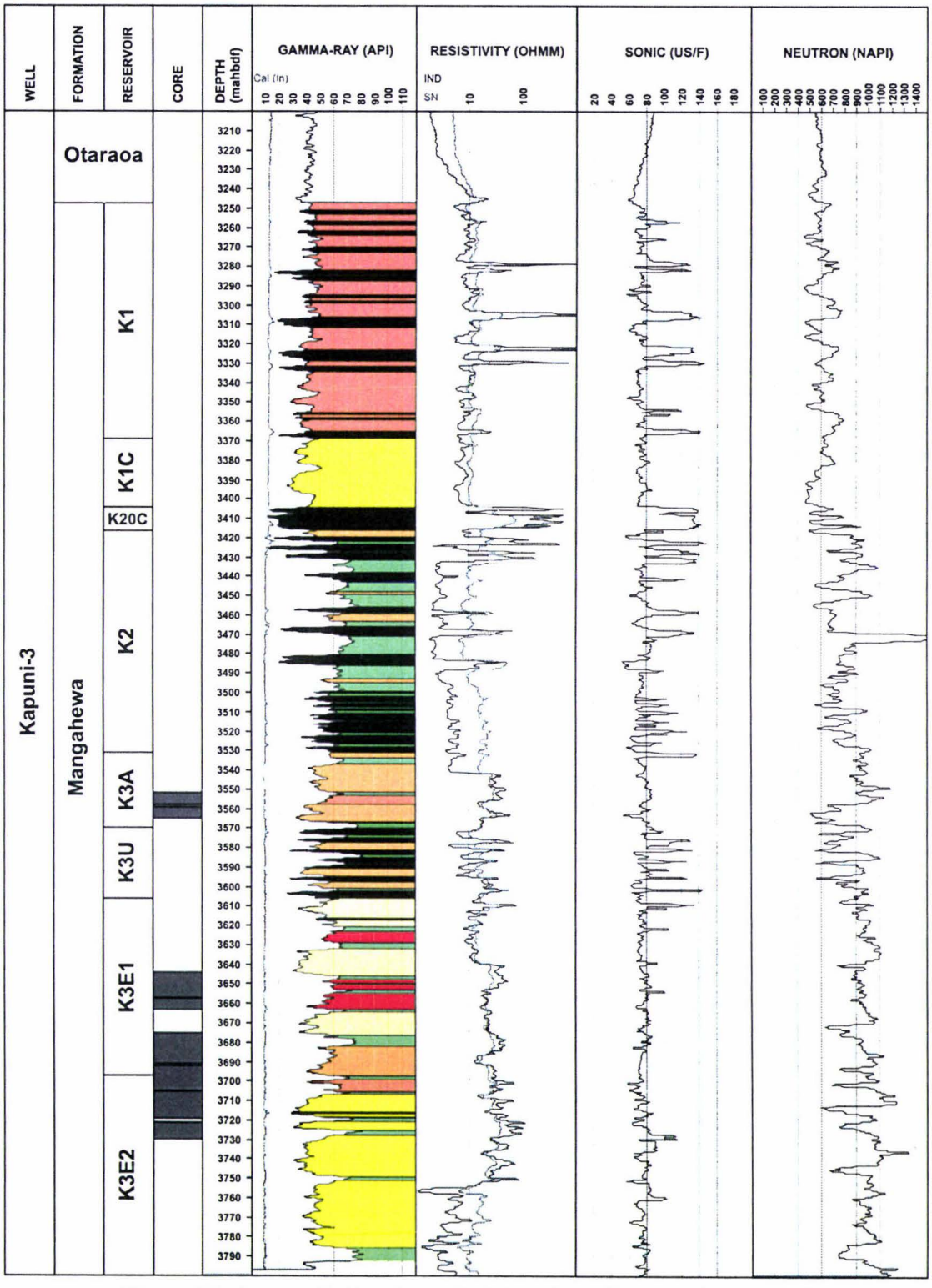

Figure 3.5: Log motifs identified in the Mangahewa Formation in Kapuni-3

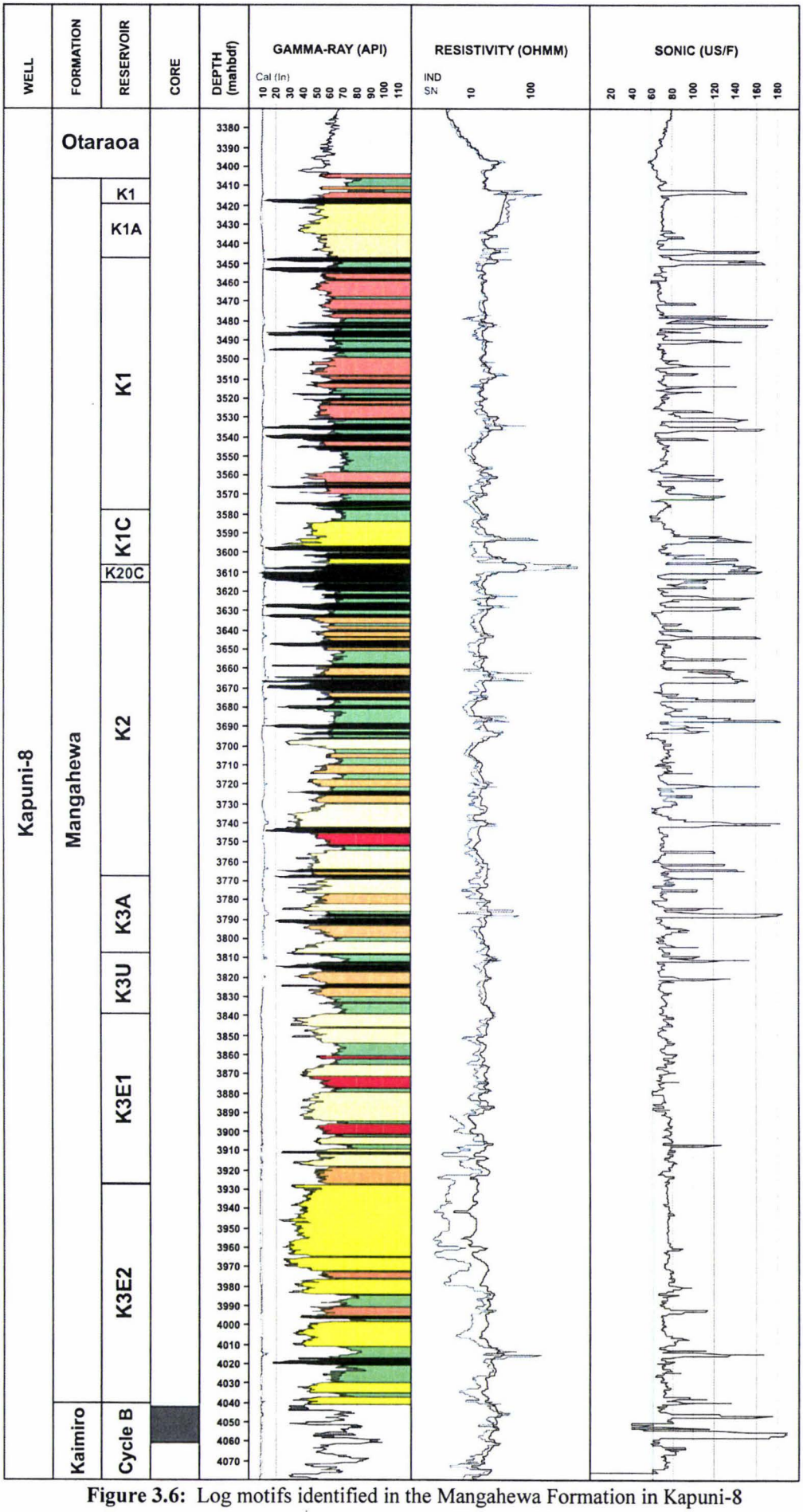

Figure 3.6: Log motifs identified in the Mangahewa Formation in Kapuni-8

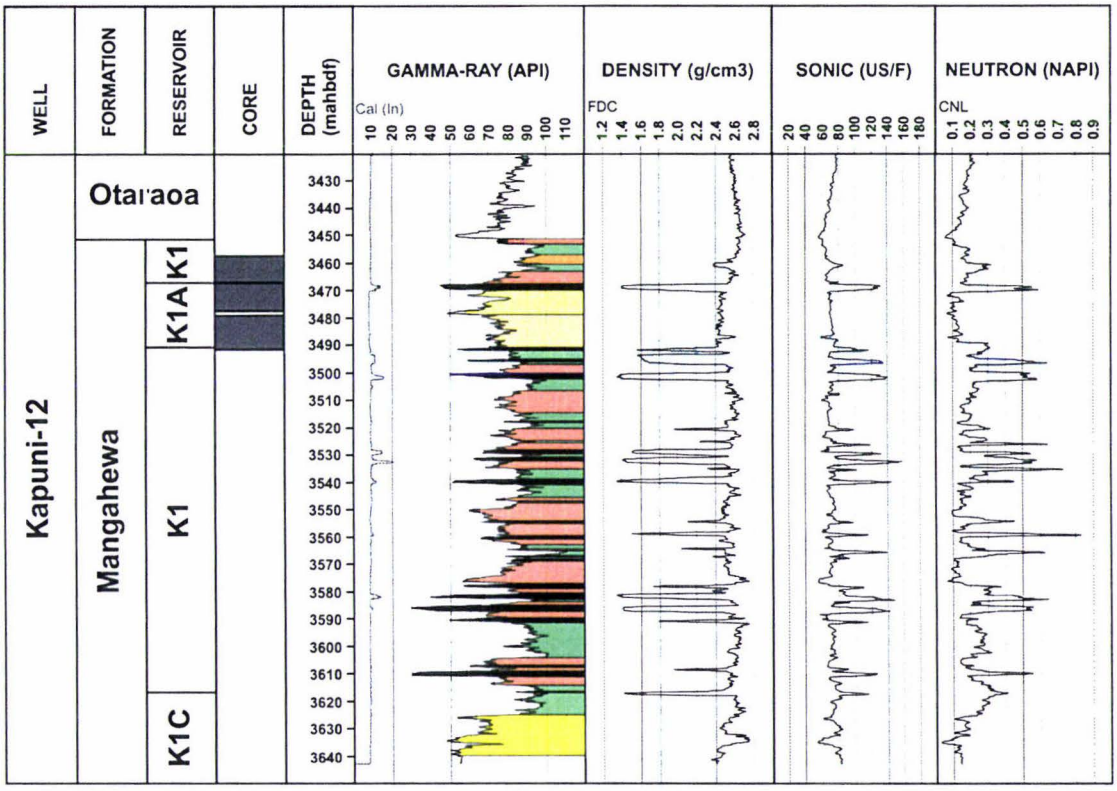

Figure 3.7: Log motifs identified in the Mangahewa Formation in Kapuni-12

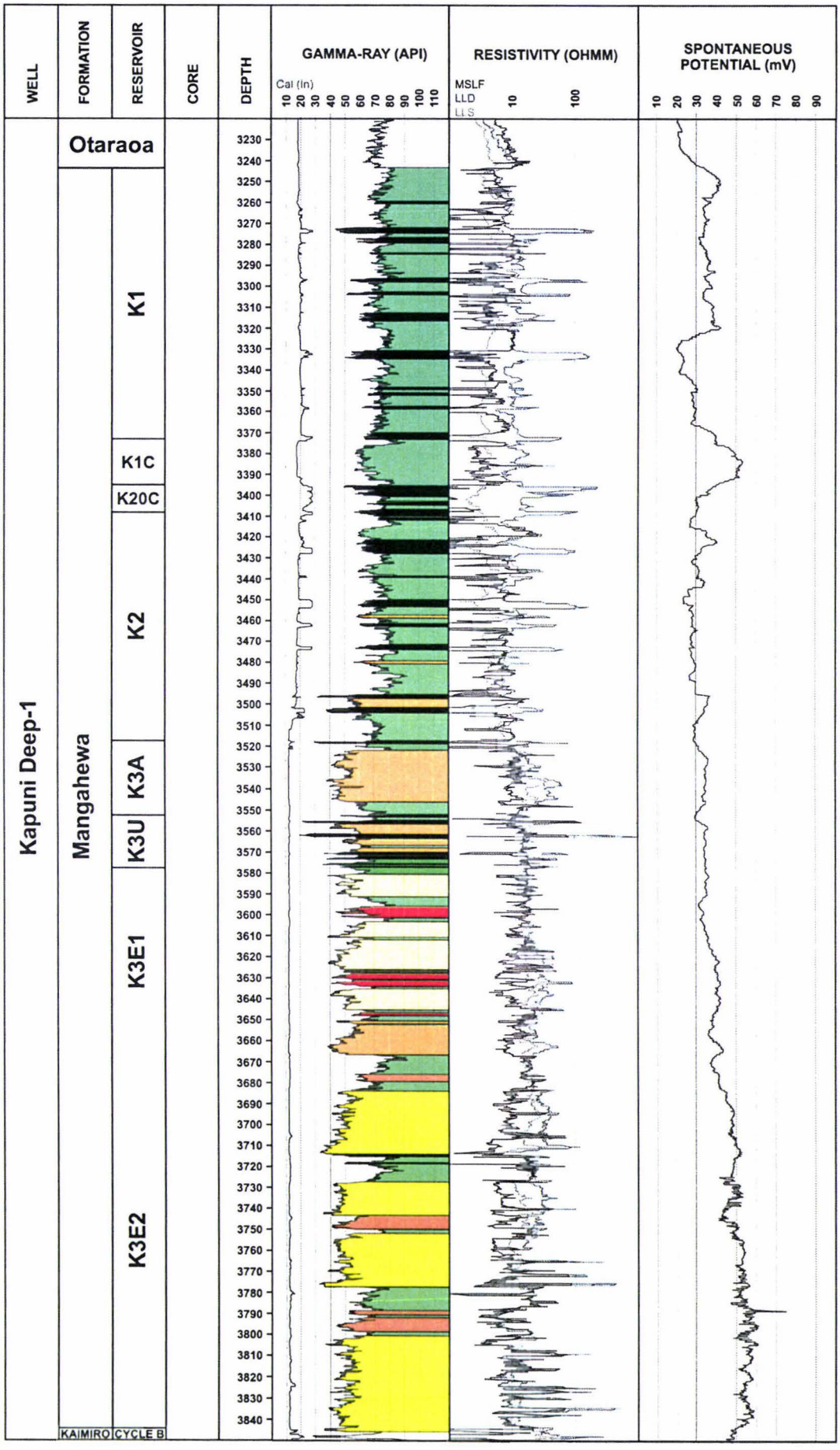

Figure 3.8: Log motifs identified from in the Mangahewa Formation in Kapuni Deep-1

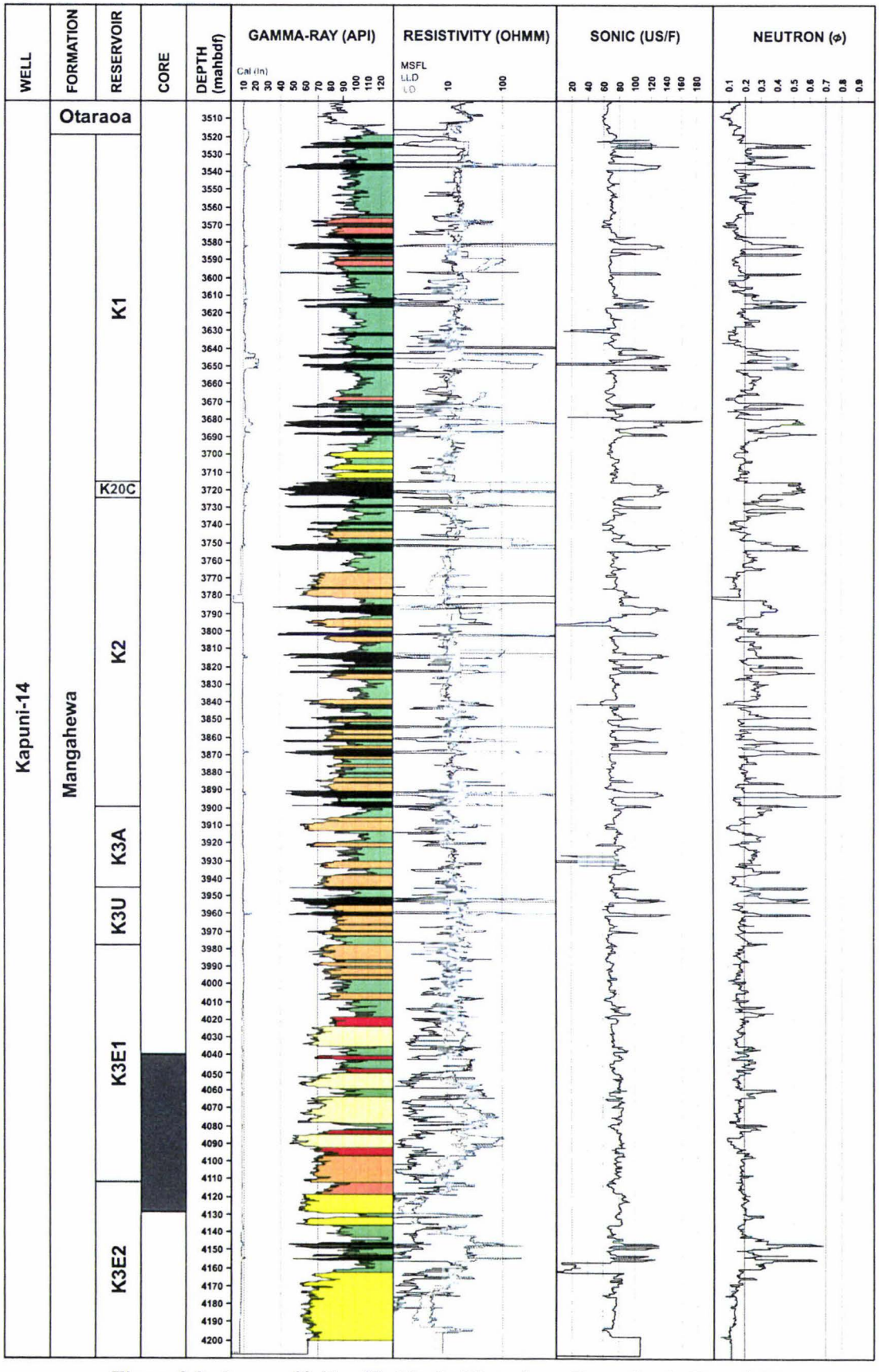

Figure 3.9: Log motifs identified in the Mangahewa Formation in Kapuni-14

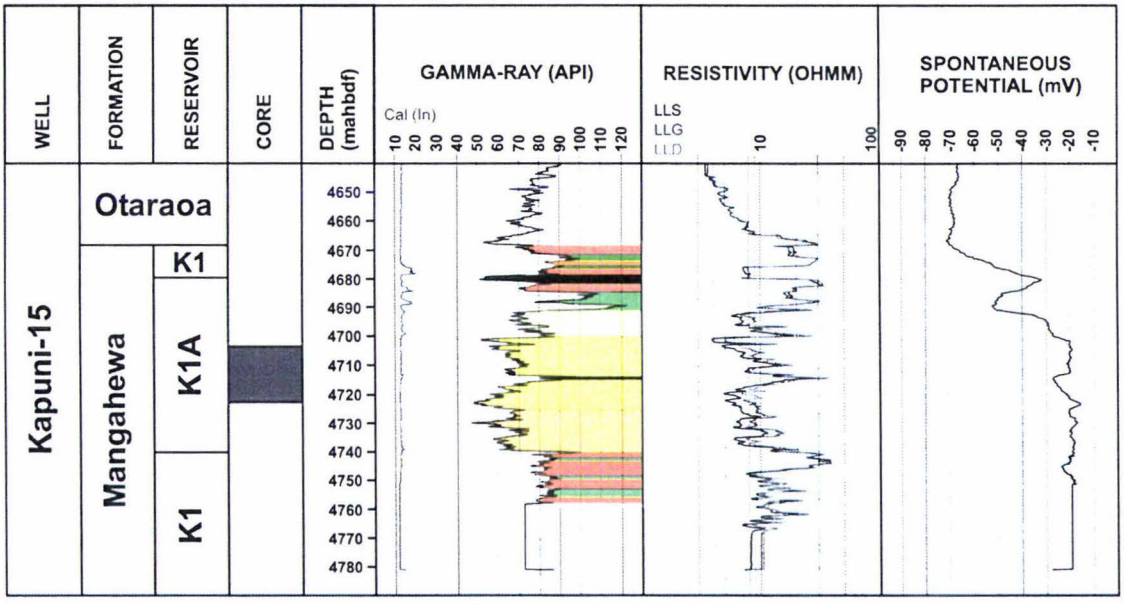

Figure 3.10: Log motifs identified in the Mangahewa Formation in Kapuni-15

3.9 CLASSIFICATION OF RESERVOIR INTERVALS

Reservoir intervals in the Mangahewa Formation in the Kapuni Field wells were originally defined by Hicks (1962), van Wijlen (1963), Haskell (1975) and Bryant and Bartlett (1992). Extrapolation of log motifs in this study has allowed reclassification of these reservoir intervals to incorporate the dominant log motifs identified. The K3 reservoir now comprises the K3E2, K3E1, K3U and K3A units. The K3E2 unit occurs at the base of the Mangahewa Formation and consists of predominantly rafted coal sandstone (Ss-rc), subordinate fine sandstone/mudstone (SM-f) and lenticular bedded mudstone/sandstone (MS-lb) and minor coal (C) log motifs. The K3E1 unit is delineated by a basal massive bedded sandstone (Ss-mb) log motif overlain by alternating coarse sandstone (Ss-c), coarse sandstone/mudstone (SM-c) and lenticular bedded mudstone/sandstone (MS-lb) log motifs. The K3U and K3A units embody predominantly massive bedded sandstone (Ss-mb), lenticular bedded mudstone/sandstone (MS-lb) and coal (C) log motifs with coarse sandstone (Ss-c) and coarse sandstone/mudstone (SM-c) log motifs also present in the Kapuni-8 well.

The K2 reservoir interval incorporates primarily lenticular bedded mudstone/sandstone (MS-lb) and coal (C) log motifs, with subordinate massive bedded sandstone (Ss-mb) and minor coarse sandstone (Ss-c) log motifs. The top of the K2 interval is defined by the K20 coal, which is the thickest coal log motif in the Kapuni Field wells.

The K1 reservoir interval overlies the K20 coal comprising the K1C, K1 and K1A units. The K1C unit incorporates predominantly rafted coal sandstone (Ss-rc) log motifs, with subordinate lenticular bedded mudstone/sandstone (MS-lb) and coal (C) log motifs. The K1 consists of lenticular bedded mudstone/sandstone (MS-lb), fine sandstone/mudstone (SM-f) and coal (C) log motifs. While, the K1A unit only occurs in the Kapuni-8, -12 and -15 wells where it comprises pebbly sandstone (Ss-p), cross-bedded sandstone (Ss-cb), lenticular bedded mudstone/sandstone (MS-lb) and coal (C) log motifs, in addition to the flood-tidal delta log motif not distinguished in core.

SANDSTONE PETROGRAPHY

4.1 METHODOLOGY

Petrographic studies were conducted to identify the composition (framework grains, matrix and cements), porosity and texture of the Kapuni Group sandstones. Fifty-four sandstone core samples were collected from lithofacies in the Kapuni-1, -3, -8, -12, -Deep-1, -14 and -15 wells. The sandstones were studied using a polarising microscope, x-ray diffraction (XRD), differential thermal analysis (DTA), infra-red analysis (IR) and scanning electron microscope (SEM). Core samples were impregnated with epoxy resin containing blue dye before thin-sections were made. Thin-sections were studied using a petrographic microscope to determine sandstone composition (300 point grain count), visible porosity, pore morphology and textural characteristics. Clay minerals were identified and their relative percentages determined by orientated (untreated, heated and glycerated) and non-orientated XRD, DTA and IR analysis (see Appendix 4). SEM was used to investigate intergranular pore spaces and crystallinity of the clay minerals. Total carbonate content was calculated in thin-section and individual carbonate minerals identified and their relative percentages ascertained by non-orientated XRD.

4.2 FRAMEWORK GRAINS

Framework grains, which range in size from coarse silt to sand-sized particles in the Kapuni Group sandstones are composed predominantly of quartz and feldspar with subordinate rock fragments, mica, heavy minerals, glauconite, carbonaceous fragments and bioclasts (Table 4.1). These detrital grains comprise from 49.5% to 85.0% of the rock.

4.2.1 Quartz

Quartz is the dominant framework mineral in the Kapuni Group sandstones, comprising from 26.9% to 65.2% of total rock composition. Quartz occurs as single (monocrystalline) grains and subordinate composite (polycrystalline) grains. Both monocrystalline and polycrystalline quartz grains display undulose extinction patterns (< 5°) when the stage is rotated under the crossed polarisers of the petrographic microscope. The number of monocrystalline quartz grains exhibiting undulose extinction is typically greatest in the Mangahewa Formation (61.0% - 83.7%). Undulose monocrystalline quartz is less common in the Kaimiro Formation (58.7% - 68.6%) and Farewell Formation (57.4% - 59.5%). Blatt and Christie (1963) attribute undulatory extinction in grains to

SAMPLE ID.	WELL NO.	DEPTH (mSSTVD)	FORMATION	RESERVOIR INTERVAL	LITHOLOGICAL FACIES	FRAMEWORK GRAINS																			MATRIX		CEMENT					POROSITY			TOTAL
						Quartz					Feldspar			Rock Fragments				Other Grains																		
						Mono-Crystalline		Poly-Crystalline																													
						Undulose	Non-undulose	2 - 3 crystals	> 3 crystals	Quartz Total	K-Feldspar	Plagioclase	Feldspar Total	Volcanic	Metamorphic	Sedimentary	Rock Fragments Total	Mica	Heavy Minerals	Glauconite	Carbonaceous Fragments	Bioclasts	Other Total	Framework Total	Clay	Matrix Total	Carbonate	Quartz Overgrowths	Feldspar Overgrowths	Pyrite	Cement Total	Primary Porosity	Secondary Porosity	Porosity Total	
1	Kapuni-1	3265.00	Mangahewa	K1	SM-f	16.8	8.1	0.6	2.7	28.2	13.7	5.1	18.8	1.5	8.5	2.5	12.5	1.5	0.8	0.0	2.0	2.0	6.3	65.8	27.5	27.5	4.4	1.2	0.0	1.1	6.7	0.0	0.0	0.0	100
2		3331.50			SM-f	14.8	6.6	0.9	4.6	26.9	16.5	1.7	18.2	0.4	7.2	3.5	11.1	2.1	0.0	0.0	1.9	3.0	7.0	63.2	18.5	18.5	14.3	3.0	0.5	0.5	18.3	0.0	0.0	0.0	100
3		3901.00	Kaimiro	Cycle B	SM-f	20.4	12.4	1.9	5.6	40.3	20.9	1.0	21.9	1.0	4.6	6.9	12.5	0.5	1.0	0.0	1.3	0.9	3.7	78.4	10.1	10.1	6.6	4.0	0.0	0.9	11.5	0.0	0.0	0.0	100
4		3902.00			SM-f	20.8	12.6	1.1	4.8	39.3	14.0	4.5	18.5	0.5	3.1	4.5	8.1	2.0	0.6	0.0	3.2	3.5	9.3	75.2	16.6	16.6	2.0	4.0	0.5	1.7	8.2	0.0	0.0	0.0	100
5		3906.00			Ss-mb	20.5	13.0	3.6	7.2	44.3	17.1	2.0	19.1	0.9	4.3	2.6	7.8	1.0	0.0	0.0	3.0	3.0	7.0	78.2	10.3	10.3	6.0	4.0	0.5	1.0	11.5	0.0	0.0	0.0	100
6		3970.00			Ss-mb	22.9	11.7	6.5	8.5	49.6	18.3	1.5	19.8	0.0	1.9	4.6	6.5	0.0	0.0	0.0	0.8	1.0	1.8	77.7	11.0	11.0	3.0	5.0	1.0	1.1	10.1	0.0	1.2	1.2	100
7	Kapuni-3	3551.00	Mangahewa	K3A	SM-f	18.4	8.8	2.7	3.2	33.1	15.7	0.5	16.2	1.0	4.4	2.0	7.4	2.0	1.2	0.0	7.8	5.6	16.6	73.3	12.3	12.3	5.2	5.6	0.9	1.2	12.9	0.0	1.5	1.5	100
8		3557.50			Ss-mb	19.3	7.7	1.9	4.2	33.1	11.9	1.4	13.3	1.0	1.8	3.4	6.2	0.0	0.5	0.0	2.6	0.0	3.1	55.7	9.5	9.5	26.2	5.0	1.0	1.3	33.5	0.0	1.3	1.3	100
9		3561.50			Ss-mb	29.4	11.4	1.9	3.6	46.3	16.9	1.0	17.9	0.6	1.5	2.0	4.1	0.5	1.5	0.0	1.3	0.0	3.3	71.6	5.0	5.0	13.8	5.3	0.0	0.9	20.0	0.0	3.4	3.4	100
10		3641.50		K3E1	Ss-c	31.4	7.5	5.0	7.0	50.9	16.7	0.6	17.3	0.0	1.6	1.0	2.6	0.0	0.0	0.0	0.2	0.0	0.2	71.0	9.0	9.0	1.0	2.4	0.5	0.0	3.9	0.0	16.1	16.1	100
11		3655.00			Ss-mb	32.9	6.4	2.5	6.4	48.2	16.3	1.3	17.6	0.0	0.6	2.6	3.2	0.0	1.0	0.0	2.5	0.7	4.2	73.2	9.6	9.6	2.5	6.0	1.8	1.1	11.4	0.0	5.8	5.8	100
12		3659.50			Ss-mb	34.1	10.6	3.7	3.2	51.6	15.9	1.5	17.4	0.7	1.0	3.4	5.1	0.0	1.2	0.0	0.5	1.0	2.7	76.8	9.1	9.1	2.0	7.6	1.3	0.0	10.9	0.0	3.2	3.2	100
13		3691.50		K3E2	SM-f	21.3	10.9	1.3	3.3	36.8	10.5	0.6	11.1	0.0	0.9	0.0	0.9	0.0	0.0	0.0	1.0	0.5	1.5	50.3	6.1	6.1	40.0	1.9	0.7	1.0	43.6	0.0	0.0	0.0	100
14		3697.00			SM-f	29.8	9.1	2.3	5.9	47.1	17.0	2.4	19.4	0.0	2.0	1.7	3.7	0.5	1.0	0.0	0.5	2.0	4.0	74.2	14.4	14.4	6.4	3.8	0.7	0.5	11.4	0.0	0.0	0.0	100
15		3701.00			SM-f	28.5	9.7	3.0	3.7	44.9	16.0	2.0	18.0	0.7	1.3	1.7	3.7	0.7	1.2	0.0	1.5	3.5	6.9	73.5	11.4	11.4	6.1	7.5	1.0	0.5	15.1	0.0	0.0	0.0	100
16		3706.50			Ss-rc	28.5	12.3	3.4	3.5	47.7	7.8	1.5	9.3	1.0	2.0	3.0	6.0	0.8	1.0	0.0	6.0	4.0	11.8	74.8	15.7	15.7	3.0	3.0	2.0	1.5	9.5	0.0	0.0	0.0	100
17		3708.50			SM-f	22.8	13.0	0.5	1.8	38.1	7.6	0.5	8.1	0.0	0.0	1.5	1.5	0.0	0.5	0.0	1.3	0.0	1.8	49.5	7.9	7.9	37.9	4.2	0.0	0.5	42.6	0.0	0.0	0.0	100
18		3710.50			Ss-rc	31.0	16.5	4.8	6.9	59.2	7.6	1.0	8.6	0.0	0.9	2.3	3.2	0.0	1.0	0.0	1.0	0.0	2.0	73.0	5.4	5.4	0.9	9.1	0.9	0.0	10.9	3.2	7.5	10.7	100
19		3721.00			Ss-rc	31.7	20.0	4.8	6.9	63.4	6.5	1.2	7.7	0.0	2.5	3.0	5.5	0.0	1.0	0.0	1.5	0.0	2.5	79.1	11.8	11.8	3.0	3.0	0.0	0.0	6.0	0.0	3.1	3.1	100
20		3725.50			SM-f	19.0	15.0	3.4	2.8	40.2	15.7	2.2	17.9	1.1	3.0	1.5	5.6	1.0	0.5	0.0	1.8	4.5	7.8	71.5	20.0	20.0	3.0	4.5	0.5	0.5	8.5	0.0	0.0	0.0	100
21	Kapuni-8	4045.00	Kaimiro	Cycle B	SM-f	20.2	14.2	2.5	1.7	38.6	8.7	2.5	11.2	1.0	6.5	2.0	9.5	3.5	0.0	0.0	7.0	0.0	10.5	69.8	23.5	23.5	1.0	2.0	0.9	0.5	4.4	0.0	2.3	2.3	100
22		4056.00			SM-f	24.8	12.3	1.4	1.8	40.3	8.8	6.1	14.9	0.5	7.6	2.0	10.1	3.2	0.0	0.0	3.0	0.0	6.2	71.5	18.7	18.7	3.3	5.0	1.0	0.5	9.8	0.0	0.0	0.0	100
23		4060.00			SM-f	24.7	11.3	0.7	3.4	40.1	10.9	5.5	16.4	1.0	5.1	1.5	7.6	3.0	0.0	0.0	4.0	0.0	7.0	71.1	19.4	19.4	3.5	4.5	0.5	1.0	9.5	0.0	0.0	0.0	100
24	Kapuni-12	3461.00	Mangahewa	K1	Ss-s	19.7	5.1	3.2	5.6	33.6	7.5	0.9	8.4	0.5	0.0	2.0	2.5	0.0	1.5	21.5	0.0	0.0	23.0	67.5	7.9	7.9	9.0	12.0	0.7	0.9	22.6	0.0	2.0	2.0	100
25		3469.00			SM-f	22.7	6.9	1.2	2.9	33.7	12.0	1.0	13.0	0.9	2.5	3.5	6.9	5.6	1.9	0.0	4.2	0.0	11.7	65.3	25.5	25.5	0.9	3.0	0.5	2.9	7.3	0.0	1.9	1.9	100
26		3471.00		K1A	Ss-p	31.7	13.3	3.0	9.5	57.5	13.1	1.0	14.1	0.7	1.5	1.5	3.7	0.0	1.9	0.0	0.0	0.0	1.9	77.2	5.3	5.3	1.0	8.2	0.7	0.5	10.4	2.0	5.1	7.1	100
27		3473.00			Ss-p	23.3	11.2	2.1	8.4	45.0	15.0	4.6	19.6	1.0	1.0	2.5	4.5	4.0	1.2	0.0	1.2	0.0	6.4	75.5	20.6	20.6	2.2	1.7	0.0	0.0	3.9	0.0	0.0	0.0	100
28		3478.00			Ss-p	42.5	14.3	4.0	4.4	65.2	10.3	1.2	11.5	0.0	0.0	1.6	1.6	0.0	1.4	0.0	0.0	0.0	1.4	79.7	4.5	4.5	1.8	2.3	0.0	0.0	4.1	4.7	7.0	11.7	100
29		3481.00			Ss-cb	23.6	5.8	4.0	3.3	36.7	15.5	1.5	17.0	0.0	0.0	2.6	2.6	1.0	1.8	0.0	3.5	0.0	6.3	62.6	21.0	21.0	2.2	6.6	0.0	0.5	9.3	3.0	4.1	7.1	100
30		3485.00			Ss-cb	24.2	7.8	4.3	4.3	40.6	14.5	2.1	16.6	1.0	0.5	2.5	4.0	1.0	0.0	0.0	3.5	0.0	4.5	65.7	23.0	23.0	2.0	4.6	0.0	0.5	7.1	0.0	4.2	4.2	100
31		3489.00			Ss-cb	37.7	2.6	3.3	3.3	46.9	11.1	1.3	12.4	0.0	1.0	1.0	2.0	0.0	0.0	0.0	1.0	0.0	1.0	62.3	13.1	13.1	2.2	5.0	1.9	0.0	9.1	4.2	11.3	15.5	100

Table 4.1: Summary of thin-section petrographic results

SAMPLE ID.	WELL NO.	DEPTH (mSSbdf)	FORMATION	RESERVOIR INTERVAL	LITHOLOGICAL FACIES	FRAMEWORK GRAINS																				MATRIX		CEMENT					POROSITY			TOTAL
						Quartz					Feldspar			Rock Fragments				Other Grains																			
						Mono-Crystalline		Poly-Crystalline																														
						Undulose	Non-undulose	2 - 3 crystals	> 3 crystals	Quartz Total	K-Feldspar	Plagioclase	Feldspar Total	Volcanic	Metamorphic	Sedimentary	Rock Fragments Total	Mica	Heavy Minerals	Glauconite	Carbonaceous Fragments	Bioclasts	Other Total	Framework Total	Clay	Matrix Total	Carbonate	Quartz Overgrowths	Feldspar Overgrowths	Pyrite	Cement Total	Primary Porosity	Secondary Porosity	Porosity Total	
32	Kapuni Deep-1	5183.00	Farewell	Cycle A	SM-c	15.9	11.8	3.1	3.1	33.9	13.5	15.0	28.5	1.5	5.0	0.0	6.5	1.5	0.0	0.0	0.9	0.0	2.4	71.3	18.7	18.7	3.1	4.5	0.9	0.0	8.5	0.0	0.5	1.5	100
33		5189.00			SM-c	13.8	9.5	2.7	2.7	28.7	19.6	13.9	33.5	1.5	7.2	0.0	8.7	2.2	0.3	0.0	1.7	0.0	4.2	75.1	16.8	16.8	2.5	3.5	0.6	1.0	7.6	0.0	0.5	0.5	100
34		5517.00			SM-c	14.1	10.0	2.0	1.5	27.6	14.6	10.6	25.2	2.0	3.5	0.0	5.5	3.0	0.5	0.0	0.7	0.0	4.2	62.5	10.6	10.6	22.9	3.0	0.5	0.5	26.9	0.0	0.0	0.0	100
35	Kapuni-14	4041.50	Mangahewa	K3E1	SM-c	30.6	19.1	2.3	3.6	55.6	6.2	1.6	7.8	0.0	0.6	1.9	2.5	0.0	0.8	0.0	2.5	0.0	3.3	69.2	4.3	4.3	0.7	3.2	0.0	1.3	5.2	3.3	18.0	21.3	100
36		4050.50			Ss-c	34.6	13.3	2.6	4.2	54.7	3.0	1.8	4.8	0.5	1.0	1.5	3.0	0.7	0.5	0.0	1.5	0.0	2.7	65.2	3.2	3.2	7.6	2.0	0.0	1.0	10.6	3.3	17.7	21.0	100
37		4052.50			Ss-c	35.0	14.5	3.0	7.5	60.0	7.7	1.4	9.1	0.0	0.0	2.3	2.3	0.0	0.5	0.0	0.0	0.0	0.5	71.9	9.8	9.8	1.0	5.0	1.0	0.9	7.9	3.8	6.6	10.4	100
38		4058.50			Ss-c	34.2	14.8	1.3	6.9	57.2	6.0	0.7	6.7	0.0	0.3	1.7	2.0	0.0	1.0	0.0	2.1	0.0	3.1	69.0	2.7	2.7	0.5	10.1	0.5	0.0	11.1	3.5	13.7	17.2	100
39		4069.50			Ss-c	35.3	16.8	1.2	4.9	58.2	7.0	1.0	8.0	0.0	1.3	0.7	2.0	0.0	0.5	0.0	2.0	0.0	2.5	70.7	8.0	8.0	2.4	4.5	0.2	0.7	7.8	3.8	9.7	13.5	100
40		4077.50			Ss-c	35.2	17.8	1.3	6.9	61.2	5.0	0.7	4.4	0.7	0.7	0.0	1.4	0.0	0.5	0.0	0.0	0.0	0.5	67.5	3.7	3.7	1.5	3.4	0.5	0.0	5.4	2.6	20.8	23.4	100
41		4088.50			Ss-c	36.1	19.5	1.8	4.8	62.2	3.2	0.6	3.8	0.0	1.0	2.0	3.0	0.0	0.5	0.0	0.0	0.0	0.5	69.5	2.0	2.0	1.2	3.0	0.0	0.0	4.2	2.2	22.1	24.3	100
42		4094.50			SM-c	34.1	16.3	2.6	3.9	56.9	8.9	1.6	10.5	0.0	1.0	1.6	2.6	0.5	0.0	0.0	0.5	0.0	1.0	71.0	4.5	4.5	3.4	12.0	0.6	0.5	16.5	3.0	5.0	8.0	100
43		4105.50			Ss-mb	27.6	14.0	0.6	8.9	51.1	8.6	0.6	9.2	0.0	1.0	1.6	2.6	1.0	1.0	0.0	1.1	0.0	3.1	66.0	5.0	5.0	2.0	8.6	0.9	0.0	11.5	4.5	13.0	17.5	100
44		4114.50		K3E2	SM-f	26.0	13.1	2.7	3.9	45.7	10.5	1.3	11.8	0.7	1.0	1.8	3.5	0.7	0.7	0.0	2.0	0.0	3.4	64.4	22.5	22.5	3.8	7.3	0.0	0.5	11.6	0.0	1.5	1.5	100
45		4122.00			Ss-rc	36.0	10.6	4.5	6.3	57.4	4.7	0.8	5.5	0.9	1.2	1.2	3.3	0.0	0.0	0.0	1.0	0.0	1.0	67.2	8.1	8.1	0.9	3.0	0.0	0.2	4.1	4.5	16.1	20.6	100
46	Kapuni-15	4701.00	Mangahewa	K1A	Ss-p	33.0	15.0	3.0	3.2	54.2	11.8	4.8	16.6	1.5	0.0	2.0	3.5	0.7	1.0	0.0	0.0	0.0	1.7	76.0	9.7	9.7	1.5	8.5	2.3	0.0	12.3	0.0	2.0	2.0	100
47		4703.00			Ss-p	31.0	17.1	2.8	4.1	55.0	13.6	4.9	18.5	1.0	1.5	2.6	5.1	0.5	0.9	0.0	0.0	0.0	1.4	80.0	7.7	7.7	2.2	5.5	1.9	0.0	9.6	0.0	2.7	2.7	100
48		4704.00			Ss-p	28.5	18.0	1.7	3.8	52.0	14.4	2.1	16.5	0.9	0.0	1.9	2.8	0.0	0.9	0.0	0.9	0.0	1.8	73.1	4.5	4.5	1.0	14.4	3.7	0.0	19.1	0.0	3.3	3.3	100
49		4705.50			Ss-p	25.4	14.7	2.9	3.6	46.6	14.9	6.5	21.4	0.5	2.0	5.5	8.0	0.7	1.0	0.0	0.7	0.0	2.4	78.4	7.0	7.0	1.8	8.9	2.7	0.0	13.4	0.0	1.2	1.2	100
50		4707.50			Ss-p	29.6	18.9	2.2	3.7	54.4	13.7	5.0	18.7	0.0	1.7	2.5	4.2	0.8	0.8	0.0	1.2	0.0	2.8	80.1	5.4	5.4	2.0	6.1	0.7	0.0	8.8	0.0	5.7	5.7	100
51		4711.00			Ss-p	26.6	16.1	2.3	2.1	47.1	17.5	4.6	22.1	0.0	1.4	2.2	3.6	0.5	0.8	0.0	3.5	2.0	6.8	79.6	10.9	10.9	2.0	6.5	0.0	1.0	9.5	0.0	0.0	0.0	100
52		4712.50			Ss-p	21.2	14.2	5.7	6.5	47.6	19.9	4.0	23.9	1.2	2.5	5.9	9.6	0.9	1.0	0.0	2.0	0.0	3.9	85.0	8.5	8.5	2.5	1.5	0.5	0.0	4.5	0.0	2.0	2.0	100
53		4714.50			Ss-p	33.0	18.7	2.9	3.9	58.5	17.6	3.0	20.6	0.0	1.9	2.5	4.4	0.0	0.8	0.0	0.0	0.0	0.8	84.3	5.0	5.0	2.2	4.8	1.3	0.0	8.3	0.0	2.4	2.4	100
54		4717.00			Ss-p	34.0	19.7	2.2	3.1	59.0	16.0	2.0	18.0	1.0	0.0	2.8	3.8	0.0	0.5	0.0	0.0	0.0	0.5	81.3	4.0	4.0	2.0	8.0	0.5	0.0	10.5	0.0	4.2	4.2	100

Table 4.1 continued: Summary of thin-section petrographic results

deformation and strain of the crystal lattice that occurred either in the source rock or from deformation of the sandstone itself. In some samples minor fracturing of quartz has occurred, with the deposition of clay minerals (kaolinite), carbonate (siderite and calcite) or secondary quartz cement in the fracture zones.

4.2.2 Feldspar

Feldspar species and abundance vary between formations in the Kapuni Group. In the Mangahewa and Kaimiro formations feldspars constitute from 3.8% to 23.9% and 11.2% to 21.9% respectively. Alkali feldspars (K-feldspars) comprising orthoclase, with subordinate microcline and rare perthite encompass most of the feldspar content. While plagioclase feldspars (albite) are less common. Feldspar content is significantly higher in sandstones of the deeper Farewell Formation ranging from 25.2% to 33.5%. Plagioclase (albite) is also more abundant in the Farewell Formation, occurring in similar quantities to K-feldspars. K-feldspars are predominantly sanidine with orthoclase, microcline and rare perthite also present. In the Kapuni Group sandstones feldspars range from fresh to extensively leached. Plagioclase grains exhibit the greatest degrees of alteration in the Mangahewa and Kaimiro formations, while sanidine feldspars are the most altered in the Farewell Formation. Both clay (kaolinite and illite) and carbonate minerals (siderite, calcite and dawsonite) are observed replacing altered feldspar grains. In some sandstones feldspars are fractured, with the deposition of kaolinite, siderite and calcite minerals filling the open voids.

4.2.3 Rock Fragments

Rock fragments comprise between 0.9% and 12.5% of the sandstones. Rock fragments are dominantly low-grade metamorphics, exhibiting foliate fabrics and abundant phyllosilicates. Quartzite, gneiss, phyllite, argillite and schist occur in abundance in that order in the sandstones. Sedimentary lithics comprise predominantly cryptocrystalline chert, siltstone and rare shale. Acid volcanic rock fragments are also present, exhibiting porphyritic textures in sandstones of the Mangahewa and Kaimiro formations and trachytic textures in the Farewell Formation. Plutonic rock fragments were not identified in this study, but have been reported in previous studies of the Kapuni Group in the Kapuni Field by Yunalis and Izhan (1995) and Smale *et al.* (1999). Very coarse-grained rocks such as granites typically yield clasts greater than coarse-sand size (Boggs, 2001). Their coarse grain-size, therefore, explains why plutonic rock fragment may be absent in thin-section studies.

4.2.4 Other Grains

Other framework grains comprise from 0.2% to 23.0% of the sandstones. These minerals include mica, heavy minerals, glauconite, carbonaceous fragments and bioclasts. Mica occurs in most sandstones in percentages <3.5%. Muscovite is the most abundant mica mineral, with rare biotite also present. Where biotite occurs it is occasionally partially altered to chlorite along grain margins. The micas generally occur as rounded thin basal flakes aligned along bedding planes or as disseminated grains, and are commonly bent around and between other grains within the sandstones. In hand-specimen mica is often concentrated where mudstone laminae occur in the sandstones. Heavy minerals including zircon, rutile and garnets were identified in amounts <1.9%. Zircon and rutile were the most common heavy minerals, with rare garnets belonging to the spessartite species also present. Glauconite minerals were only identified in the Mangahewa Formation speckled sandstone (Ss-s) lithofacies where they comprise a significant percentage (21.5%) of the sandstone composition. Glauconite occurs as pellets with irregular lobate forms (Plate 4.1). The glauconite also exhibits a cauliflower texture and conforms to type 2a as described by McConchie and Lewis (1980). Carbonaceous fragments occur in most sandstones in varying amounts up to 7.8%, although they are most abundant in the Mangahewa and Kaimiro formation fine sandstone/mudstone (SM-f) lithofacies. Carbonaceous fragments identified in hand-specimen include reworked coal and pieces of woody material ranging in size up to 3cm. In thin-section carbonaceous material occurs as irregular discontinuous laminae often associated with clay laminae or as sub-angular to sub-rounded fragments (Plate 4.2). Bioclasts consist of fecal pellets ranging up to 300μm in size. In thin-section these pellets typically were identified along the surface of bedding planes. Fecal pellets were only identified in the Mangahewa and Kaimiro formations fine sandstone/mudstone (SM-f) and massive bedded sandstone (Ss-mb) lithofacies where they comprise <5.6% of the rock.

4.3 MATRIX

The matrix of sandstones is comprised of minerals <30μm in size which fill interstitial spaces between framework grains (Miall, 1990). Matrix includes quartz, feldspars and micas; however, clay minerals form the bulk of matrix minerals in the sandstones. Clay minerals are defined to include sheet silicate minerals which consist of oxygen, silicon, aluminium, magnesium, iron and water (H_2O, OH^-) in the <2μm fraction (Heinrich, 1965). According to this classification quartz and feldspar clay-sized minerals were excluded from the analysis. To identify clay minerals and determine their relative abundance, thin-section studies were supplemented with x-ray diffraction (XRD), differential thermal analysis (DTA) and infrared analysis (IR) studies.

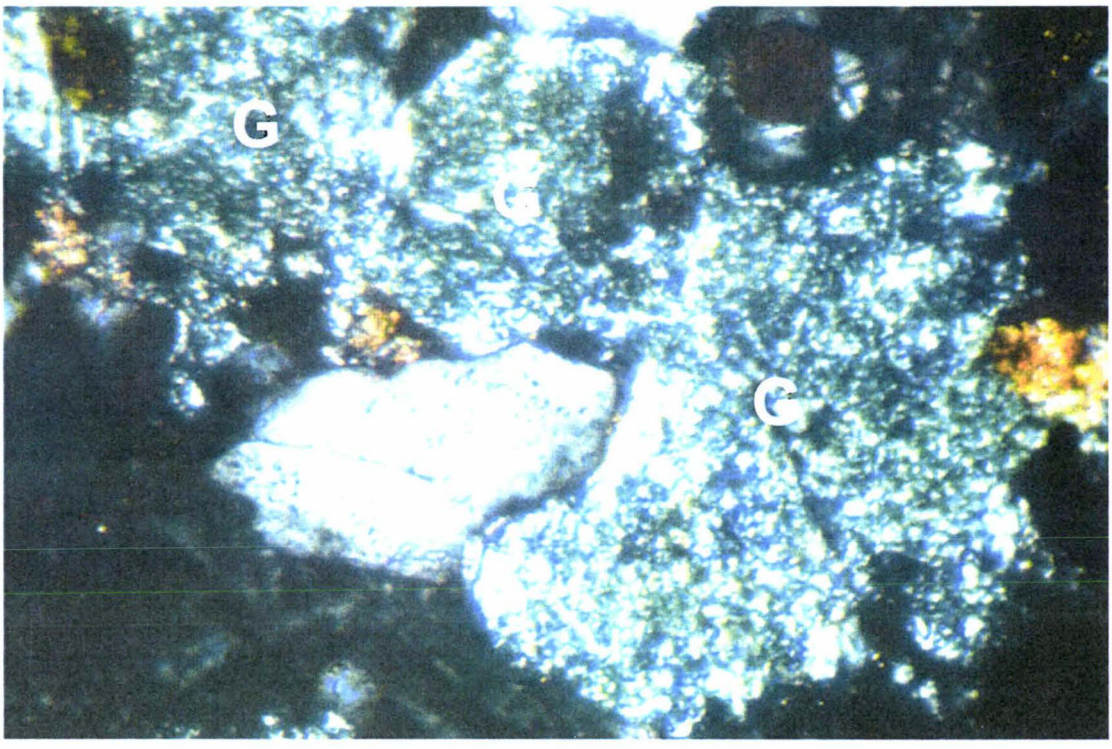

Plate 4.1: Cross-polarised photomicrograph of glauconite pellets (G) in the Mangahewa Formation speckled sandstone (Ss-s) lithofacies (Q = Quartz), photomicrograph x10 (Sample 24, Kaapuni-12)

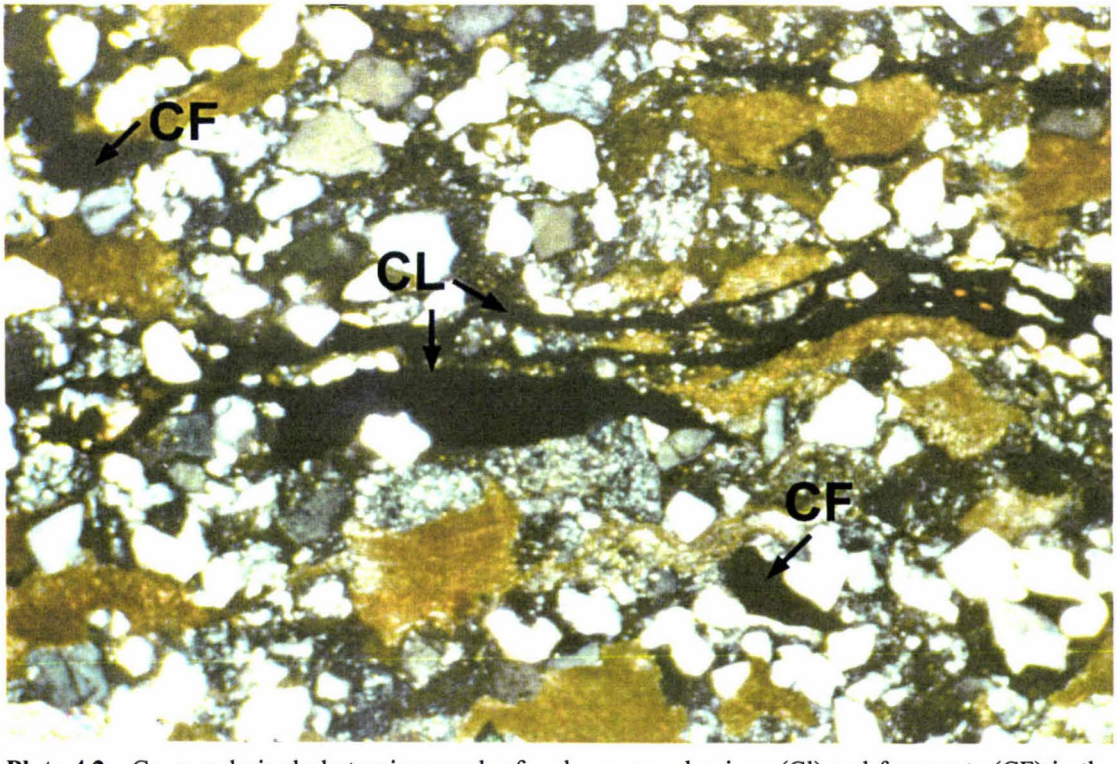

Plate 4.2: Cross-polarised photomicrograph of carbonaceous laminae (Cl) and fragments (CF) in the Kaimiro Formation fine sandstone/mudstone (SM-f) lithofacies, photomicrograph x2.0 (Sample 23, Kpuni-8)

Clay minerals identified in this study include kaolinite, illite, vermiculite, chlorite, smectite and a number of mixed-layer clays (Table 4.2). Mixed-layer clay minerals are those that comprise composite physical layers of phyllosilicates in which two or more clay types are intermixed in a vertical stacking sequence (Eslinger and Pevear, 1988). Total clay percentages in the Kapuni Group sandstones range from 2.0% to 27.5%. The fine sandstone/mudstone (SM-f) lithofacies generally comprise the highest clay totals of all Kapuni Group lithofacies.

4.3.1 Kaolinite

Kaolinite, one of the main clay minerals identified in the Kapuni Group sandstones ranges in abundance from 0.7% to 16.5% of the sandstone and 14% to 66% of the total clay content. Kaolinite percentages are typically higher in the Mangahewa and Kaimiro formations, than in underlying Farewell Formation. Furthermore, in this study recorded kaolinite percentages are generally much lower than those previously reported for the Kapuni Group sandstones in the Kapuni Field by Hogan (1979), Challis and Mildenhall (1986) and Yunalis and Izhan (1995). X-ray diffraction peaks and SEM studies demonstrate that kaolinite is well-crystallised. The well-crystallised nature of kaolinite, however, appears to exaggerate the intensity of the XRD peaks making it easy to overestimate the amount of kaolinite present relative to other clay minerals (Personal Communication J. Whitton, 2002). To obtain accurate kaolinite percentages DTA and IR analysis studies were conducted to verify XRD results and eliminate the possibility of amorphous material.

4.3.2 Illite

Illite is another common clay mineral. Illite comprises from 0.9% to 16.5% of the rock and from 16% to 85% of the total clay content. Illite occurs in greater abundance in sandstones of the Mangahewa and Kaimiro formations than in the Farewell Formation. X-ray diffraction peaks are generally not as well-defined as those for kaolinite. Interpretation of broad XRD peaks indicate that illite is often partially or completely transformed to mixed-layer clay types, namely; illite/vermiculite illite/smectite and illite/chlorite. Illite/ vermiculite is a common mixed-layer clay in the Mangahewa and Kaimiro formations, while illite/smectite occurs in the Mangahewa and Farewell formations. Rare illite/chlorite is present only in the Mangahewa Formation.

4.3.3 Other Clays

A number of other clay minerals occur in the Kapuni Group sandstones, including vermiculite, chlorite and smectite. Vermiculite occurs as a minor clay in the Mangahewa Formation where it accounts for <1.9% of the rock and <22% of total clay. Mixed-layer

SAMPLE ID.	WELL NO.	DEPTH (mbbdf)	FORMATION	RESERVOIR INTERVAL	LITHOLOGICAL FACIES	CLAY MINERAL TOTALS AND NORMALISED VALUES										TOTAL CLAY %/ NORMALISED CLAY TOTAL
											MIXED-LAYER CLAYS					
						Kaolinite	Illite	Vermiculite	Smectite	Chlorite	Illite/ Vermiculite	Illite/ Smectite	Illite/ Chlorite	Chlorite/ Vermiculite	Chlorite/ Smectite	
1	Kapuni-1	3265.00	Mangahewa	K1	SM-f	16.5/ 60	9.6/ 35	1.4/ 5	-	-	-	-	-	-	-	27.5/ 100
2		3331.50	Mangahewa	K1	SM-f	8.1/ 44	10.4/ 56	-	-	-	-	-	-	-	-	18.5/ 100
3		3901.00	Kaimiro	Cycle B	SM-f	4.1/ 41	4.1/ 40	-	-	-	1.9/ 19	-	-	-	-	10.1/ 100
4		3902.00	Kaimiro	Cycle B	SM-f	5.3/ 32	8.5/ 51	-	-	-	2.8/ 17	-	-	-	-	16.6/ 100
5		3906.00	Kaimiro	Cycle B	Ss-mb	4.1/ 40	5.2/ 50	-	-	-	1.0/ 10	-	-	-	-	10.3/ 100
6		3970.00	Kaimiro	Cycle B	Ss-mb	4.4/ 40	4.0/ 36	-	-	2.6/ 24	-	-	-	-	-	11.0/ 100
7	Kapuni-3	3551.00	Mangahewa	K3A	SM-f	5.9/ 48	4.1/ 33	-	-	-	0.9/ 8	1.4/ 11	-	-	-	12.3/ 100
8		3557.50	Mangahewa	K3A	Ss-mb	5.3/ 56	3.4/ 36	-	-	-	-	-	0.8/ 8	-	-	9.5/ 100
9		3561.50	Mangahewa	K3A	Ss-mb	3.2/ 63	1.5/ 30	-	-	-	0.3/ 7	-	-	-	-	5.0/ 100
10		3641.50	Mangahewa	K3E1	Ss-c	3.7/ 41	4.5/ 50	-	-	-	-	0.8/ 8	-	-	-	9.0/ 100
11		3655.00	Mangahewa	K3E1	Ss-mb	6.0/ 63	3.6/ 37	-	-	-	-	-	-	-	-	9.6/ 100
12		3659.50	Mangahewa	K3E1	Ss-mb	4.9/ 53	2.8/ 31	-	-	-	-	0.9/ 10	-	-	0.5/ 6	9.1/ 100
13		3691.50	Mangahewa	K3E2	SM-f	2.8/ 46	2.4/ 39	-	-	-	-	-	0.9/ 15	-	-	6.1/ 100
14		3697.00	Mangahewa	K3E2	SM-f	5.6/ 39	8.8/ 61	-	-	-	-	-	-	-	-	14.4/ 100
15		3701.00	Mangahewa	K3E2	SM-f	7.2/ 63	4.2/ 37	-	-	-	-	-	-	-	-	11.4/ 100
16		3706.50	Mangahewa	K3E2	Ss-rc	7.7/ 49	6.1/ 39	-	-	-	-	1.9/ 12	-	-	-	15.7/ 100
17		3708.50	Mangahewa	K3E2	SM-f	3.3/ 42	2.7/ 34	-	-	1.9/ 24	-	-	-	-	-	7.9/ 100
18		3710.50	Mangahewa	K3E2	Ss-rc	2.1/ 39	3.3/ 61	-	-	-	-	-	-	-	-	5.4/ 100
19		3721.00	Mangahewa	K3E2	Ss-rc	4.7/ 40	7.1/ 60	-	-	-	-	-	-	-	-	11.8/ 100
20		3725.50	Mangahewa	K3E2	SM-f	8.8/ 44	8.6/ 43	2.6/ 13	-	-	-	-	-	-	-	20.0/ 100
21	Kapuni-8	4045.00	Kaimiro	Cycle B	SM-f	9.4/ 40	10.3/ 44	-	-	1.4/ 6	2.4/ 10	-	-	-	-	23.5/ 100
22		4056.00	Kaimiro	Cycle B	SM-f	12.3/ 66	6.4/ 34	-	-	-	-	-	-	-	-	18.7/ 100
23		4060.00	Kaimiro	Cycle B	SM-f	8.0/ 41	11.4/ 59	-	-	-	-	-	-	-	-	19.4/ 100
24	Kapuni-12	3461.00	Mangahewa	K1	Ss-s	1.2/ 15	6.7/ 85	-	-	-	-	-	-	-	-	7.9/ 100
25		3469.00	Mangahewa	K1	SM-f	11.7/ 46	13.8/ 54	-	-	-	-	-	-	-	-	25.5/ 100
26		3471.00	Mangahewa	K1A	Ss-p	2.1/ 39	2.3/ 44	-	-	0.9/ 17	-	-	-	-	-	5.3/ 100
27		3473.00	Mangahewa	K1A	Ss-p	9.3/ 45	11.3/ 55	-	-	-	-	-	-	-	-	20.6/ 100
28		3478.00	Mangahewa	K1A	Ss-p	1.3/ 29	3.2/ 71	-	-	-	-	-	-	-	-	4.5/ 100
29		3481.00	Mangahewa	K1A	Ss-cb	8.4/ 40	12.6/ 60	-	-	-	-	-	-	-	-	21.0/ 100
30		3485.00	Mangahewa	K1A	Ss-cb	9.2/ 40	6.7/ 29	-	-	-	-	7.1/ 31	-	-	-	23.0/ 100
31		3489.00	Mangahewa	K1A	Ss-cb	3.9/ 30	5.0/ 38	-	1.4/ 11	-	-	2.8/ 21	-	-	-	13.1/ 100
32	Kapuni Deep-1	5183.00	Farewell	Cycle A	SM-c	2.6/ 14	3.0/ 15	-	9.5/ 51	-	-	1.3/ 7	-	2.3/ 12	-	18.7/ 100
33		5189.00	Farewell	Cycle A	SM-c	2.4/ 14	3.0/ 18	-	7.7/ 46	-	-	1.3/ 8	-	2.4/ 14	-	16.8/ 100
34		5517.00	Farewell	Cycle A	SM-c	2.0/ 19	2.0/ 19	-	4.9/ 46	-	-	1.2/ 11	-	0.5/ 5	-	10.6/ 100
35	Kapuni-14	4041.50	Mangahewa	K3E1	SM-c	2.2/ 52	1.5/ 34	-	-	-	0.6/ 13	-	-	-	-	4.3/ 100
36		4050.50	Mangahewa	K3E1	Ss-c	1.7/ 54	1.2/ 38	-	-	0.3/ 8	-	-	-	-	-	3.2/ 100
37		4052.50	Mangahewa	K3E1	Ss-c	5.2/ 53	3.8/ 39	-	-	0.8/ 8	-	-	-	-	-	9.8/ 100
38		4058.50	Mangahewa	K3E1	Ss-c	0.7/ 26	1.6/ 59	-	-	-	0.4/ 15	-	-	-	-	2.7/ 100
39		4069.50	Mangahewa	K3E1	Ss-c	3.8/ 47	1.2/ 15	-	-	-	3.0/ 37	-	-	-	-	8.0/ 100
40		4077.50	Mangahewa	K3E1	Ss-c	1.4/ 37	2.3/ 63	-	-	-	-	-	-	-	-	3.7/ 100
41		4088.50	Mangahewa	K3E1	Ss-c	0.9/ 45	0.7/ 33	0.4/ 22	-	-	-	-	-	-	-	2.0/ 100
42		4094.50	Mangahewa	K3E1	SM-c	2.5/ 56	1.4/ 31	0.6/ 13	-	-	-	-	-	-	-	4.5/ 100
43		4105.50	Mangahewa	K3E1	Ss-mb	2.8/ 56	2.2/ 44	-	-	-	-	-	-	-	-	5.0/ 100
44		4114.50	Mangahewa	K3E2	SM-f	12.6/ 56	9.9/ 44	-	-	-	-	-	-	-	-	22.5/ 100
45		4122.00	Mangahewa	K3E2	Ss-rc	3.9/ 48	3.0/ 37	1.2/ 15	-	-	-	-	-	-	-	8.1/ 100
46	Kapuni-15	4701.00	Mangahewa	K1A	Ss-p	4.9/ 50	3.4/ 35	-	-	-	1.4/ 15	-	-	-	-	9.7/ 100
47		4703.00	Mangahewa	K1A	Ss-p	3.0/ 39	2.7/ 35	1.2/ 15	-	-	0.8/ 11	-	-	-	-	7.7/ 100
48		4704.00	Mangahewa	K1A	Ss-p	1.7/ 38	2.1/ 46	-	-	-	0.7/ 16	-	-	-	-	4.5/ 100
49		4705.50	Mangahewa	K1A	Ss-p	2.2/ 32	3.4/ 49	-	-	-	1.4/ 19	-	-	-	-	7.0/ 100
50		4707.50	Mangahewa	K1A	Ss-p	2.1/ 40	2.1/ 40	-	-	-	-	1.2/ 20	-	-	-	5.4/ 100
51		4711.00	Mangahewa	K1A	Ss-p	6.9/ 63	2.6/ 24	-	-	-	1.4/ 13	-	-	-	-	10.9/ 100
52		4712.50	Mangahewa	K1A	Ss-p	3.0/ 35	4.0/ 47	-	-	-	-	1.5/ 18	-	-	-	8.5/ 100
53		4714.50	Mangahewa	K1A	Ss-p	2.4/ 48	1.0/ 21	-	-	-	-	1.1/ 22	0.5/ 9	-	-	5.0/ 100
54		4717.00	Mangahewa	K1A	Ss-p	1.5/ 37	1.5/ 38	-	-	-	1.0/ 25	-	-	-	-	4.0/ 100

Table 4.2: Summary of clay mineral results identified by XRD

vermiculite consists of illite/vermiculite in the Mangahewa and Kaimiro formations, and chlorite/vermiculite which only occurs in the Farewell Formation. Chlorite occurs in the Mangahewa and Kaimiro formations, comprising <1.9% of the sandstone composition and <24% of the total clay content. Mixed-layer chlorite/smectite was identified in sandstones from the Mangahewa and Kaimiro formations, while chlorite/vermiculite is restricted exclusively to Farewell Formation sandstones. Smectite is present only in sandstones from the Farewell Formation. In these samples, smectite clays constitute 1.3% – 8.1% of the rock and form a significant part of the total clay composition (<51%). As previously mentioned, smectite also occurs as a mixed-layer clay, interlayered with both illite and chlorite in sandstones from the Mangahewa and Kaimiro formations.

4.4 CEMENTS

Cements are recrystallised or diagenetically precipitated intergranular material that augment and lithify sandstones (Dapples, 1979). Cements identified in this study include syntaxial overgrowths on detrital siliclastic grains, carbonate minerals and pyrite. These authigenic cements collectively constitute from 3.9% to 43.6% of the Kapuni Group sandstones.

4.4.1 Overgrowths

Overgrowths occur on both detrital quartz and feldspar grains in the Kapuni Group sandstones. These overgrowths are difficult to distinguish in thin-section due to the common absence of 'dust rims' on the surface of original grains. Syntaxial quartz overgrowths are more common than those that occur on feldspar grains. Overgrowths primarily occur on monocrystalline quartz and less commonly on polycrystalline quartz grains. Overgrowths on detrital quartz grains often exhibit one or more euhedral crystal faces where overgrowth development is complete. The degree of diagenetic quartz overgrowth development varies between the sandstones, with overgrowths being more common in the Mangahewa Formation pebbly sandstone (Ss-p) and speckled sandstone (Ss-s) lithofacies where they constitute up to 14.4% and 12% respectively. Secondary feldspar overgrowths also occur comprising up to 3.7% of the rock. These overgrowths are analogous to those that occur on detrital quartz grains displaying similar form and habit. Feldspar overgrowths are generally observed on the skeletal remains of leached plagioclase and microcline feldspars.

4.4.2 Carbonate Minerals

Core observations suggest that well-cemented carbonate horizons are common near concentrations of organic matter or thin coal beds in the sandstones. Carbonate minerals were identified in thin-section and the respective relative abundance of each carbonate

was determined by XRD. The limit of XRD detection may exclude carbonate minerals that constitute <2% of the rock. Carbonate minerals identified included siderite and calcite with subordinate dolomite, dawsonite and laumontite (Table 4.3). The Mangahewa Formation massive bedded sandstone (Ss-mb) and fine sandstone/mudstone (SM-f) lithofacies typically comprise the highest carbonate totals in the Kapuni Group with <28.2% and <40% respectively.

i. Siderite

Siderite is the most common carbonate cement occurring in percentages <24.3% and ranging from 1% to 100% of the total carbonate present. In the sandstones siderite is commonly found as euhedral rhombs, concentrated as nodules or as thin laminae. In thin-section siderite is observed as a uniform to patchy distributed cement filling pores and fractures, replacing feldspars and corroding quartz and feldspar grains and overgrowths. Siderite cement is particularly abundant in the Mangahewa Formation massive bedded sandstone (Ss-mb) and fine sandstone/mudstone (SM-f) lithofacies and Farewell Formation coarse sandstone/mudstone (SM-c) lithofacies.

ii. Calcite

Calcite is the second most common carbonate mineral, generally occurring in quantities <5.8%, although, in two samples from the Mangahewa Formation fine sandstone/mudstone (SM-f) lithofacies calcite accounts for 37.9% and 40.0% of the rock. Calcite occurs as grain replacing micrite and pore-filling spar. Micrite most often replaces orthoclase and microcline feldspars. Whilst, pore-filling spar composed of microcrystalline crystals exhibits a uniform to patchy distribution in the sandstones, where it frequently corrodes quartz and feldspar grains and overgrowths, and occasionally fills grain fractures.

iii. Other Carbonate Minerals

Minor cement forming carbonate minerals include dolomite, dawsonite and laumontite. Dolomite is a rare carbonate mineral (<0.3%) only identified by XRD in samples from the Mangahewa Formation cross-bedded sandstone (Ss-cb) and fine sandstone/mudstone (SM-f) lithofacies. Dawsonite occurs in amounts <0.5% in the Mangahewa and Farewell formation sandstones as fibrous aggregates, replacing calcic feldspars. Although, not technically regarded as a carbonate mineral, the calcium zeolite laumontite was identified by XRD in the Mangahewa Formation pebbly sandstone (Ss-p) lithofacies comprising <0.5% of the rock.

SAMPLE ID.	WELL NO.	DEPTH (subsdf)	FORMATION	RESERVOIR INTERVAL	LITHOLOGICAL FACIES	CARBONATE TOTAL/ CARBONATE % TOTAL					TOTAL
						Calcite	Dolomite	Siderite	Laumontite	Dawsonite	
1	Kapuni-1	3265.00	Maeg-kewa	K1	SM-f	0.6/ 13	*	3.8/ 87	*	*	4.4/ 100
2		3331.50			SM-f	*	*	11.6/ 81	*	2.7/ 19	14.3/ 100
3		3901.00	Kaimiro	Cycle B	SM-f	0.3/ 5	*	6.1/ 92	*	0.2/ 3	6.6/ 100
4		3902.00			SM-f	*	*	1.9/ 94	*	0.1/ 6	2.0/ 100
5		3906.00			Ss-mb	*	*	5.7/ 95	*	0.3/ 5	6.0/ 100
6		3970.00			Ss-mb	0.9/ 30	*	2.1/ 70	*	*	3.0/ 100
7	Kapuni-3	3551.00	Mangahewa	K3A	SM-f	0.4/ 7	*	4.8/ 93	*	*	5.2/ 100
8		3557.50			Ss-mb	1.9/ 7	*	24.3/ 93	*	*	26.2/ 100
9		3561.50			Ss-m	5.8/ 42	*	8.0/ 58	*	*	13.8/ 100
10		3641.50		K3E1	Ss-c	*	*	1.0/ 100	*	*	1.0/ 100
11		3655.00			Ss-mb	0.8/ 31	*	1.7/ 69	*	*	2.5/ 100
12		3659.50			Ss-mb	0.3/ 16	*	1.7/ 84	*	*	2.0/ 100
13		3691.50		K3E2	SM-f	39.4/ 99	*	0.6/ 1	*	*	40.0/ 100
14		3697.00			SM-f	*	*	6.4/ 100	*	*	6.4/ 100
15		3701.00			SM-f	1.7/ 28	*	4.4/ 72	*	*	6.1/ 100
16		3706.50			Ss-rc	*	*	2.8/ 95	*	0.2/ 5	3.0/ 100
17		3708.50			SM-f	36.0/ 95	*	1.9/ 5	*	*	37.9/ 100
18		3710.50			Ss-rc	0.4/ 40	*	0.5/ 60	*	*	0.9/ 100
19		3721.00			Ss-rc	*	*	3.0/ 100	*	*	3.0/ 100
20		3725.50			SM-f	*	*	3.0/ 100	*	*	3.0/ 100
21	Kapuni-8	4045.00	Kaimiro	Cycle B	SM-f	*	*	1.0/ 100	*	*	1.0/ 100
22		4056.00			SM-f	1.9/ 57	*	1.4/ 43	*	*	3.3/ 100
23		4060.00			SM-f	1.3/ 36	*	2.2/ 64	*	*	3.5/ 100
24	Kapuni-12	3461.00	Mangahewa	K1	Ss-s	2.4/ 26	*	6.6/ 74	*	*	9.0/ 100
25		3469.00			SM-f	0.2/ 25	*	0.7/ 75	*	*	0.9/ 100
26		3471.00		K1A	Ss-p	*	*	0.9/ 90	*	0.1/ 10	10.0/ 100
27		3473.00			Ss-p	0.7/ 30	*	1.3/ 61	*	0.2/ 9	2.2/ 100
28		3478.00			Ss-p	1.0/ 57	*	0.6/ 31	*	0.2/ 12	1.8/ 100
29		3481.00			Ss-cb	1.9/ 88	*	0.3/ 12	*	*	2.2/ 100
30		3485.00			Ss-cb	1.2/ 60	*	0.8/ 40	*	*	2.0/ 100
31		3489.00			Ss-cb	0.7/ 33	0.3/ 13	1.2/ 54	*	*	2.2/ 100
32	Kapuni Deep-1	5183.00	Farewell	Cycle A	SM-c	2.2/ 71	*	0.9/ 29	*	*	3.1/ 100
33		5189.00			SM-c	1.6/ 63	*	0.5/ 20	*	0.4/ 17	2.5/ 100
34		5517.00			SM-c	*	*	22.9/ 100	*	*	22.9/ 100
35	Kapuni-14	4041.50	Mangahewa	K3E1	SM-c	0.4/ 61	*	0.3/ 39	*	*	0.7/ 100
36		4050.50			Ss-c	*	*	7.6/ 100	*	*	7.6/ 100
37		4052.50			Ss-c	*	*	1.0/ 100	*	*	1.0/ 100
38		4058.50			Ss-c	0.2/ 36	*	0.3/ 64	*	*	0.5/ 100
39		4069.50			Ss-c	1.5/ 63	*	0.9/ 37	*	*	2.4/ 100
40		4077.50			Ss-c	0.5/ 31	*	1.0/ 69	*	*	1.5/ 100
41		4088.50			Ss-c	0.6/ 48	*	0.4/ 33	*	0.2/ 19	1.2/ 100
42		4094.50			SM-c	1.1/ 32	*	2.3/ 68	*	*	3.4/ 100
43		4105.50			Ss-mb	0.5/ 26	*	1.5/ 74	*	*	2.0/ 100
44		4114.50		K3E2	SM-f	0.3/ 7	0.3/ 7	3.3/ 86	*	*	3.8/ 100
45		4122.00			Ss-rc	0.5/ 56	*	0.4/ 44	*	*	0.9/ 100
46	Kapuni-15	4701.00	Mangahewa	K1A	Ss-p	0.6/ 37	*	0.9/ 63	*	*	1.5/ 100
47		4703.00			Ss-p	1.1/ 50	*	1.1/ 50	*	*	2.2/ 100
48		4704.00			Ss-p	0.4/ 37	*	0.6/ 63	*	*	1.0/ 100
49		4705.50			Ss-p	1.1/ 64	*	*	*	0.7/ 36	1.8/ 100
50		4707.50			Ss-p	0.6/ 28	*	1.4/ 72	*	*	2.0/ 100
51		4711.00			Ss-p	0.5/ 23	*	1.4/ 70	0.1/ 7	*	2.0/ 100
52		4712.50			Ss-p	1.4/ 54	*	1.1/ 46	*	*	2.5/ 100
53		4714.50			Ss-p	2.2/ 100	*	*	*	*	2.2/ 100
54		4717.00			Ss-p	1.5/ 76	*	*	0.5/ 24	*	2.0/ 100

Table 4.3: Summary of carbonate mineral results identified by XRD and thin-section

4.4.3 Pyrite

Pyrite is a minor (<2.9%) cement. SEM studies indicate that pyrite occurs as nodules of euhedral crystals or cubes commonly with a framboidal habit in the sandstone. In thin-section pyrite formation is commonly associated with and observed replacing carbonaceous intraclasts and laminae. Pyritised microfossils with a framboidal habit were also observed in the Mangahewa Formation coarse sandstone (Ss-c), pebbly sandstone (Ss-p) and coarse sandstone/mudstone (SM-c) lithofacies.

4.5 POROSITY

Sandstone porosity is the volume of the rock that is void space or pores, either isolated in nature or forming an interconnected network (Tissot and Welte, 1978). These pores are commonly classified in thin-section as primary or secondary according to origin and pore texture (Appendix 5). Primary porosity is pore space existing from the time of deposition, while secondary porosity is that which forms after deposition (Schmidt and McDonald, 1979a). In the Kapuni Group sandstones intergranular porosity is the only form of primary pore textures identified. While, secondary porosity includes intra-constituent, moldic, oversized and fracture pore textures. Total visible porosity is variable in the Kapuni Group sandstones ranging up to 24.3%. The highest total porosity values primarily occur in the Mangahewa Formation coarse sandstone (Ss-c) lithofacies (13.5% to 24.3%) and coarse sandstone/mudstone (SM-c) lithofacies (8% to 21.3%) In other Mangahewa Formation sandstones total visible porosity rarely exceeds 15%. Porosity is negligible in sandstones of the underlying Kaimiro and Farewell formations. Table 4.4 summarises total visible porosities and porosity types for the Kapuni Group sandstones.

4.5.1 Primary Porosity

i. Intergranular Pores

Intergranular porosity preserved between framework grains, matrix and cements is not common in the sandstones (Plate 4.3). Original pore space has generally been reduced by compaction and the filling of pores by authigenic cements (siliclastic, carbonate and pyrite) or clay minerals. Intergranular porosity is most common in the Mangahewa Formation coarse sandstone (Ss-c) lithofacies and coarse sandstone/mudstone (SM-c) lithofacies, but, was also identified in samples from the pebbly sandstone (Ss-p), cross-bedded sandstone (Ss-cb), rafted coal sandstone (Ss-rc) and massive bedded sandstone (Ss-mb) lithofacies. In the Kapuni Group sandstones visible intergranular porosity does not exceed 4.7% of the rock.

SAMPLE ID.	WELL NO.	DEPTH (mSSRDF)	FORMATION	RESERVOIR INTERVAL	LITHOLOGICAL FACIES	VISIBLE POROSITY						TOTAL
						PRIMARY	SECONDARY					
						Intergranular	Grain Intra-constituent	Matrix Intra-constituent	Moldic	Oversized Dissolution	Grain Fracture	
1	Kapuni-1	3265.00	Mangahewa	K1	SM-f	-	-	-	-	-	-	0.0
2		3331.50			SM-f	-	-	-	-	-	-	0.0
3		3901.00	Kaimiro	Cycle B	SM-f	-	-	-	-	-	-	0.0
4		3902.00			SM-f	-	-	-	-	-	-	0.0
5		3906.00			Ss-mb	-	-	-	-	-	-	0.0
6		3970.00			Ss-mb	-	1.2	-	-	-	-	1.2
7	Kapuni-3	3551.00	Mangahewa	K3A	SM-f	-	1.5	-	-	-	-	1.5
8		3557.50			Ss-mb	-	1.3	-	-	-	-	1.3
9		3561.50			Ss-mb	-	3.4	-	-		-	3.4
10		3641.50		K3E1	Ss-c	-	3.3	3.0	2.5	7.3	-	16.1
11		3655.00			Ss-mb	-	4.3	1.5	-	-	-	5.8
12		3659.50			Ss-mb	-	3.2	-	-	-	-	3.2
13		3691.50		K3E2	SM-f	-	-	-	-	-	-	0.0
14		3697.00			SM-f	-	-	-	-	-	-	0.0
15		3701.00			SM-f	-	-	-	-	-	-	0.0
16		3706.50			Ss-rc	-	-	-	-	-	-	0.0
17		3708.50			SM-f	-	-	-	-	-	-	0.0
18		3710.50			Ss-rc	3.2	5.0	1.3	1.2	-	-	10.7
19		3721.00			Ss-rc	-	3.1	-	-	-	-	3.1
20		3725.50			SM-f	-	-	-	-	-	-	0.0
21	Kapuni-8	4045.00	Kaimiro	Cycle B	SM-f	-	2.3	-	-	-	-	2.3
22		4056.00			SM-f	-	-	-	-	-	-	0.0
23		4060.00			SM-f	-	-	-	-	-	-	0.0
24	Kapuni-12	3461.00	Mangahewa	K1	Ss-s	-	1.2	-	0.8	-	-	2.0
25		3469.00			SM-f	-	1.9	-	-	-	-	1.9
26		3471.00		K1A	Ss-p	2.0	4	0.9	-	-	0.2	7.1
27		3473.00			Ss-p	-	-	-	-	-	-	0.0
28		3478.00			Ss-p	4.7	4.9	1	0.9	-	0.2	11.7
29		3481.00			Ss-cb	3.0	3.7	0.4	-	-	-	7.1
30		3485.00			Ss-cb	-	4.2	-	-	-	-	4.2
31		3489.00			Ss-cb	4.2	2.8	-	-	8.5	-	15.5
32	Kapuni Deep-1	5183.00	Farewell	Cycle A	SM-c	-	0.5	-	-	-	-	1.5
33		5189.00			SM-c	-	0.5	-	-	-	-	0.5
34		5517.00			SM-c	-	-	-	-	-	-	0.0
35	Kapuni-14	4041.50	Mangahewa	K3E1	SM-c	3.3	2.5	1.2	-	14	0.3	21.3
36		4050.50			Ss-c	3.3	2.8	1.0	0.5	13.2	0.2	21.0
37		4052.50			Ss-c	3.8	2.0	0.5	-	3.6	0.5	10.4
38		4058.50			Ss-c	3.5	3.4	1.5	-	8.8	-	17.2
39		4069.50			Ss-c	3.8	3.0	-	-	6.2	0.5	13.5
40		4077.50			Ss-c	2.6	2.8	-	-	17.8	0.2	23.4
41		4088.50			Ss-c	2.2	1.6	1.0	-	19.0	0.5	24.3
42		4094.50			SM-c	3.0	4.2	-	0.3	-	0.5	8.0
43		4105.50			Ss-mb	4.5	5.0	-	-	8.0	-	17.5
44		4114.50		K3E2	SM-f	-	1.5	-	-	-	-	1.5
45		4122.00			Ss-rc	4.5	1.0	-	-	15.1	-	20.6
46	Kapuni-15	4701.00	Mangahewa	K1A	Ss-p	-	2.0	-	-	-	-	2.0
47		4703.00			Ss-p	-	2.7	-	-	-	-	2.7
48		4704.00			Ss-p	-	2.6	0.2	0.5	-	-	3.3
49		4705.50			Ss-p	-	1.2	-	-	-	-	1.2
50		4707.50			Ss-p	-	4.3	0.7	0.7	-	-	5.7
51		4711.00			Ss-p	-	-	-	-	-	-	0.0
52		4712.50			Ss-p	-	2.0	-	-	-	-	2.0
53		4714.50			Ss-p	-	2.4	-	-	-	-	2.4
54		4717.00			Ss-p	-	3.2	1.0	-	-	-	4.2

Table 4.4: Summary of thin-section visible porosity results

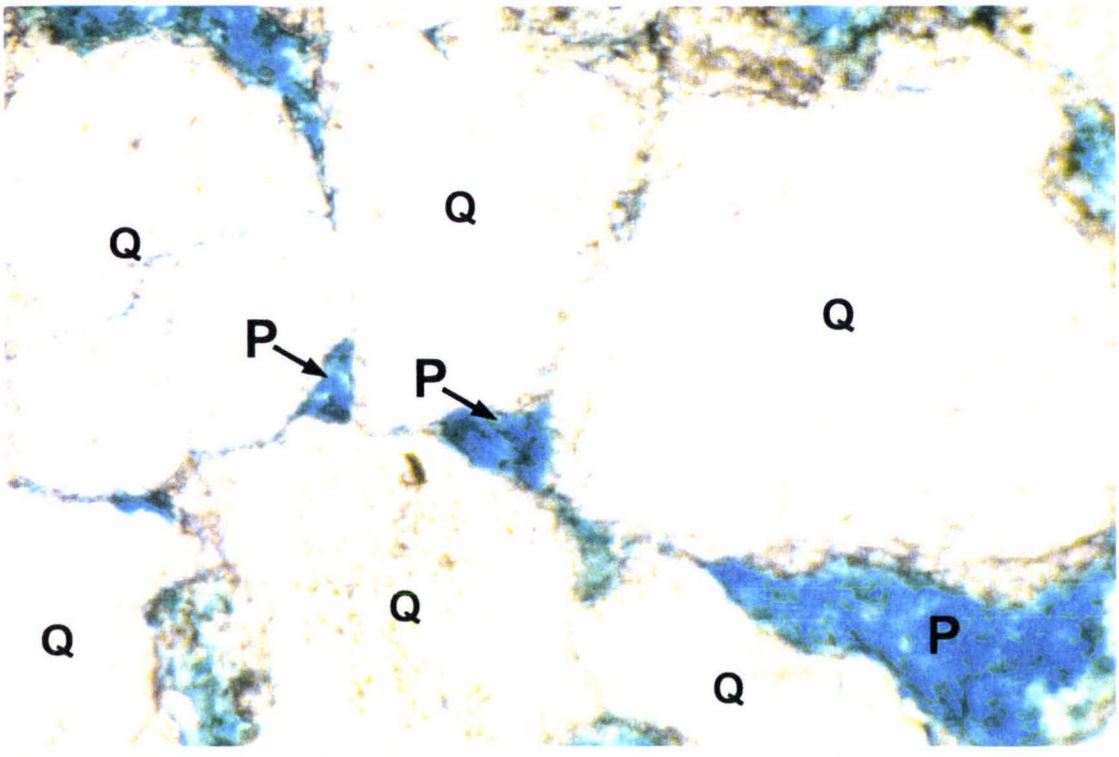

Plate 4.3: Plane-polarised photomicrograph of intergranular primary porosity (P) preserved between framework grains (Q = Quartz) in the Mangahewa Formation coarse sandstone (Ss-c) lithofacies (Q = Quartz), photomicrograph x10 (Sample 38, Kapuni-14)

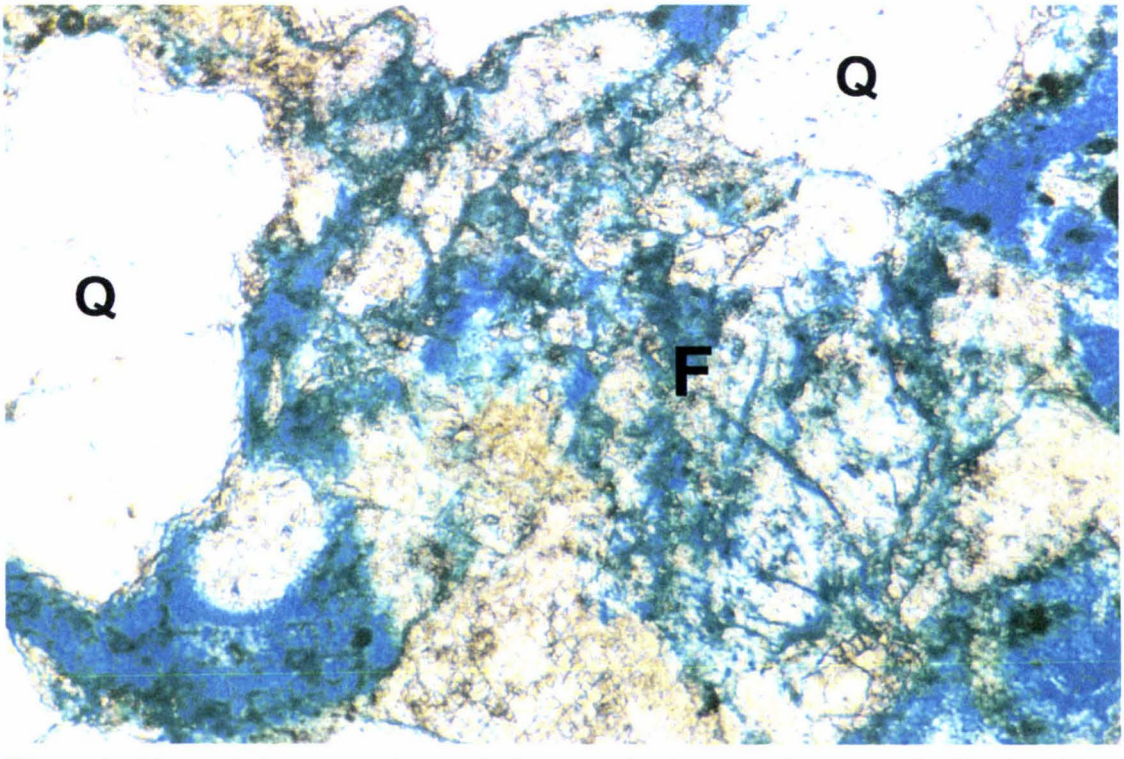

Plate 4.4: Plane-polarised photomicrograph demonstrating intra-constituent porosity (blue) within a corroded feldspar grain (F = Feldspar, Q = Quartz) in the pebbly sandstone (Ss-p) lithofacies, photomicrograph x6.4, (Sample 25, Kapuni-12)

4.5.2 Secondary Porosity

i. Intra-constituent Pores

Intra-constituent porosity in the Kapuni Group sandstones is generally intragranular, forming through the internal dissolution of grains, but may have also developed through the leaching of carbonate minerals which partially replaced grains. Such porosity occurs between patches of the remnant grain (Plate 4.4). Grains with a high percentage of intragranular porosity have been described as 'honeycomb grains' (Schmidt and McDonald, 1979b), 'skeleton grains' (Rowsell and De Swardt, 1974) and 'leached grains' (Fox *et al.*, 1975). The dissolution of feldspar grains is the most common form of secondary porosity development, although porosity enhancement in typically low not exceeding 5.7% in the sandstones. In the Mangahewa and Kaimiro formations fine sandstone/mudstone (SM-f), Kaimiro Formation massive bedded sandstone (Ss-mb) and Farewell Formation coarse sandstone/mudstone (SM-c) lithofacies intra-constituent dissolution provides the only form of secondary porosity development.

Intra-constituent porosity also occurs through intra-matrix dissolution, with the selective dissolution of clay minerals, primarily kaolinite. Cay matrix dissolution primarily occurs in the Mangahewa Formation coarse sandstone lithofacies (Ss-c) and subordinately in the massive bedded sandstone (Ss-mb), rafted coal sandstone (Ss-rc), pebbly sandstone (Ss-p), cross-bedded sandstone (Ss-p) and coarse sandstone/mudstone lithofacies where such porosity does not exceed 3.0%.

ii. Moldic Pores

Grain-mold porosity involves the complete dissolution of grains, creating pore space in the void of their precursors. Complete grain dissolution, primarily concerns the leaching of feldspars creating minor secondary porosity (<2.5) in the Mangahewa Formation coarse sandstone (Ss-c), massive bedded sandstone (Ss-mb), pebbly sandstone (Ss-p), rafted coal sandstone, speckled sandstone (Ss-s) and coarse sandstone/mudstone (SM-c) lithofacies.

iii. Oversized pores

Oversized pores in sandstones are recognised texturally as pore apertures, other than those produced by fracturing, larger than the diameter of adjacent grains by a factor of at least 1.2 (Schmidt and McDonald, 1979b). Oversized pores in the sandstones have predominantly formed through the selective dissolution of replacive carbonate minerals and less importantly through the dissolution of soluble grains (primarily feldspars) and clay matrix (Plate 4.5). The development of oversized pores is most common in the Mangahewa Formation coarse sandstone (Ss-c) and coarse sandstone/mudstone (SM-c) lithofacies, where they account for the higher total porosity values in these sandstones.

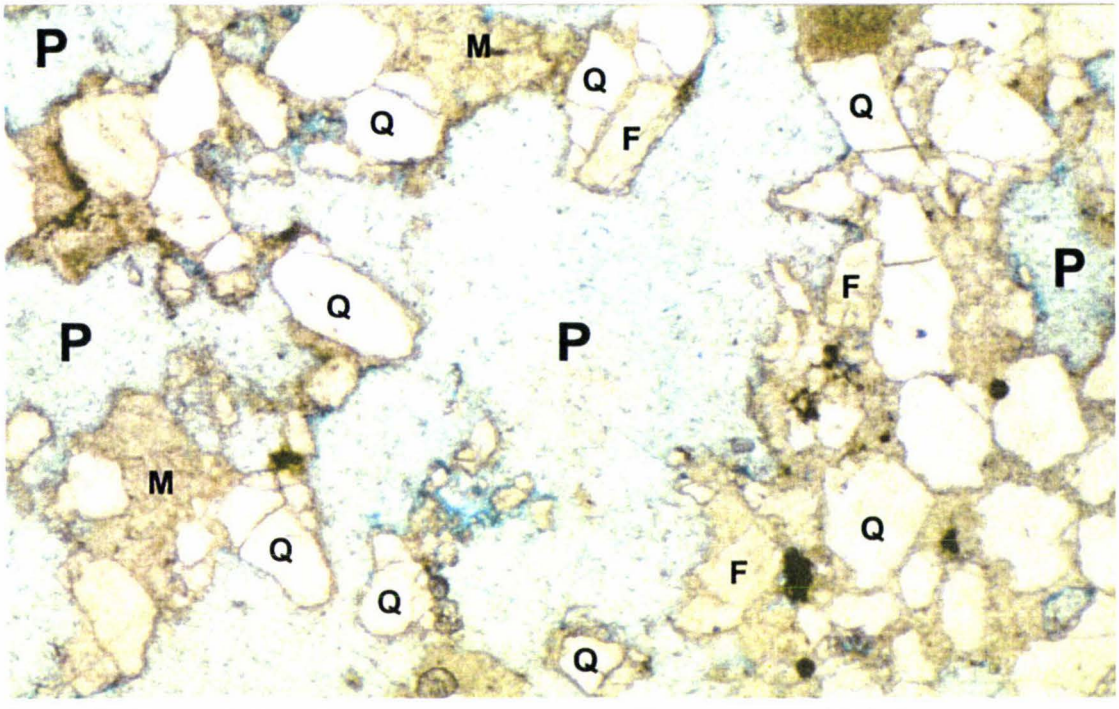

Plate 4.5: Plane-polarised photomicrograph of oversized dissolution pores (P) in the coarse sandstone (Ss-c) lithofacies (Q = Quartz, F = Feldspar, M = Matrix), photomicrograph x4 (Sample 41, Kapuni-14)

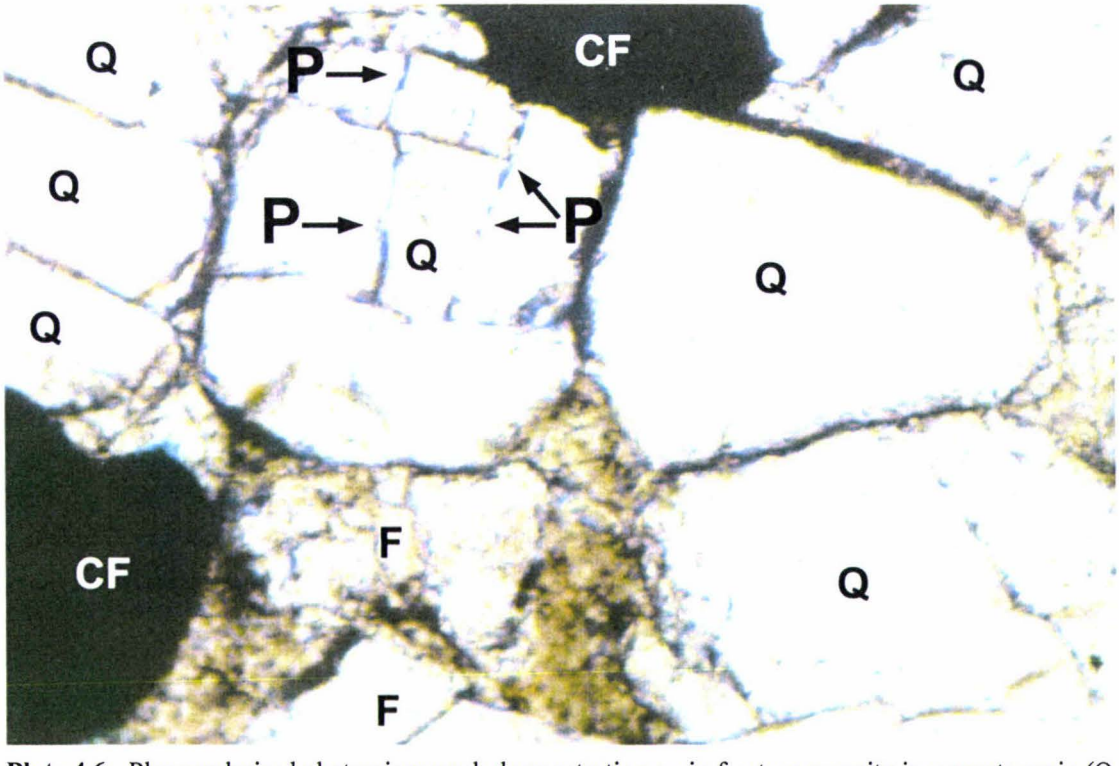

Plate 4.6: Plane-polarised photomicrograph demonstrating grain fracture porosity in a quartz grain (Q = Quartz, F= Feldspar, CF = Carbonaceous Fragment) in the coarse sandstone (Ss-c) lithofacies, photomicrograph x6.4, (Sample 40, Kapuni-14)

iv. Open Grain Fractures

Fracture of detrital grains has created pore space between the openings of individual grains. In the Kapuni Group sandstones grain fractures are frequently filled by authigenic clay (kaolinite), carbonate (siderite, calcite) or siliceous minerals (quartz). However, the dissolution of these minerals has given rise to porosity within the "reopened" fractures (Plate 4.6). Porosity created by grain fractures only occurs in the Mangahewa Formation coarse sandstone (Ss-c), coarse sandstone/mudstone (SM-c) and pebbly sandstone (Ss-p) lithofacies. Fractured grains provide an insignificant amount of porosity (<0.5%), but increase permeability in the sandstones.

4.6 TEXTURE

Sediment texture concerns the grain-size, grain morphology and fabric characteristics of sandstones (see Appendix-6). These textural characteristics are largely a reflection of the depositional processes that were operating when the sandstones were being deposited (Pettijohn *et al.*, 1987). North (1985) suggests that textural properties are important considerations in sandstones as they are the prime factors governing porosity and permeability. Table 4.4 summarises textural results from thin-section studies of the Kapuni Group sandstones.

4.6.1 Grain Size

Grain-size distribution of the sandstones was studied and the samples classified using the Wentworth standard grain-size scale. Both grain-size range and the average grain-size were recorded. In the Kapuni Group sandstones grain-size varies from very-fine sand to very-fine pebbles. The Mangahewa Formation pebbly sandstone (Ss-p) lithofacies are the coarsest-grained with an average grain-size of very-coarse sand (1.35mm). The Mangahewa and Farewell formations coarse sandstone (Ss-c) and coarse sandstone/mudstone (SM-c) lithofacies generally comprise a medium to coarse grain-size. The finest grain-size occurs in the Mangahewa and Kaimiro formations fine sandstone/mudstone (SM-f) lithofacies. Other Kapuni Group sandstone lithofacies typically encompass an average medium grain-size.

4.6.2 Grain Morphology

Grain morphology concerns the sphericity and roundness of individual grains. Roundness measures are generally more important textural characteristic than sphericity (Boggs, 2001); therefore, sphericity was only recorded as the percentage of low sphericity grains in each sample. Grain roundness was classified into six classes ranging from very angular to well-rounded. In the Mangahewa Formation grains are typically sub-angular to sub-rounded, although a greater percentage of angular grains are. noted in the fine

SAMPLE ID.	WELL NO.	DEPTH (mbbdf)	FORMATION	RESERVOIR INTERVAL	LITHOLOGICAL FACIES	CLASSIFICATION	TEXTURAL FEATURES					
							Grain Size	Average Grain Size	Sphericity	Roundness	Sorting	Grain Contacts
1	Kapuni-1	3265.00	Mangakewa	K1	SM-f	Lithic Arkose	vf-m	0.13mm (f)	L (82.7%)	a-sr	p	pnt>pln
2		3331.50			SM-f	Lithic Arkose	vf-m	0.16mm (f)	L (78.7%)	a-sr	p	pnt=pln
3		3901.00	Kaimiro	Cycle B	SM-f	Lithic Arkose	vf-m	0.16mm (f)	L (89.1%)	sa-sr	p-m	pnt=pln>con
4		3902.00			SM-f	Lithic Arkose	vf-m	0.24mm (f)	L (87.0%)	sa-sr	m	pnt=pln
5		3906.00			Ss-mb	Lithic Arkose	vf-m	0.20mm (f)	L (85.0%)	a-sr	m	pln>pnt>con
6		3970.00			Ss-mb	Arkose	lm-vc	0.45mm (m)	L (80.0%)	sa-sr	m	pnt=pln
7	Kapuni-3	3551.00	Mangahewa	K3A	SM-f	Lithic Arkose	vf-m	0.18mm (f)	L (83.0%)	a-sr	p-m	pln>pnt
8		3557.50			Ss-mb	Lithic Arkose	vf-c	0.31mm (m)	L (89.2%)	a-sr	m	pnt>pln
9		3561.50			Ss-mb	Arkose	vf-c	0.46mm (m)	L (88.4%)	sa-sr	m	pln>con
10		3641.50		K3E1	Ss-c	Arkose	vf-vc	0.50mm (c)	L (86.5%)	sa-sr	m	pnt>pln
11		3655.00			Ss-mb	Arkose	vf-c	0.30mm (m)	L (82.8%)	a-sr	m	pnt=pln
12		3659.50			Ss-mb	Arkose	vf-c	0.32mm (m)	L (75.5%)	sa-sr	mw	pnt=pln
13		3691.50		K3E2	SM-f	Subarkose	vf-c	0.30mm (m)	L (79.2%)	a-sr	m	pnt>pln
14		3697.00			SM-f	Arkose	vf-m	0.21mm (f)	L (73.2%)	sa-sr	m	pnt>pln
15		3701.00			SM-f	Arkose	vf-c	0.26mm (m)	L (77.6%)	sa-sr	m	pln=pnt
16		3706.50			Ss-rc	Subarkose	vf-m	0.22mm (f)	L(88.7%)	sa-sr	m	pnt>pln
17		3708.50			SM-f	Arkose	vf-c	0.31mm (m)	L (86.1%)	a-sr	m	pnt>pln
18		3710.50			Ss-rc	Subarkose	vf-vc	0.39mm (m)	L (79.0%)	sa-sr	mw	pnt=pln>con
19		3721.00			Ss-rc	Subarkose	f-c	0.38mm (m)	L (60.0%)	a-sr	mw	pnt>pln
20		3725.50			SM-f	Arkose	vf-m	0.22mm (f)	L (78.2%)	a-sr	m	pnt>pln>con
21	Kapuni-8	4045.00	Kaimiro	Cycle B	SM-f	Lithic Arkose	vf-m	0.13mm (f)	L (65.0%)	a-sr	m	pln=con=pnt
22		4056.00			SM-f	Lithic Arkose	vf-m	0.20mm (f)	L (76.7%)	a-sr	m	con>pln>pnt
23		4060.00			SM-f	Lithic Arkose	vf-c	0.23mm (f)	L (73.5%)	a-sr	m	con>sut
24	Kapuni-12	3461.00	Mangahewa	K1	Ss-s	Subarkose	vf-c	0.40mm (m)	L (83.1%)	sa-sr	m	pln=pnt>con
25		3469.00			SM-f	Lithic Arkose	f-c	0.22mm (f)	L (71.0%)	a-sr	m	pln=pnt>con
26		3471.00		K1A	Ss-p	Subarkose	f-c	0.50mm (c)	L (77.0%)	sa-sr	mw	pln=pnt=con
27		3473.00			Ss-p	Arkose	vf-vfp	0.26mm (m)	L (73.0%)	a-sr	mw	pln>pnt>con
28		3478.00			Ss-p	Subarkose	vf-vfp	1.22mm (vc)	L (62.6%)	sa-sr	mw	pln=pnt>con
29		3481.00			Ss-cb	Arkose	vf-vfp	1.10mm (vc)	L (78.1%)	sa-sr	p	pln>con
30		3485.00			Ss-cb	Arkose	vf-vc	0.30mm (m)	L (74.0%)	a-sr	m	pln>con>pnt
31		3489.00			Ss-cb	Subarkose	f-vc	0.43mm (m)	L (73.0%)	sa-sr	m	pnt>pln>con
32	Kapuni Deep-1	5183.00	Farewell	Cycle A	SM-c	Arkose	vf-c	0.29mm (m)	L (77.7%)	sa-sr	w	con>sut>pln
33		5189.00			SM-c	Arkose	vf-c	0.30mm (m)	L (79.8%)	a-sr	mw	con>sut>pln
34		5517.00			SM-c	Arkose	vf-m	0.24mm (f)	L (68.3%)	a-sr	mw	con=sut>pln
35	Kapuni-14	4041.50	Mangahewa	K3E1	SM-c	Subarkose	vf-vc	0.90mm (c)	L (76.6%)	sa-sr	w	pln>pnt
36		4050.50			Ss-c	Subarkose	vf-c	0.50mm (c)	L (77.8%)	sa-sr	mw	pln>pnt
37		4052.50			Ss-c	Subarkose	vf-vfp	0.50mm (c)	L (70.8%)	sa-sr	w	pln=pnt
38		4058.50			Ss-c	Subarkose	vf-vfp	0.40mm (m)	L (75.8%)	sa-sr	mw	pln > pnt
39		4069.50			Ss-c	Subarkose	vf-c	0.38mm (m)	L (77.8%)	sa-sr	w	pln>pnt
40		4077.50			Ss-c	Subarkose	vf-c	0.50mm (c)	L (79.9%)	sa-sr	w	pln>pnt
41		4088.50			Ss-c	Subarkose	vf-c	0.35mm (m)	L (67.8%)	sa-sr	w	pln>pnt
42		4094.50			SM-c	Subarkose	vf-vc	0.39mm (m)	L (63.2%)	sa-sr	mw	pln>pnt
43		4105.50			Ss-mb	Subarkose	vf-c	0.44mm (m)	L (75.4%)	sa-sr	m	pln>con>pnt
44		4114.50		K3E2	SM-f	Arkose	vf-m	0.21m (f)	L (85.6%)	sa-sr	p-m	pln>con.pnt
45		4122.00			Ss-rc	Subarkose	vf-c	0.46 (m)	L (73.5%)	sa-sr	m	pln>pnt
46	Kapuni-15	4701.00	Mangahewa	K1A	Ss-p	Arkose	vf-vc	0.42mm (m)	L (75.8%)	sa-sr	m	pln>con
47		4703.00			Ss-p	Arkose	vf-c	0.34mm (m)	L (76.7%)	sa-sr	m	pln=con>pnt
48		4704.00			Ss-p	Arkose	vf-vc	0.53mm (c)	L (77.6%)	sa-sr	m	pln=con>pnt
49		4705.50			Ss-p	Lithic Arkose	vf-c	0.31mm (m)	L (71.5%)	sa-sr	m	pln>con
50		4707.50			Ss-p	Arkose	vf-c	0.45mm (m)	L (77.5%)	sa-sr	mw	pln >con
51		4711.00			Ss-p	Arkose	vf-c	0.29mm (m)	L (89.8%)	sa-sr	m	pln>con
52		4712.50			Ss-p	Lithic Arkose	vf-c	0.31mm (m)	L (87.5%)	sa-sr	m	pln>con
53		4714.50			Ss-p	Arkose	vf-vc	0.51mm (c)	L (77.4%)	sa-sr	m	con>pln
54		4717.00			Ss-p	Arkose	vf-vfp	1.35mm (vc)	L (78.8%)	sa-sr	m	con>pln

Table 4.5: Summary of textural characteristics in thin-section

TEXTURAL SUMMARY

Grain Size
vf - very fine sand
f - fine sand
m - medium sand
c - coarse sand
vc - very coarse sand
vfc - very fine pebble

Grain Shape
va - very angular
a - angular
sa - sub-angular
sr - sub-rounded
r - rounded
wr - well rounded

Grain Sorting
p - poor
m - moderate
mw - moderately well
w - well

Grain Sphericity
L - low
H - high

Grain Contacts
pnt - point
pln - planar
con - concavo-convex
sut - sutured

sandstone/mudstone (SM-f) lithofacies. The proportion of angular grains is much greater in the underlying Kaimiro and Farewell formations. The Kapuni Group sandstones comprise from 60.0% to 89.8% low sphericity grains. No discernable sphericity trends for any of the sandstone lithofacies were identified.

4.6.3 Sediment Fabric

Sediment fabric was examined in respect to the sorting and nature of grain contacts in the sandstones. Grain sorting was classified into five categories from poorly- to well-sorted. The most pronounced grain sorting is observed in the Mangahewa Formation coarse sandstone (Ss-c) and coarse sandstone/mudstone (Ss-rc) lithofacies, which are moderately-well-to well-sorted. Grain sorting is lowest in the fine sandstone/mudstone lithofacies which are generally poorly- to moderately-sorted. Other Kapuni Group sandstone lithofacies are predominantly moderately-sorted.

Grain contacts were described as point, planar, concavo-convex or sutured. Point and planar contacts are most common in the Mangahewa Formation coarse sandstone (Ss-c), pebbly sandstone (Ss-p), rafted coal sandstone (Ss-rc) and coarse sandstone/mudstone (SM-c) lithofacies. Other sandstone lithofacies in the Mangahewa Formation predominately comprise planar, point and minor concavo-convex contacts. Concavo-convex contacts occur in greater amounts in the Kaimiro Formation sandstones. Whilst in sandstones from the Farewell Formation concavo-convex contacts predominated over sutured and planar contacts.

4.7 SANDSTONE CLASSIFICATION

Sandstones in the Kapuni Group were classified by their dominant framework components, according to the scheme of Folk *et al.* (1970). The composition of each sample in terms of quartz (Q), feldspar (F) and rock fragments (R) have been plotted on a ternary diagram and classified (Figure 4.1). In the Mangahewa Formation the coarse sandstone (Ss-c), coarse sandstone/mudstone (SM-c), rafted coal sandstone (Ss-rc) and speckled sandstone (Ss-s) lithofacies are all classified as subarkose sandstones. Samples from the pebbly sandstone (Ss-p), cross-bedded sandstone (Ss-cb) and massive bedded sandstone (Ss-mb) lithofacies also comprise subarkose sandstones. Arkose sandstones are most prominent in the Mangahewa Formation pebbly sandstone (Ss-p) and cross-bedded sandstone (Ss-cb) lithofacies, and Farewell Formation sandstone/mudstone lithofacies (SM-c). Arkose sandstones are also recognised in some Mangahewa Formation fine sandstone/mudstone (SM-f) and Mangahewa and Kaimiro formations massive bedded sandstone (Ss-mb) lithofacies. Lithic arkose sandstones predominantly occur in the Mangahewa Formation fine sandstone/mudstone (SM-f) and Kaimiro Formation massive bedded sandstone (Ss-mb) lithofacies.

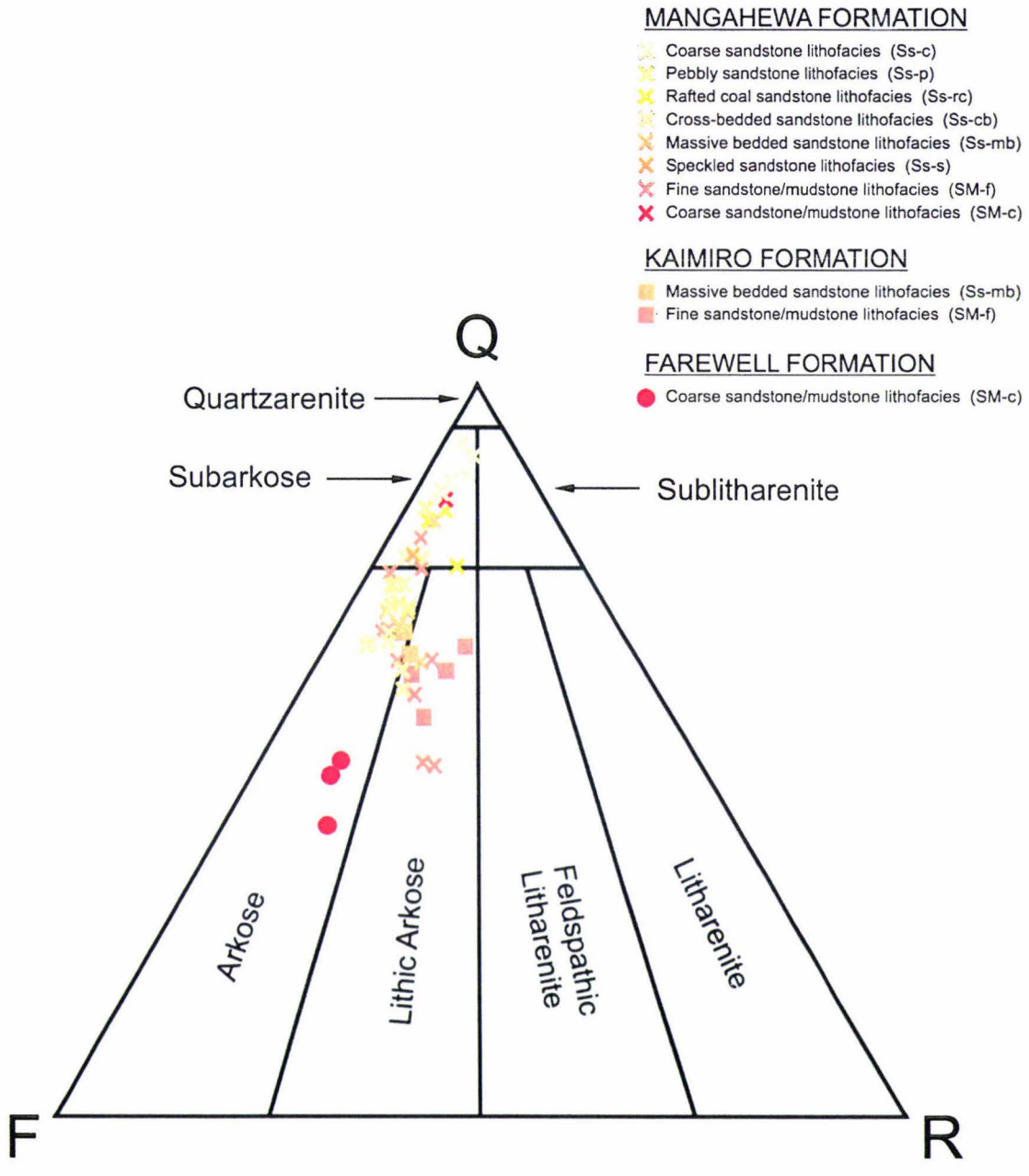

Figure 4.1: Modal analyses of the Kapuni Group sandstones in terms of quartz (Q), feldspar (F) and rock fragments (R) (after Folk *et al.*, 1970)

4.8 PROVENANCE

4.8.1 Mineralogy

Framework minerals including rock fragments, quartz, feldspar and heavy minerals have been used in this study to elucidate the provenance of the sandstones. Rock fragments are considered the most informative and direct evidence of source rock lithology (Tucker, 1991). Rock fragments in the Kapuni Group sandstones are predominantly low-grade metamorphics; comprising quartzite, gneiss, phyllite, argillite and schist. Sedimentary rock fragments including chert and siltstone were also identified. While, volcanic rock fragments occur in the Mangahewa and Kaimiro formations exhibiting porphyritic textures and Farewell Formation with trachytic textures.

Quartz is the most common component of the Kapuni Group sandstones. Basu *et al.* (1975) suggest that the proportions of strained to unstrained medium quartz grains can provide provenance information when the relative percentages are plotted on a four-variable diamond diagram. Following this method, monocrystalline quartz with undulose extinction (>5°), monocrystalline quartz with nonundulose extinction (<5°), polycrystalline quartz with 2 - 3 crystal units and polycrystalline quartz with >3 crystal units were plotted as relative percentages on a diamond diagram (Figure 4.2). The results demonstrate a low-rank metamorphic source for the Kapuni Group sandstones.

A useful framework for relating feldspar varieties to common source rocks was developed by Pittman (1970), and later expanded on by Lewis and McConchie (1994). According to this framework K-feldspars are an essential component of alkaline and acidic igneous rocks and their volcanic equilivants. Orthoclase is typical of granites or acid volcanics, microcline and perthite of granites, while sanidine is predominantly derived from acid volcanic rocks. In contrast, plagioclase (albite) feldspars are essential constituents of a wide-range of igneous, low-grade metamorphic and intermediate volcanics rocks.

Rice *et al.* (1976) suggest that heavy minerals are useful provenance indicators as they involve a much wider range of minerals than the abundant light grain fraction. However, an impoverished heavy mineral suite in the Kapuni Group sandstones means that source rock evidence can only be gathered from a limited range of heavy minerals, namely; zircon, rutile and garnets. Zircon and rutile are common components of igneous plutonic rocks, but are also found in sedimentary and metamorphic rocks. Little source rock evidence can be gathered from zircon and rutile because their resistance means they often survive more than one cycle of weathering and sedimentation (Deer *et al.*, 1971). Garnets, however, are generally only found in higher rank metamorphic rocks.

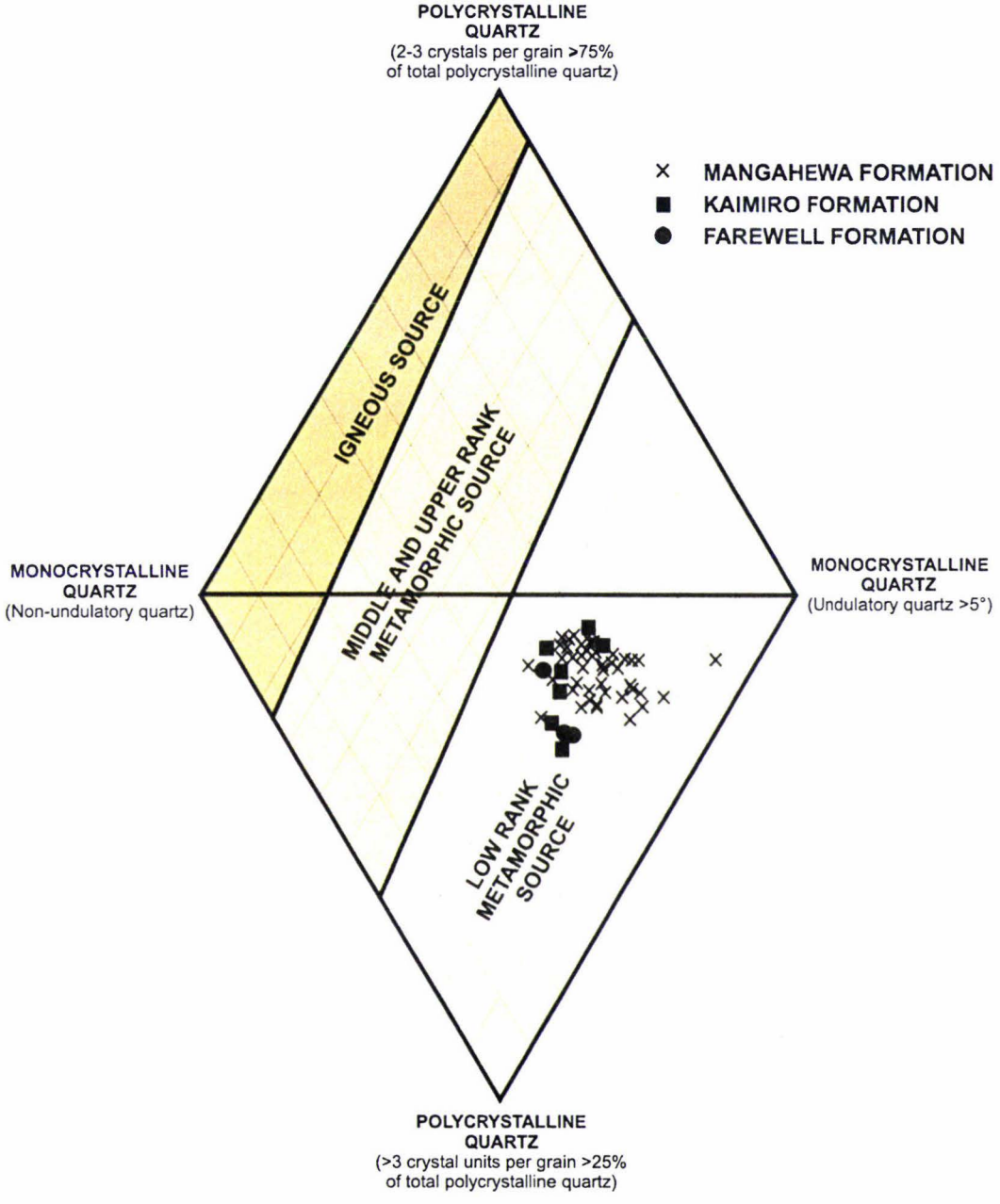

Figure 4.2: Four-variable plot of medium sand sized quartz indicating provenance (after Basu *et al.*, 1975).

4.8.2 Tectonic Setting

The mineral composition of sandstone can help in determining the tectonic setting of provenance areas. Three principal types of provenances are identified including continental block, magmatic arc and recycled orogen. To differentiate sediment derived from the three major tectonic provenances, Dickinson *et al.* (1983) suggest the use of triangular composition diagrams using the proportions of quartz, feldspar and rock fragments. The triangular diagram allows differences in provenance areas amongst the Kapuni Group formations to be distinguished (Figure 4.3). The Mangahewa Formation sandstones were predominantly derived from continental block (craton interior and transitional continental) and recycled orogen provenances. The Kaimiro Formation sandstones were derived from a recycled orogen provenance. Whilst, the Farewell Formation sandstones were derived from a magmatic arc (dissected arc) and/or continental block (basement uplift) provenances.

4.8.3 Summary

The mineralogy of the Kapuni Group sandstones indicate various input from low-grade metamorphic, granitic, sedimentary and acid volcanic sources. Based on thin-section observations and provenance plots metamorphic source rocks seem to be the most important sediment source for the Kapuni Group sandstones. However, although a strong metamorphic source rock component is undisputable based on the evidence, it is commonly thought by a number of authors including Smale (1996) and King and Thrasher (1996), that alkali granites are dominant provenance for the Kapuni Group in the Taranaki Basin. A dominant plutonic provenance cannot be discounted for several reasons. Firstly, the mineralogy of the sandstones is compatible with an alkali granite source. Secondly, as previously mentioned plutonic rock fragments are often not found in thin-section. Thirdly, granites can contain shear zones where a high percentage of undulatory quartz can occur. Lastly, modal analyses in this study indicate a cratonic *(type)* origin for some sandstones in the Mangahewa Formation.

Metamorphic and plutonic source rocks both outcrop in the northwest Nelson area in the south of the Taranaki Basin. In this region a variety of metasedimentary rocks including gneisses, quartzites, phyllites, argillites and schists of Lower Cambrian to Permian age are present. Also in northwest Nelson the only outcropping plutonic rocks of the Separation Point and Karamea alkali granites in New Zealand occur. Although a correlative of the Separation Point Granite is identified in the Maui-4 well (Wodzicki, 1974). Separation Point and Karamea granites can be differentiated by their mineralogy. On the basis of abundant K-feldspars, presence of biotite and muscovite micas, absence of sphene and epidote, and scarcity of magnetite the older Karamea granite is the more compatible granitic source for the Kapuni Group.

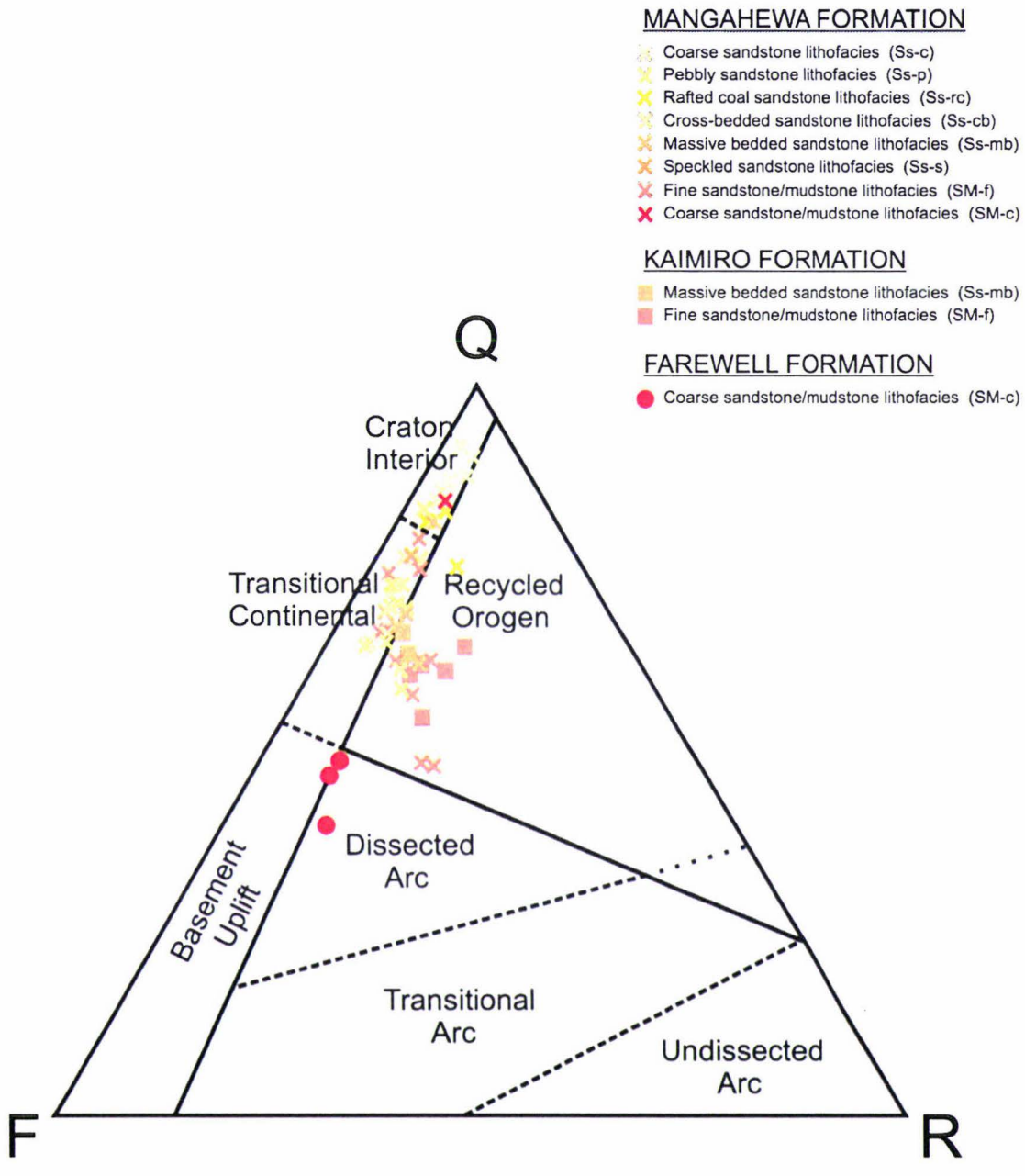

Figure 4.3: Modal analysis of the Kapuni Group sandstones in terms of quartz (Q), feldspar (F) and rock fragments (R) demonstrating relationship between framework composition and tectonic setting (after Dickinson *et al.*, 1983).

Chert, siltstone and shale lithics specifically indicate some degree of sedimentary input, particularly in the Kaimiro and Mangahewa Formations. A sedimentary source is supported by a modal analysis of the sandstones for both these formations. Potential sources include the greywacke-argillite sedimentary rocks of Triassic and Jurassic age that crop out to the northeast, east and southeast of the Taranaki Basin. While to the south of the basin the Upper Cretaceous Pakawau Group sediments consisting of conglomerates and coarse sandstones overlain by alternating sandstones, carbonaceous mudstones and coals (Bishop, 1971), outcrop in northwest Nelson. Both sedimentary sources are compatible and therefore neither can be discounted.

A volcanic source is also identified for the Kapuni Group sandstones. Feldspar mineralogy and modal analysis suggest that a volcanic source but may have been more important during deposition of the basal Farewell Formation, than in overlying Kaimiro and Mangahewa formations. Tasman-1 terminated in a post-Permian-pre-Upper Cretaceous red breccia containing a variety of acid volcanics (Wodzicki, 1974), although paleogeographic reconstructions by Palmer (1985), Robinson and King (1988), Palmer and Andrews (1993) and King and Thrasher (1996) negate this as a possible source for the Kapuni Group. The preferred source is acid volcanic rocks of Pre Cambrian to Upper Cretaceous age that occur in the northwest Nelson area.

Evidence from framework mineralogy and modal analysis clearly indicates that the Kapuni Group sandstones were derived from more than one main rock type. An interpretation of the evidence suggests that vertical changes in the composition of the Kapuni Group sandstones dominantly reflect source rock changes in the south of the Taranaki Basin, around the northwest Nelson area.

SANDSTONE DIAGENESIS

5.1 INTRODUCTION

Sandstone diagenesis is defined to include the many physical and chemical processes that affect sediment from the time it is deposited until metamorphism (Blatt, 1979). During burial, temperature and pressure increase and changes occur in pore-water chemistry, which result in the dissolution, precipitation and transfer of minerals, and the modification of primary textures, porosity and permeability. The purpose of this study is to identify diagenetic features in the Kapuni Group sandstones and resolve how post-depositional processes have modified the original sediment. Diagenetic processes recognised include compaction, clay mineral formation, precipitation of cements and the dissolution of detrital grains, matrix and cements.

5.2 MECHANICAL AND CHEMICAL COMPACTION

Mechanical and chemical compaction of the sandstones is due primarily to increasing weight of the overburden during burial. Overburden pressures cause water to be squeezed out of the rock, resulting in a significant decrease in rock volume and reduction in gross porosity. The effects of compaction in the Kapuni Group sandstones are characterised by the reorganisation of grains, deformation of ductile framework grains and fracturing of brittle grains.

5.2.1 Reorganisation of Grains

The reorganisation of grains demonstrates varying degrees of mechanical and chemical compaction in the Kapuni Group sandstones. In thin-section grain reorganisation is least pronounced in the coarse-grained, moderately-well to well-sorted Mangahewa Formation sandstones, such as the coarse sandstone (Ss-c) lithofacies. Greater degrees of grain reorganisation are recognised by the dominance of concavo-convex contacts in the Mangahewa and Kaimiro formations fine-grained, poorly to moderately sorted sandstones e.g. fine sandstone/mudstone (SM-f) lithofacies. Grains reorganisation is most pronounced in the deeper Farewell Formation coarse sandstone (Ss-c) lithofacies where concavo-convex and sutured grain boundaries predominate. In the Kapuni Group sandstones concavo-convex and sutured boundaries involve grains dissolving at their point of contact and are a minor form of pressure solution.

5.2.2 Plastic Deformation of Grains

Mechanical Compaction has resulted in the plastic deformation of ductile grains, causing them to be bent and penetrated by rigid grains and overgrowths and squeezed into adjacent pores. The plastic deformation of ductile grains is most pronounced in sandstones that are fine-grained and poorly- to moderately-sorted. Bent and kinked mica flakes and argillaceous rock fragments are the most commonly deformed grains (Plate 5.1). Plastic deformation of fecal pellets is greatest in the Mangahewa and Kaimiro fine sandstone/mudstone (SM-f) and subordinately in the massive bedded sandstone (Ss-mb) lithofacies. While, deformed glauconite pellets are common in the speckled sandstone (Ss-s) lithofacies. Plastic deformation of grains in the Kapuni Group sandstones appears not to have significantly affected quartz overgrowth development (Plate 5.2).

5.2.3 Fracturing of Grains

Grain fractures observed in thin-section may be attributed to mechanical compaction or localised tectonic movement along fault crush zones. It is not possible to differentiate between these processes based on thin-section observations, core or log data, therefore, their cause remains unclear in this study. Nevertheless, the brittle fracture of predominantly feldspars, brittle rock fragments and subordinate quartz grains is common and most pronounced in the coarser-grained, better sorted Mangahewa Formation coarse sandstone (Ss-c), pebbly sandstone (Ss-p) and coarse sandstone/mudstone (SM-c) lithofacies. Grain fractures in these sandstones are commonly filled with kaolinite, quartz, siderite or calcite. Where these fractures are not filled by authigenic minerals, they provide restricted areas of minor (<0.5%) secondary porosity in the sandstones.

5.3 CLAY MINERALS

Clay minerals in the Kapuni Group sandstones are both detrital and authigenic in origin. Detrital clays are those that were introduced into the sandstone during deposition by physical or biological processes. In contrast, authigenic clays are those which have formed in the sandstone either via precipitation from interstitial pore waters or through reactions between precursor minerals and interstitial pore waters. Composition, morphology, structure, texture and distribution allow differentiation between detrital and authigenically derived clays.

5.3.1 Detrital Clays

Detrital clays observed in thin-section include dispersed matrix, intercalated laminae, argillaceous rock fragments, carbonaceous mudstone intraclasts and fecal pellets deposited during sediment deposition. These clays were recognised as solid rounded clay

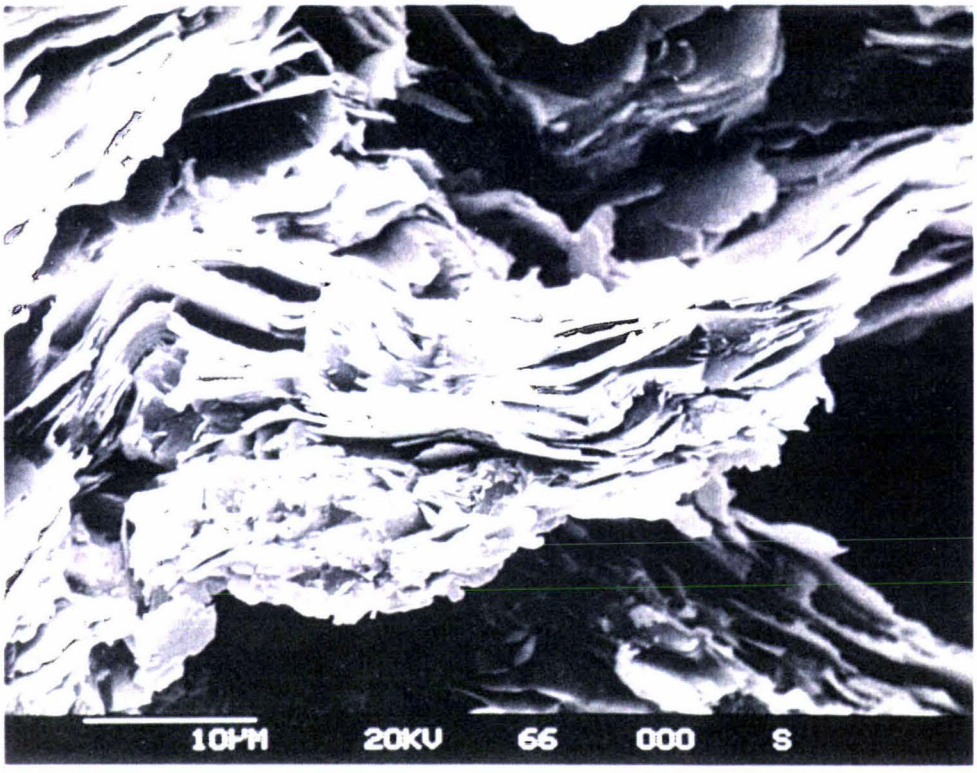

Plate 5.1: Scanning electron micrograph of bent and kinked mica (muscovite) with illite flakes forming from the margins of some mica sheets in the Mangahewa Formation fine sandstone/mudstone (SM-f) lithofacies (Sample 1, Kapuni-1)

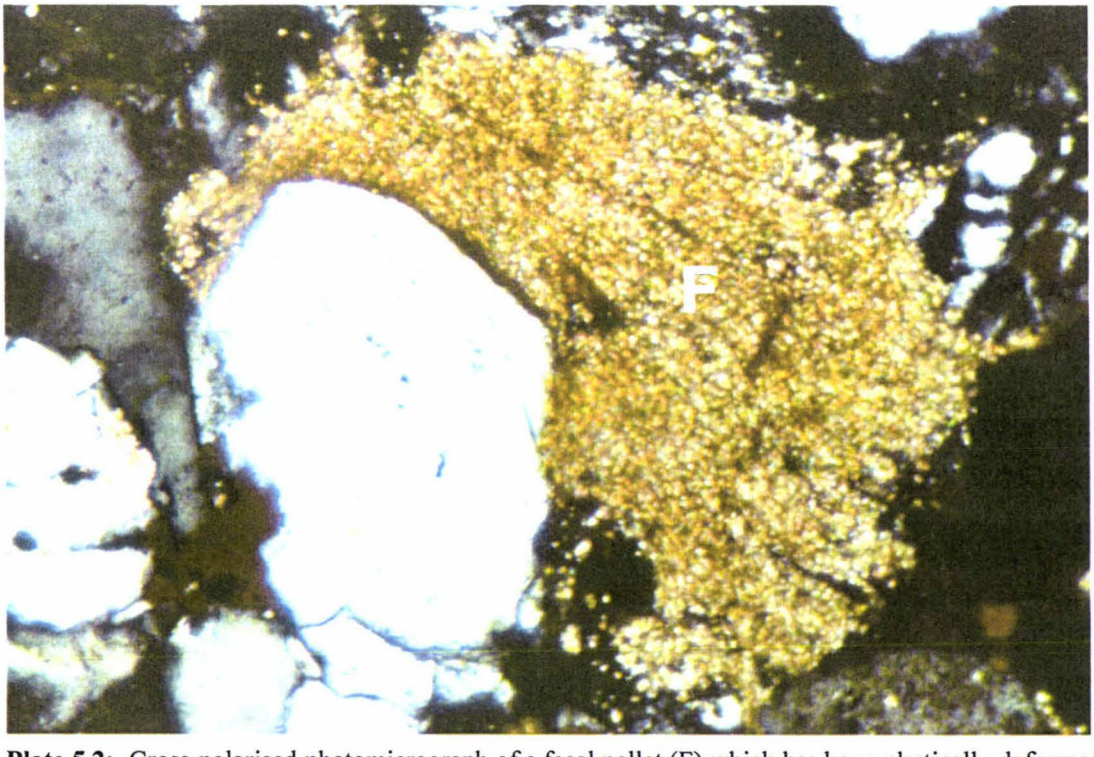

Plate 5.2: Cross-polarised photomicrograph of a fecal pellet (F) which has been plastically deformed around detrital quartz (Q) and secondary quartz overgrowth (SQ) in the Mangahewa Formation fine sandstone/mudstone (SM-f) lithofacies, photomicrograph x16 (Sample 4, Kapuni-3)

aggregates with deformed morphologies and poor crystalline habits (Plate 5.3). In SEM detrital clays were only identified in the Mangahewa Formation speckled sandstone (Ss-s), massive bedded sandstone (Ss-mb) and fine sandstone/mudstone (SM-f) lithofacies.

5.3.2 Authigenic Clays

Authigenic clays are distinguished by their high degree of crystallinity, delicate crystalline habits and large particle size (Wilson and Pittman, 1977). In the sandstones authigenic clays were observed lining pores, filling pores, filling fractures and as pseudomorph replacements. Authigenic clays identified by XRD, DTA, IR analysis and SEM included kaolinite, illite, vermiculite, chlorite and smectite. These common clays were also interstratified with one other (mixed-layered) adopting a composition, morphology, structure, texture and distribution similar to one of the participating clay minerals.

i. Kaolinite

Authigenic kaolinite occurs as crystalline, pseudohexagonal stacked platelets or books, exhibiting face-to-face stacks and vermicular (veriform) habits (Plates 5.4 and 5.5). The delicate vermicular kaolinite habit, however, is the more common form. The size and crystallinity of kaolinite varies considerably in the sandstones. Authigenic kaolinite platelets typically measure 2 - 10μm across, although some platelets occur up to 20μm in width. Two distinct size classes of kaolinite were observed in SEM, constituting discrimination as fine and coarse kaolinite series. The identification of two distinct sizes has also been previously documented in the Kapuni Group by Hogan (1979) and Collen (1988) in the Kapuni Field and elsewhere in the Taranaki Basin.

In the Kapuni Group sandstones the finer kaolinite series (2 - 10μm) is more common. The finer kaolinite consists of tightly to loosely packed booklets, which often exhibit dissolution effects along the surface and margins of the platelets and books (Plate 5.6). The coarser kaolinite series (10 - 20μm) occurs as localised aggregates of crystalline platelets that are typically tightly stacked, and appear relatively fresh (Plate 5.7). The coarse kaolinite is less common and although not exclusive too, is most prevalent in the coarse sandstone (Ss-c), pebbly sandstone (Ss-p), rafted coal sandstone (Ss-rc), and coarse sandstone/mudstone (SM-c) lithofacies. Frequently these two sizes occur side by side (Plate 5.8).

Kaolinite has been predominantly derived from the neotransformation of feldspar as a pseudomorphous replacement. In SEM kaolinite is observed partially to completely replacing feldspars grains or infilling voids left by the dissolution of detrital grains (Plate 5.9). In most cases, where feldspar has been replaced the texture of the host grain has been preserved. Kaolinite platelets and books are occasionally grooved or notched (Plate

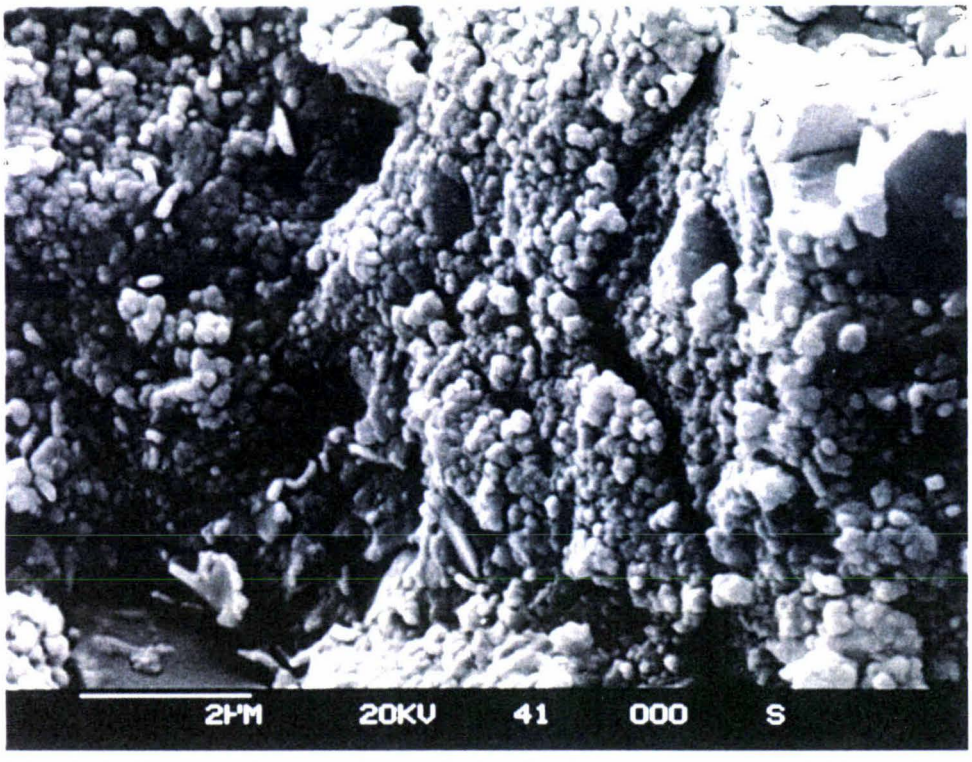

Plate 5.3: Scanning electron micrograph showing fine aggregates of detrital clay in the Mangahewa Formation fine sandstone/mudstone (SM-f) lithofacies (Sample 20, Kapuni-3)

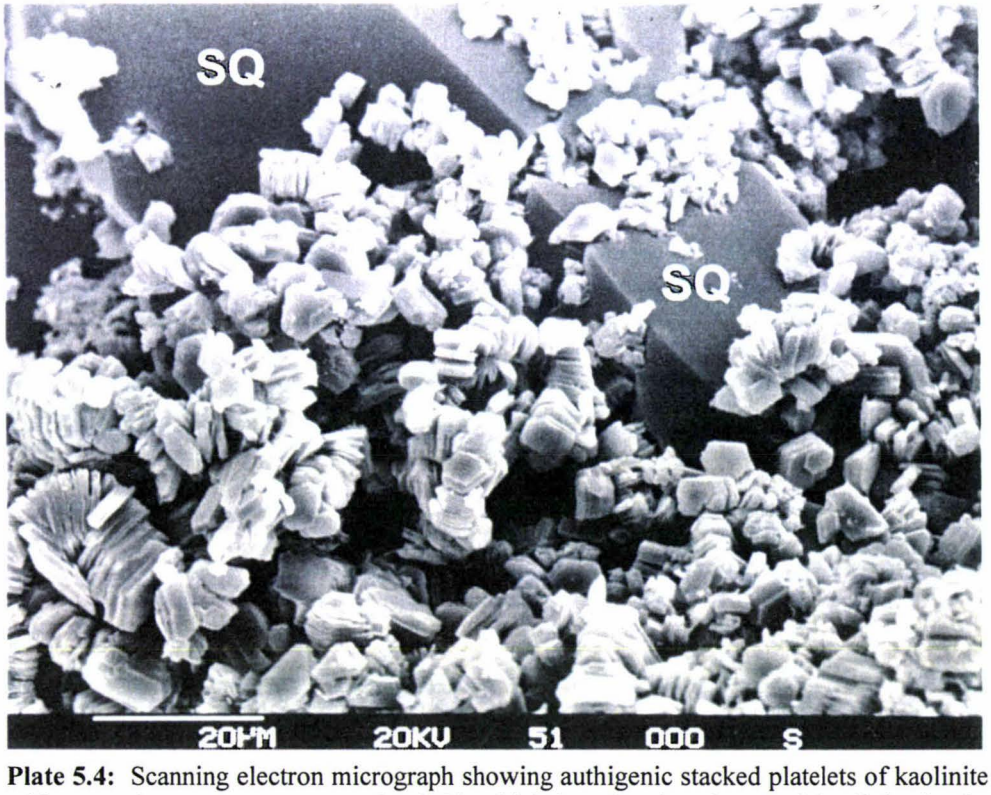

Plate 5.4: Scanning electron micrograph showing authigenic stacked platelets of kaolinite with secondary quartz overgrowths (SQ) which has developed around kaolinite in the Mangahewa Formation rafted coal sandstone (Ss-rc) lithofacies (Sample 45, Kapuni-14)

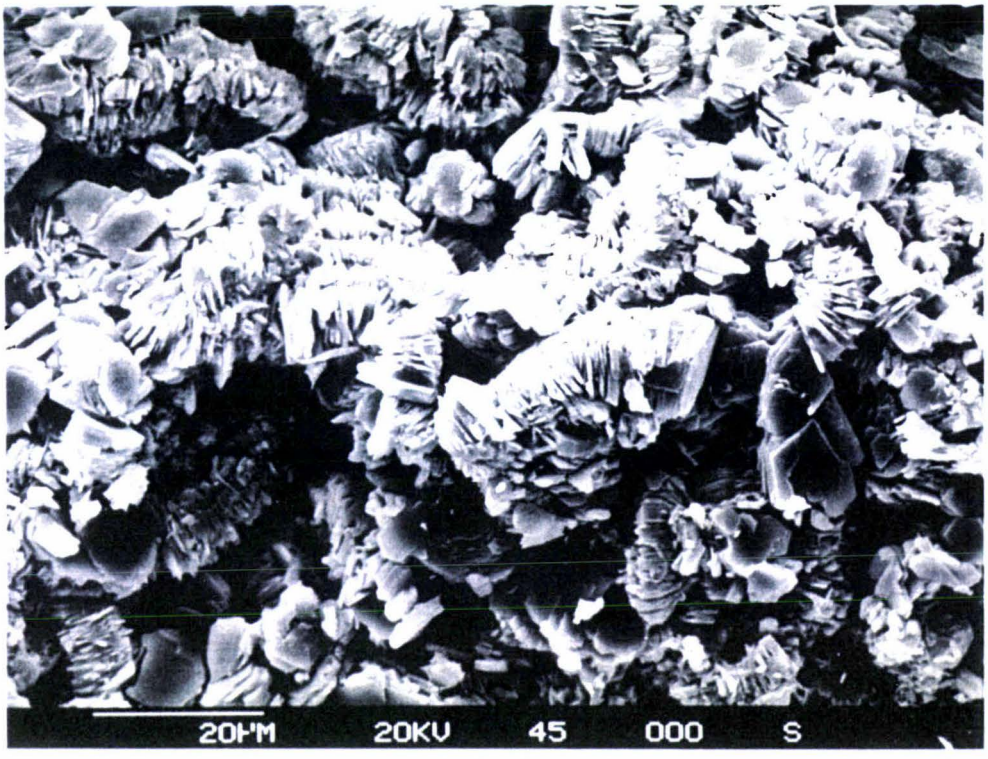

Plate 5.5: Scanning electron micrograph showing authigenic vermicular kaolinite in the Mangahewa Formation speckled sandstone (Ss-s) lithofacies (Sample 24, Kapuni-12)

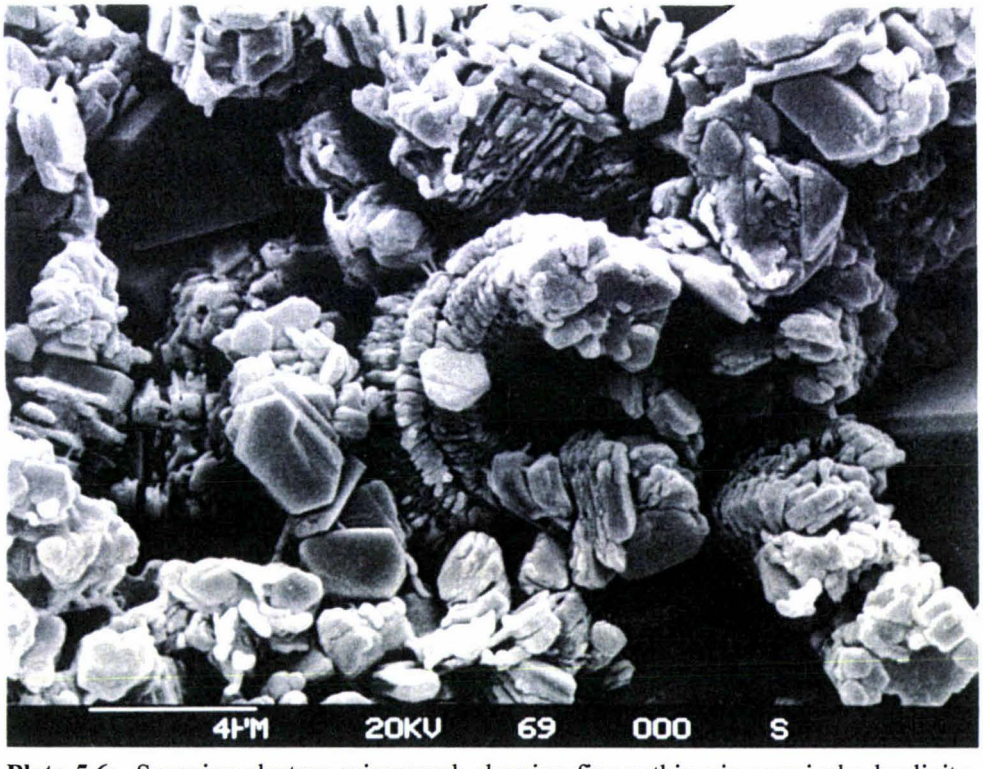

Plate 5.6: Scanning electron micrograph showing fine authigenic vermicular kaolinite platelets that exhibit dissolution effects along their margins in the Mangahewa Formation coarse sandstone/mudstone (SM-c) lithofacies (Sample 35, Kapuni-14)

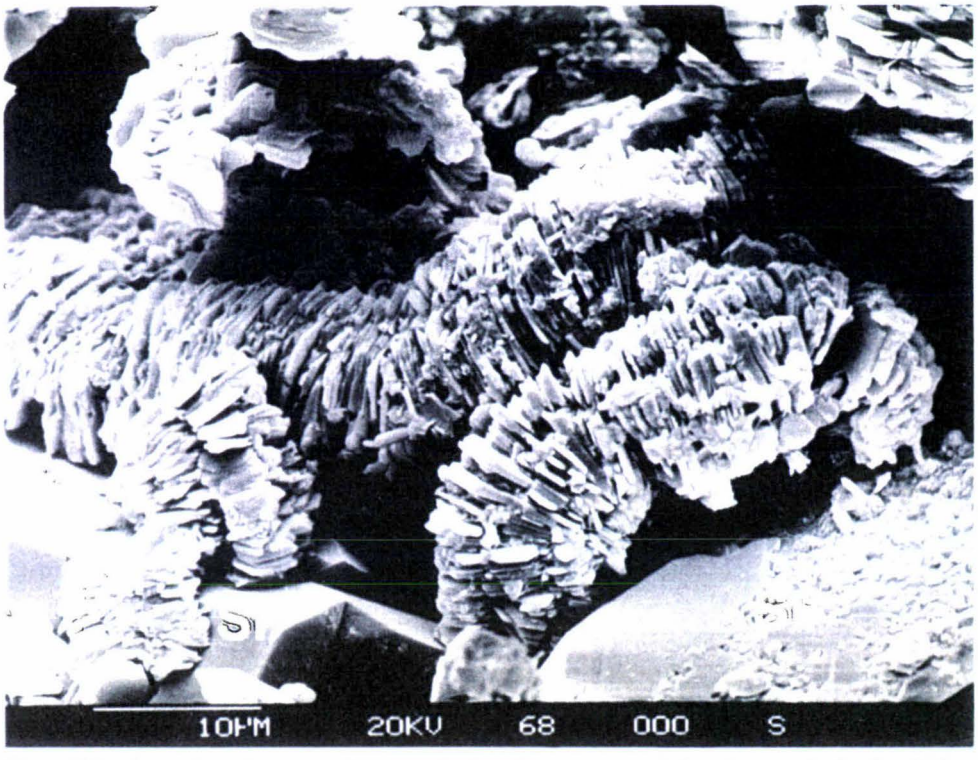

Plate 5.7: Scanning electron micrograph showing coarse authigenic vermicular kaolinite platelets that appear relatively fresh in the Mangahewa Formation pebbly sandstone (Ss-p) lithofacies – note the leaching of the adjacent secondary feldspar overgrowth (SF) (Sample 27, Kapuni-12)

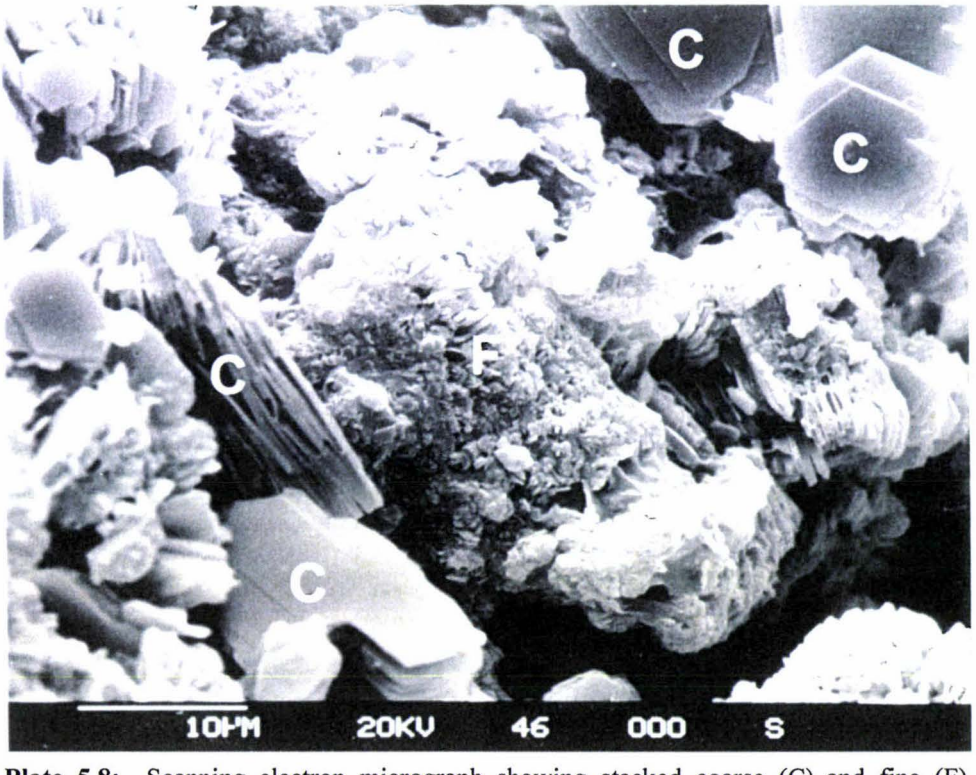

Plate 5.8: Scanning electron micrograph showing stacked coarse (C) and fine (F) authigenic kaolinite series occurring side by side in the Farewell Formation coarse sandstone/mudstone (SM-c) lithofacies (Sample 31, Kapuni Deep-1)

Plate 5.9: Scanning electron micrographs showing authigenic kaolinite deriving from the pseudomorphous replacement of feldspar: (A) Vermicular kaolinite altering from feldspar in Mangahewa Formation rafted coal sandstone (Ss-rc) lithofacies (Sample 16, Kapuni-3); (B) Kaolinite platelets with ragged edges altering from the Mangahewa Formation cross-bedded sandstone (Ss-cb) lithofacies (Sample 52, Kapuni-15); (C) Vermicular kaolinite altering from feldspar in the Mangahewa Formation pebbly sandstone (Ss-p) lithofacies (Sample 48, Kapuni-15); (D) Vermicular kaolinite preserving the original grain texture in the Kaimiro Formation fine sandstone/mudstone (SM-f) lithofacies (Sample 22, Kapuni-8)

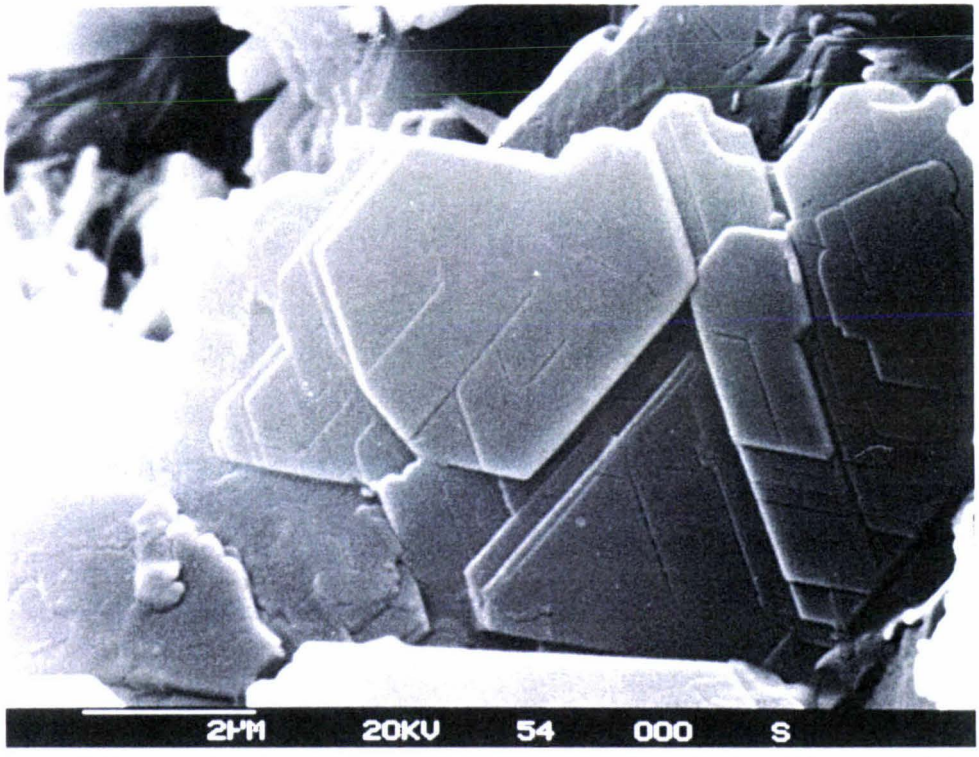

Plate 5.10: Scanning electron micrograph of grooves and notches in authigenic kaolinite platelets in the Mangahewa Formation pebbly sandstone (Ss-p) lithofacies (Sample 49, Kapuni-12)

5.10). Mansfield and Bailey (1972) suggest that such markings on kaolinite are indications of twinning that existed in the precursor mineral. In thin-section twinning was observed in detrital plagioclase and microcline feldspars.

Kaolinite has also precipitated directly from interstitial formation waters filling pores. Pore-filling kaolinite booklets plug pores, and exhibit no apparent alignment relative to the detrital grain (Plate 5.11). Thin-section studies indicate that kaolinite has also precipitated into grain fractures in some Mangahewa Formation sandstones e.g. coarse sandstone (Ss-c) lithofacies. It is also likely that kaolinite has neotransformed from detrital clays. However, such clays are difficult to distinguish from kaolinite derived from primary minerals or direct precipitation from interstitial pore waters, and despite extensive SEM studies could not be identified with certainty in this study.

The derivation of kaolinite from feldspar occurs via the removal of soluble bases in acidic conditions. As a consequence of feldspar dissolution, kaolinite precipitates according to: $2KAlSi_3O_8 + 2H^+ + 9H_2O$ *(Feldspar)* $\rightarrow AL_2Si_2O_5(OH)_4 + 4H_4SiO_4 + 2K^+$ *(Kaolinite)*. The acidic conditions required for kaolinite formation, often prevail soon after burial (Hancock, 1978; Hancock and Taylor, 1978; Sommer, 1978) or after structural inversion (Lanson, 2002). In these circumstances the required alumina for the transformation is generally bought in by fresh meteoric circulating pore waters moving fteely through the sandstones. Maturation of organic matter could have also been responsible for providing the low pH conditions required for kaolinite formation. During maturation of organic matter H_2O and CO_2 are removed as carboxyl, methoxyl and hydroxyl compounds (Füchtbauer, 1967), favouring the dissolution of feldspar and formation of kaolinite. The role of these compounds is well demonstrated by Gaupp *et al.* (1993) and Platt (1993) in their studies of the Permian Rotliegend sandstones in northwest Germany where the subsequent precipitation of kaolinite at the expense of feldspar occurred specifically at the contacts with the Carboniferous Coal Measures formation.

ii. Illite

SEM studies show that illite is authigenic in origin, occurring as irregular flakes with delicate lath-like tendrils. The morphology of illite varies in the sandstones depending on the development of these tendrils (Plate 5.12). In most cases the edges of these flakes project tendrils that are relatively short. However, occasionally, these sheets develop relatively long, delicate-appearing tendrils up to 5μm long. The commonly reported habit of long tendrils of illite forming dense masses bridging the pore spaces between framework grains (Wilson and Pittman, 1977), was not observed. However, as illite tendrils collapse on drying (McHardy *et al.*, 1982), this habit may have once been more prevalent in the sandstones than is now observed in SEM studies.

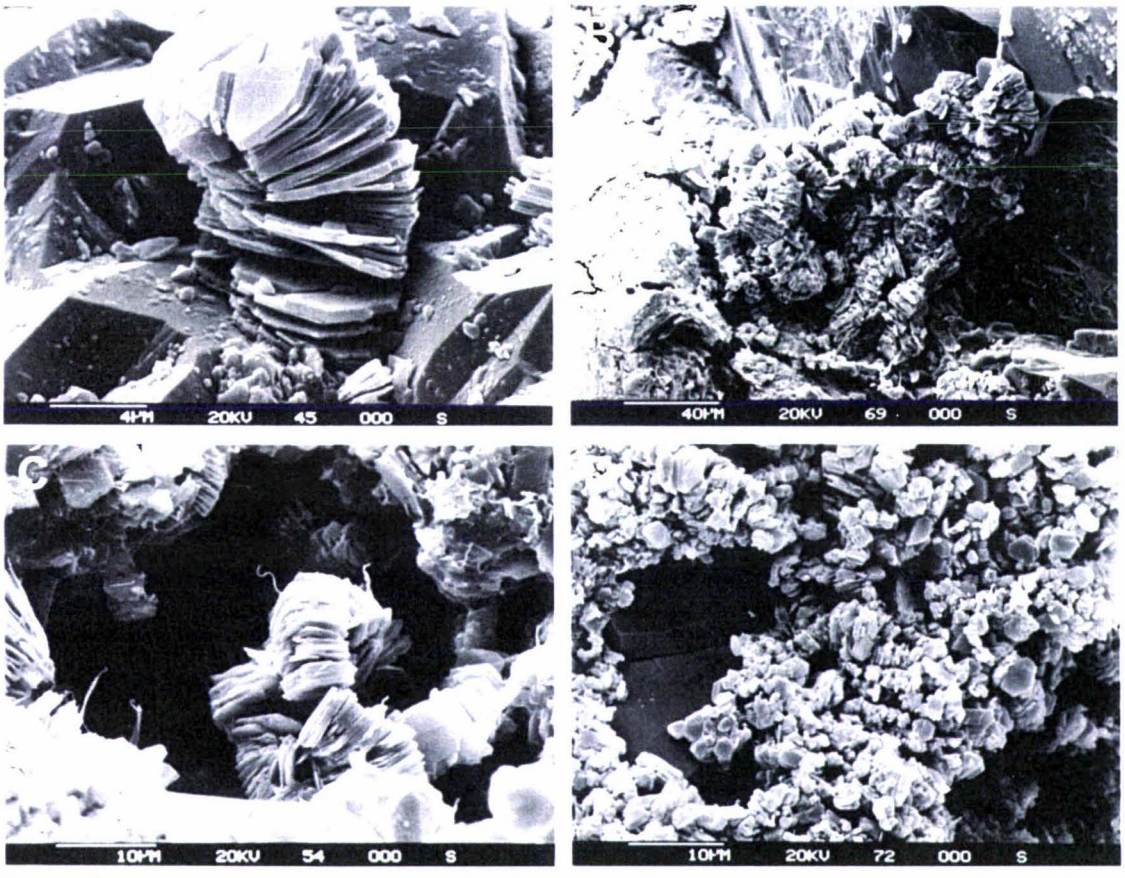

Plate 5.11: Scanning electron micrographs showing authigenic kaolinite that has precipitated from interstitial pore waters into pores throats and with no apparent alignment relative to detrital grain surfaces; (A) single vermicular kaolinite booklet attached to quartz overgrowth in the Mangahewa Formation pebbly sandstone (Ss-p) lithofacies (Sample 28, Kapuni-12); (B) vermicular kaolinite attached to the surface of a feldspar grain in the Farewell Formation coarse sandstone/mudstone (SM-c) lithofacies (Sample 32, Kapuni Deep-1); (C) vermicular kaolinite booklets filling a pore throat in the Mangahewa Formation fine sandstone mudstone (SM-f) lithofacies - note the fine illite tendrils extending from some kaolinite platelets (Sample 1, Kapuni-1); (D) kaolinite stacks filling pores in the Mangahewa Formation coarse sandstone (Ss-c) lithofacies (Sample 39, Kapuni-14)

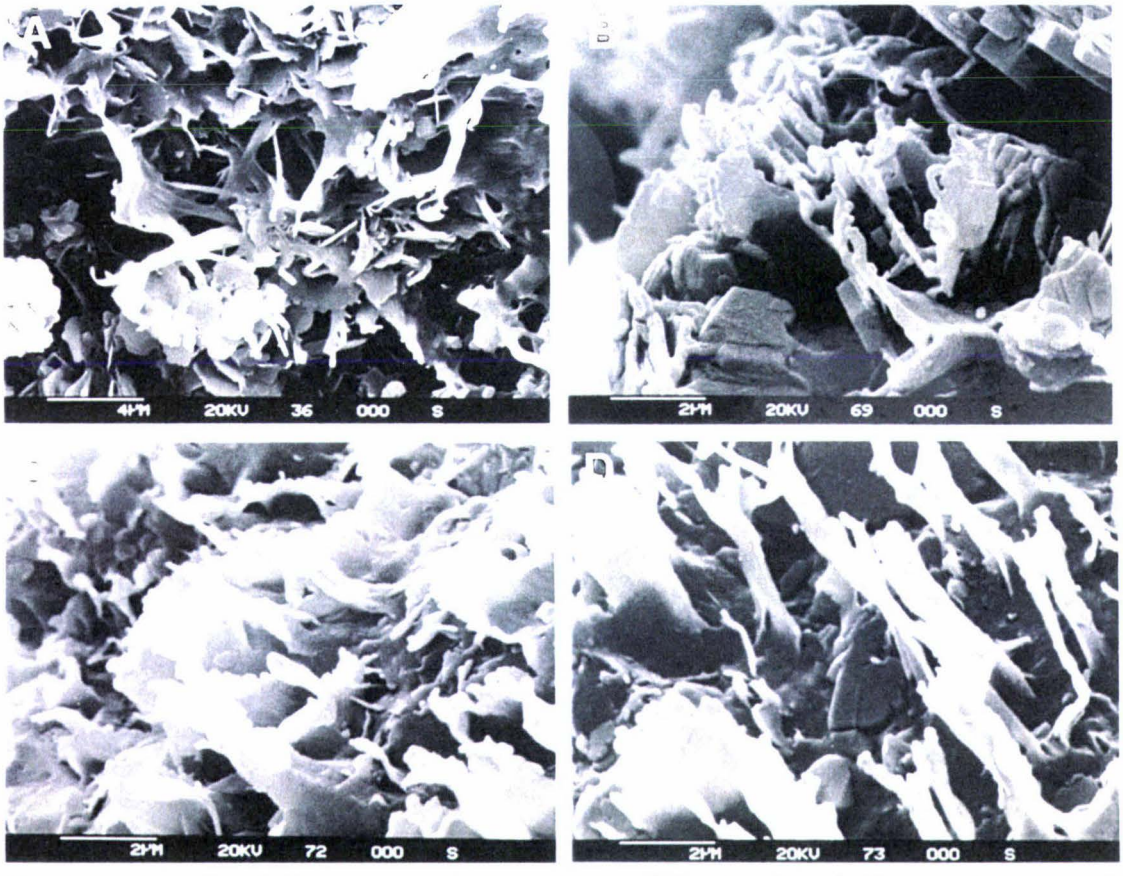

Plate 5.12: Scanning electron micrographs demonstrating different authigenic illite morphologies: (A) spiny illite tendrils in the Kaimiro Formation fine sandstone/mudstone (SM-f) lithofacies (Sample 6, Kapuni-1), (B) short illite flakes with short tendrils in the Mangahewa Formation coarse sandstone/mudstone (SM-c) lithofacies (Sample 35, Kapuni-14), (C) wide short illite flakes in the Mangahewa Formation coarse sandstone (Ss-c) lithofacies (Sample 39, Kapuni-14), (D) long illite flakes in the Mangahewa Formation coarse sandstone (Ss-c) lithofacies (Sample 41, Kapuni-14)

Illite is mostly observed in SEM neoforming from the edges of kaolinite platelets (Plate 5.13). Illite has also precipitated directly in pores and pore throats attaching to detrital grains, where they curl away from the point of attachment (Plate 5.14). Less commonly, illite has also been derived directly from feldspars and feldspar overgrowths and detrital muscovite grains (Plate 5.15 and 5.16). Mixed-layer illite is common, with XRD studies demonstrating the existence of illite/vermiculite in the Mangahewa and Kaimiro formations, illite/smectite in the Mangahewa and Farewell formations, while illite/chlorite is restricted to the Mangahewa Formation.

Illite clay minerals form where circulating pore fluids are alkaline (Hancock and Taylor, 1978). Under alkaline conditions kaolinite may alter to illite (Dunoyer de Segonzac, 1970). It is commonly observed in studies in the North Sea that a minimum temperature of ~100 - 140°C, which corresponds to an average burial depth of 3.0 – 3.5km, is required before extensive illitisation of kaolinite begins (Bjørlykke *et. al.*, 1986, Ehrenberg and Nadeau, 1989; Scotchman *et al.*, 1989 and Giles *et al.*, 1992). This temperature threshold corresponds to the thermodynamical destabilisation temperature of kaolinite and K-feldspar (+ quartz) assemblage (Lanson *et al.*, 2002), according to the reaction: $KAlSi_3O_8$ *(K-feldspar)* + $Al_2Si_2O_5(OH)_4$ *(Kaolinite)* → $KAl_3Si_3O_{10}(OH)_2$ *(illite)* + $2SiO_{2(aq)}$ + H_2O *(quartz)*. The maturation of organic matter at the latter stages of coalification may have been important for illite development during burial causing the pH of pore waters to rise to neutral or slightly alkaline.

iii. Vermiculite

Vermiculite resembles mica in structure and only differs by having a lower layer charge and the presence of inter-layered water. Authigenic vermiculite was not observed in SEM, but it presence was confirmed by XRD. Vermiculite clay is formed through the alteration of biotite or illite precursor minerals (Bjørlykke *et al.*, 1989). Neoformation of vermiculite from these minerals is therefore inferred for the Kapuni Group sandstones. Furthermore, the identification of mixed-layer illite/vermiculite and chlorite/vermiculite suggests that transformation occurs through these inter-layered precursors. Vermiculite forms in pore waters with a high pH. The latter stages of organic matter maturation may have been responsible for raising the pore waters to neutral or slightly alkaline favouring the formation of vermiculite.

iv. Chlorite

Chlorite was identified by XRD in the Mangahewa and Kaimiro formations. In SEM authigenic chlorite has a pore-lining habit, exhibiting a cellular structure composed of idiomorphic crystals commonly 2 - 3μm across in diameter, which are attached at their edges to framework grains. In SEM these crystals have a face-to-edge orientation, are

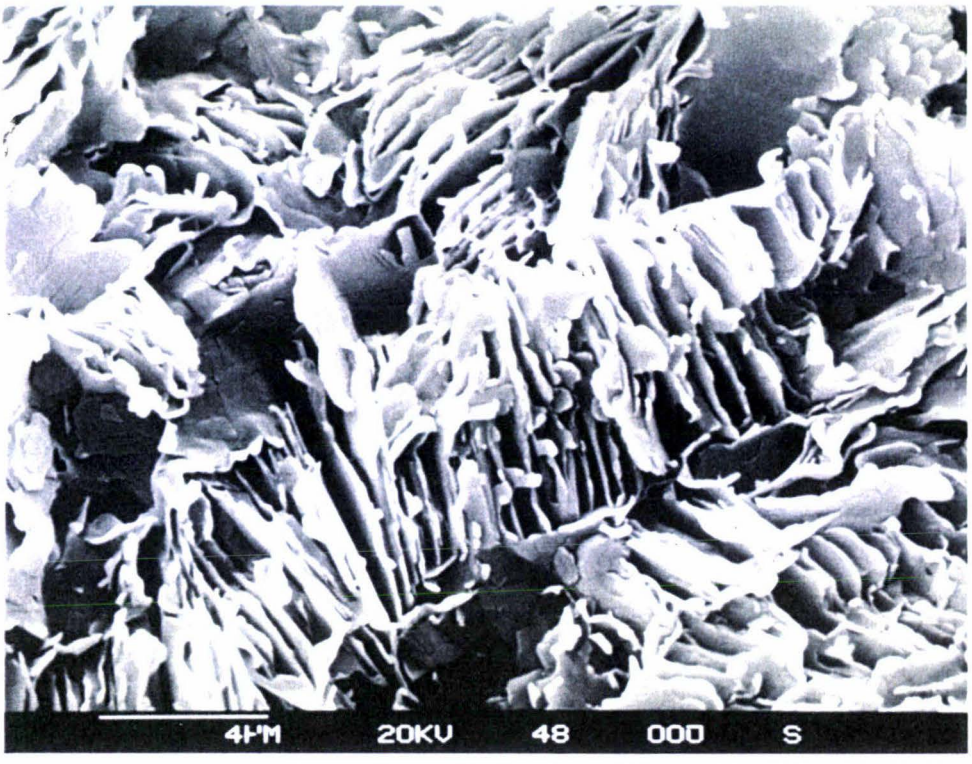

Plate 5.13: Scanning electron micrograph showing authigenic illite flakes developing from kaolinite platelets in the Kaimiro Formation fine sandstone/mudstone (SM-f) lithofacies (Sample 32, Kapuni-8)

Plate 5.14: Scanning electron micrograph showing authigenic illite which has precipitated in pore throats onto quartz overgrowths where they characteristically curl away from their point of attachment in the Mangahewa Formation massive bedded sandstone (Ss-mb) lithofacies (Sample 10, Kapuni-3)

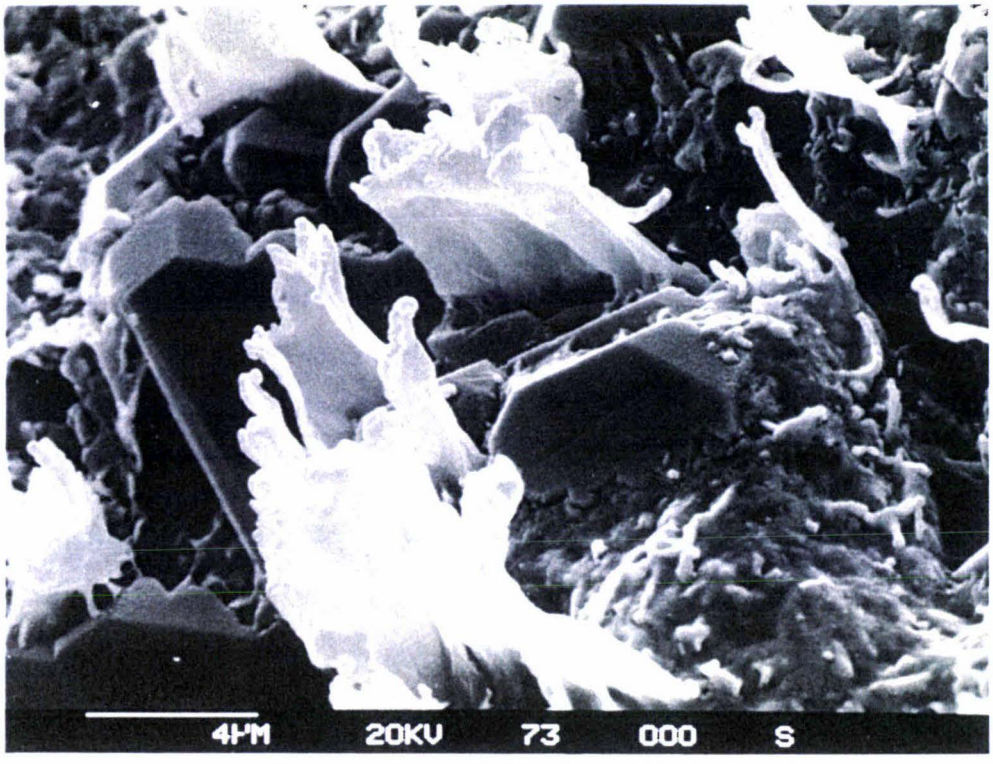

Plate 5.15: Scanning electron micrograph showing authigenic illite flakes developing directly from detrital feldspar grains and feldspar overgrowths in the Mangahewa Formation coarse sandstone (Ss-c) lithofacies (Sample 40, Kapuni-14)

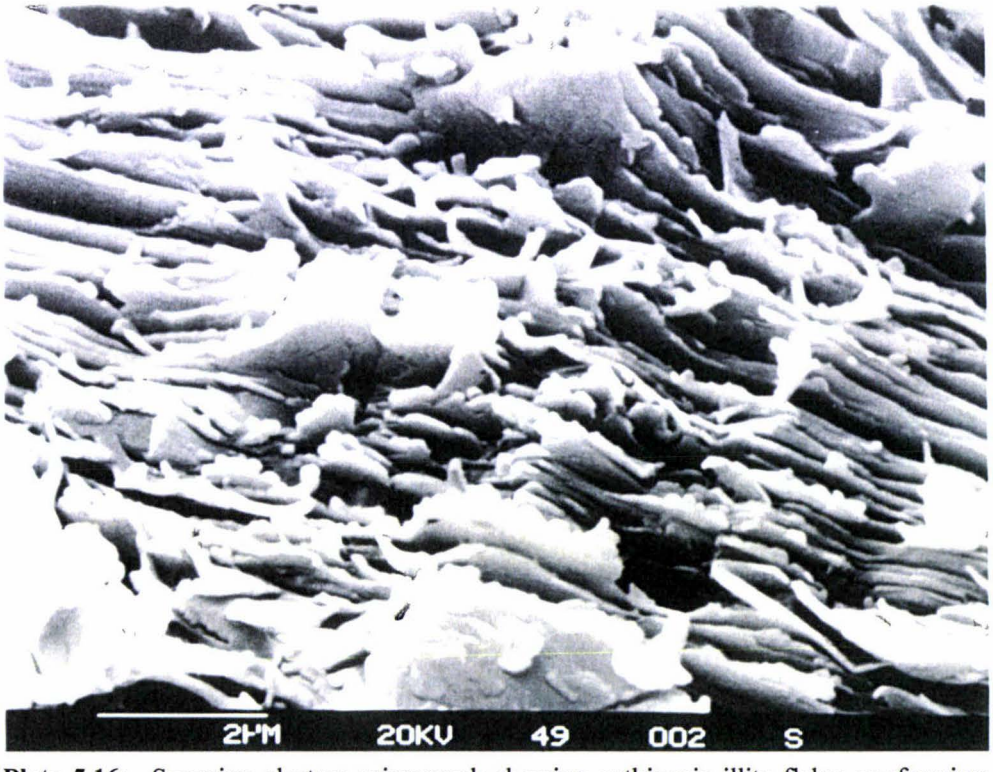

Plate 5.16: Scanning electron micrograph showing authigenic illite flakes neoforming from muscovite sheets in the Farewell Formation coarse sandstone (Ss-c) lithofacies (Sample 33, Kapuni Deep-1)

commonly curved and intersect, giving them a characteristic honeycomb pattern. Thin-section observations suggest that chlorite has developed from the alteration of precursor biotite, either directly or from illite/chlorite, chlorite/vermiculite or chlorite/smectite mixed-layered clays. Mixed-layer illite/chlorite and chlorite/smectite occur in the Mangahewa Formation, while chlorite/vermiculite was identified in the Farwell Formation. Chlorite forms in pore waters with a high pH. The final stages of organic matter maturation may have been responsible for raising the pore waters to neutral or slightly alkaline favouring the formation of chlorite.

vi. Smectite

Smectite clays were only identified in the Farewell Formation. Authigenic smectite occurs as pore-lining clay, with honeycomb aggregates forming a cellular structure (Plate 5.17). SEM and XRD studies revealed that smectite is more commonly found inter-layered with other clay species, within the Mangahewa and Farewell formations. Illite/smectite is the most common mixed-layer clay, identified in the Mangahewa and Farewell formations. Rare chlorite/smectite also occurs in the Mangahewa Formation. The presence of mixed-layer illite/smectite and chlorite/smectite, indicate that this transformation occurs through inter-layered clay precursors. Smectite forms in neutral or slightly alkaline pore waters. Such conditions occur at the latter stages of organic matter maturation.

5.4 CARBONATE CEMENTATION AND NEOFORMATION

5.4.1 Siderite

Siderite is the most abundant carbonate mineral in the Kapuni Group sandstones, and was particularly abundant in the Mangahewa Formation massive bedded sandstone (Ss-mb) and fine sandstone/mudstone (SM-f), and Farewell Formation coarse sandstone/mudstone (SM-c) lithofacies. In the sandstones siderite occurs as disseminated grains, concentrated as nodules or thin laminae. SEM studies demonstrate the typical euhedral habit of authigenic siderite, occurring as rhombs either singly or more commonly as clusters (Plate 5.18). In thin-section siderite is a uniform to patchy distributed cement, filling pores and fractures and corroding the margins of detrital quartz and feldspars and secondary syntaxial overgrowths on these grains (Plate 5.19).

5.4.2 Calcite

Authigenic calcite was identified by XRD in most Kapuni Group sandstone lithofacies. In thin-section calcite occurs as micritic intraclasts (micrite), and pore-filling microcrystalline cement (spar). Micrite is observed partially to completely replacing detrital feldspar grains and overgrowths (Plate 5.20). Plagioclase and microcline are the

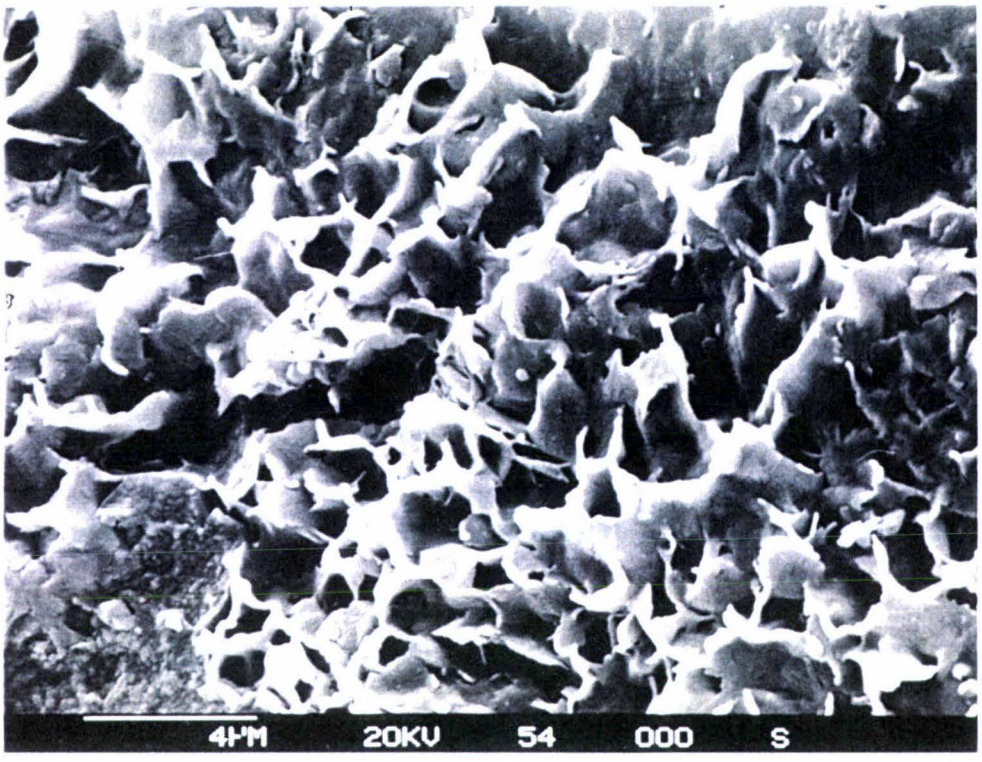

Plate 5.17: Scanning electron micrograph of smectite occurring as honeycomb aggregates with a cellular structure in the Farewell Formation coarse sandstone/mudstone (SM-c) lithofacies (Sample 32, Kapuni Deep-1)

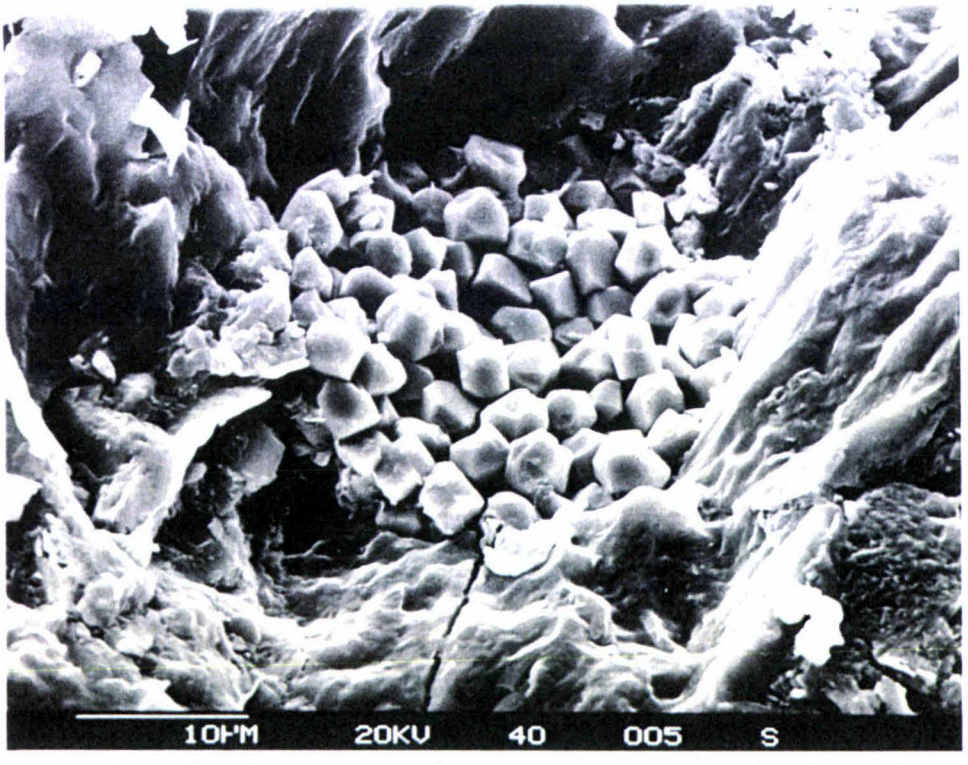

Plate 5.18: Scanning electron micrograph showing euhedral siderite rhombs concentrated as a nodule in a corroded feldspar grain in the Mangahewa Formation rafted coal sandstone (Ss-rc) lithofacies (Sample 18, Kapuni-3)

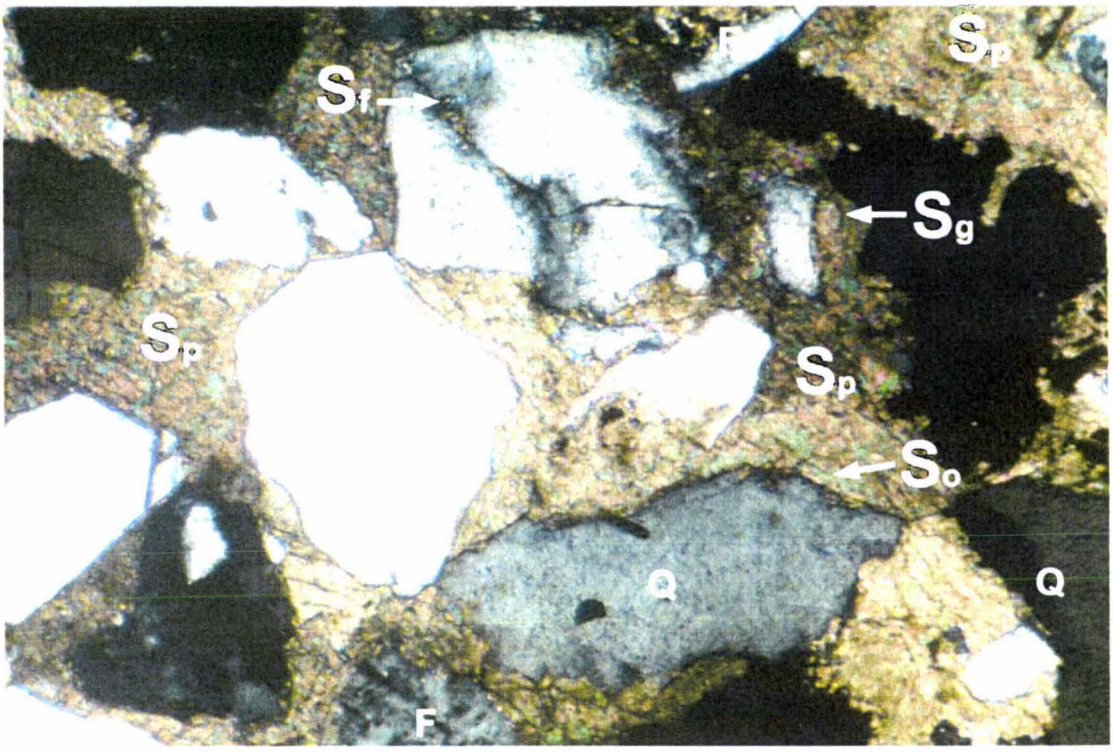

Plate 5.19: Cross-polarised photomicrograph showing uniform siderite cement filling pores (S_p) filling fractures (S_f) and corroding detrital grains (S_g) and secondary overgrowths (S_o) in the Mangahewa Formation fine sandstone/mudstone (SM-f) lithofacies (note Q = Quartz and F = Feldspar), photomicrograph x10 (Sample 2, Kapuni-1)

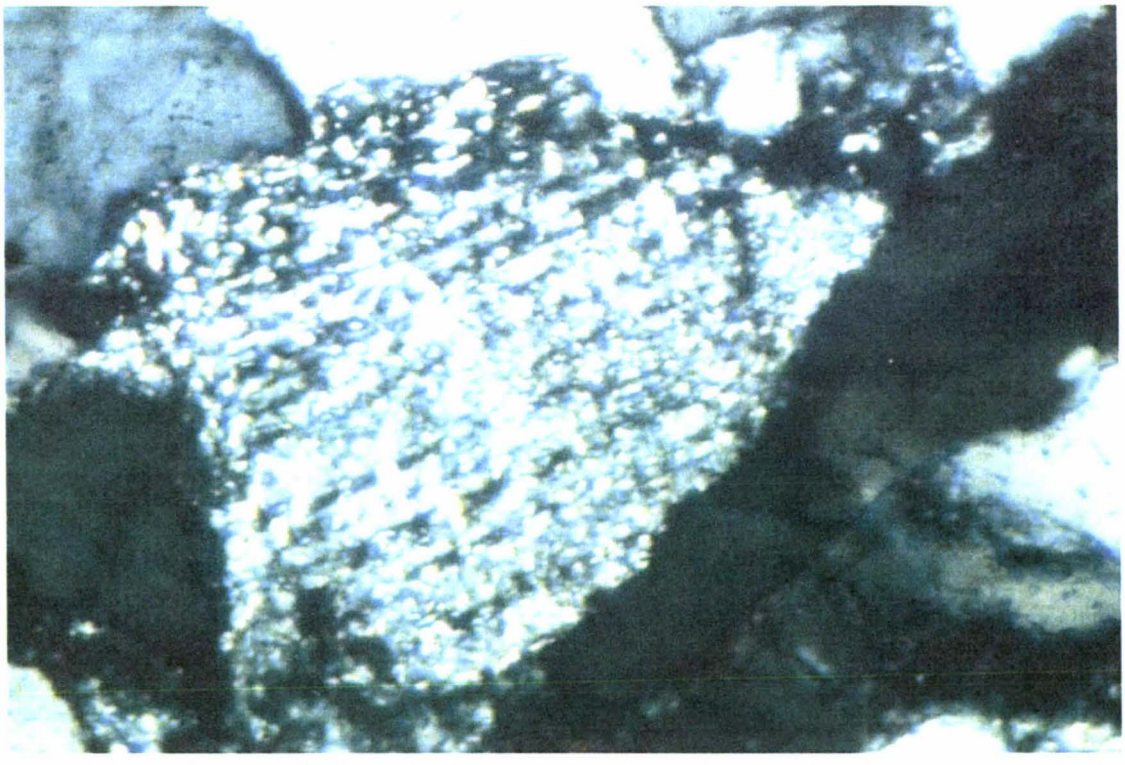

Plate 5.20: Cross-polarised photomicrograph showing micritic calcite intraclasts extensively replacing plagioclase feldspar and secondary overgrowth in the Farewell Formation coarse sandstone/mudstone (SM-c) lithofacies, photomicrograph x18 (Sample 33, Kapuni Deep-1)

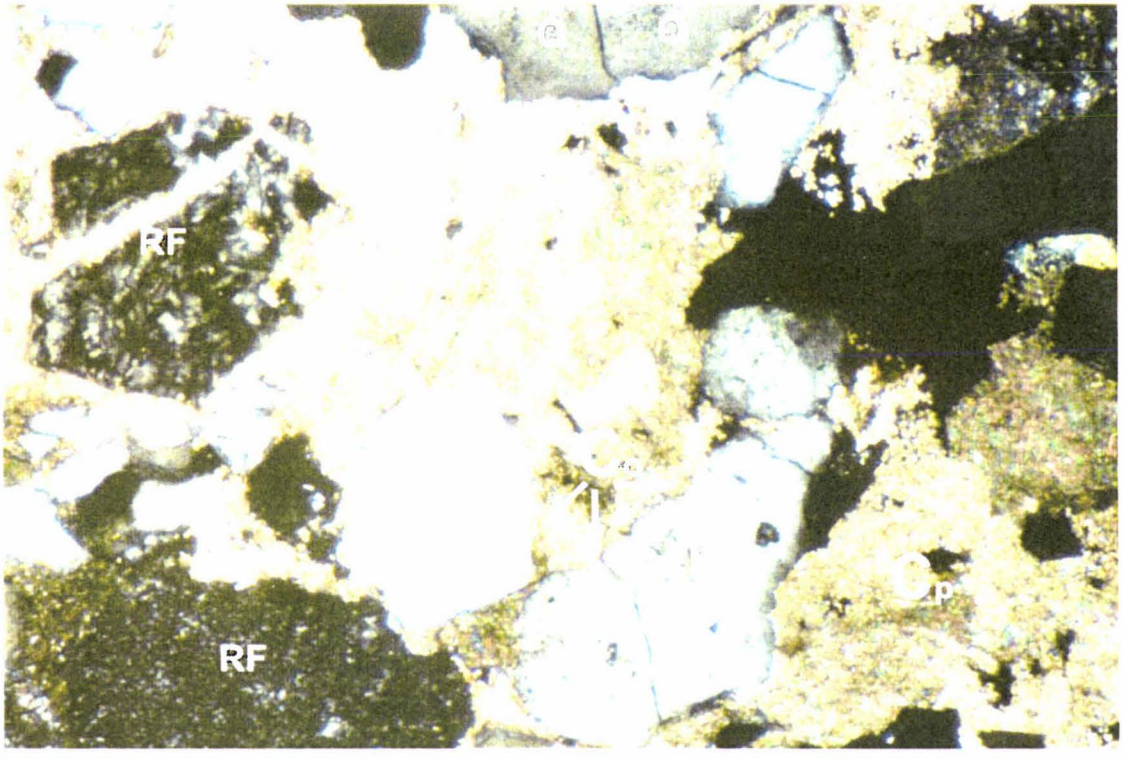

Plate 5.21: Cross-polarised photomicrograph showing uniform microcrystalline calcite cement filling pores and corroding grains (C_g) and secondary overgrowths (C_o) in the Mangahewa Formation fine sandstone/mudstone (SM-f) lithofacies (note Q = Quartz, F = Feldspar and RF = Rock Fragment), photomicrograph x6.3 (Sample 17, Kapuni-3)

most common grains affected by micrite replacement. Spar occurs as a uniform and patchy distributed pore-filling cement, corroding quartz and feldspar grains and secondary overgrowths and is also observed filling grain fractures in the sandstones (Plate 5.21). In some Mangahewa Formation fine sandstone/mudstone (SM-f) lithofacies spar occupies up to 40% of the rock.

5.4.3 Other Carbonate Minerals

Minor cement forming carbonate minerals include dolomite, dawsonite and laumontite. Dolomite is a rare authigenic carbonate mineral filling pores and was only identified in some Mangahewa Formation pebbly sandstone (Ss-p) and fine sandstone/mudstone (SM-f) lithofacies. Authigenic dolomite was only identified by XRD in the Mangahewa Formation fine sandstone/mudstone (SM-f) lithofacies and cross-bedded sandstone (Ss-cb) lithofacies. Authigenic dawsonite occurs in the Mangahewa and Farewell formations as fibrous aggregates, replacing calcic feldspars. The calcium zeolite laumontite was not observed in thin-section, but was identified by XRD in the Mangahewa Formation pebbly sandstone (Ss-p) lithofacies. Mason (1966) notes that laumontite is generally authigenic where it is identified in sedimentary rocks.

The composition and crystal habit of carbonate minerals depend on both the physical and chemical environment of the sandstones. In their study of the Mangahewa Formation in the Inglewood-1 well Hill and Collen (1978) found evidence to suggest that calcareous horizons are concentrated around coal seams, where the maturation of organic matter creates alkaline conditions favourable for carbonate deposition. These findings are consistent with this study, as well-cemented calcareous horizons were frequently observed in core near thin coal beds or near concentrations of organic matter. Carbonate cementation and neoformation can occur in sandstones over a wide-range of temperatures and burial depths and are a function of pH and Eh of the circulating pore fluids (North, 1985). The pore waters containing carbonate may be meteoric or they may be squeezed from shales during decarboxylation of organic matter.

The salinity of the pore waters and the Ca/Mg/Fe ratio are of particular importance in determining the type of carbonate mineral precipitated. Siderite precipitation is entirely dependent on the Eh of the environment as it will only form reducing conditions where Fe is present (Krumbein and Garrels, 1952; Garrels and Christ, 1965). Blanche and Whitaker (1978) documented in a study of the Brent Sand Formation (Middle Jurassic) in the northern part of the North Sea Basin that siderite precipitation requires a rise in the pH of the environment and that a temperature increase may be significant in creating such conditions. The precipitation of calcite occurs in neutral or slightly alkaline conditions and is primarily dependent on the availability of calcium ions. Precipitation of

dolomite is thought to relate to the metasomatic action of magnesium-bearing pore waters (Mason, 1966). Laumontite constitutes hydrated silicates of aluminium and may form through the replacement of plagioclase in alkaline conditions (Shelley, 1974). While, dawsonite occurs through the neoformation of calcic feldspars.

5.5 QUARTZ CEMENTATION

Quartz cement in the Kapuni Group sandstones occurs as syntaxial overgrowths on detrital quartz grains. In some cases clay coatings on the surface of quartz grains have preserved the original outline of the grain, allowing it to be distinguished in thin-section. In most cases, however, it is optically difficult to distinguish overgrowths from the original grain. Overgrowths occur on both monocrystalline and polycrystalline quartz. Polycrystalline grains have similar overgrowth morphology to those that occur on monocrystalline grains, although each individual quartz crystal has a separate overgrowth with corresponding crystallographic orientation and extinction. Quartz overgrowths were generally thinner on polycrystalline quartz grains. Worden and Morad (2000) suggest that this is due to competitive growth between separate and differently orientated nuclei on the surface of polycrystalline quartz grains.

Quartz overgrowth development is syntaxial, governed by the crystallographic structure and orientation of the host grain. The overgrowths occur as both rhombohedra and prism structures. In SEM studies rhombohedral faces are, however, more abundant. Hayes (1979) suggests rhombohedral overgrowth structures are typically more prolific in sandstones as they tend to grow faster than prismatic structures. In cases where pore space has allowed rhombohedra and prism structures have amalgamated to form euhedral crystal faces. However, quartz overgrowth development is commonly inhibited or restricted by the presence of kaolinite on grain surfaces (Plate 5.22).

It is commonly thought that quartz cementation occurs in acidic conditions at temperatures <100°C, commensurate to burial depths of 2000 – 3000m (Land *et al.*, 1987; McBride, 1989). Apart from temperature, quartz cementation also requires large amounts of dissolved silica in sufficient concentration. There are several potential internal and external sources of silica, although some likely to be more volumetric than others in the Kapuni Group sandstones. Internal sources for dissolved silica include grain contact dissolution, the alteration and hydrolysis of feldspars and clay mineral neoformation eg. illitisation of kaolinite. While, silica may also be externally redistributed from mudstones, transported from more deeply buried sandstones or brought in from elsewhere in the Taranaki Basin by tectonic activity. Although quantifying possible silica source is beyond the scope of this study, external sources for quartz cementation are commonly advocated for quartz cementation despite the low

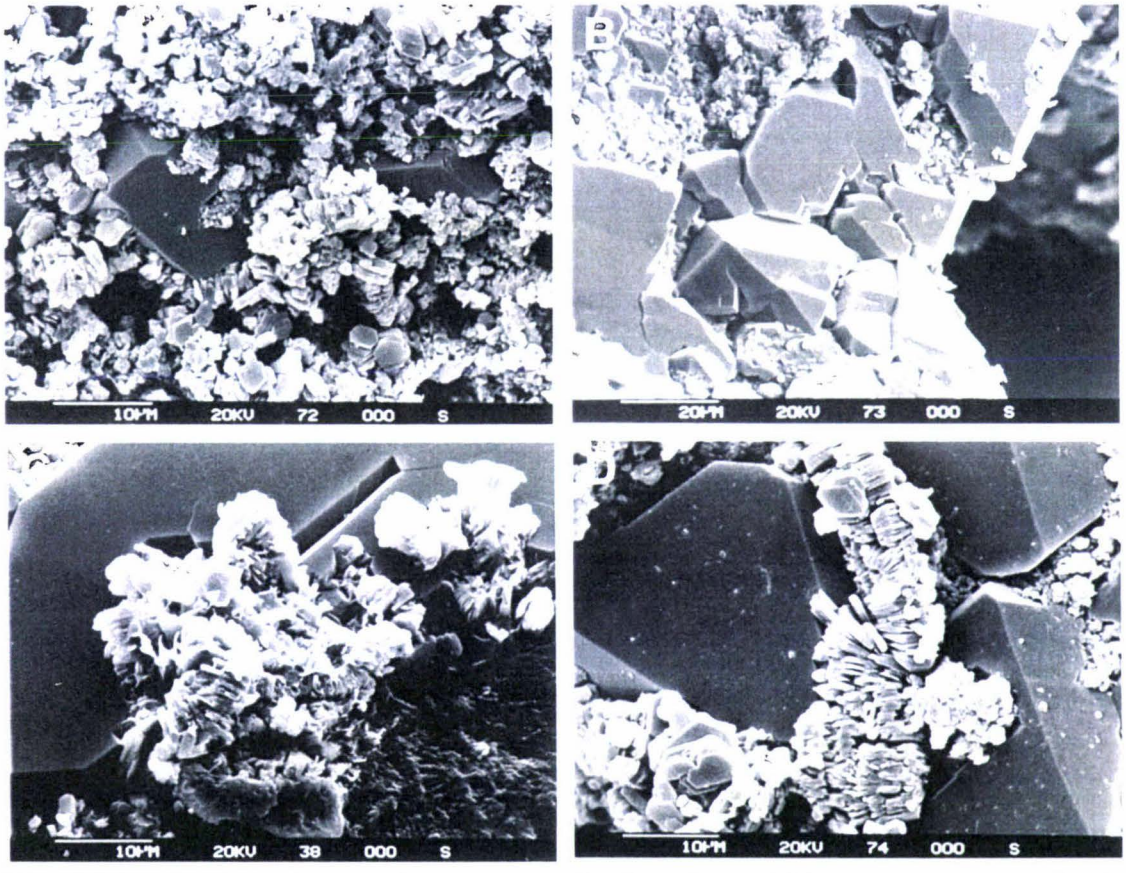

Plate 5.22: Scanning electron micrographs showing kaolinite prohibiting quartz overgrowths at various stages of development: (A) Mangahewa Formation rafted coal sandstone (Ss-rc) lithofacies (Sample 45, Kapuni-14); (B) Mangahewa Formation coarse sandstone (Ss-c) lithofacies (Sample 39, Kapuni-14); (C) Mangahewa Formation massive bedded sandstone (Ss-mb) lithofacies (Sample 43, Kapuni-14); (D) Mangahewa Formation coarse sandstone (Ss-c) lithofacies (Sample 40, Kapuni-14)

solubility of silica in solution and vast quantities of water required to accomplish quartz cementation. For example, in quartzose sandstones of the Green River Basin in Wyoming, Stone and Siever (1996) concluded that silica was imported from other areas in the basin during episodes of fluid flow related to deep-basin mineral dehydration and tectonic activity.

5.6 FELDSPAR CEMENTATION

Authigenic feldspar occurs as overgrowths on detrital feldspar grains. These overgrowths have developed through similar processes and in a similar manner to the overgrowths on detrital quartz grains. Feldspar overgrowths are most commonly identified on partially to extensively leached grains, particularly plagioclase although they also occur on microcline grains (Plate 5.23). The overgrowths seem to have been arrested at the early stages of development as few overgrowths exhibit euhedral crystal faces due to the presence of kaolinite clay minerals on grain surfaces and/or as a result of change in the chemistry of interstitial pore waters (Plate 5.24). Feldspar overgrowths are most abundant in the Mangahewa Formation pebbly sandstone (Ss-p) and speckled sandstone (Ss-s) lithofacies. Overgrowth development on detrital feldspar requires an alkaline environment (Mason, 1966), with available potassium, aluminium and silicon ions (Waugh, 1978).

5.7 PYRITE CEMENTATION

Pyrite occurs as a minor cement in the Kapuni Group sandstones. In SEM studies pyrite is observed as authigenic nodules of euhedral crystals or cubes (Plate 5.25). In thin-section pyrite formation is commonly associated with and observed replacing carbonaceous intraclasts and laminae. Also, in the Mangahewa Formation pyritised microfossils with a framboidal habit were observed in the coarse sandstone (Ss-c), pebbly sandstone (Ss-p) and coarse sandstone/mudstone (SM-c) lithofacies (Plate 5.26). Pyrite formation requires low Eh, reducing conditions and the availability of iron and sulphur (Gautier *et. al*, 1985).

5.8 FELDSPAR DISSOLUTION

Feldspars identified in Kapuni Group sandstones include orthoclase, microcline, perthite and plagioclase, with sanidine present only in the Farewell Formation. Feldspar grains demonstrate varying degrees of alteration. In the Mangahewa Formation feldspars range from fresh to extensively leached, with plagioclase the most extensively leached and altered. Mason (1966) attributes extensive and preferential alteration of plagioclase in sandstones to the fact that they have the lowest chemical stability of the feldspar species

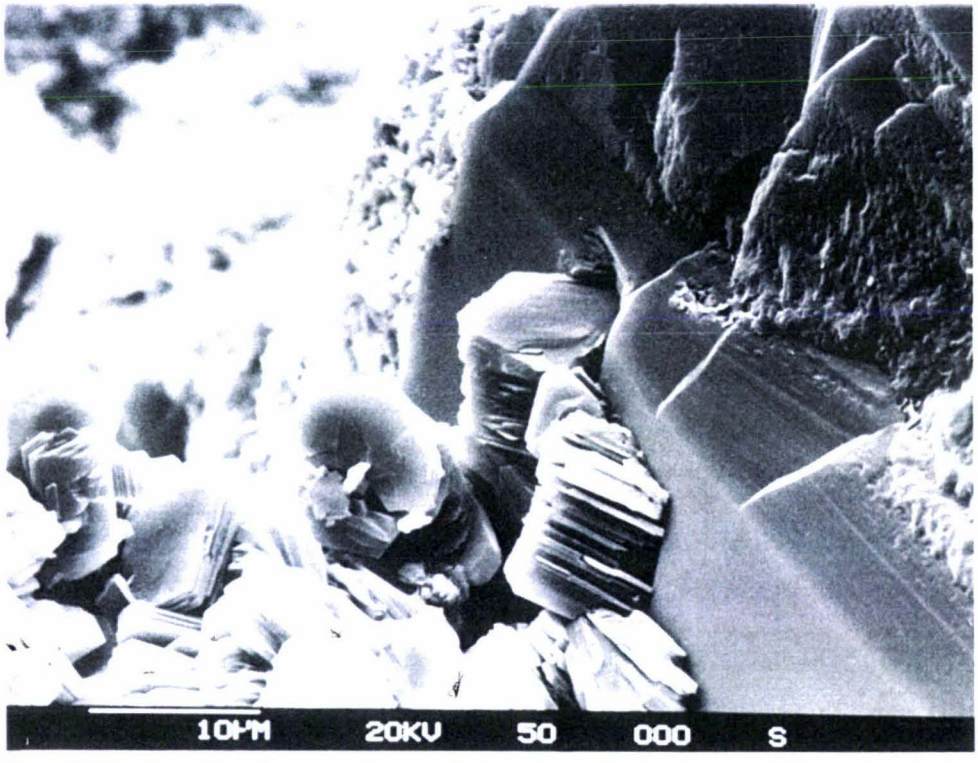

Plate 5.23: Scanning electron micrograph showing feldspar overgrowth development on partially leached feldspar grain in the Mangahewa Formation fine sandstone/mudstone (SM-f) lithofacies (Sample 44, Kapuni-14)

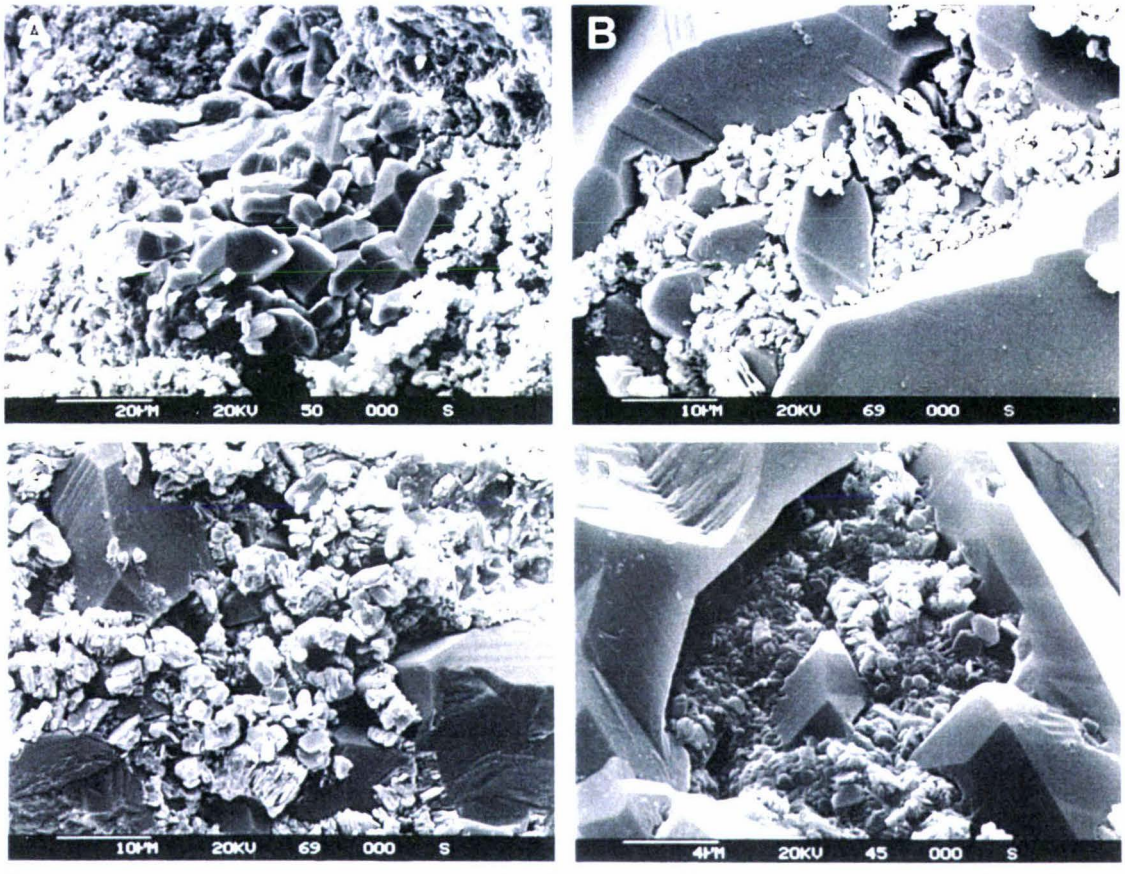

Plate 5.24: Scanning electron micrographs showing authigenic kaolinite prohibiting feldspar overgrowths at various stages of development: (A) small euhedral feldspar overgrowths developing from an extensively leached feldspar and coalescing around kaolinite in the Mangahewa Formation coarse sandstone/mudstone (SM-c) lithofacies (Sample 42, Kapuni-14); (B) feldspar overgrowths beginning to enclose kaolinite in the Mangahewa Formation cross-bedded sandstone (Ss-cb) lithofacies, note the groves on the overgrowths which are reflections of twinning in the host grain (Sample 30, Kapuni-12); (C) feldspar overgrowth development restricted by veriform kaolinite in the Mangahewa Formation pebbly sandstone (Ss-p) lithofacies (Sample 26, Kapuni-14); (D) feldspar overgrowths almost completely enclosing kaolinite in the Mangahewa Formation rafted coal sandstone (Ss-rc) lithofacies (Sample 16, Kapuni-3)

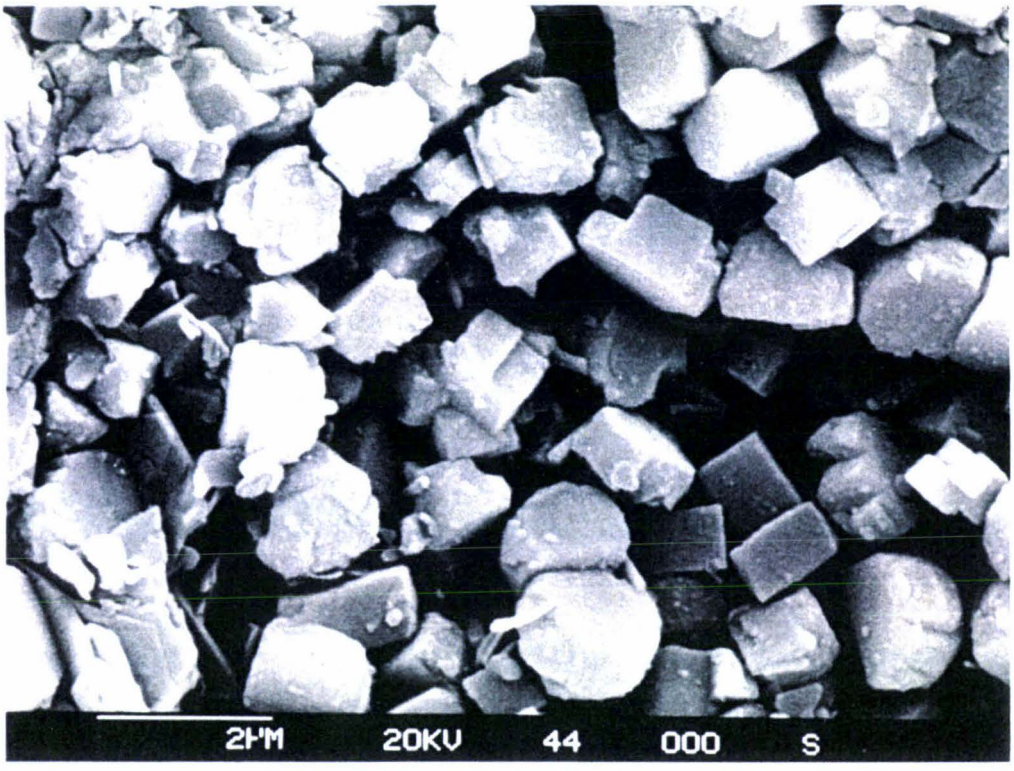

Plate 5.25: Scanning electron micrograph of authigenic pyrite cubes, with some cubes exhibiting minor dissolution in the Mangahewa Formation coarse sandstone (Ss-c) lithofacies (Sample 38, Kapuni-14)

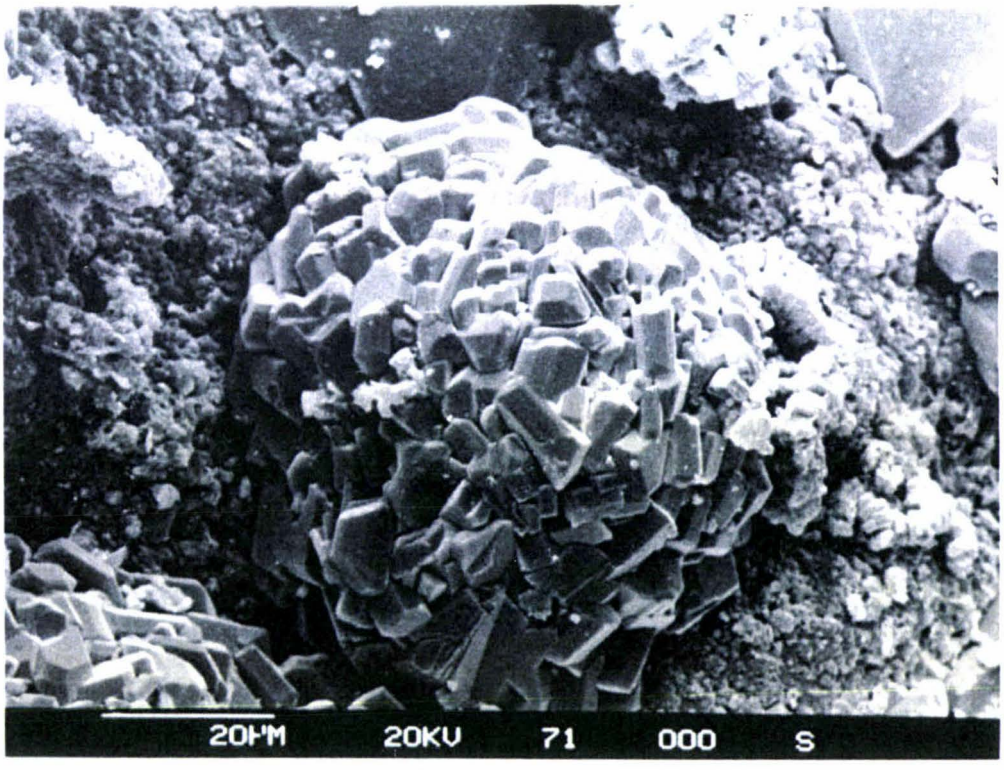

Plate 5.26: Scanning electron micrograph showing pyritised microfossils with a framboidal habit in the Mangahewa Formation coarse sandstone/mudstone (SM-c) lithofacies (Sample 35, Kapuni-14)

and are thus altered preferentially in the source area. Microcline and perthite feldspars have also been altered with leaching most pronounced in the Mangahewa Formation coarse sandstone/mudstone (SM-c), pebbly sandstone (Ss-p), cross-bedded sandstone (Ss-cb) and rafted coal sandstone (Ss-rc) lithofacies. Feldspar alteration is less common in the Kaimiro Formation with only minor plagioclase, microcline and perthite leaching. In the Farewell Formation sanidine is the most commonly leached feldspar, whilst plagioclase occurs both fresh and leached.

In SEM studies the dissolution of feldspar is observed along grain surfaces, grain margins and within grains (Plate 5.27). Incipient chemical alteration of feldspars has involved replacement by clay and carbonate minerals that have been deposited in etched or pitted crystal faces, along cleavages or entirely replacing grains. Carbonate minerals replacing feldspar include siderite, calcite, dawsonite and laumontite. Most feldspar grains, however, are observed altering to clay minerals, predominantly kaolinite, while illite is also common. Leaching of feldspar grains has also created restricted areas of minor secondary porosity in most Kapuni Group sandstones.

5.9 QUARTZ DISSOLUTION

The most common form of quartz dissolution occurs at grain boundaries, where grain interpenetration has created widespread concavo-convex and minor sutured contacts. Minor replacement of quartz by carbonate is observed in thin-section and SEM studies, although such leaching may have been more important in some Mangahewa Formation sandstones where widespread carbonate is inferred in this study to have been removed. Schmidt and McDonald (1979a) report that quartz is often replaced by carbonate minerals, which are later dissolved, with such leaching mistakenly attributed to direct dissolution by pore waters. Thin-section observations indicate that quartz grains and overgrowths are frequently corroded by carbonate minerals. In SEM minor corrosion of quartz is evidenced by dissolution pits (typically $< 4\mu m$) on the surface of both detrital quartz grains and secondary quartz overgrowths (Plate 5.28). In most cases micritic calcite intraclasts are commonly preserved with in these embayments.

5.10 CLAY DISSOLUTION

The dissolution of clay matrix is not common in the Kapuni Group sandstones. Kaolinite is the only clay observed in SEM exhibiting minor dissolution effects along the margins of books and platelets. In thin-section studies the dissolution of clay matrix has created intra-constituent secondary porosity. Although, this form of secondary porosity development is a minor form of porosity enhancement, the dissolution of clay may have also been important in the formation of oversized pores in some Mangahewa Formation sandstones.

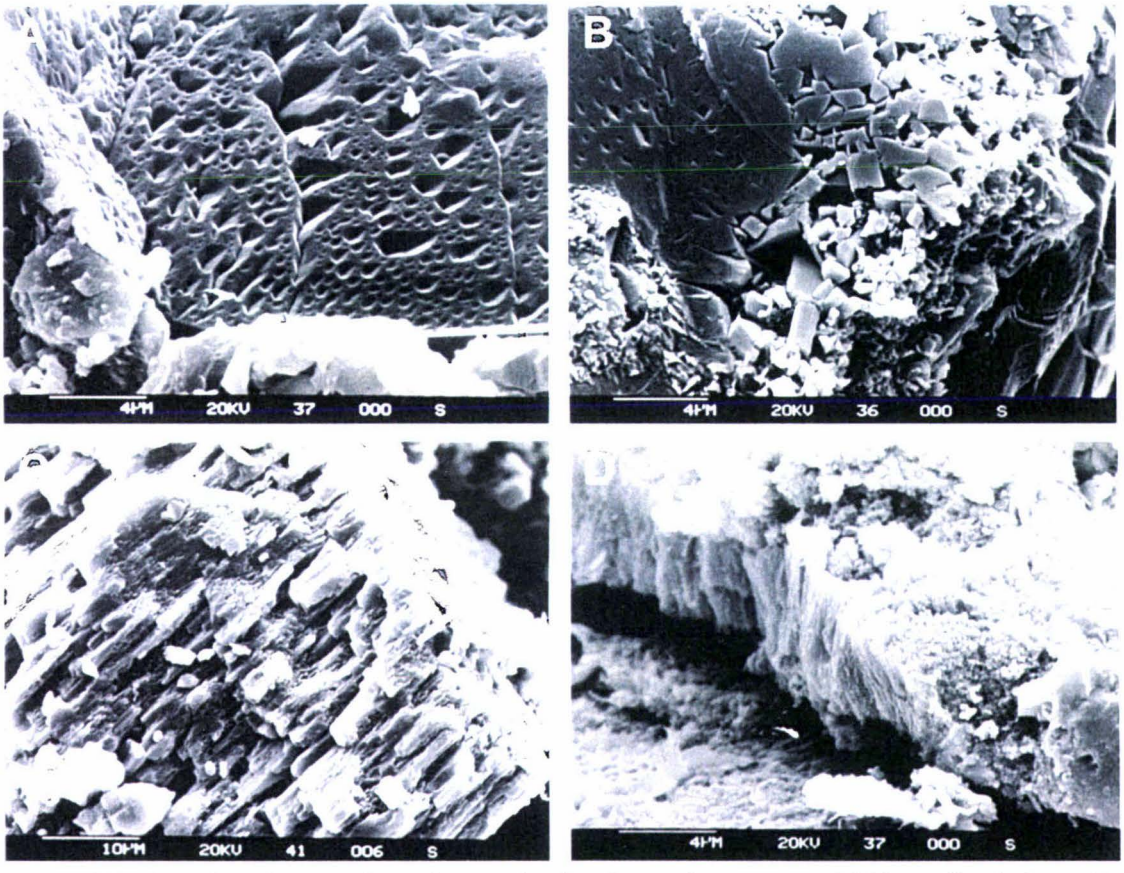

Plate 5.27: Scanning electron photomicrographs showing various stages of feldspar dissolution: (A dissolution pits on the surface of a feldspar grain in the Kaimiro Formation massive bedded sandstone (Ss-mb) lithofacies (Sample 6, Kapuni-1); (B) dissolution along the edges of a feldspar grain in the Mangahewa Formation cross-bedded sandstone (Ss-cb) lithofacies (Sample 31, Kapuni-12), (C) feldspar dissolution along cleavage planes in the Mangahewa Formation rafted coal sandstone (Ss-rc) lithofacies (Sample 19, Kapuni-3); (D) extensive dissolution of a feldspar grain along cleavage in the Mangahewa Formation fine sandstone/mudstone (SM-f) lithofacies (Sample-1, Kapuni-1)

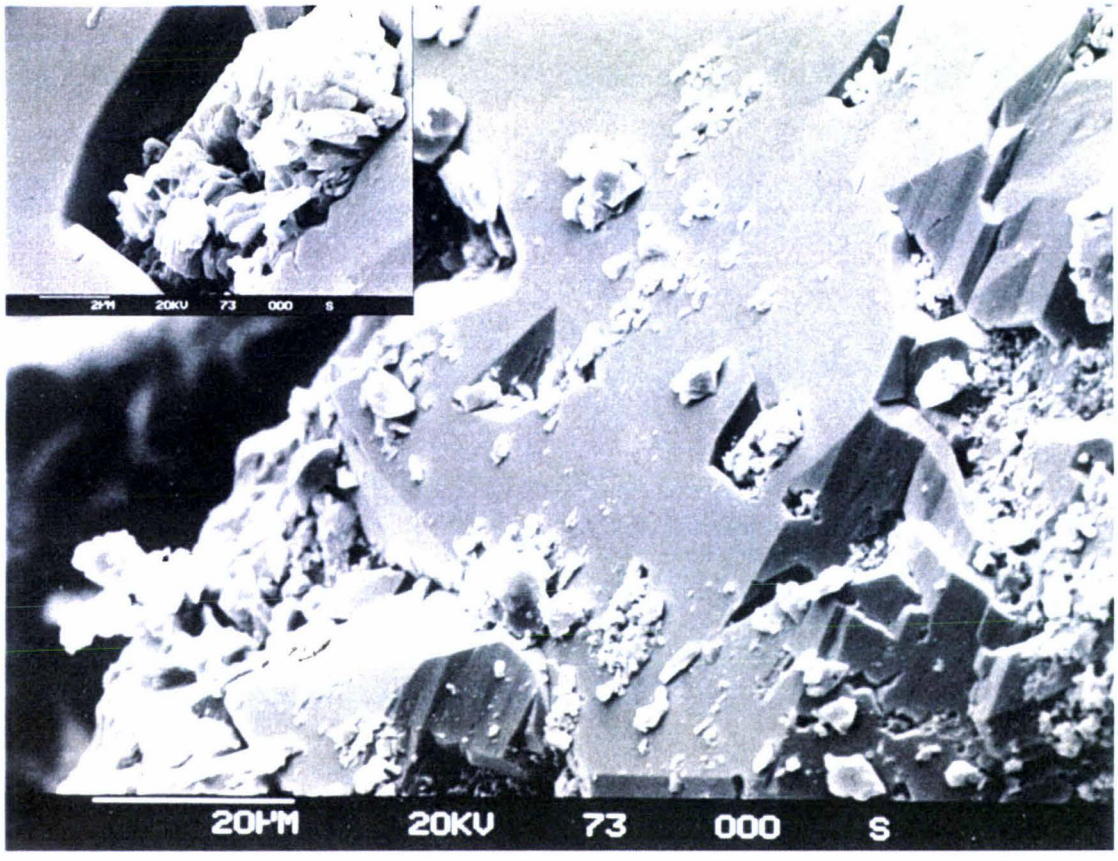

Plate 5.28: Scanning electron micrograph showing quartz dissolution pits on secondary quartz overgrowths in the Mangahewa Formation coarse sandstone (Ss-c) lithofacies (Sample 41, Kapuni-14)

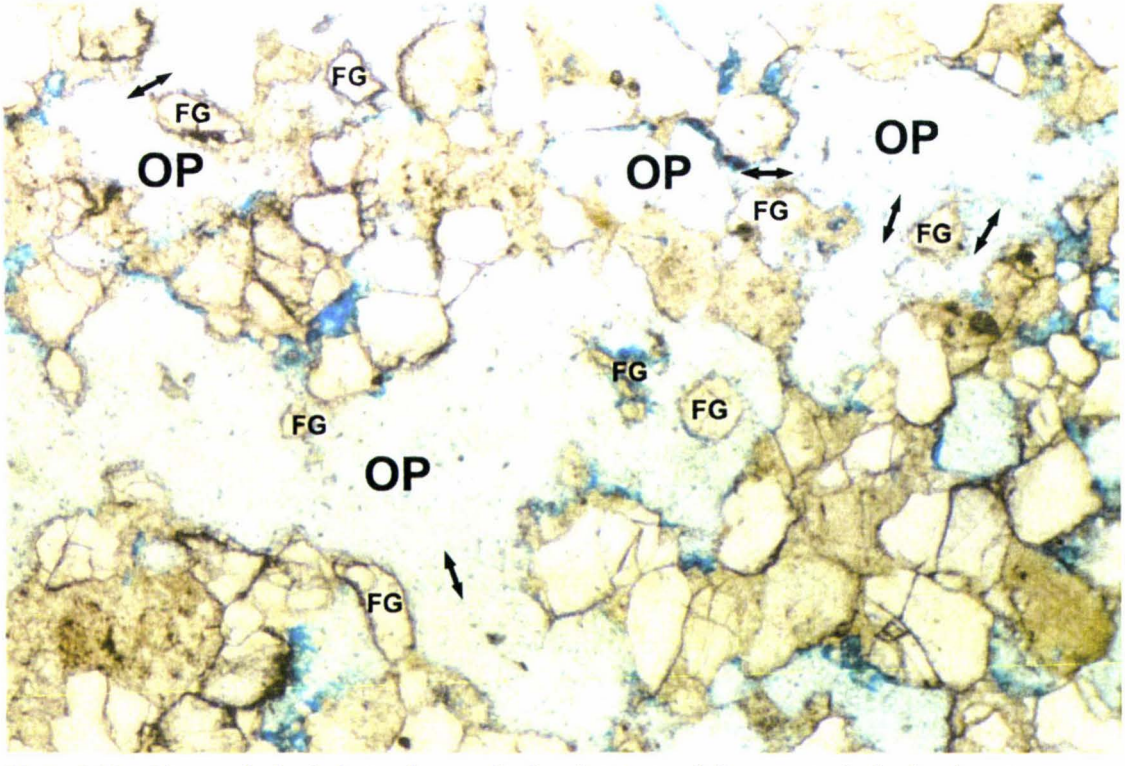

Plate 5.29: Plane-polarised photomicrograph showing textural features typical of carbonate cement dissolution including oversized dissolution pores (OP), solution channels (⟷) and floating grains (FG) indicative of carbonate cement dissolution in the Mangahewa coarse sandstone (Ss-c) lithofacies (Sample 40, Kapuni-14)

5.11 CARBONATE DISSOLUTION

Carbonate cement dissolution in the sandstones is evidenced by oversized dissolution pores, solution channels and floating grains (Plate 5.29). Schmidt and McDonald (1979b) describe these as typical textural characteristics of secondary porosity development through the dissolution of once pre-existing carbonate cements. Secondary porosity development by the removal of carbonate minerals is primarily observed in the Mangahewa Formation coarse sandstone (Ss-c) and coarse sandstone/mudstone (SM-c) lithofacies. On the basis of textural evidence in thin-section carbonate dissolution appears not to have been important in other Kapuni Group sandstones.

Carbonate solubility generally decreases with burial depth and increasing temperature (Blatt, 1979). The dissolution and removal of carbonate cements commonly involves the presence of carbon dioxide and/or organic acids (Beggs 1989; Schmidt and McDonald, 1979a; Surdam *et al.* 1989). The presence of carbon dioxide and organic acids in sandstones is commonly the result of microbial activities near the surface or thermal maturation of organic matter during burial (Schmidt and McDonald, 1979a).

5.12 PARAGENESIS

Diagenetic processes have significantly modified the physical and chemical composition of the Kapuni Group sandstones. The paragenetic sequence of events records these diagenetic changes throughout their geological history. Figure 5.1 presents the generalised diagenetic stages for the Mangahewa, Kaimiro and Farewell Formations in the Kapuni Field.

Compaction of the Kapuni Group sandstones commenced soon after deposition, and was greatest in the initial stages of burial during removal of the high water content from the sandstones. The effects of mechanical during this time were not homogenous in the Kapuni Group sandstones. In the Mangahewa and Kaimiro formations plastic deformation and the reorganisation of grains is more advanced in the fine-grained, poorly to moderately sorted sandstones, but has had less effect in coarse-grained, moderately-well to well-sorted sandstones. With increasing burial the rate of plastic deformation and grain rotation decreased and the dissolution of grains became an increasingly important process, as evidenced in sandstones of the deeper Farewell Formation.

Acid conditions are represented by early and late phases of quartz cementation, kaolinite formation and feldspar dissolution. Early quartz cementation, kaolinite formation and feldspar dissolution events were coeval with the main period of compaction. Early quartz cementation in the sandstones is demonstrated by the presence of plastically deformed

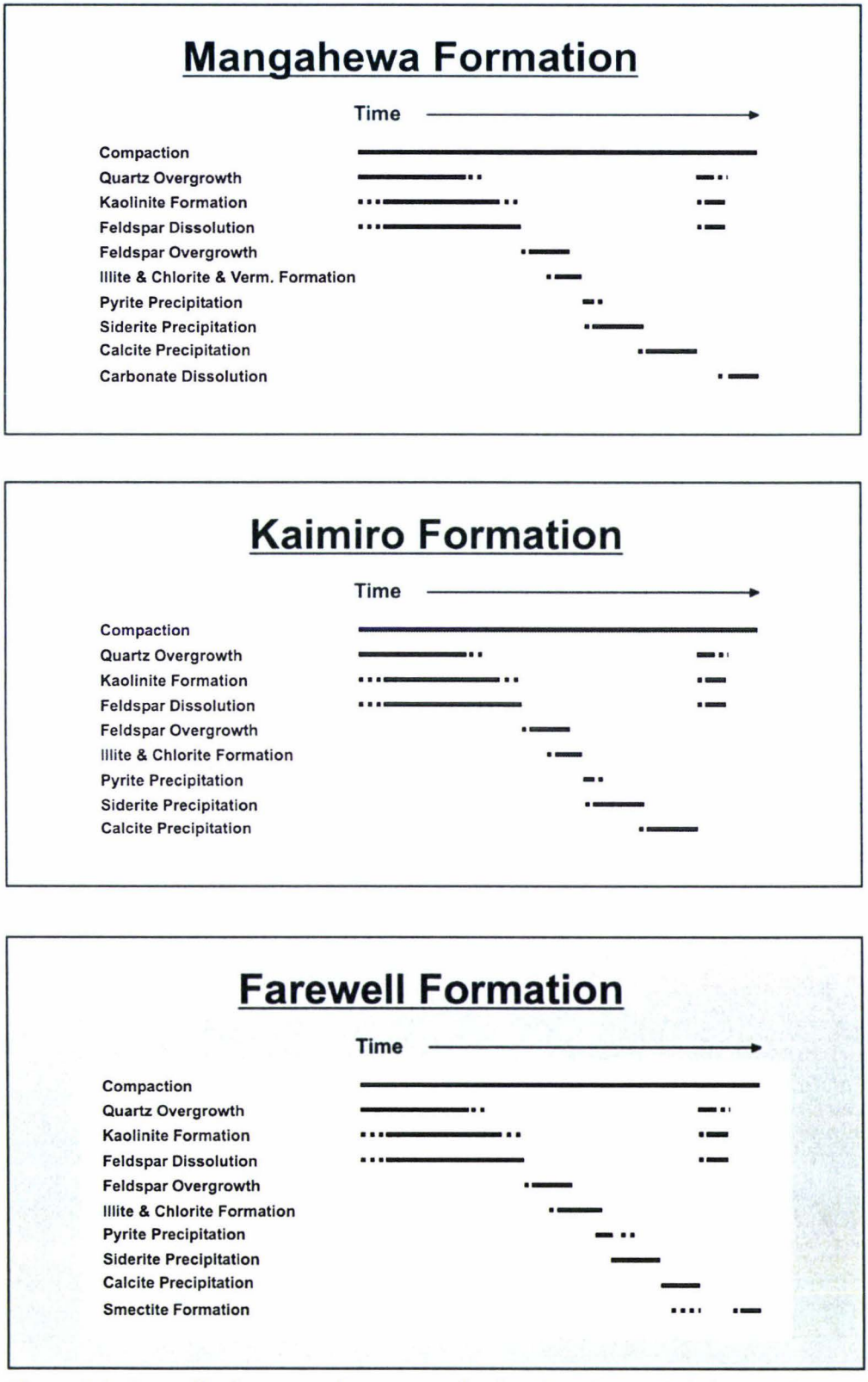

Figure 5.1: Generalised paragenetic sequence for the Mangahewa, Kaimiro and Farewell Formations in the Kapuni Field

grains around syntaxial quartz overgrowths. Quartz overgrowth development has been frequently inhibited or restricted by the precipitation of authigenic kaolinite. As quartz overgrowths locally grow around kaolinite, kaolinite formation must have occurred either simultaneously with or prior to quartz overgrowth development. Kaolinite as a pseudomorphous replacement of extensively leached plagioclase and lesser altered perthite and microcline feldspars is further evidence for coexisting development. A late phase of quartz cementation, kaolinite formation and feldspar dissolution also occurred in the sandstones. Late development is supported by the presence of both fresh and leached overgrowths on detrital quartz grains and the distinction of two kaolinite series exhibiting different sizes and degrees of dissolution. These observations suggest two phases of development, occurring before and after carbonate deposition.

Acid conditions could not be maintained indefinitely in the sandstones. Buffering by mineral reactions and the declining supply of carbon dioxide from organic maturation resulted in an increase in the pH of interstitial pore waters to neutral or slightly alkaline. The change in pore water chemistry and greater depth of burial would have favoured feldspar cementation, illite, chlorite and vermiculite formation and carbonate (siderite and calcite) precipitation. Authigenic feldspar occurs as overgrowths on extensively leached detrital feldspar grains, they therefore post-date feldspar dissolution. The neoformation of illite primarily from kaolinite and subordinately from leached feldspar grains and overgrowths indicate that precipitation post-dates both kaolinite and feldspar overgrowth development. The neoformation of chlorite and vermiculite from precursor biotite is likely to have occurred at a similar time to illite neoformation, in response to differing pore water compositions.

Carbonate cementation post-dates the main period of compaction, overgrowth development on feldspar and quartz grains, and clay mineral formation. The relative timing of siderite and calcite as the two main carbonates is difficult to distinguish. They are unlikely to have occurred together, as they are not precipitated in the same chemical environment. The precipitation of calcite is primarily influenced by the availability of calcium ions and the pH of the environment, whereas the precipitation of siderite is dependent on the oxidation-reduction balance of the environment, forming only in reducing conditions. Both siderite and calcite are observed corroding detrital and authigenic quartz and feldspar and filling grain fractures, therefore post-dating these processes. On the basis of relative abundance, siderite is likely to have been the first carbonate precipitated, with the later precipitation of calcite. At a similar time to siderite cementation, pyrite cementation would have also occurred in the sandstones as siderite and pyrite form in the same chemical environment.

At the latest stages of diagenesis in the Mangahewa and Kaimiro formations and late stage in the Farewell Formation acid conditions again prevailed. As mentioned previously, the result was late quartz overgrowth development, kaolinite formation and dissolution of detrital and authigenic feldspar in the coarser-grained, better sorted sandstones. The dissolution of carbonate cements also occurred at a similar time in the Mangahewa Formation sandstones. While, in the Farewell Formation greater depth of burial and the development of alkaline to slightly alkaline conditions as the latest stages of diagenesis, has resulted in the complete neotransformation of smectite from illite.

DISCUSSION

6.1 INTRODUCTION

This study has primarily focused on the Mangahewa Formation, due to the abundance of core and geophysical log data and its economic significance in providing the producing reservoir sandstones in the Kapuni Field. Limited core and geophysical log data from the underlying Kaimiro and Farewell formations therefore constrain the discussion on depositional setting to the Mangahewa Formation. Nevertheless, the relative importance of depositional and post-depositional processes on reservoir quality in the Kapuni Group are discussed and the implications of this study for future reservoir development locally in the Kapuni Field, and exploration regionally in the Taranaki Basin will be elucidated.

6.2 DEPOSITIONAL SETTING OF THE MANGAHEWA FORMATION

The Mangahewa Formation consists of lithofacies that are indicative of tidal sand bar, tidal-inlet channel, fluvial-tidal channel, sand flat, spit platform, shallow marine, tidal channel, meandering tidal channel, mud flat, swamp and marsh environments. Log motifs of these lithofacies were identified and characterised on geophysical logs and extrapolated to uncored sections of the Mangahewa Formation. Correlation between wells was then conducted on the principle that major coal units are laterally contiguous in the field (Enclosure 1).

Core and log data indicate that the Mangahewa Formation was deposited in an overall transgressive estuarine depositional setting. The nature and organisation of lithofacies is typical of an estuarine environment possessing a three-fold zonation of an outer marine-dominated high energy zone, a relatively low-energy central zone and an inner river dominated (but marine influenced) zone headward. Dalrymple *et al.* (1992) define an estuary as the seaward portion of a drowned valley extending from the landward limit of tidal facies at its head to the seaward limit of coastal facies at its mouth. Essential to the definition of estuarine systems is the net landward movement of sediment and the deposition of lithofacies influenced by tide, wave and fluvial processes (Dalrymple *et al.* 1992). Estuarine development in the Mangahewa is discussed in conjunction with reservoir intervals previous defined in the study.

i. K3 Reservoir Interval

A transgressive surface marks the initial stages of tide-dominated estuary development in the Mangahewa Formation. The K3 reservoir incorporates those lithofacies deposited at the beginning of this transgression (Figure 6.1a). Fluvial-tidal channel deposits

immediately overlie the transgressive surface at the base of the K3E2 reservoir and together with meandering tidal channel sediments constitute the K3E2 reservoir unit. The K3E1 reservoir unit comprises marine sand bodies consisting of two strongly contrasting lithofacies, the tidal sand bar zone (tidal sand bars and tidal channels) and sand flats. The former lie seaward of the tidal-energy maximum (Harris 1988; Dalrymple and Zaitlin 1989; Dalrymple *et al.*, 1990) and the latter coincide with the tidal-energy maximum displaying a braided channel pattern where the estuary is unconfined, merging into a single channel headward (Hamilton 1979; Lambiase 1980; Dalrymple *et al.*, 1990). The K3U and K3A reservoir units consist primarily of sand flat, mud flat and swamp/marsh environments. Both the K3U and K3A are inferred to represent lateral movement of the main sand flat channels and deposition away from the estuary margins, encroachment of mudflats and stabilisation by swamp/marsh environments. Coarsening upward tidal sand bars and tidal channels are also present in the K3A in the northern Kapuni-8 well indicating periods of progradation were also occurring at this time.

ii. K2 Reservoir Interval

The K2 reservoir interval consists for the most part of mud flat and swamp/marsh deposits, although sand flat, tidal sand bars and tidal channels increase in the basal section of the K2 reservoir interval towards the north. The K2 reservoir interval corresponds with continuing lateral movement of sand flat, tidal sand bar and tidal channel environments and infilling of the estuary, through progradation at the landward margin of the embayment (Figure 6.1b). Like true tide-dominated estuaries such as the Severn Estuary (Harris and Collins, 1985) progradation occurred through tidal sand bar, tidal flat and marsh environments. Dalrymple *et al.* (1990) suggest that as estuaries fill there is an expansion and shallowing of the sandbars and the seaward movement of the tidal meandering zone. These estuarine processes are not determinable with the present log data; however, they are consistent with the sequence of log motifs identified in the K2 reservoir interval.

ii. K20 Coal

Overlying the K2 reservoir interval is the K20 coal (K20c). This coal represents complete or partial infilling of the estuary (Figure 6.1b). The coal corresponds to the last stages of progradation (forced regression) during a sea-level standstill, or during the early part of sea-level fall. The great thickness of the coal (~ 10m) indicates a period of low sea-level that existed for an extended period of time.

iii. K1 Interval

The K1C reservoir unit characterises renewed transgression in the Mangahewa Formation, however, at this time lithofacies and log motifs indicate a change in estuary morphology from tide-dominated to wave-dominated (Figure 6.1c). Resembling most

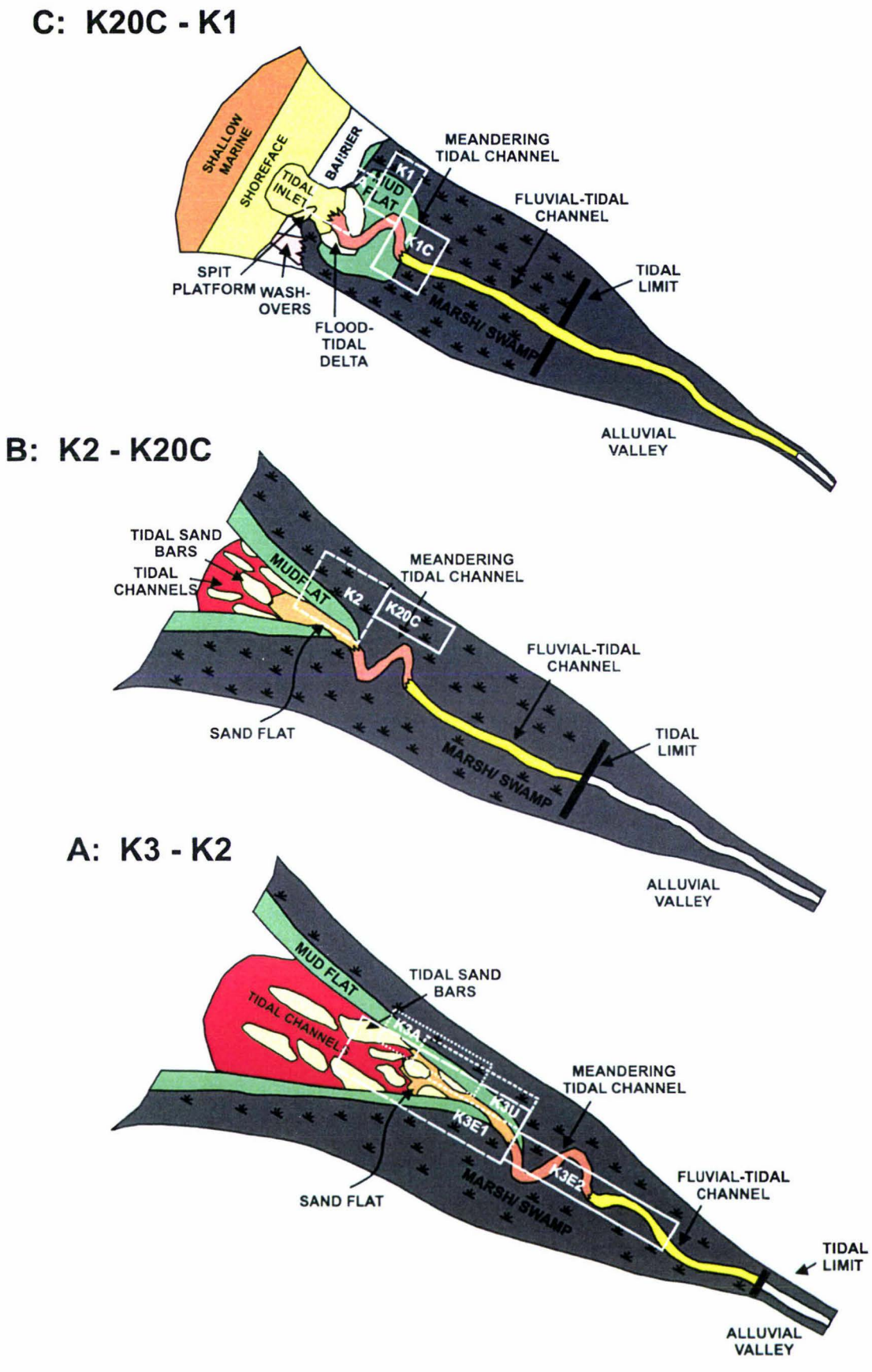

Figure 6.1: Environmental setting for deposition of the Mangahewa Formation in terms of the (A) K3 - K2 (B) K2 - K20C and (C) K1 reservoir intervals

wave-dominated estuaries such as those described by Roy *et al.* (1980) and Zaitlin and Schultz (1990); a clearly-defined, "tripartite" distribution of lithofacies (coarse-fine-coarse) is observed. Where preserved the basal K1C reservoir interval incorporates fluvial-tidal sediments overlying the unconformity with the K20 coal. Such deposits represent the bay-head delta typically associated with wave-dominated estuarine systems (Nichol, 1991).

The K1 reservoir unit predominantly incorporates mud flat, swamp/marsh and meandering tidal channel environments. These log motifs represent the low-energy central part of the estuary. A lagoon may have been present at this time acting as the prodelta region, however, Dörjes and Howard (1975) point out that in shallow (nearly filled) estuaries the equivalent area contains extensive marsh and swamp environments crossed by meandering tidal channels, which pass directly into fluvial-tidal channels. The stratigraphic succession and dominance of meandering tidal channel, mud flat and marsh/swamp environments indicated by log motifs suggest a lagoon was probably not present. Of particular note in the K1 reservoir is the greater extent of meandering tidal deposits and absence of mud flat deposits in the southern Kapuni-3 well. The basis for increased thickness of these deposits cannot be interpreted directly from the geophysical log data available, but may relate to the headward extent of the meander zone where straightening of meandering tidal channels occurred or to the restriction of channel migration by topographic barriers.

The K1A reservoir unit only occurs in the northern Kapuni Field wells (Kapuni-8, -12 and -15). Collectively log motifs are consistent with a barrier system. The barrier is a composite feature composed of the deeper lithofacies, which have a higher preservation potential during transgression. Core lithofacies and log motifs indicate the presence of spit platform, tidal-inlet channel, flood-tidal delta, meandering tidal channel and shallow marine environments. Erosion of the barrier complex from the middle and southern wells later occurred during shoreface retreat and/or tectonic uplift of the Kapuni anticline.

6.2 DEPOSITIONAL PROCESSES ON SANDSTONE RESERVOIR QUALITY

6.2.1 Provenance

Provenance has exerted the primary control on the detrital composition of the Kapuni Group sandstones. Detrital mineral assemblages forming the main framework component in the sandstones differ between the younger Mangahewa and Kaimiro formations and older Farewell Formation. In general detrital composition in terms of quartz, feldspar and rock fragments are comparable between lithofacies in the Mangahewa and Kaimiro formations. However, there is a distinct difference in feldspar variety and abundance and rock fragment composition in the Farewell Formation. The presence of sanidine and

relative increase in plagioclase feldspar, coincidental with an increase in acid volcanic rock fragments with trachytic textures indicate a different source for the Farewell Formation. Provenance has therefore been an important factor differentiating initial reservoir characteristics of sandstones in the Mangahewa and Kaimiro formations from those in the Farewell Formation.

6.2.2 Depositional Environment

The Kapuni Group sandstone lithofacies were deposited in a range of environments including tidally influenced fluvial channels, meandering tidal channels, sand flat, tidal sand bars, tidal channels, tidal-inlet channels, spit-platform and shallow marine environments. Each of these environments exhibits different hydrodynamic conditions, which have influenced directly or indirectly the diversity and stratigraphic heterogeneity of the sandstones and produced sandstone lithofacies with characteristic detrital compositions and sedimentary textures. At one end of the hydrodynamic spectrum, are the lithofacies of the low energy tidal meandering channels that generally comprise low quartz totals, greater proportions of plastically deformed grains, fine grain-size and poor- to moderate-sorting. In contrast, high energy lithofacies of the tidal sand bars and tidal channels are characterised by greater proportions of quartz, negligible ductile grains, coarse grain-size and moderately-well to well-sorted sandstones. Other sandstone lithofacies of the Kapuni Group in general fall in between these end member lithofacies comprising variable detrital compositions, an average medium grain-size and moderate sorting. An exception is the speckled sandstone lithofacies (Ss-s) of shallow marine origin which is characterised by plastically deformed glauconite pellets and coarse-grain size.

6.3 POST-DEPOSITIONAL PROCESSES ON SANDSTONE RESERVOIR QUALITY

Diagenesis consists of a set of competitive post-depositional processes or reactions which tend to preserve, enhance or destroy sandstone reservoir quality. Diagenesis can be discussed in terms of those processes that reduce and those processes that enhance reservoir quality. Diagenetic processes reducing reservoir quality of the Kapuni Group sandstones include compaction, clay mineral formation and cementation. While processes enhancing reservoir quality include the dissolution of carbonate, framework grains and clay matrix.

6.3.1 Processes Reducing Reservoir Quality

i. Mechanical and Chemical Compaction

Mechanical compaction was one of the first and most critical factors reducing reservoir quality of the sandstones. Mechanical compaction and the resultant reduction in porosity

was greatest in the initial stages of burial where the rotation and closer packing of the grains occurred; then, as burial progresses the deformation, fracture and chemical dissolution of grains become increasingly important processes. The effects of compaction can be related directly to the textural and mineralogical maturity and depth of burial of the sandstones. In the Mangahewa and Kaimiro formations compaction is greatest in the fine-grained, poorly- to moderately-sorted lithic arkose sandstones of meandering tidal channel environments. In these sandstones the greater proportion of plastically deformed ductile grains would have resulted in a significant reduction in primary porosity and permeability during the early period of water removal. However, in the Mangahewa Formation coarse-grain, moderately-well to well-sorted subarkose sandstones of tidal sand bar and tidal-inlet channel environments, compaction has been a less important factor in reducing porosity. Greater depth of burial of sandstone in the Farewell Formation has result in a greater degree of grain reorganisation, with chemical compaction (grain contact dissolution) a more important process in these sandstones.

ii. Clay Mineral Formation

Porosity and permeability are markedly affected by clay mineral abundance and distribution in the sandstones. Clay mineral percentages in the Kapuni Group sandstones seem to correlate with initial textural characteristics i.e. higher authigenic clay percentages occur in sandstones which are fine-grained and poorly sorted. Whereas, the type of clay mineral deposited is constrained by temperature (depth of burial) and composition of interstitial pore waters. In the Kapuni Group sandstones a transition from kaolinite to illite, vermiculite and chlorite and finally smectite is observed with paleo-depth. The distribution and reactivity of these clay minerals have profound effects during drilling, completion and stimulation production programs (Eslinger and Pevear, 1988). As clay types and abundance vary considerable in the Kapuni Group sandstones it is important to accurately identify and determine relative clay percentages, inorder to properly assess their effect on reservoir quality. X-ray diffraction, differential thermal analysis and infra-red analysis studies in combination are therefore required.

Kaolinite is one of the main clays, forming at early and late stages of diagenesis. Kaolinite abundance is highest in sandstones of the Mangahewa and Kaimiro formations but also occurs in the Farewell Formation. Kaolinite extensively replaces leached feldspars and occludes pores and pore throats reducing permeability and total porosity. Microporosity, however, is generally increased where kaolinite is present[6], although it is not effective porosity because the small pores are poorly connected. Microporosity was not recorded in point count analysis in this study and therefore differences between visible porosity totals identified in thin-section and air-mercury porosity values described

[6] Microporosity includes pores with a pore-aperture radii less than 0.5μm (Pittman, 1979)

by Reiman (1962); Elskamp and van Benten (1976) and Shell-Todd Oil Services Limited (1988) can most likely be attributed to microporosity.

Illite and mixed-layered illite (illite/vermiculite, illite/smectite and illite/chlorite) are also abundant in the Mangahewa and Kaimiro formations and less common in the Farewell Formation. Illite has neoformed predominantly from kaolinite, but also formed as an alteration product of feldspar and mica and precipitated in pores and pore throats from circulating interstitial pore waters. In this study illite and mixed-layer illite were identified in greater than previously reported studies by Hogan (1979), Challis and Mildenhall (1986) and Yunalis and Izhan 1995) of the Kapuni Group. Such findings are important because illitic clays have a detrimental effect on reservoir quality, greatly reducing permeability.

Chlorite and mixed-layered chlorite (illite/chlorite, chlorite/vermiculite and chlorite/smectite) and vermiculite (illite/vermiculite and chlorite/vermiculite) occur at a similar diagenetic stage to illite in the Kapuni Group sandstones. Both chlorite and vermiculite have formed from precursor biotite. Although these clay minerals have reduced porosity and permeability their relatively low abundance means that their effect on reservoir quality is not as important as other clay species in the Kapuni Group.

Smectite and mixed-layer smectite (illite/smectite and illite/chlorite) are also important clay minerals. Mixed-layer smectite occurs throughout the Kapuni Group generally as a minor clay component. Smectite, however, is restricted to the Farewell Formation sandstones where is has neoformed as a result of greater paleo-burial depth from predominantly illite and infrequently chlorite. Smectite clay has a detrimental effect on reservoir quality because interlayered water causes it to swell, significantly reducing porosity and permeability in these sandstones.

iii. Cementation

Authigenic cements in the Kapuni Group sandstones consist of overgrowths on detrital grains, carbonate minerals and pyrite. Secondary overgrowths and carbonate minerals form the dominant cements in the sandstones. Pyrite is a rare cement and its effect on reducing reservoir quality is minor and as such will not be discussed further.

Syntaxial overgrowths on quartz grains occurred at early and late stages of diagenesis as demonstrated by the two phases (fresh and leached) of quartz overgrowth development. Differences between depositional lithofacies are recognised, with overgrowth development in sandstone lithofacies related to pore size and permeability. Pore-waters can only play a significant role in quartz cementation if enough water can be moved through the rock (Sibley and Blatt, 1976). Therefore, where quartz overgrowths are more

extensively developed, primary porosity and/or secondary porosity in these sandstones would have had to been relatively high. This explains why overgrowths are less abundant in the fine-grained, poorly- to moderately-sorted sandstones and more abundant in the coarse-grained moderately-well to well-sorted sandstones. Syntaxial overgrowths also occur on detrital feldspar grains after initial feldspar dissolution. These overgrowths are less abundant than those that occur on detrital quartz grains in the sandstones. However, similar distinctions in overgrowth abundance between lithofacies are not observed. Feldspar overgrowths in comparison only have a minor effect on reducing reservoir quality in the Kapuni Group sandstones.

Carbonate cementation occurred after clay mineral formation in the Kapuni Group sandstones. Carbonate minerals have precipitated in pores, coated framework grains, increased areas of grain-to-grain contact and decreased porosity in the Kapuni Group sandstones. Where carbonate cements are present they are detrimental to porosity and permeability as they create barriers to fluid flow and pressure compartments. Carbonate minerals identified include predominantly siderite, calcite and less common dolomite, dawsonite and laumontite. Carbonate cement type and relative abundance do not exhibit any relationship with sandstone lithofacies or depth. In this respect, carbonate formation is likely to have been primarily influenced by pore water composition, textural characteristics, prior diagenetic modifications and structural or stratigraphic controls on the sandstones.

6.3.2 Processes Enhancing Reservoir Quality

Secondary porosity development during diagenesis has been critical for improving the reservoir quality of most Kapuni Group sandstones. Secondary porosity development is not as regularly distributed as primary porosity. Zones of high secondary porosity often occur adjacent areas that are tightly cemented or comprise abundant clay matrix. This gives the Kapuni Group sandstones a wide range of porosity and permeability values within and between sandstone lithofacies, although, general trends are distinguished in this study. Secondary porosity development is greatest in the Mangahewa Formation coarse-grained, moderately well- to well-sorted sandstones and least developed in fine-grained, poorly- to moderately-sorted sandstones. The development of secondary porosity is variable in the medium-grained and moderately-sorted lithofacies of the Mangahewa Formation and negligible in the Kaimiro and Farewell formations. Secondary porosity development has occurred through the dissolution of authigenic replacement minerals (carbonates and clays), grains and grain fractures.

The formation of secondary porosity through the dissolution of replacive carbonate-cements, unstable framework grains and clay matrix is volumetrically the most important reservoir-enhancing feature that occurs in the Kapuni Group sandstones. However, such

porosity development is typically restricted to sandstone lithofacies of the tidal sand bar and tidal channel environments in the Mangahewa Formation. The lack of carbonate cement dissolution in other Kapuni Group sandstone lithofacies can be attributed to compaction significantly reducing porosity and permeability before carbonate cementation occurred and/or the loss of porosity and permeability at the late stage of diagenesis preventing the dissolution of carbonate cements by organic acids.

Minor porosity enhancement has occurred through partial grain dissolution and moldic grain dissolution, matrix dissolution and the fracturing of grains to vary degrees in all Kapuni Group sandstone lithofacies. Of these diagenetic processes the most common is the dissolution of feldspar grains, primarily plagioclase, which is most advanced in the Mangahewa Formation. Although this type of porosity is common, it is uncertain as to whether reservoir porosity is actually enhanced due to the fact that pores are very poorly interconnected, mainly isolated by rims of remnant feldspar, and are often surrounded by densely packed detrital grains. Furthermore, due to low solubility of Al bearing minerals some authors e.g. Hayes (1979) suggest that feldspar dissolution leads to precipitation of clay minerals and quartz with in the rock with little/no net gain in porosity and a potential loss of permeability.

6.4 FUTURE RESERVOIR DEVELOPMENT AND PREDICTIONS

As identified depositional and post-depositional processes have to varying degrees determined the ultimate reservoir quality of the Kapuni Group sandstones in the Kapuni Field. In assessing these processes and their relative importance it is possible to apply the findings of this study to areas of future reservoir development in the Kapuni Field and in a wider sense make some inferences and predictions to future exploration in the Taranaki Basin.

6.4.1 Kapuni Field

Future reservoir development in the Kapuni Field should focus on identifying and exploiting those Mangahewa Formation sandstone lithofacies deposited in tidal sand bar, and tidal channel environments. These sandstone lithofacies contain the best reservoir sandstone characteristics in the field, with preserved primary porosity and well developed secondary porosity. In this study a classification scheme has been devised which allows lithofacies to be distinguished by their characteristic log motifs on the gamma-ray. Log motif correlations between Kapuni wells for the Mangahewa Formation indicate an increase in occurrence and thickness of lithofacies representing tidal sand bar and tidal channel environments in the northern Kapuni-8, -12 and -15 wells of the field at all reservoir intervals. Future production programs should therefore concentrate on draining

the northern extent of the Kapuni anticline where these lithofacies occur above the water zone.

6.4.2 Taranaki Basin

In the Taranaki Basin all significant hydrocarbon accumulations occur in structural traps, except for the Kupe South Field, where lithology-dependent diagenetic effects may partially control reservoir distribution (King, 1994). Concerted exploration efforts in the basin now mean that most large structural traps have already been identified and completed. As previously recognised by Orr (1987) and King (1994) exploration efforts, must now focus on identifying reservoir sandstones within smaller structures, but more importantly stratigraphic traps. North (1985) defines stratigraphic traps as those that occur through variations in the stratigraphy and that are independent of structural deformation other than regional tilting. Sandstone lithofacies identified in the Kapuni Group have stratigraphic trapping potential formed by lithofacies or unconformity pinchouts or up-dip cementation.

In the Kapuni Field estuarine depositional lithofacies were identified in the Mangahewa Formation and are inferred to have existed at least in the upper part of the Kaimiro Formation due to the recognition of similar lithofacies in core. Tidal sand bar and tidal channel environments were not identified in limited core available from the Kaimiro Formation, but it is highly likely that they exist, due to the presence of sand flat, meandering tidal channel, mud flat and marsh/swamp environments collectively typical of tidally-influenced estuarine systems. Also, petrographic studies indicate similar detrital composition, textural characteristics, and diagenetic modification of sandstone lithofacies (meandering tidal channel and sand flat environments) that occur in both the Mangahewa and Kaimiro Formations. It is highly likely, therefore, that where present, tidal sand bar and tidal channel lithofacies are likely to comprise similar reservoir characteristics both within the Kapuni Field and elsewhere in the Taranaki Basin.

Future exploration in the Taranaki Basin should focus on identifying and recognising sandstones lithofacies that characterise estuarine deposits of the Mangahewa and Kaimiro formations. The advantages to exploration are firstly that they have high preservation potential because of their location within paleovalleys (Dermarest and Kraft, 1987) and secondly they provide the ideal habit for hydrocarbons because of well-sorted lenticular or linear sandstone bodies representative of various environments that thin out gradually or abruptly both along and across their strike. The potential is also high for multiple complexes of interlocking fluvial, estuarine and beach deposits separated from one another by hydraulic barriers of shale or coal. These factors combined with the overall transgression nature and associated forced regressions that occur in estuaries, mean that

the potential for stratigraphic or unconformity pinchouts is high in both the Mangahewa and Kaimiro formations.

Estuarine deposits also provide environmental settings favouring the development of stratigraphic traps formed by variations in cementation. In this study and other studies by Hill and Collen (1978), Collen (1988) and Fairburn (1980) of the Kapuni Group, there is evidence to suggest the updip cementation of reservoir sandstones. Traps rarely contain only one homogeneous reservoir rock (North, 1985) and lateral and/or vertical variations in porosity and permeability occur between and with in sandstone lithofacies of the Kapuni Group. Thus the potential is high for stratigraphic traps in the Kapuni Group.

CONCLUSIONS

Lithofacies in the Kapuni Group have been identified in core and their environments of deposition recognised. Log motifs were distinguished for the sandstone lithofacies in the Mangahewa Formation and extrapolated to determine the depositional setting. The composition, texture and porosity of the sandstone lithofacies were ascertained, provenance identified and diagenetic processes and paragenesis elucidated. Depositional and diagenetic factors controlling reservoir quality have been discussed and their relative importance established. These findings have then been applied to aid in future reservoir development in the Kapuni Field and exploration in the Taranaki Basin. The main conclusion of this study are:

- Lithofacies in core from the Mangahewa Formation elucidate to tidal sand bar, tidal-inlet channel, fluvial/tidal channel, spit platform, sand flat, shallow marine, tidal channel, meandering tidal channel, mud flat, swamp and marsh environments. The Kaimiro Formation comprises lithofacies of meandering tidal channel, sand flat, mud flat, swamp and marsh environments. While the Farewell Formation lithofacies represent tidal channel and mud flat depositional environments.

- Log signatures on the gamma-ray when correlated with core provide a useful means for distinguishing lithofacies in the Mangahewa Formation based on log curve shape and characteristics (log motifs). Log motifs allowed reservoir intervals in the Mangahewa Formation to be redefined, to correspond with stages in the depositional history of the formation.

- The crystallinity of kaolinite exaggerates XRD peaks leading to an overestimation of kaolinite relative to other clay minerals. Accurate assessment of clay percentages in the Kapuni Group therefore necessitates the use of XRD supplemented with DTA and IR analysis studies.

- Evidence from framework mineralogy clearly indicates that the Kapuni Group sediments were derived from more than one main rock type. The dominant sediment sources for the Kapuni Group are low -grade metamorphic rock of Lower Cambrian to Permian age and the Permian to Carboniferous Karamea Granite that occur in northwest Nelson. A sedimentary source may include greywacke-argillite sedimentary rocks of Triassic and Jurassic age that crop out to the northeast, east and southeast of the Taranaki Basin and/or Upper Cretaceous Pakawau Group

sediments also to the south of the Taranaki Basin in the northwest Nelson area. Pre Cambrian to Upper Cretaceous acid volcanic rocks that also occur in the northwest Nelson area are an important source in the Farewell Formation, but minor source in the Mangahewa and Kaimiro Formations.

- The Mangahewa Formation was deposited in an overall transgressive environment. Initially tide-dominated estuarine conditions predominated. The estuary infilled through progradation of tidal sand bar, mud flat and swamp/marsh development. The K20 coal represents a period of maximum infilling and low sea-level. After deposition of the K20 coal another transgressive episode reflecting wave-dominated estuarine conditions prevailed. The marine barrier sand body deposited during the later stages of Mangahewa Formation deposition was later eroded from wells in the middle and south of the field by marine erosion and/or tectonic uplift.

- Diagenetic process have reduced reservoir quality in the Kapuni Group by mechanical and chemical compaction, clay formation (predominantly kaolinite and illite in the Mangahewa and Kaimiro formation and smectite in the Farewell Formation), quartz and feldspar overgrowths and carbonate cementation (primarily siderite and calcite). Diagenetic processes have enhanced reservoir quality primarily through the dissolution of replacive carbonate cements and subordinately by the dissolution of framework grains and clay matrix and grain fractures.

- Sandstone reservoir quality in the Kapuni Group is highest in the Mangahewa Formation lithofacies of tidal sand bar and tidal channel environments. In these sandstones primary porosity is preserved and secondary porosity is best developed.

- Future development in the Kapuni Field should focus on identifying and exploiting lithofacies of the tidal sand bar and tidal channel and tidal environments. These sandstone lithofacies provide the best reservoir characteristics in the field.

- Future exploration in the Taranaki Basin should focus on identifying reservoir sandstones within smaller structures and stratigraphic traps. Sandstones lithofacies of the Mangahewa and Kaimiro Formation are very likely to contain stratigraphic traps formed by lithofacies or unconformity pinchouts or up-dip cementation.

REFERENCES

Abbott, W.O. (1990). Kapuni Field. In E.A. Beaumont and N.H. Foster, (Eds.), *Structural traps; I, tectonic fold traps: AAPG Treatise of Petroleum Geology, Atlas of oil and gas fields* (pp. 27 - 49). Tulsa: American Association of Petroleum Geologists.

Anderson, F.E., Black, L., Watling, L.E., Mook, W., and Mayer, L.M. (1981). A temporal and spatial study of mud flat erosion and deposition. *Journal of Sedimentary Petrology, 51*, 729 -736.

Andrews, P.B. (1982). *Revised guide to recording field observations in sedimentary sequences, New Zealand Geological Survey Report NZGS 102.* Lower Hutt: Department of Scientific and Industrial Research.

Bal, A.A. (1994). Cessation of Tasman Sea spreading recorded as a sequence boundary: Interpretation of an early Paleocene unconformity in the Pakawau sub-basin, northwest Nelson, New Zealand. In G.J. van der Lingen, K.M. Swanson, and R.J. Muir (Eds.), *Evolution of the Tasman Sea Basin: Preceedings of the Tasman Sea Conference, Christchurch, New Zealand* (pp. 105 – 117). Rotterdam: Balkema

Basu, A., Young, S.W., Suttner, L.J., James, W.C., and Mack, G.H. (1975). Re-evaluation of the use of undulatory extinction and polycrystallinity in detrital quartz for provenance interpretation. *Journal of Sedimentary Petrology, 45*, 873 – 882.

Beggs, J.M. (1989). *Diagenetic effects of petroleum emplacement into sandstone reservoirs: New Zealand Geological Survey Record, 40* (pp. 61 – 66). Wellington: New Zealand Department of Scientific and Industrial Research.

Bell, D.L., and Goodell, H.G. (1967). A comparative study of glauconite and the associated clay fraction in modern marine sediments. *Sedimentology, 9*, 169 – 202.

Bishop, D.G. (1971). *Sheets S1, S3 and pt. S4. Farewell Spit – Collingwood* (1st ed.) *Geological Map of New Zealand 1:63,360.* Wellington: New Zealand Department of Scientific and Industrial Research.

Bjørlykke, K., Aagaard, P., Dypvik, H., Hastings, D.S., and Harper, A.S. (1986). Diagenesis and reservoir properties of Jurassic sandstones from the Haltenbanken area, offshore Mid-Norway. In A.M Spencer (Ed.), *Habitat of hydrocarbons on the Norwegian Continental Shelf* (pp. 275 – 286). London: Graham and Trotman.

Bjørlykke, K., Ramm, M., and Saigal, G.C. (1989). Sandstone diagenesis and porosity modification during basin evolution. In H.S. Poelchau and U. Mann (Eds.), *Geologic modelling – aspects of integrated basin analysis and numerical simulation* (pp. 243 – 268). Geol Rundsch.

Blanche, J.B., and Whitaker, J.H. (1978). Diagenesis of part of the Brent Sand Formation (Middle Jurassic) of the northern North Sea Basin. *Journal of Geological Society of London, 135*, 73 – 82.

Blatt, H. (1979). Diagenetic processes in sandstones. In P.A. Scholle and P.R Schluger (Eds.), *Aspects of Diagenesis: SEPM Special Publication No.26* (pp. 141 – 159). Tulsa: Society of Economic Paleontologists and Mineralogists.

Blatt, H. (1982).Sedimentary Petrology. San Francisco: W.H. Freeman.

Blatt, H., and Christie, J.M. (1963). Undulatory extinction in quartz of igneous and metamorphic rocks and its significance in provenance studies of sedimentary rocks. *Journal of Petrology, 37*, 401 – 424.

Boggs, S. (2001). *Principles of sedimentology and stratigraphy* (3rd ed.). New Jersey: Prentice Hall.

Brekelmans, H., Bryant, I.D., van Rossem, S.J., Soek, H.F., and Stulemeijer, I.P.J.M. (1991). Reservoir geological modelling of the Mangahewa Formation, Kapuni Field (onshore New Zealand): Unpublished Shell Report (RKER 91.018). New Plymouth: Shell BP Todd Oil Services Limited.

Bryant, I.D., and Bartlett, A.D. (1992). *Kapuni 3D reservoir model and reservoir simulation.* In *1991 New Zealand oil exploration conference proceedings* (pp. 404 – 412). Wellington: Ministry of Commerce.

Bulte, G.A. (1988). Styles of compressional wrench faulting, Taranaki Basin, New Zealand. In *Preceedings of the 7th offshore South East Asia conference* (pp. 79 – 91). Singapore.

Cant, D.J. (1992). Subsurface facies analysis. In R.G. Walker, and N.P. James (Eds.) (1994). *Facies models: response to sea-level change* (2nd ed.) (pp. 27 - 47). Ontario: Geological Society of Canada.

Challis, G.A., and Mildenhall, D.C. (1986). *Petrography and diagenesis of sandstones from Kapuni-12 well between 3489.9m and 3460.8m.* Unpublished Petroleum Report PR1224. Wellington: Ministry of Commerce.

Collen, J.D. (1988). Diagenetic control of porosity and permeability in Pakawau and Kapuni Group sandstones, Taranaki Basin, New Zealand. *Energy, Exploration and Exploitation, 6*, 263 - 280.

Collinson, J.D., and Thompson, D.B. (1989). *Sedimentary structures* (2nd ed.). London: Unwin Hyman Limited.

Crown Minerals (2000). *Explore New Zealand Petroleum.* Wellington: Crown Minerals, Ministry of Economic Development.

Crown Minerals (2001). *Explore New Zealand Petroleum.* Wellington: Crown Minerals, Ministry of Economic Development.

Crown Minerals (2002). *Explore New Zealand Petroleum.* Wellington: Crown Minerals, Ministry of Economic Development.

Crown Minerals (2003). *Explore New Zealand Petroleum.* Wellington: Crown Minerals, Ministry of Economic Development.

Dalrymple, R.W. (1992). Tidal depositional systems. In R.G. Walker and N.P. James (Eds.) *Facies models: response to sea-level change* (2nd ed.) (pp 195 – 219). Ontario: Geological Society of Canada.

Dalrymple, R.W., Knight, R.J., Zaitlin, B.A., and Middleton, G.V. (1990) Dynamics and facies model of a macro-tidal sand-bar complex, Cobequid Bay-Salmon river estuary, (Bay of Fundy). *Sedimentology, 37*, 577 - 612.

Dalrymple, R.W., and Zaitlin, B.A. (1989). Tidal sedimentation in the macrotidal, Cobequid Bay-Salmon river estuary, Bay of Fundy: In *Canadian Society of Petroleum Geologists Field Guide, Second International Symposium on Clastic Tidal Deposits, Calgary, Alberta* (pp 84).Alberta: Canadian Society of Petroleum Geologists.

Dalrymple, R.W., Zaitlin, B.A., and Boyd, R. (1992). Estuarine facies models: conceptual basis and stratigraphic implications. *Journal of Sedimentary Petrology, 62*(6), 1130 – 1146.

Dapples, E.C. (1979). Diagenesis of sandstones. In G. Larsen, and G.V. Chilingar (Eds.), *Development in sedimentology: Diagenesis in sediments and sedimentary rocks.* Amsterdam: Elsevier Scientific Publishing Company.

Davis, R.A. (1992). *Depositional Systems: An introduction to sedimentology and stratigraphy* (2nd ed.). New Jersey: Prentice Hall.

de Boer, G.J.W. (1973). *Interpretation of the 1971 and 1973 seismic surveys in Mining Licence 839, Kapuni Area, New Zealand: Unpublished Shell-BP-Todd EP 44946III.* New Plymouth: Shell BP Todd Oil Services Limited.

Deer, W.A., Howie, R.A., and Zussman, J. (1971). *An introduction to the rock forming minerals*. London: Longman.

Dermarest, J.M., II., and Kaft, J.C. (1987). Stratigraphic record of Quaternary sea levels: implications for more ancient strata. In D. Nummedal, O.H. Pilkey and J.D. Howard (Eds.). *Sea-level fluctuations and coastal evolution: SEPM Special Publication 41* (pp. 223 – 239). Tulsa: Society of Economic Paleontologists and Mineralogists.

Dickinson, W.R., Beard, L.S., Brakenridge, G.R., Erjavec, J.L., Ferguson, R.C., Inman, K.F., Knepp R.A., Lindberg, F.A., and Ryberg, P.T. (1983). Provenance of North American Phanerozic sandstones in relation to tectonic setting. *Geological Society America Bulletin, 94*, 222 – 235.

Donaldson, A.C., Martin, R.H., and Kanes, W.H. (1970). Holocene Guadalupe delta of Texas Gulf Coast. In J.P. Morgan (Eds.) *Deltaic sedimentation modern and ancient: SEPM Special Publication 15* (pp. 45 – 68). Tulsa: Society of Economic Paleontologists and Mineralogists.

Dörjes, J., and Howard, J.D. (1975). Estuaries of Georgia Coast, U.S.A: Sedimentology and Biology, IV, fluvial-marine transition indicators in an estuarine environment, Ogeecheee River-Ossabaw Sound. *Senckenbergiana Maritima, 7*, 137-179.

Dunoyer de Segonzac, G. (1970). The transformation of clay minerals during diagenesis and low-grade metamorphism: A review. *Sedimentology, 15*, 281 – 346.

Ehrenberg, S.N., and Nadeau, P.H. (1989). Formation of diagenetic illite in sandstones of the Garn formation, Haltenbanken area, mid-Norwegian continental shelf, *Clay Minerals, 24*, 233 – 253.

Eslinger, E., and Pevear, D. (1988). *Clay Minerals for Petroleum Geologists and Engineer: SEPM short course no.22.* Tulsa: Society of Economic Paleontologists and Mineralogists.

Elskamp, P.T., and van Benten, J.A. (1976). *Investigation of cores from well Kapuni-3, PML38839.* Unpublished Petroleum Report PR1402. Wellington: Ministry of Economic Development.

Fairburn, S.G. (1980). *Diagenesis of the Kapuni Formation, offshore south Taranaki.* Unpublished BSc(Hons) dissertation, Victoria University of Wellington, Wellington, New Zealand.

Flores, R.M., Beggs, J.M., and King, P.R. (1993). Sedimentology of tide-dominated reservoir sandstones in the Eocene Kapuni Group, Taranaki Basin, New Zealand. In *American Association of Petroleum Geologists 1993 annual convention abstracts* (pp 102). Tulsa: American Association of Petroleum Geologists.

Folk, R.L., Andrews, P.B., and Lewis, D.W. (1970). Detrital sedimentary rock classification and nomenclature for use in New Zealand. *New Zealand Journal of Geology and Geophysics, 13*, 937 - 968.

Fox, J.E., Lambert, P.W., Mast, R.F., Nuss, N.W., and Rein, R.D. (1975). Porosity variation in the Tensleep and its equivalent, the Weber Sandstone, western Wyoming; a log and petrographic analysis. In D.W. Bolyard (Ed.), *Deep drilling frontiers of the central Rocky Mountains* (pp. 185 – 216). Denver, Colorado: Rocky Mountains Association of Geologists.

Frey, R.W., and Basan, P.B. (1985). Coastal salt marshes. In R.A Davis Jnr. (Ed.). *Coastal sedimentary environments* (2nd Ed.) (pp. 225 – 302). New York: Springer-Verlag.

Füchtbauer, H. (1967). Influence of different types of diagenesis of sandstone porosity. *7th World Petroleum Congress, Proceedings 2*, 353 – 380.

Garrels, R.M., and Christ, C.L (1965). *Solutions, minerals and equilibria.* London: Harper and Row.

Gaupp, R., Matter, A., Platt, J., Ramseyer, K., and Walzebuck, J. (1993). Diagenesis and fluid evolution of deeply buried Permian (Rotliegende) gas reservoir, Northwest Germany. *American Association of Petroleum Geologists Bulletin, 77*, 111 – 1128.

Gautier, D.L., Kharaka, Y.K., and Surdam, R.C. (1985). *Relationship of organic matter and mineral diagenesis: SEPM Short Course No.17.* Tulsa: Society of Economic Paleontologists and Mineralogists.

Geosearch. (1991). *Petroleum resources of New Zealand: Resource Information Report 10.* Wellington: Energy and Resources Division, Ministry of Commerce.

Giles, M.R., Stevenson, S., Martin, S., Cannon, S.J.C., Hamilton, P.J., and Samways, G.M. (1992). The reservoir properties and diagenesis of the Brent Group: A regional perspective. In A.C. Morton, R.S. Haszeldine, M.R Giles and S. Brown (Eds.), *Geology of the Brent Group: Geological Society of London Special Publication 61* (pp. 289 – 327). London: Geological Society of London.

Glennie, K.W., and Jaeckli, R. (1956). *The Oligocene formations of Taranaki.* Unpublished N.Z. Geological Survey report PR409.Wellington: New Zealand Geological Survey.

Hamilton, D. (1979). The high energy sand and mud regime of the Severn Estuary, S.W. Britain. In R.T. Severn, D. Dineley and L.E. Hawker (Eds.), Tidal power and estuary management. *Albuquerque Transatlantic Arts Incorporated, Colston Paper 30,* 162 – 172.

Hancock, N.J. (1978). Possible causes of Rotliegend sandstone diagenesis in northern West Germany. *Journal of the Geological Society of London, 135,* 35 – 40.

Hancock, N.J., and Taylor, A.M. (1978). Clay mineral diagenesis and oil migration in the Middle Jurassic Brent Sand Formation. *Journal of Geological Society of London, 135,* 69 – 72.

Harris, P.T. (1988). Large-scale bedforms as indicators of mutually evasive sand transport and the sequential infilling of wide-mouthed estuaries. *Sedimentary Geology, 57,* 273 – 298.

Harris, P.T., and Collins, M.B. (1985). Bedform distribution and sediment transport paths in the Bristol Channel and Severn Estuary. *Marine Geology, 62,* 153 – 166.

Harrison, J. (1979). *Coal percentage and sandstone-shale ratio maps, Kapuni Formation, Taranaki.* Unpublished Petroleum Report PR745. Wellington: Ministry of Commerce New Zealand

Haskell, T.R. (1975). *Geological Review of the Kapuni Field.* Unpublished Petroleum Report PR65. Wellington: Ministry of Commerce.

Haskell, T.R. (1989). *Study of structural development sandstone depositional systems and hydrocarbon accumulation, Taranaki Basin.* Unpublished Petroleum Report PR1502. Wellington: Ministry of Commerce.

Hayes, J.B. (1979). Sandstone Diagenesis – The hole truth. In P.A. Scholle and P.R Schluger (Eds.), *Aspects of Diagenesis: SEPM Special Publication No.26* (pp. 127 – 139). Tulsa: Society of Economic Paleontologists and Mineralogists.

Hayward, B.W. (1987). *Paleobathymetry and structural and tectonic history of Cenozoic drillhole sequences in Taranaki Basin: New Zealand Geological Survey report PAL122.* Wellington: Department of Scientific and Industrial Research.

Hayward, B.W., and Wood, R.A. (1989). *Computer-generated geohistory plots for Taranaki drillhole sequences: New Zealand Geological Survey report PAL147.* Wellington: Department of Scientific and Industrial Research.

Hicks, P.F. (1962). *Remarks on the Kapuni Structure.* Unpublished Petroleum Report PR440. Wellington: Ministry of Economic Development.

Hill, P.J., and Collen, J.D. (1978). The Kapuni sandstones from Inglewood-1 well, Taranaki – petrology and the effect of diagenesis on reservoir characteristics. *New Zealand Journal of Geology and Geophysics, 21*, 215 - 228.

Hogan, J.A. (1979). *Stratigraphy and sedimentology of the Kapuni Formation. Taranaki, New Zealand.* Unpublished MSc dissertation, Victoria University of Wellington, Wellington, New Zealand.

Holstege, G.C.J., and Bishop, D.J. (1998). Structural evolution of the Kapuni Field, New Zealand. *In 1998 New Zealand oil exploration conference proceedings* (223 – 231). Wellington: Ministry of Commerce.

Isaac, M.J., Herzer, R.H., Brook, F.J., and Hayward, B.W. (1994). *Cretaceous and Cenozoic sedimentary basins of Northland, New Zealand: Institute of Geological and Nuclear Sciences monograph 8.* (pp. 203).Wellington: Institute of Geological and Nuclear Sciences Limited.

Katz, H.R. (1968). Potential oil formation in New Zealand and their stratigraphic position as related to basin evolution. *New Journal of Geology and Geophysics, 11*, 1077 – 1133.

Katz, H.R. (1971). Petroleum developments in New Zealand during 1970. *American Association of Petroleum Geologists Bulletin, 55*, 1657 – 1661.

Katz, H.R. (1973). Petroleum developments in New Zealand during 1972. *American Association of Petroleum Geologists Bulletin, 57*, 2109 – 2113.

Katz, H.R. (1974). Recent exploration for oil and gas. In G.J. Williams (Ed.) *Economic geology of New Zealand: the T.J McKee memorial volume: Australian Institute of Mining and Metallurgy monograph series 4* (pp. 463 – 480). Victoria: Australian Institute of Mining and Metallurgy.

Katz, H.R. (1975a). Petroleum developments in New Zealand during 1974. *American Association of Petroleum Geologists Bulletin, 59*, 2011 – 2013.

Katz, H.R. (1975b). The story of oil. *New Zealand's Nature Heritage, 6*(83) 2317 – 2324.

Katz, H.R. (1976a). Developments in New Zealand and Southwest Pacific Island Region 1975. *American Association of Petroleum Geologists Bulletin, 60*, 1947 – 1956.

Katz, H.R. (1976b). Sedimentary basins and petroleum prospects, onshore and offshore New Zealand. In M.T. Halbouty, J.C. Maher, H.M. Lian, and J.C. Hazzard (Eds.), *Circum-Pacific energy and mineral resources: papers from a Circum-Pacific energy and mineral resources conference, AAPG memoir 25* (pp. 217 – 228). Tulsa: American Association of Petroleum Geologists.

Kear, D. (1967). The Kapuni gas-condensate field, New Zealand: a case study. In United Nations, *Economic Commission for Asia and the Far East, case histories of oil and gas*

fields in Asia and the Far Eas: Mineral resources development series 29. (pp. 86 – 91). New York: United Nations.

King, P.R. (1988a). *Well summary sheets, onshore Taranaki: New Zealand Geological Survey report G125.* Wellington: New Zealand Geological Survey.

King, P.R. (1988b). *Well summary sheets, offshore Taranaki: New Zealand Geological Survey report G127.* Wellington: New Zealand Geological Survey.

King, P.R. (1990). Polyphase evolution of the Taranaki Basin, New Zealand: changes in sedimentary and structural style. In *1989 New Zealand oil exploration conference proceedings* (pp. 134 – 150). Wellington: Ministry of Commerce.

King, P.R. (1991). *Physiographic maps of the Taranaki Basin – Late Cretaceous to Recent: New Zealand Geological Survey report G155.* Wellington: Department of Scientific and Industrial Research.

King, P.R. (1994). The habitat of oil and gas in Taranaki Basin. In *1994 New Zealand petroleum conference proceedings* (pp. 180 – 203). Wellington: Ministry of Commerce

King, P.R., and Beggs, J.M. (1991). Geological controls on oil and gas occurrence in Taranaki Basin, New Zealand. In *American Association of Petroleum Geologists 1991 Annual Convention, Program and Abstracts* (pp. 49). Tulsa: American Association of Petroleum Geologists.

King, P.R., and Cook, R.A. (1987). Summary of the petroleum geology of onshore Taranaki. *Petroleum Exploration in New Zealand News, 15,* 4 - 12.

King, P.R. and Robinson, P.H. (1988). An overview of Taranaki region geology, New Zealand. *Energy Exploration and Exploitation, 6,* 213 - 232.

King, P.R., and Thrasher, G.P. (1992). Post-Eocene development of the Taranaki Basin, New Zealand: convergent overprint of a passive margin. In J.S. Watkins, F. Zhiqiang and K.J McMillen (Eds), *Geology and geophysics of continental margins: AAPG memoir 53* (pp. 93 – 118). Tulsa: American Association of Petroleum Geologists.

King, P.R., and Thrasher, G.P. (1996). *Cretaceous-Cenozoic geology and petroleum systems of the Taranaki Basin, New Zealand: monograph 13.* Wellington: Institute of Geological and Nuclear Sciences Limited.

Knox, G.J. (1982). Taranaki Basin, structural style and tectonic setting. *New Zealand Journal of Geology and Geophysics, 25,* 125 - 140.

Krumbein, W.C., and Garrels, R.M. (1952). Origin and classification of chemical sediments in terms of pH and oxidation-reduction potentials. *Journal of Geology, 60,* 1 – 33.

Kumar, N., and Sanders J.E. (1974). Inlet sequence: a vertical succession of sedimentary structures and textures created by the lateral migration of tidal inlets. *Sedimentology, 21,* 491 - 532.

Lambiase, J.J. (1980). Sediment dynamics in the macrotidal Avon River Estuary, Bay of Fundy. *Canadian Journal of Earth Science, 17*, 1628 – 1641.

Land, L.S., Milliken, K.L., and McBride, E.F. (1987). Diagenetic evolution of Cenozoic sandstones, Gulf of Mexico sedimentary basin. *Sedimentary Geology, 50*, 195 – 225.

Lanson, B., Beaufort, D., Berger, G., Bauer, A., Cassagnabère, A., and Meunier, A. (2002). Authigenic kaolin and illitic minerals during burial diagenesis of sandstones: a review. *Clay Minerals, 37*, 1 – 22.

Lewis, D.W., and McConchie, D. (1994). *Practical Sedimentology* (2nd ed.). New York: Chapman and Hall.

Lutz, M. (1964). *Lower coastal plain deposits of the Eocene Mangaotaki Formation (New Zealand)*: Unpublished Shell-BP-Todd EP 3498. New Plymouth: Shell BP Todd Oil Services Limited.

Mansfield, C.F. and Bailey, S.W. (1972). Twin and pseudotwin intergrowths in kaolinite. *American Mineralogy, 57*, 411 - 425.

Mason, B. (1966). *Principles of geochemistry* (3rd ed.). New York: John Wiley and Sons.

McAlpine, A., and Bussell, R. (1994). *Taranaki hydrocarbon crawl: Geological Society of New Zealand Conference Field Trip Guide* (pp 127 – 151). Geological Society of New Zealand.

McBeath, M. (1976). *Kapuni and Maui gas-condensate fields of New Zealand – summary, AAPG Memoir 25* (pp. 211 – 216). Tulsa: American Association of Petroleum Geologists.

McBeath, M. (1977). Gas-condensate fields of the Taranaki Basin, New Zealand. *New Zealand Journal of Geology and Geophysics, 20*, 99 – 129.

McBride, E.F. (1989). Quartz cement in sandstones: a review. *Earth Science Review, 26*, 69 – 112.

McConchie, D.M., and Lewis, D.W. (1980). Varieties of glauconite in late Cretaceous and early tertiary rocks of the South Island of New Zealand, and new proposals for classification. *New Zealand Journal of Geology and Geophysics, 23*, 413 - 437.

McHardy, W.J., Wilson, M.J., and Tait, J.M. (1982). Electron microscope and x-ray diffraction studies of filamentous illitic clay from sandstones of the Magnus Field. *Clay Minerals, 17*, 23 - 39.

McLernon, C.R. (1972). *Oil prospecting wells drilled in New Zealand - 1865 – 1970: Industrial Minerals and Rocks: New Zealand Department of Scientific and Industrial Research Information Series 88*. Wellington: New Zealand Department of Scientific and Industrial Research.

McLernon, C.R. (1976). *Oil prospecting wells drilled in New Zealand 1971 – 1973 with additions to oil prospecting wells 1865 – 1970: Industrial Minerals and Rocks No. 7*. Wellington: New Zealand Department of Scientific and Industrial Research.

McLernon, C.R. (1978). *Indications of petroleum in New Zealand. New Zealand.* unpublished petroleum report PR839. Wellington: Ministry of Commerce
Miall, A.D. (1990). *Principles of sedimentary basin analysis* (2nd ed). New York: Springer-Verlag.

Mildenhall, D.C. (1988). *Palynology of core and sidewall samples from well Kapuni-14, New Zealand: New Zealand Geological Survey Report DCM 98/88.* Wellington: Department of Scientific and Industrial Research.

Moslow, T.F., and Tye, R.S., (1985). Recognition and characterization of Holocene tidal inlet sequences: *Marine Geology, 63*, 129 – 151.

Neall, V.E. (1979). *Sheets P19, P20 and P21, New Plymouth, Egmont and Manaia. Geological map of New Zealand 1:50,000.* Wellington: Department of Scientific and Industrial Research.

Nichol, S.L. (1991). Zonation and sedimentology of estuarine facies in an incised valley, wave-dominated, microtidal setting. In D.G. Smith, G.E. Reinson, B.A. Zaitlin, and R.A. Rahmani (Eds.), *Clastic tidal sedimentology, Canadian Society of Petroleum Geologists Memoir 16* (41 – 58). Ontario: Canadian Society of Petroleum Geologists.

North, F.K. (1985). *Petroleum Geology*. London: Unwin Hyman.

Odin, G.S. (1988). *Green marine clays, Developments in sedimentology, 45.* Amsterdam: Elsevier.

Orr, M.D.M. (1987). *Petrology and diagenesis of the Kapuni Group sandstone reservoirs of the Maui gas-condensate field, Taranaki Basin, New Zealand.* Unpublished BSc (Hons) dissertation, Victoria University of Wellington, Wellington, New Zealand.

Palmer, J.A. (1980). *Description of core material from Kapuni Formation, onshore Taranaki, New Zealand: Geology Department of Geology Publication No. 18.* Wellington: Victoria University of Wellington.

Palmer, J.A. (1985). Pre-Miocene lithostratigraphy of Taranaki Basin, New Zealand. *New Zealand Journal of Geology and Geophysics, 28*, 197 - 216.

Palmer, J.A., and Andrews, P.B. (1993). Cretaceous – Tertiary sedimentation and implied tectonic controls on the structural evolution of Taranaki Basin. In P.F. Balance (Ed.), *South Pacific sedimentary basin: Sedimentary basins of the world* 2 (pp. 309 – 328). Amsterdam: Elsevier.

Palmer, J.A., and Bulte, G. (1991). Taranaki Basin, New Zealand. In K.T. Biddle (Ed.) *Active margin basins: AAPG Geologists memoir 52* (pp. 261 – 282). Tulsa: American Association of Petroleum Geologists.

Pettijohn, F.J., Potter, P.E. and Siever, R. (1987). *Sand and sandstone* (2nd ed.). New York: Springler-Verlag.

Pilaar, W.F.H., and Wakefield, L.L. (1978). Structural and stratigraphic evolution of the Taranaki Basin, offshore North Island, New Zealand. *Australian Petroleum Exploration Association Journal, 18*, 93 – 101.

McLernon, C.R. (1978). *Indications of petroleum in New Zealand. New Zealand.* unpublished petroleum report PR839. Wellington: Ministry of Commerce
Miall, A.D. (1990). *Principles of sedimentary basin analysis* (2nd ed). New York: Springer-Verlag.

Mildenhall, D.C. (1988). *Palynology of core and sidewall samples from well Kapuni-14, New Zealand: New Zealand Geological Survey Report DCM 98/88.* Wellington: Department of Scientific and Industrial Research.

Moslow, T.F., and Tye, R.S., (1985). Recognition and characterization of Holocene tidal inlet sequences: *Marine Geology, 63*, 129 – 151.

Neall, V.E. (1979). *Sheets P19, P20 and P21, New Plymouth, Egmont and Manaia. Geological map of New Zealand 1:50,000.* Wellington: Department of Scientific and Industrial Research.

Nichol, S.L. (1991). Zonation and sedimentology of estuarine facies in an incised valley, wave-dominated, microtidal setting. In D.G. Smith, G.E. Reinson, B.A. Zaitlin, and R.A. Rahmani (Eds.), *Clastic tidal sedimentology, Canadian Society of Petroleum Geologists Memoir 16* (41 – 58). Ontario: Canadian Society of Petroleum Geologists.

North, F.K. (1985). *Petroleum Geology.* London: Unwin Hyman.

Odin, G.S. (1988). *Green marine clays, Developments in sedimentology, 45.* Amsterdam: Elsevier.

Orr, M.D.M. (1987). *Petrology and diagenesis of the Kapuni Group sandstone reservoirs of the Maui gas-condensate field, Taranaki Basin, New Zealand.* Unpublished BSc (Hons) dissertation, Victoria University of Wellington, Wellington, New Zealand.

Palmer, J.A. (1980). *Description of core material from Kapuni Formation, onshore Taranaki, New Zealand: Geology Department of Geology Publication No. 18.* Wellington: Victoria University of Wellington.

Palmer, J.A. (1985). Pre-Miocene lithostratigraphy of Taranaki Basin, New Zealand. *New Zealand Journal of Geology and Geophysics, 28*, 197 - 216.

Palmer, J.A., and Andrews, P.B. (1993). Cretaceous – Tertiary sedimentation and implied tectonic controls on the structural evolution of Taranaki Basin. In P.F. Balance (Ed.), *South Pacific sedimentary basin: Sedimentary basins of the world* 2 (pp. 309 – 328). Amsterdam: Elsevier.

Palmer, J.A., and Bulte, G. (1991). Taranaki Basin, New Zealand. In K.T. Biddle (Ed.) *Active margin basins: AAPG Geologists memoir 52* (pp. 261 – 282). Tulsa: American Association of Petroleum Geologists.

Pettijohn, F.J., Potter, P.E. and Siever, R. (1987). *Sand and sandstone* (2nd ed.). New York: Springier-Verlag.

Pilaar, W.F.H., and Wakefield, L.L. (1978). Structural and stratigraphic evolution of the Taranaki Basin, offshore North Island, New Zealand. *Australian Petroleum Exploration Association Journal, 18*, 93 – 101.

Pirson, S.J., (1970). *Geologic well log analysis.* Houston: Gulf Publishing.
Pittman, E.D. (1970). Plagioclase feldspar as an indicator of provenance in sedimentary rocks. *Journal of Sedimentary Petrology, 40,* 591 – 598.

Pittman, E.D. (1979). Porosity, diagenesis and productive capability of sandstone reservoirs. In P.A. Scholle and P.R. Schluger (Eds.). *Aspects of Diagenesis, SEPM Special Publication No.26* (pp.159 – 175). Tulsa: Society of Economic Paleontologists and Mineralogists.

Platt, J.D. (1993). Controls on clay mineral distribution and chemistry in the early Permian Rotliegend of Germany. *Clay Minerals, 28,* 393 – 416.

Potter, P.E. (1967). Sand bodies and sedimentary environments: a review. *The American Association of Petroleum Geologists Bulletin, 51*(3), 337 – 365.

Powers, M.C. (1953). *A new roundness scale for sedimentary particles. Journal of Sedimentary Petrology, 23,* 117 – 119.

Raine, J.I. (1984). *Biostratigraphy of Kapuni Formation, SBPT Kapuni Deep-1 well, Taranaki: New Zealand Geological Survey Report. PAL 71.* Wellington: Department of Scientific and Industrial Research.

Raine, J.I. (1987). *Palynology of samples from Kapuni Group, SBPT Kapuni-8 well, Taranaki.* Unpublished Petroleum Report PR1299. Wellington: Ministry of Commerce.

Reading, H.G., and Levell, B.K. (1996). Controls on the sedimentary rock record. In H.G. Reading (Ed.), *Sedimentary environments: processes, facies and stratigraphy* (3rd ed.) (pp. 5 – 36). Oxford: Blackwell Science Limited.

Reiman, K. (1962). *Analysis of core samples from well Kapuni-3, PML38839.* Unpublished Petroleum Report PR1400. Wellington: Ministry of Economic Development.

Reineck, H.E., and Singh, I.B. (1975). *Depositional sedimentary environments.* New York: Springler-Verlag.

Reinson, G.E. (1992). Transgressive barrier island and estuarine systems. In R.G. Walker and N.P. James (Eds.) *Facies models: response to sea-level change* (2nd ed.) (pp. 179 – 195). Ontario: Geological Society of Canada.

Rice, R.M., Gorsline, D.S., and Osborne, R.H. (1976). Relationships between sand input from rivers and composition of sands from beaches of Southern California. *Sedimentology, 23,* 689 – 703.

Robinson, P.H., and King, P.R. (1988). Hydrocarbon reservoir potential of the Taranaki Basin, Western New Zealand. *Energy, Exploration and Exploitation, 5*(3), 248 - 262.

Robinson, P.H., Thomson, B., King, P.R., Hayward, B.W., Raine, J.I., and Scott, G.H. (1986a). Depositional history of Eocene - Oligocene sediments, Taranaki Basin, New Zealand. In *12th International Sedimentological Congress, Canberra, Australia. Abstracts volume,* 259.

Robinson, P.H., Thomson, B., King, P.R., Hayward, B.W., Raine, J.I., and Scott, G.H. (1986b). Depositional history of Eocene - Oligocene sediments, Taranaki Basin, New Zealand. In *Geological Society of New Zealand annual conference, Palmerston North. Programme and Abstracts,* (p.87). Geological Society of New Zealand Miscellaneous publication 35A.

Robinson, P.H., Thomson, B., King, P.R., Hayward, B.W., Raine, J.I., and Scott, G.H. (1986c). *Preliminary diagrams on the depositional history of Eocene – Oligocene sediments, Taranaki Basi: New Zealand, New Zealand Geological Survey Report G112.* Wellington: Department of Scientific and Industrial Research.

Rowsell, D.M., and De Swardt, A.M.J. (1974). Secondary leaching porosity in Middle Ecca Sandstones: *Geological Society of South Africa Transactions and Proceedings, 77,* 131 – 140.

Roy, P.S., Thom, B.G., and Wright, L.D. (1980). Holocene sequences on an embayed high energy coast: and evolutionary model. *Sedimentary Geology, 26,* 1 - 19.

Schmidt, V. and McDonald, D.A. (1979a). The role of secondary porosity in the course of sandstone diagenesis. In P.A. Scholle and P.R. Schluger (Eds.), *Aspects of Diagenesis, SEPM Special Publication No.26* (pp. 175 – 207). Tulsa: Society of Economic Paleontologists and Mineralogists.

Schmidt, V. and McDonald, D.A. (1979b). Texture and recognition of secondary porosity in sandstones. In P.A. Scholle and P.R. Schluger (Eds.), *Aspects of Diagenesis, SEPM Special Publication No.26* (pp. 209 – 225). Tulsa: Society of Economic Paleontologists and Mineralogists.

Schmidt, V., McDonald, D.A. and Platt, R.L. (1977). Pore geometry and reservoir aspects of secondary porosity in sandstones. *Bulletin Canadian Petroleum Geology, 25,* 271 – 290.

Schmidt, D.S. and Robinson, P.H. (1990). The structural setting for the Kupe South Field, Taranaki Basin. In *Preceedings 1989 New Zealand oil exploration conference proceedings* (pp. 151 – 172). Wellington: Ministry of Commerce.

Scotchman, I.C., Johnes, L.H., and Miller, R.S. (1989). Clay diagenesis and oil migration in Brent group sandstones of NW Hutton field, UK North Sea. *Clay Minerals, 24,* 339 – 374.

Selley, R.C. (1976). Subsurface environmental analysis of North Sea sediments. *American Association of Petroleum Geologists Bulletin, 60*(2) 184 – 195.

Selley, R.C. (1978). *Concepts and methods of subsurface facies analysis: American Association of Petroleum Geologists, Continuing Education Course Notes Series 9.* Tulsa: American Association of Petroleum Geologists.

Serra, O. (1985). *Sedimentary environments from wireline logs.* Montrouge: Schlumberger Limited.

Serra, O., and Sulpice, L. (1975). Sedimentological analysis of shale-sand series from well logs. *Transactions of the SPWLA 16th Annual Logging Symposium, Paper W,* 23

Shell BP Todd Oil Services Limited (1984). *Geological summary Kapuni Deep-1, PML 38839, Taranaki, New Zealand.* Unpublished Petroleum Report PR1024, Wellington: Ministry of Commerce.

Shell BP Todd Oil Services Limited (1988). *Geological and petrophysical analysis of cores from well KA-14 PML38836 (SBPT Report No. 88/037).* Unpublished Petroleum Report PR1373. Wellington: Ministry of Commerce.

Shell Todd Oil Services Limited (1992). *Well Resume Kapuni-15 (KA-15), Kapuni-15A (KA-15A), PML 38839 Taranaki New Zealand.* Unpublished Petroleum Report PR1832, Wellington: Ministry of Commerce.

Shelley, D. (1974). *Optical Mineralogy* (2nd ed.). Christchurch: Department of Geology, University of Canterbury.

Short, K.C. (1962). *The stratigraphy of the Taranaki Peninsula structure.* Unpublished petroleum report PR438. Wellington: Ministry of Commerce.

Sibley, D.F., and Blatt, H. (1976). Intergranular pressure solution and cementation of the Tuscarora Orthoquartzite. *Journal of Sedimentary Petrology, 46*, 881 – 896.

Smale, D. (1992). Provenance of sediments in Taranaki Basin: an assessment from heavy minerals. In *1991 New Zealand oil exploration conference proceedings*, (pp. 245 - 254) Wellington: Ministry of Commerce.

Smale, D. (1996). *Petrographic summaries of Taranaki petroleum* reports: *Institute of Geological and Nuclear Sciences Science Report 96/1.* Wellington: Institute of Geological and Nuclear Sciences.

Smale, D., Mauk, J.L., Palmer, J., Soong, R., and Blattner, P. (1999). Variations in sandstone diagenesis with depth, time, and space, onshore Taranaki wells, New Zealand. *New Zealand Journal of Geology and Geophysics, 42*, 137 - 154.

Stone, W.N., and Siever, R. (1996). Quantifying compaction, pressure solution and quartz cementation in moderately- and deeply-buried quartzose sandstones from the Greater Green River Basin, Wyoming. In L.J. Crossey, R. Loucks, and M.W. Totten (Eds.) *Siliclastic Diagenesis and Fluid Flow, Society for Sedimentary Geology Special Publication 55*, 129 – 150.

Sommer, F. (1978). Diagenesis of Jurassic sandstones in the Viking Graben. *Journal of the Geological Society of London, 135*, 63 – 67.

Suggate, R.P. (1956). Puponga coalfield. *New Zealand Journal of Science and Technology, 37*, 539 – 559.

Surdam, R.C., Crossey, L.J., Hagen, E.S., and Heasler, H.P. (1989). Organic-inorganic interactions and sandstone diagenesis. *American Association of Petroleum Geologists Bulletin, 73*, 1 - 23.

Taylor, J.M. (1950). Pore reduction in sandstones. *American Association of Petroleum Geologists Bulletin, 34*, 701 - 706.

Terwindt, .H.J. (1988). Paleo-tidal reconstructions of inshore tidal depositional environments. In P.L. De Boer, A. van Gelder and S.D. Nio (Eds.), *Tide influenced sedimentary environments and facies* (pp. 233 – 263). Boston: Reidel Publishing Company.

Thrasher, G.P. (1990). Tectonics of the Taranaki Rift. In *1989 New Zealand oil exploration conference proceedings* (pp. 124 – 133). Wellington: Ministry of Commerce.

Thrasher, G.P. (1992). *Late Cretaceous geology of Taranaki Basin, New Zealand.* Unpublished PhD dissertation, Victoria University of Wellington, Wellington, New Zealand.

Tissot, B.P., and Welte, D.H. (1978). Petroleum Formation and Occurrence: a new approach to oil and gas exploration. Berlin: Springer-Verlag.

Tucker, M.E. (1991). *Sedimentary Petrology: an introduction to the origin of sedimentary rocks* (2nd ed.). London: Blackwell Scientific Publications.

United States Geological Survey. (1990). *Grain-size scale: United States Geological Survey.open file report 03-001.* Washington: United States Geological Survey

van der Klugt, S., van der Sijp, J.W.C.M., and Geiger, M.E. (1959). *Exploration well resume, Kapuni-1.* Unpublished Petroleum Report PR427. Wellington: Ministry of Commerce.

van der Lingen, G.J., Challis, G.A., Robinson, P.H., Smale, D.A., and Watters, W.A. (1988). Siliclastic diagenesis in Paleocene-Eocene reservoir sandstones of the Taranaki Basin, New Zealand. *Energy Exploration and Exploitation, 6*(2), 151 - 169.

van der Sijp, J.W.C.M. (1958a). *Tertiary paleogeography of the Taranaki Basin, New Zealand.* Unpublished petroleum report PR421. Wellington: Ministry of Commerce.

van der Sijp, J.W.C.M. (1958b). *Interim compilation of west Taranaki geology. New Zealand.* Unpublished petroleum report PR415. Wellington: Ministry of Commerce.

van der Sijp, J.W.C.M. (1959). *The geology of Taranaki (a compilation report). New Zealand.* Unpublished petroleum report PR821. Wellington: Ministry of Commerce.

van Wijlen, H.A. (1963). *Production - geology report on the Kapuni structure, South Taranaki Peninsula, New Zealand.* Unpublished Shell-BP-Todd EP 33850. New Plymouth: Shell BP and Todd Oil Services Limited.

Voggenreiter, W.R. (1991). *Kapuni 3D interpretation: imaging Eocene paleogeography. In 1991 New Zealand oil exploration conference proceedings* (pp. 287 – 298). Wellington: Ministry of Commerce.

Voggenreiter, W.R. (1993). Structure and evolution of the Kapuni Anticline, Taranaki Basin, New Zealand: evidence from the Kapuni 3D seismic survey. *New Zealand Journal of Geology and Geophysics, 36*, 77 - 94.

Walcott, R.I. (1987). *Geodetic strain and the deformation history of the North Island of New Zealand during the Cainozoic, Philosophical Transactions of the Royal Society of London A321* (pp. 163 – 181). London: Royal Society.

Waugh, B. (1978). Authigenic K-feldspar in British Permo-Triassic sandstones. *Journal of Geological Society of London, 135,* 51 – 56.

Weimer, R.J., Howard, J.D., and Lindsay, D.R. (1982). Tidal flats and associated tidal channels In P.A. Scholle, and D. Spearing (Eds.), *Sandstone depositional environments: AAPG Memoir 31* (pp. 191 – 245). Tulsa: American Association of Petroleum Geologists.

Whitton, J.S., and Churchman, G.J. (1987). *Standard Methods for mineral analysis of survey samples for characterisation and classification in NZ Soil Bureau: NZ Soil Bureau Scientific Report 79.* Lower Hutt: NZ Soil Bureau, Department of Scientific and Industrial Research.

Wilson, M.D., and Pittman, E.D. (1977). Authigenic clays in sandstones: Recognition and influence on reservoir properties and paleoenvironmental analysis. *Journal of Sedimentary Petrology, 47,* 3 - 31.

Wodzicki, A. (1974). Geology of the pre-Cenozoic basement of the Taranaki-Cook Strait-Westland area New Zealand, based on recent drillhole data. *New Zealand Journal of Geology and Geophysics, 17,* 747 – 757.

Worden, R.H., and Morad, S. (2000). Quartz cementation in oil field sandstones: a review of the key controversies. In R.H. Worden and S. Morad (Eds), *Quartz Cementation in Sandstones: Special Publication Number 29 of the International Association of Sedimentologists* (pp. 1 – 21). Oxford: Blackwell Science Limited.

Yunalis, P., and Izhan, W. (1995). *A petrographic study of core plug and chip samples from reservoirs K1A, K3A, K3E in wells KA-03, KA-12, KA-14, KA-15, Kapuni Field, New Zealand.* Unpublished Petroleum Report PR2334. Wellington: Ministry of Commerce.

Zaitlin, B.A., and Schultz, B.C. (1990). Wave-influenced estuarine sand body, Senlac heavy oil pool, Saskatchewan, Canada, In J.H. Barwis, J.G. McPherson, J.R.J Studlick (Eds.), *Sandstone Petroleum Reservoirs* (pp. 363 – 387). New York: Springer-Verlag.

Appendix 1

CORE INFORMATION

WELL No.	FORMATION	RESERVOIR INTERVAL	CORE No.	CORE INTERVAL (mahbdf)	CORE LOG INTERVAL (mahbdf)	LENGTH CORED (m)	AMOUNT RECOVERED (m)	% RECOVERED
Kapuni-1	Mangahewa	K1	4	3260.75 - 3266.85	3259.92 - 3266.02	6.10	5.25	86%
		K1	5	3328.11 - 3334.21	3331.25 - 3337.35	6.10	5.19	97%
		K20C	6	3419.86 - 3425.96	3419.86 - 3425.96	6.10	2.14	35%
	Kaimiro	Cycle B	7	3900.53 - 3906.63	3900.53 - 3906.63	6.10	4.88	80%
		Cycle B	8	3966.67 - 3972.46	3966.67 - 3972.46	5.79	5.79	100%
Kapuni-3	Mangahewa	K3A	1	3548.48 - 3554.58	3551.56 - 3557.66	6.10	2.60	42.50%
		K3U	2	3555.49 - 3565.25	3558.57 - 3568.33	9.75	8.78	90%
		K3E1	3	3641.14 - 3656.08	3643.74 - 3658.68	14.94	13.75	92%
		K3E1	4	3656.08 - 3660.50	3658.68 - 3663.10	14.94	5.38	36%
		K3E1	5	3672.84 - 3687.78	3675.72 - 3690.66	14.94	13.74	92%
		K3E1/ K3E2	6	3687.78 - 3703.02	3691.16 - 3706.40	15.24	14.33	94%
		K3E2	7	3703.62 - 3717.04	3706.60 - 3720.02	13.42	9.80	73%
		K3E2	8	3718.56 - 3727.70	3720.83 - 3729.97	9.14	7.31	80%
Kapuni-8	Kaimiro	Cycle B	1	4041.65 - 4059.94	4042.29 - 4060.58	18.29	18.29	100%
Kapuni-12	Mangahewa	K1	1	3460.00 - 3470.00	3458.08 - 3468.08	10.00	9.68	97%
		K1A	2	3470.00 - 3480.10	3470.00 - 3480.10	10.10	10.10	100%
		K1A/ K1	3	3481.10 - 3493.50	3480.10 - 3493.50	12.40	12.00	96%
Kapuni Deep-1	Farewell	Cycle A	1	5181.00 - 5189.60	5176.52 - 5185.12	8.60	8.60	100%
		Cycle A	2	5515.00 - 5519.35	5521.20 - 5525.55	4.35	4.35	100%
Kapuni-14	Mangahewa	K3E1	1	4040.00 - 4044.42	4040.00 - 4044.42	4.42	4.42	100%
		K3E1	2	4044.42 - 4045.46	4044.42 - 4045.46	1.04	1.04	100%
		K3E1	3	4045.46 - 4055.08	4045.46 - 4055.08	9.62	9.14	95%
		K3E1	4	4055.08 - 4070.50	4055.08 - 4070.50	15.42	15.42	100%
		K3E1	5	4070.50 - 4086.57	4070.50 - 4086.57	16.07	16.07	100%
		K3E1	6	4086.57 - 4100.21	4086.57 - 4100.21	13.64	13.64	100%
		K3E1/ K3E2	7	4100.21 - 4128.15	4100.21 - 4128.15	27.94	27.94	100%
Kapuni-15	Mangahewa	K1/ K1A	1	4700.00 - 4718.60	4703.90 - 4722.50	18.60	18.60	100%

Appendix 2

SEDIMENTOLOGICAL CONVENTIONS

COLOUR

Term	Modifying Objective
Black	Dark
Blue	Dusky
Brown	Light
Green	Moderate
Grey	Mottled
Olive	Pale
Orange	Variegated
Pink	Weathering
Purple	
Red	
White	
Yellow	

Colour terms and modifying objectives (Andrews, 1982)

SORTING

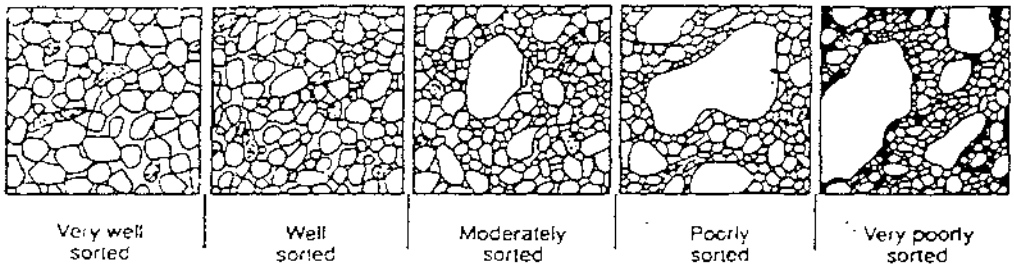

Sediment Sorting Comparator (Blatt, 1982)

GRAIN SHAPE

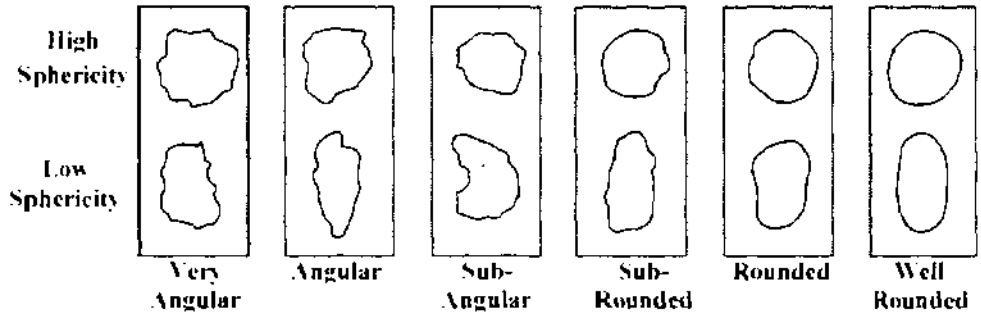

Classes for determining the roundness of sand sized grains (Powers, 1953)

GRAIN-SIZE

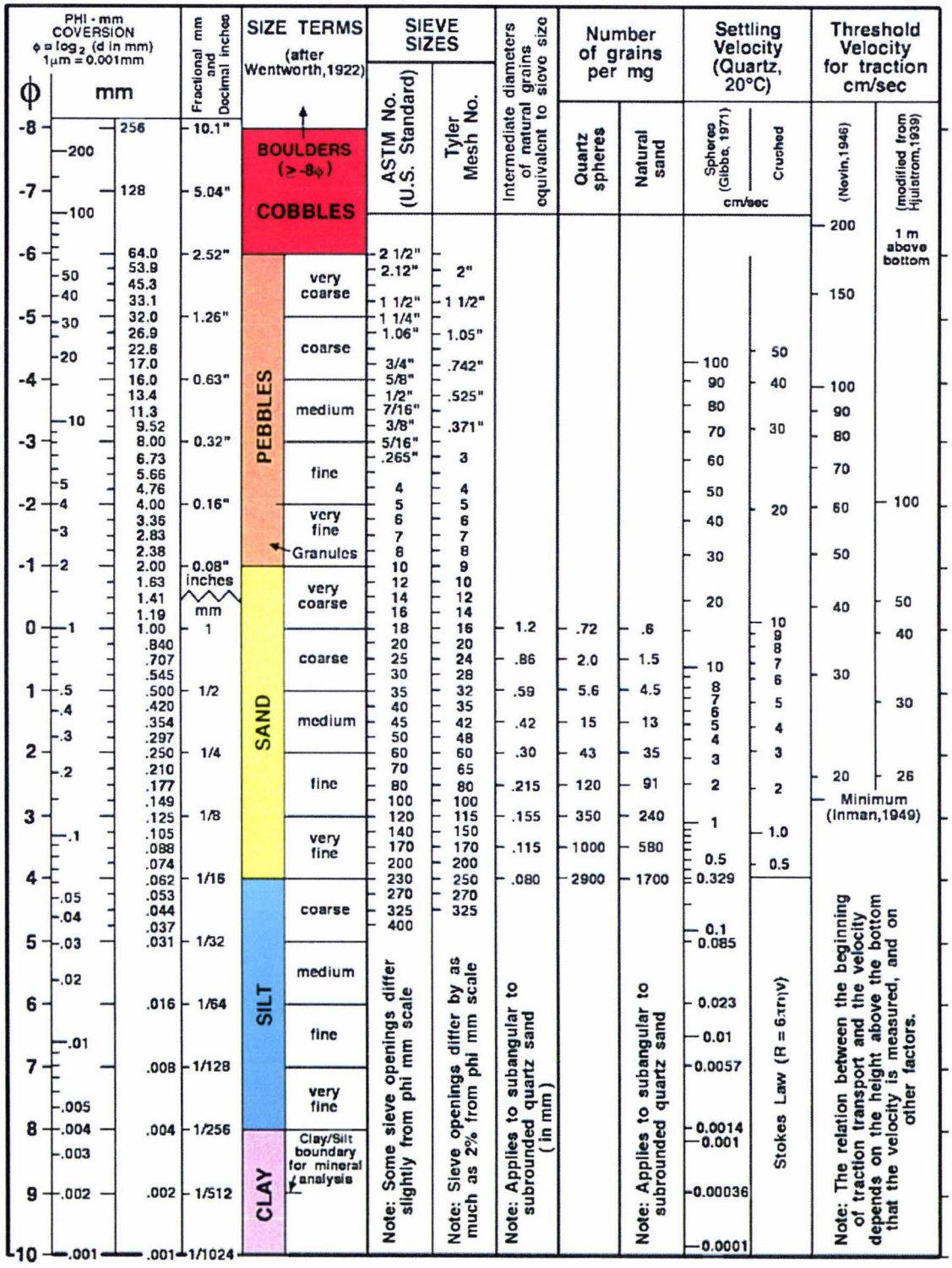

The Wentworth grain-size scale for sediments (United States Geological Survey, 1990)

BEDDING STRUCTURES

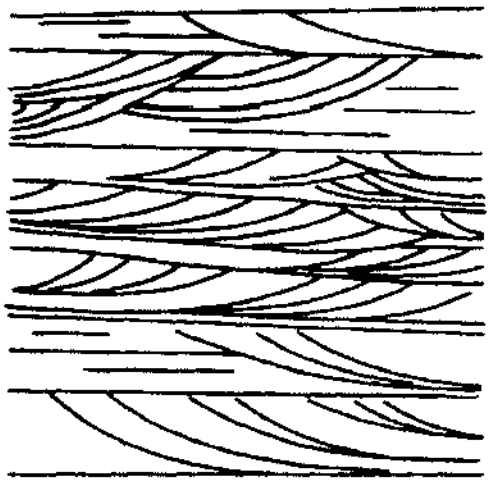

Current Bedding

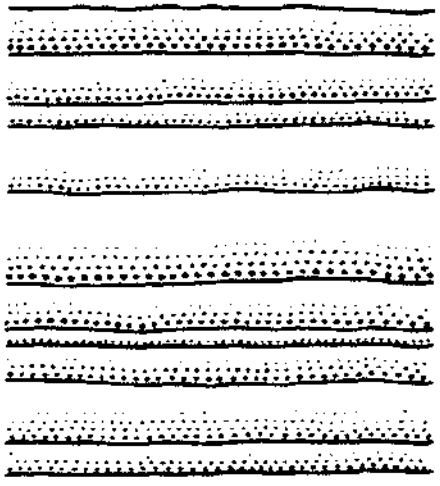

Normal Graded Bedding

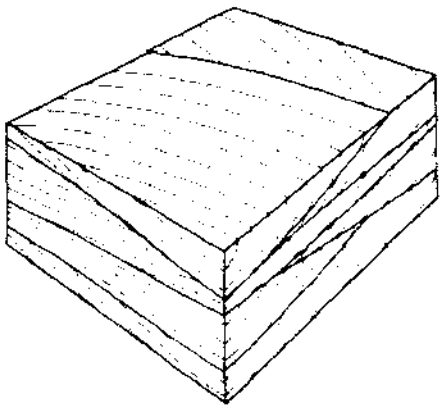

Planar Cross-Bedding

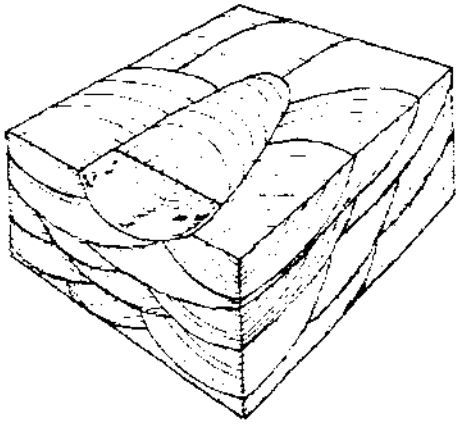

Trough Cross-Bedding

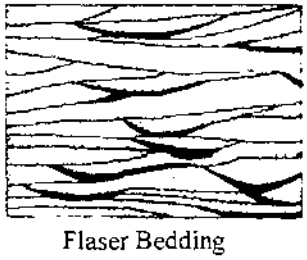

Flaser Bedding

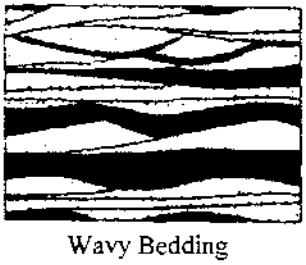

Wavy Bedding

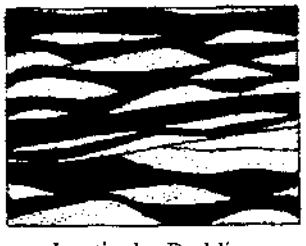

Lenticular Bedding

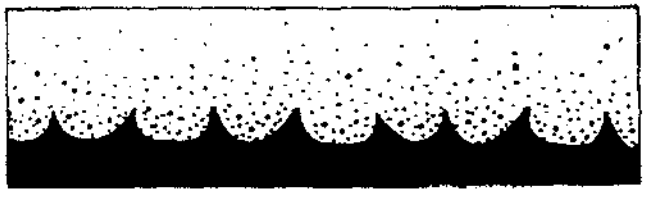

Load Structures

Identification of sedimentary structures (Reineck and Singh, 1975)

Appendix 3

CORE DESCRIPTIONS

KAPUNI-1

Core 4: 3260.75m – 3266.85m

3260.75m - 3264.03m (MS-lb)
Mudstone/Sandstone: dark grey to brownish-black, wavy bedded (2mm - 2cm, average 5mm), carbonaceous mudstone and silty mudstone interbedded with light grey to moderate grey to greyish-brown, very fine-grained, poorly to moderately sorted, sub-rounded, wavy bedded (2mm - 4.5cm, average 3mm), silty sandstone, lenticular bedding at c.3263.50m, some convolute laminae, common bioturbation, mottled, common black coal intraclasts (<2mm by <8mm) between 3262.68m - 3263.49m, occasional reddish-brown siderite grains and orange-pink siderite laminae (<1cm), common mica flakes along bedding planes, lower bedding contact not observed

3264.03m - 3266.85m (SM-f)
Sandstone/Mudstone: light greyish-brown to moderate dark grey, very fine- to fine-grained, poorly to moderately sorted, sub-rounded, wavy bedded (1mm – 5cm, average 1.5cm) sandstone interbedded with dark grey, faint, wavy bedded (1mm – 2cm, average 5mm) silty mudstone, black, shiny, brittle fracture, resinous, coal streaks (<3mm) occur between 3266.44m - 3266.49m and 3266.62m - 3266.67m, common bioturbation, common black coal and brownish-black carbonaceous mudstone intraclasts (<2mm by <5mm) increasing in concentration below c.3264.90m, occasional moderate yellowish-brown pyrite nodules and pale red siderite grains, common mica flakes along bedding planes, lower bedding contact not observed

Core 5: 3328.11m - 3334.21m

3328.11m - 3333.15m (SM-f)
Sandstone/Mudstone: light greyish-brown, medium-grained, poorly to moderately sorted, sub-rounded, wavy bedded (2mm - 5cm, average 2.5cm) sandstone, interbedded with dark brownish-grey, faint, wavy bedded (1mm - 5mm, average 3mm) silty mudstone, occasional light brown and moderate orange-pink siderite laminae (<3mm), common bioturbation between 3328.47m - 3328.72m, occasional black carbonaceous mudstone intraclasts (<2mm by <1cm) occur between 3331.16m - 3333.15m, lower bedding contact not observed

3333.15m - 3334.21m (MS-lb)
Mudstone/Sandstone: dark brownish-black, wavy bedded (2mm - 3cm, average 1cm) carbonaceous mudstone interbedded with light grey, fine-grained, poorly to moderately sorted, sub-rounded, wavy bedded (2mm - 3.5cm, average 1.2cm) sandstone, some convolute bedding, occasional light brown siderite laminae (<1cm), lower bedding contact not observed

Core 6: 3419.86m - 3425.96m

3419.86m - 3422.05m (C)
Coal: black, shiny, brittle fracture, resinous, planar-bedded (2mm – 1cm, average, 5mm) coal interbedded with brownish-black planar laminated (2mm – 7mm, average 3mm) carbonaceous mudstone

3422.05m – 3423.10m
Core missing

3423.10m - 3425.96m (C)
Coal: black, shiny, brittle fracture, resinous, lower bedding contact not observed

Core 7: 3900.53m - 3906.63m

3900.53m - 3902.56m (SM-f)
Sandstone/Mudstone: light brownish-grey, medium- to fine-grained, moderately sorted, sub-rounded, wavy bedded (2mm - 1.5cm, average 5mm) and planar cross-bedded (2mm - 1cm, average 5mm) at c.3901.92m to 3902.02m sandstone interbedded with brownish-black, faint, wavy laminated (1 - 5mm, average 2mm) mudstone, black, shiny, brittle fracture, resinous, coal laminae (1cm) occurs at c.3902.02m, minor bioturbation, common pinkish-grey siderite laminae and lenses (<2mm), some olive grey pyrite nodules, vertical fractures at c.3901.75m and c.3902.05m (vertical offsets = 3mm), lower bedding contact not observed

3902.56m - 3902.66m
Core missing

3902.66m - 3903.60m (MS-lb)
Mudstone/Sandstone: brownish-black, planar bedded (2mm – 3cm, average 1.5cm) carbonaceous mudstone interbedded with grey, fine-grained, moderately sorted, sub-rounded, planar bedded (1mm - 1cm, average 5mm), sandstone, lenticular bedding occurs above 3903.27m, lower bedding contact not observed

3903.60m - 3903.88m
Core missing

3903.88m - 3906.63m (Ss-mb)
Sandstone/Mudstone: light brownish-grey, fine- to medium-grained, moderately sorted, sub-rounded, wavy bedded (2mm - 3.5cm, average 8mm) and planar cross-bedded (2mm - 3cm, average 8mm) at 3904.00m to 3904.45m, sandstone interbedded with brownish-black, faint, wavy laminated (2 - 8mm, average 3mm) carbonaceous mudstone, common pinkish-grey siderite laminae and lenses (<2mm), occasional olive grey pyrite nodules, lower bedding contact not observed

Core 8: 3966.67m - 3972.46m

3966.67m - 3972.46m (Ss-mb)
Sandstone: light-grey, medium- to coarse-grained, moderately to well sorted, sub-rounded, planar laminated (5mm - 3cm, average 8mm), common grey-pink siderite laminae (<3mm), common mica flakes along bedding planes, lower bedding contact not observed

KAPUNI-3

Core 1: 3548.48m - 3554.58m

3548.48m - 3554.58m (SM-f)
Sandstone/Mudstone: light grey, fine-grained, moderately sorted, sub-angular to sub-rounded, wavy bedded (2mm - 3.0cm, average 1cm), sandstone interbedded with dark grey planar and wavy laminated (1mm - 1cm, average 3mm) mudstone, lenticular bedding near c.3550.95m, common load structures (<1cm by <2.5cm), common pink-grey siderite nodules and laminae (2mm – 3mm), lower bedding contact not observed

Core 2: 3555.49m - 3565.25m

3555.49m – 3563.42m (Ss-mb)
Sandstone: light greyish-brown, medium- to coarse-grained, moderately sorted, sub-rounded, massive bedded sandstone, occasional faint wavy carbonaceous mudstone laminae (<2cm), black coal intraclasts (<5mm by <3cm) below 3558.24m, slightly to moderately calcareous, some dark reddish-brown siderite laminae (<1cm), lower bedding contact not observed

3563.42m - 3564.33m (Mc)
Mudstone: brownish-black, massive bedded, carbonaceous mudstone, organic matter increases with depth, black, shiny, brittle fracture, resinous coal at bed (2cm) at c.3564.03m, common dark reddish-brown siderite grains, lower bedding contact not observed

3564.33m – 3565.25m
Core missing

Core 3: 3641.14m - 3656.08m

3641.14m – 3641.80m (Ss-c)
Sandstone: light brownish-grey, coarse-grained, moderately sorted, sub-angular to sub-rounded, planar cross-bedded (3mm – 2cm, average 1cm) sandstone, scoured lower bedding contact

3641.80m – 3643.27m (Ss-mb)
Sandstone: brownish-grey, medium- to coarse-grained, moderately sorted, sub-rounded, bioturbated, sandstone, with dark grey, faint, bioturbated mudstone, mottled, common black carbonaceous intraclasts (1cm by 4cm), horizontal burrows 1cm by <4cm *(Teichichnus)*, strongly bioturbated, common orange-brown disseminated siderite grains, gradational lower bedding contact

3643.27m - 3645.30 (MS-lb)
Mudstone: dark grey, planar laminated (2mm – 4cm, average 8mm) carbonaceous mudstone interbedded with greyish-brown, medium-grained, moderately sorted, sub-rounded, planar bedded (5mm - 3cm, average 1cm) sandstone, flaser bedding below c.3644.34m, common black carbonaceous intraclasts (2mm by 1cm), horizontal burrows 1cm by <5cm *(Teichichnus)*, black, shiny, brittle fracture, resinous coal streaks (<3mm) from 3644.34m – 3644.49m, common orange-brown disseminated siderite grains, lower bedding contact not observed

3645.30m – 3646.75m (Ss-mb)
Sandstone: light brownish-grey, medium- to coarse-grained, moderately sorted, sub-rounded, massive bedded, sandstone with dark-grey, faint, wavy-laminated (2mm – 5mm, average 3mm) mudstone, sharp lower bedding contact

3646.75m – 3648.30m (MS-lb)
Mudstone/Sandstone: dark grey, planar laminated (2mm – 12cm, average 1cm) carbonaceous mudstone interbedded with light brownish-grey, medium-grained, moderately sorted, sub-angular to sub-rounded, planar bedded (3mm - 5cm, average 5mm) and small-scale ripple bedded (1mm - 1cm, average, 3mm) at c.3647.90m and lenticular bedded below 3648.00m sandstone, mottled, 8mm by <1.5cm and 1cm by <3cm horizontal burrows *(Chondrites, Teichichnus)*, strongly bioturbated, dark reddish-brown siderite laminae (<5mm), common mica flakes along bedding planes, sharp lower bedding contact

3648.30m – 3649.90m (Ss-mb)
Sandstone: light brownish-grey, medium- to coarse-grained, moderately sorted, sub-rounded, planar bedded (5mm - 8cm, average 1cm) and planar cross-bedded (1mm – 4cm, average 3cm) at c.3648.80m sandstone, with dark grey, planar laminated (2mm – 5mm, average 3mm) mudstone, gradational lower bedding contact

3649.90m – 3651.80m (MS-lb)
Mudstone/Sandstone: dark grey, planar laminated (2mm – 2cm, average 5mm) carbonaceous mudstone interbedded with light brownish-grey, medium-grained, moderately sorted, sub-angular to sub-rounded, planar laminated (1mm - 1.2cm, average 3mm) and lenticular bedded (1mm – 1cm, average 3mm) sandstone, strongly bioturbated from 3650.20m – 3651.20m, 1cm by <2cm horizontal burrows *(Teichichnus)*, black carbonaceous intraclasts (<3mm by <1cm), common dark reddish-brown siderite laminae (<3mm) occur associated with the mudstone laminae, common mica along bedding planes, lower bedding contact not observed

3651.80m – 3656.08m (Ss-mb)
Sandstone: light brownish-grey, medium- to coarse-grained, moderately sorted, sub-rounded, wavy-bedded (5mm - 15cm, average 5cm) sandstone, with dark grey, faint, wavy laminated (2mm – 5mm, average 3mm) carbonaceous mudstone, horizontal burrows 1cm by 6cm *(Teichichnus)* and 1cm by <25cm and 2cm by <10cm vertical burrows *(Skolithos, Ophiomorpha)*, strongly bioturbated from 3652.30m – 3653.00m and 3656.50m – 3656.08m, black carbonaceous intraclasts (5mm by <1cm) and dark reddish-brown siderite laminae (<3mm)

Core 4: 3656.08m - 3660.50m

3656.08m - 3660.35m (Ss-mb)
Sandstone: light brownish-grey, medium- to coarse-grained, moderately sorted, sub-angular to sub-rounded, planar bedded (3mm - 7cm, average 1.5cm) and massive bedded between 3657.75m 3660.74m sandstone, with dark grey, planar laminated (2mm – 2cm, average 3mm) mudstone, <1.5cm by <4cm horizontal burrows *(Teichichnus)*, strongly bioturbated from 3656.08m – 3657.75m, brownish-black carbonaceous mudstone intraclasts (<5mm by <1cm), slightly calcareous, dark reddish-brown siderite laminae (<3mm), sharp lower bedding contact

3660.35m - 3660.50m (C)
Coal: black, shiny, brittle fracture, resinous coal, lower bedding contact not observed

Core 5: 3672.84m - 3687.78m

3672.84m - 3679.37m (MS-lb)
Mudstone/Sandstone: brownish-black, planar laminated (2mm - 3cm, average 5mm) mudstone, interlaminated with greyish-brown, medium-grained, moderately sorted, sub-rounded, planar laminated (2mm – 2cm, average 3mm), silty sandstone, occasional load structures (<3mm by <3cm), mottled, black, shiny, brittle fracture, resinous coal streaks (<3mm) particularly abundant above c.3675.00m, common bioturbation, lower bedding contact not observed

3679.37m – 3680.51m (SM-f)
Sandstone: light grey to greyish-white, medium-grained, moderately sorted, sub-rounded, planar bedded (1cm – 8cm, average 5cm), sandstone, with brown, faint, discontinuous wavy laminated (1mm – 5mm, average 2mm) mudstone, reddish-brown siderite laminae and lenses (<2mm), brownish-black carbonaceous intraclasts (5mm by 1cm) and occasional dark yellowish-grey pyrite nodules, lower bedding contact not observed

3680.51m - 3687.78m (Ss-mb)
Sandstone: light greyish-brown, medium-grained, moderately to well sorted, sub-rounded, massive bedded, sandstone, abundant dark grey carbonaceous mudstone intraclasts (<1cm by <3cm) occur particularly above c.3683.00m, brownish-black, faint, planar laminated (<3mm) mudstone occurs at c.3682.80m and c.368320m, common reddish-brown siderite laminae (<3mm) replacing mudstone, occasional dark yellowish-grey pyrite nodules, lower bedding contact not observed

Core 6: 3687.78m - 3703.02m

3687.78m – 3689.60m (Ss-mb)
Sandstone: light grey to light greyish-brown, medium- to coarse-grained, moderately to well sorted, sub-rounded, massive bedded, sandstone, abundant dark grey carbonaceous mudstone intraclasts (<2mm by <3cm), calcareous, some reddish-brown siderite grains, occasional dark yellowish-grey pyrite nodules (<5mm), lower bedding contact not observed

3689.60m - 3694.00m (SM-f)
Sandstone: light grey to greyish-white, medium-grained, moderately sorted, sub-rounded, planar laminated (2mm – 1cm, average 5mm), sandstone, with brown, faint, planar laminated (1mm – 5mm, average 2mm) mudstone, occasional reddish-brown siderite laminae and lenses (<3mm), occasional dark yellowish-grey pyrite nodules, common mica along bedding planes, lower bedding contact not observed

3694.00m - 3696.12m (MS-lb)
Mudstone/Sandstone: brownish-black, planar laminated (2mm - 3cm, average 5mm), mudstone interlaminated with greyish-brown, medium-grained, moderately sorted, sub-rounded, planar laminated (2mm – 2cm, average 3mm) silty sandstone, some occasional bioturbation, abundant brownish-black carbonaceous mudstone intraclasts (<2mm by <1cm), small fracture at c.3694.18m (vertical offset = 5mm), common brownish-orange siderite nodules, lower bedding contact not observed

3696.12m - 3698.53m (SM-f)
Sandstone/Mudstone: light greyish-brown, fine- to medium-grained, moderately sorted, sub-rounded, planar bedded (5mm – 8cm, average 3cm), interbedded with dark grey, faint, wavy laminated (1mm – 1cm, average 5mm), silty mudstone, dark grey carbonaceous mudstone intraclasts (<5mm by <3.5cm), lower bedding contact not observed

3698.53m – 3698.93m (Ss-rc)
Sandstone: light brownish-grey, coarse- to very-coarse grained, moderately sorted, sub-rounded, normal graded bedded (5cm - 15cm, average 8cm), sandstone, common black coal intraclasts (<5mm by <3cm), common disseminated grains of orange siderite, lower bedding contact not observed

3698.93m - 3703.02m (SM-f)
Sandstone/Mudstone: light greyish-brown, fine- to medium-grained, moderately sorted, sub-rounded, planar bedded (1cm – 10cm, average 4cm) sandstone, interbedded with dark grey, faint, wavy-laminated (1mm – 1cm, average 5mm), silty mudstone, carbonaceous mudstone intraclasts (<5mm by <3.5cm), lower bedding contact not observed

Core 7: 3703.62m - 3717.04m

3703.62m - 3704.16m (MS-lb)
Mudstone/Sandstone: brownish-black, planar-laminated (2mm - 3cm, average 5mm) mudstone, interlaminated with greyish-brown, fine-grained, moderately sorted, sub-rounded, planar laminated (2mm – 1.8cm, average 2mm) silty sandstone, abundant mica in sandstone, lower bedding contact not observed

3704.16m – 3704.97m (Ss-rc)
Sandstone: light brownish-grey, coarse-grained, moderately sorted, sub-rounded, massive bedded sandstone, some black, wavy coal streaks (2mm - 5mm, average 3mm) and intraclasts (3mm by 1cm), lower bedding contact not observed

3704.97m - 3706.50m (SM-f)
Sandstone: light pinkish-grey, medium-grained, moderately sorted, sub-rounded, planar bedded (1cm – 15cm, average 5cm) sandstone, with dark grey, faint, wavy laminated (2mm – 1cm, average 5mm) mudstone, clay-lined <1.8cm by <2.5cm sub-vertical burrows at c.3706.40m *(Ophiomorpha)*, lower bedding contact not observed

3706.50m – 3708.20m (Ss-rc)
Sandstone: light brownish-grey, coarse-grained, moderately sorted, sub-rounded, massive bedded sandstone, lower bedding contact not observed

3708.20m – 3709.22m (SM-f)
Sandstone, light pinkish-grey, medium-grained, moderately sorted, sub-rounded, planar bedded (1cm – 15cm, average 5cm): with dark grey, faint, wavy-laminated (2mm – 5mm, average 3mm) mudstone, calcareous, common reddish-brown siderite laminae (<3mm), common mica, lower bedding contact not observed

3709.22m - 3712.72m (Ss-rc)
Sandstone: light brownish-grey, coarse-grained, moderately sorted, sub-rounded, normal graded bedded (2cm – 10cm) sandstone, common disseminated grains of orange siderite, lower contact not observed

3712.72m – 3716.38m
Core missing

3716.38m - 3716.56m (C)
Coal: black, shiny, brittle fracture, resinous, planar bedded (<8cm) coal with dark grey, planar laminated (2mm - 2cm, average 5mm) carbonaceous mudstone, lower bedding contact not observed

3716.56m – 3717.04m (MS-lb)
Mudstone/Sandstone: brownish-black, planar laminated (2mm - 5cm, average 5mm), mudstone and greyish-brown, medium-grained, moderately sorted, sub-rounded, planar laminated (2mm – 1.8cm, average 2mm), sandstone, horizontal burrows <8mm by <1.5cm *(Chondrites)*, common bioturbation, lower bedding contact not observed

Core 8: 3718.56m - 3727.70m

3718.56m - 3722.73m (Ss-rc)
Sandstone: light brownish-grey, coarse- to very-coarse grained, moderately sorted, sub-rounded, normal graded bedded (2cm - 20cm, average 10cm sandstone), with brownish-grey, wavy laminated (2 - 5mm, average 3mm), mudstone and coal, common black carbonaceous intraclasts (<2mm by <2cm), common disseminated grains of orange siderite, lower contact not observed

3722.73m - 3724.76m (MS-lb)
Mudstone/Sandstone: brownish-black, planar bedded (2mm - 5cm, average 1.5cm) silty mudstone interbedded with greyish-brown, fine-grained, moderately sorted, sub-rounded, planar bedded (2mm – 5cm, average 1cm), silty sandstone, common lenticular bedding throughout, some black carbonaceous mudstone intraclasts (<3mm by <1cm), common bioturbation, vertical fracture at c.3722.22 (vertical offset = 10mm), lower bedding contact not observed

3724.76m - 3727.70m (SM-f)
Sandstone/Mudstone: light greyish-brown, medium-grained, moderately sorted, sub-rounded, planar cross-bedded (1cm – 5cm, average 2cm) sandstone, interbedded with brownish-black, planar cross-bedded (1mm – 1cm, average 5mm) mudstone, black carbonaceous mudstone intraclasts (<5mm by <1.5cm), load structures <3cm by <5cm occur at c.3724.70m, common reddish-brown siderite laminae above c.3724.40m, common mica flakes along bedding planes, lower bedding contact not observed

KAPUNI-8

Core 1: 4041.65m – 4059.94m

4041.65m – 4042.57m (SM-f)
Sandston/Mudstone: grey, fine- to medium-grained, moderately to poorly sorted, sub-angular to sub-rounded, planar bedded (1cm – 5cm, average 2cm) sandstone, interbedded with brownish-black, wavy laminated (1mm – 2cm, average 2mm) carbonaceous mudstone, pinching out of mudstone laminae, common black carbonized plant fragments (<5mm by <2cm), occasional grains of resin, common slickensides, occasional pyrite nodules, abundant mica along bedding planes

4042.57m – 4044.60m (SM-f)
Sandstone/Mudstone: light greyish-white, fine-grained, poorly sorted, sub-angular to sub-rounded, planar laminated (2mm – 11cm, average 4cm), sandstone, interbedded with dark grey, planar laminated (1mm – 2cm, average 3mm) carbonaceous mudstone, strongly bioturbated, common black, common black carbonised plant fragments (<2mm by <2cm), dark yellowish-grey pyrite nodules, lower bedding contact not observed

4044.60m – 4044.84m
Core missing

4044.84m – 4046.12m (C)
Coal: black, brittle fracture, resinous, planar bedded coal interbedded with brownish-black, planar bedded (5mm – 10cm, average 3cm) argillaceous mudstone, common mica flakes along bedding planes, abundant slickensides, sharp lower bedding contact

4046.12m – 4046.63m (MS-lb)
Mudstone/Sandstone: dark greyish-brown, wavy laminated (1mm – 1cm, average 3mm), mudstone with brownish-grey, fine-grained, moderately sorted, sub-angular to sub-rounded wavy laminated (1mm – 1cm, average 2mm) silty sandstone, black carbonised plant fragments (<2mm by 1cm), strongly bioturbated, abundant mica flakes, common slickensides, sharp lower bedding contact

4046.63m – 4050.51m (SM-f)
Sandstone/Mudstone, grey to brownish-grey, fine-grained, moderately sorted, sub-angular to sub-rounded, planar laminated (1mm – 5cm, average 2mm) sandstone, interlaminated with planar laminated (1mm – 5mm, average 1mm) carbonaceous sandy mudstone and mudstone, some convolute laminations, <1.5cm by <10cm vertical burrows infilled with fine clean sand *(Skolithos)*, common bioturbation, abundant mica flakes, scoured lower bedding contact

4050.51m – 4050.94m (C)
Coal: black, brittle fracture, resinous, planar bedded (2mm - 2cm, average 1cm) coal interbedded with brownish-black, planar-laminated (2mm - 1cm, average 3mm), silty mudstone, common black carbonised plant fragments (<2mm by 3cm), some pinching out of sandy shale laminae, common mica along bedding planes, gradational lower bedding contact

4050.94m – 4051.76m (Mc)
Mudstone: brownish-black, faint, planar-laminated (2mm - 1cm, average 3mm) carbonaceous mudstone, common carbonised plant fragments (<2mm by <4cm), abundant mica flakes, sharp lower bedding contact

4051.76m – 4052.21m (C)
Coal: black, brittle fracture, slightly resinous, planar bedded (5mm – 12cm, average, 5cm) coal interbedded with brownish-black, planar laminated (1mm – 5mm, average 2mm), mudstone, occasional pyrite nodules, common mica flakes along bedding planes, sharp lower bedding contact

4052.21m – 4052.80m (SM-f)
Sandstone/Mudstone: brownish-grey, fine-grained, moderately sorted, sub-angular, planar laminated (1mm – 1cm, average 1mm) and planar cross-bedded (5mm – 1cm, average 7mm) above 4052.58m sandstone interbedded with dark brownish-black, faint, planar laminated (1mm – 1cm, average 1mm) mudstone, common black carbonised plant fragments (<1cm by <3.5cm), <1cm by <10cm vertical burrows infilled with fine sand *(Skolithos)*, minor bioturbation, scoured lowered bedding contact

4052.80m – 4053.35m (C)
Coal: black, brittle, fracture, resinous, coal with brownish-black, planar laminated (1mm – 1cm, average 3mm) mudstone, common black carbonised plant fragments (<1cm by <3cm), gradational lower bedding contact

4053.35m – 4055.95m (Mc)
Mudstone: dark grey to dark greyish-brown, faint, planar laminated (1mm - 1cm, average 3mm) carbonaceous mudstone, common black carbonized plant fragments (<1cm by <3cm), occasional pyrite nodules, common mica flakes along bedding planes, slickensides, sharp lower bedding contact

4055.95m – 4056.35m (SM-f)
Sandstone/Mudstone: grey, fine-grained, moderately sorted, sub-angular to sub-rounded, parallel laminated (2mm – 1.2cm, average 5mm) and planar cross-bedding (5mm – 4cm, average 2cm) below 4056.20m sandstone interlaminated with dark greyish-brown, faint, planar laminated (2mm – 1cm, average 2mm) mudstone, mudstone laminae increasing in frequency up the unit, common bioturbation, common slickensides, common black carbonized plant fragments (<1cm by <3cm), abundant mica flakes along bedding planes, occasional pyritic nodules

4056.35m – 4056.47m
Core missing

4056.47m – 4059.94m (SM-f)
Sandstone/Mudstone: greyish-white, fine- to medium-grained, moderately-well sorted, sub-angular to sub-rounded, Herringbone cross-bedded (5mm – 6cm, average 2cm) sandstone interbedded with dark planar laminated (1mm – 3mm) greyish-brown, discontinuous carbonaceous and argillaceous mudstone, two fractures at c.4059.11m (vertical offset = 1cm and 2cm), common reddish-brown siderite laminae (<3mm), abundant mica along bedding planes, lower bedding contact not observed

KAPUNI-12

Core 1: 3460.00m – 3470.00m

3460.00m – 3461.52m (Ss-s)
Sandstone: dark greenish-grey, coarse-grained, well sorted, sub-rounded, massive bedded sandstone, common dark green glauconite pellets, lower bedding contact not observed

3461.52m – 3463.02m (Mc)
Mudstone: brownish-black, planar laminated (1mm – 8mm, average 5mm), carbonaceous mudstone, common carbonised plant fragments (<1.5cm by <3cm), a dark grey, medium-grained, poorly to moderately-well sorted,

sub-angular to sub-rounded, sandstone bed (15cm) occurs at c.3462.40m, bioturbated, gradual lower bedding contact

3463.02m – 3465.47m (SM-f)
Sandstone/Mudstone: dark grey, fine- to medium-grained, moderately sorted, sub-angular to sub-rounded, wavy laminated (2mm – 3cm, average 8mm) and above 3464.22m planar laminated (2mm – 1.5cm, average 5mm), sandstone interbedded with brownish-black, wavy laminated (2mm – 1cm, average 3mm) and planar laminated (2mm – 5mm, average 3mm), carbonaceous mudstone, common lenticular bedding, common bioturbation, common carbonised plant fragments (<1.2cm by <3cm), sharp lower bedding contact

3465.47m – 3469.68m (SM-f)
Sandstone/Mudstone: greyish-brown, medium-grained, moderately sorted, sub-angular to sub-rounded, wavy bedded (1cm – 5cm, average, 4cm) sandstone, interbedded with continuous and discontinuous carbonaceous mudstone laminae (2mm – 5mm, average 2mm), abundant coal intraclasts (<5mm by <4cm), common bioturbation, lower bedding contact not observed

3469.68m – 3470.00m
Core missing

Core 2: 3470.00m – 3480.10m

3470.00m - 3472.00m (Ss-p)
Sandstone: dark grey and greyish-brown, medium- to coarse-grained, poorly sorted, sub-angular to sub-rounded, massive bedded, sandstone, bioturbated above c.3471.00m, lower bedding contact not observed

3472.00m – 3472.90m (Ss-p)
Sandstone: light greyish-brown, medium-grained, moderately to well sorted, sub-angular to sub-rounded, small-scale ripple laminated (2mm – 8mm, average 3mm) sandstone, gradual lower bedding contact

3472.90m – 3473.90m (Ss-p)
Sandstone: light greyish-brown, medium to coarse-grained, moderately to well sorted, sub-angular to sub-rounded, planar bedded (2mm – 5cm, average 2cm), sandstone, small fracture occurs at c.3473.70m (vertical offset = 3cm), common disseminated mica flakes, lower bedding contact not observed

3473.90m – 3478.65m (Ss-p)
Sandstone: light greyish-brown, coarse-grained to very fine pebbles (2mm - 4mm), moderately to well sorted, sub-angular to sub-rounded, graded bedded (1cm – 20cm) sandstone, rare coal intraclasts (<2cm by <3.5cm) occur at c.3476.61m, thin coal beds (<3mm) occur at c.3473.95m, c.3476.10m, c.3476.20m and c.3477.60m, lower bedding contact not observed

3478.65m – 3480.10m (Ss-cb)
Sandstone: light greyish-brown, coarse-grained. moderately to well sorted, sub-angular to sub-rounded, planar-bedded (2mm – 10cm, average 3cm) from 3479.00m to 3479.80m sandstone, clay-lined <1.2cm by <2cm sub-vertical burrows and <1.2cm by <10cm vertical burrows infilled with coarse clean sand occur at c.3478.70m and below c.3479.90m *(Ophiomorpha)*, a series of small fractures occurs at c.3479.95m (vertical offsets = 3.5cm), slightly calcareous, lower bedding contact not observed

Core 3: 3481.10m – 3493.50m

3481.10m – 3485.00m (Ss-cb)
Sandstone: light greyish-brown, medium-to coarse-grained, moderately to well sorted, sub-angular to sub-rounded, ripple bedded (5mm – 4cm, average 1.5cm) and below 3481.85, herringbone cross-bedded (5mm – 5cm, average 2cm) sandstone, clay-lined <1.5cm by 1.8cm sub-vertical burrows infilled with clean coarse sand occur above 3481.20m *(Ophiomorpha)*, small fractures occur at c.3481.10m (vertical offset = 12mm) and c.3481.75m (vertical offset = 2mm), sharp lower bedding contact

3485.00m – 3485.25m (Ss-p)
Sandstone: light greyish-brown, very coarse-grained, moderately sorted, sub-angular to sub-rounded, massive bedded, sandstone, scoured lower bedding contact

3485.25m – 3486.40m (Ss-cb)
Sandstone: light greyish-brown, medium-to coarse-grained, moderately to well sorted, sub-angular to sub-rounded, herringbone cross-bedded (5mm – 5cm, average 2cm) sandstone, gradual lower bedding contact

3486.40m – 3486.60m (Ss-cb)
Sandstone: light greyish-brown, medium-grained, moderately to well sorted, sub-angular to sub-rounded, wavy bedded (1cm – 10cm, average 7cm) sandstone with dark brownish-grey, flaser bedded (1mm – 2.5cm), silty mudstone, gradational lower bedding contact

3486.60m – 3488.10m (Ss-cb)
Sandstone: light greyish-brown, medium- to coarse-grained, moderately sorted, sub-angular to sub-rounded, herringbone cross-bedded (5mm – 4cm, average 1.5cm), sandstone, slightly calcareous, lower bedding contact not observed

3488.10m – 3490.00m (Ss-cb)
Sandstone: light greyish-brown, medium- to coarse-grained, moderately sorted, sub-angular to sub-rounded, massive bedded sandstone, brownish-black mudstone intraclasts (<1cm - <3cm) occur at c.3488.35m, common clay lined <1cm by <1.5cm sub-vertical and <1.2cm by <10cm vertical burrows infilled with clean coarse sand *(Ophiomorpha)*, slightly calcareous, gradual lower bedding contact

3490.00m – 3491.10m (Ss-cb)
Sandstone: light greyish-brown, medium-grained, moderately sorted, sub-angular to sub-rounded, herringbone cross-bedded (1cm – 6cm, average, 4cm) sandstone, scoured lower bedding contact

3491.10m – 3491.40m (MS-lb)
Mudstone/Sandstone: dark brownish-grey, planar laminated (1mm – 3mm, average, 2mm) silty mudstone with grey, fine-grained, moderately sorted, sub-angular to sub-rounded, planar laminated (1mm – 3mm, average 1cm), sandstone, black coal intraclasts (<1cm by <1.5cm), pyritised clast (8cm by 12cm) occurs at c.3691.25m , abundant mica along bedding planes, gradational lower bedding contact

3491.40m – 3491.70m (C)
Coal: black, hard, resinous, coal, gradational lower bedding contact

3491.70m – 3493.50m (MS-lb)
Mudstone/Sandstone: brownish-black, planar laminated (1mm – 1cm, average 5mm), carbonaceous mudstone interlaminated with grey, fine-grained, moderately-well sorted, sub-angular to sub-rounded, wavy laminated (1mm – 3cm, average 7mm) sandstone, black coal intraclasts (1cm by 3cm), common bioturbation, abundant mica flakes along bedding planes, lower bedding contact not observed

KAPUNI DEEP-1

Core 1: 5181.00m – 5189.60m

5181.00m – 5186.37m (SM-c)
Sandstone/Mudstone: light grey, medium-grained, moderately sorted, sub-angular to sub-rounded, planar cross-bedded (5mm – 25cm, average 8cm) sandstone interlaminated with dark greyish-brown, well-bedded and faint, wavy laminated (2mm – 1.2cm, average 3mm) silty mudstone, common carbonaceous mudstone intraclasts (2cm by 3cm), common disseminated mica flakes, sharp lower bedding contact

5186.37m – 5187.58m (MS-lb)
Mudstone/Sandstone: dark grey to dark brownish-black, wavy laminated (2mm – 3cm, average 5mm), silty mudstone interlaminated with grey, medium-grained, moderately sorted, sub-angular to sub-rounded, wavy laminated (1mm – 8mm, average 5mm), sandstone, common lenticular bedding, common disseminated mica flakes, sharp lower bedding contact

5187.98m – 5189.60m (SM-c)
Sandstone: light grey, medium- to coarse-grained, moderately sorted, sub-angular to sub-rounded, massive bedded sandstone with dark greyish-brown, wavy bedded (5mm – 1.2cm, average 1cm) carbonaceous silty mudstone, common brownish-black carbonaceous mudstone intraclasts (2cm by 3cm), common disseminated mica flakes, lower bedding contact not observed

Core 2: 5515.00m – 5519.35m

5515.00m – 5519.35m (SM-c)
Sandstone/Mudstone: grey, medium-grained, moderately sorted, sub-angular to sub-rounded, planar bedded (5cm – 15cm, average 8cm) and planar cross-bedded from c.5517.64m – 5518.55m (5cm – 15cm, average 8cm) sandstone interbedded with dark brown, wavy laminated (3mm – 1cm, average, 7mm) mudstone, common load structures, some bioturbation, common carbonaceous mudstone intraclasts (2cm by 3cm), common disseminated mica, lower bedding contact not observed

KAPUNI-14

Core 1: 4040.00m – 4044.42m

4040.00m – 4042.47m (SM-c)
Sandstone/Mudstone: light grey to moderate grey, medium- to coarse-grained, moderately sorted, sub-angular-sub-rounded, ripple bedded (5mm – 15cm, average 8cm) and planar cross-bedded (5mm – 10cm, average 5cm) at

4041.30m sandstone interbedded with wavy laminated (2 - 7mm, average 3mm) mudstone, <6mm by <1.2cm sub-vertical clay-lined burrows *(Ophiomorpha)* occur from 4040.20m to 4040.70m, pyritised mudstone clast (8.5cm by 9cm) occurs at c.4041.60m, common mica flakes, common disseminated pyrite grains, lower bedding contact not observed

4042.47m – 4044.42m (MS-lb)
Mudstone/Sandstone: light grey to greyish-brown, wavy laminated (1mm – 8mm, average 3mm) mudstone interlaminated with light greyish-brown, very fine-grained, moderately sorted, sub-angular to sub-rounded, wavy laminated (1mm – 5mm, average 2mm) silty sandstone, common lenticular bedding, occasional coal streaks (<3mm), common bioturbation

Core 2: 4044.42m – 4045.46m

4044.42m – 4045.46m (MS-lb)
Mudstone/Sandstone: moderate grey to dark grey, wavy laminated (1mm – 1cm, average 5mm) mudstone interbedded with light greyish-brown, very fine-grained, moderately sorted, sub-angular to sub-rounded, wavy laminated (1mm – 1cm, average 3mm) silty sandstone, common lenticular bedding, common coaly streaks (<3mm), abundant slickensides

Core 3: 4045.46m – 4055.08m

4045.46m – 4047.48m (MS-lb)
Mudstone/Sandstone: moderate grey to dark grey, wavy laminated (1mm – 1cm, average 5mm) carbonaceous mudstone, interlaminated with light grey, very fine-grained, moderately sorted, sub-angular to sub-rounded, wavy laminated (2mm – 1cm, average 3mm) silty sandstone, common lenticular bedding, common coaly streaks (<3mm), calcareously cemented sandstone occurs between 4046.10m and 4045.60m, <1.2cm by <2.8cm sub-vertical and horizontal burrows infilled with clean sand *(Chondrites* and *Teichichnus)*, common slickensides, sharp lower bedding contact

4047.48m – 4049.90m (SM-c)
Sandstone/Mudstone: light brownish-grey, fine- to medium-grained, poorly sorted, sub-angular to sub-rounded, ripple bedded (3mm – 3.5cm, average 1cm) sandstone interbedded with moderate grey, wavy laminated (2mm – 2.5cm, average 8mm) mudstone, mudstone content increases upwards, sandstone and mudstone completely bioturbated above 4049.00m, <1cm by <4cm horizontal burrows *(Teichichnus)*, common pyrite nodules and disseminated grains, sharp lower bedding contact

4049.90m – 4054.78m (Ss-c)
Sandstone: light greyish-brown, medium-grained, moderately sorted, sub-angular to sub-rounded, bioturbated, sandstone, with medium grey to dark grey, ripple laminated (3mm – 2.5cm, average 1cm) from 4049.90m to 4051.70m, mudstone drapes, mud content increasing upwards, <1.5cm by <3cm, <1.5cm by <4cm horizontal and sub-vertical burrows some infilled with clean sand *(Teichichnus* and *Ophiomorpha)*, burrowing gives a mottled appearance, common pyrite nodules and disseminated grains, sharp lower bedding contact

4054.78m – 4056.20m (Ss-c)
Sandstone: light brownish-grey, medium- to coarse-grained, moderately sorted, sub-angular to sub-rounded, planar cross-bedded (1cm – 5cm, average 3cm) sandstone, calcareous, common pyrite nodules, sharp lower bedding contact

Core 4: 4055.08 – 4070.50m

4056.20m – 4059.00m (Ss-c)
Sandstone: light brownish-grey, medium- to coarse-grained, moderately sorted, sub-angular to sub-rounded, massive bedded (1cm – 40cm, average 10cm) sandstone with moderate grey to dark grey, wavy-laminated (1mm – 2.0cm, average 5mm) mudstone, moderately calcareous, common pyrite nodules, scoured lower bedding contact

4059.00m – 4059.16m (C)
Coal: black, bright, blocky and extensively fractured, coal, sharp lower bedding contact

4059.16m – 4063.10m (MS-lb)
Mudstone/Sandstone: dark grey to brownish-black, well-bedded, planar laminated (2mm – 1cm, average 5mm), carbonaceous mudstone interbedded with grey, well-bedded, planar laminated (2mm – 1cm, average 3mm) silty sandstone, common lenticular bedding, distinctive fine-grained wavy bedded (2mm – 3cm, average 1cm) sandstone units occur between 4061.65m – 4062.05m and 4063.00m – 4063.10m, common mudstone intraclasts (5mm by 2.5cm), extensively bioturbated between 4060.60m – 4061.15m and 4061.65m – 4062.50m, coaly streaks above 4059.50m, <1.5cm by <1.8cm horizontal burrows *(Chondrites)*, abundant slickensides, sharp lower bedding contact

4063.10m – 4070.50m (Ss-c)
Sandstone: light greyish-brown, coarse-grained, moderately sorted, sub-angular to sub-rounded, graded bedded and planar cross-bedded (1cm – 15cm , average 8cm) at c.4068.90m sandstone with medium grey, faintly bedded

wavy and discontinuous wavy laminated silty mudstone drapes (2mm – 1.5cm, average 7mm), clay-lined <1.5cm by <2cm sub-vertical and vertical burrows 1.5cm by <8cm from 4065.35m to 4066.60m infilled with clean coarse sand *(Ophiomorpha)*, calcareous

Core 5: 4070.50m – 4086.57m

4070.50m – 4073.75m (Ss-c)
Sandstone: light greyish-brown, coarse-grained, moderately sorted, sub-angular to sub-rounded, graded bedded (1cm – 15cm , average 10cm) sandstone with medium grey, faintly bedded wavy and discontinuous wavy laminated silty mudstone drapes (2mm – 1.5m, average 7mm), calcareous, gradational lower bedding contact

4073.75m – 4078.15m (Ss-c)
Sandstone: light greyish-brown, medium- to very coarse-grained, moderately sorted, sub-angular to sub-rounded, planar cross-bedded (2cm – 10cm, average 5cm) sandstone with moderate to dark grey, wavy laminated (2mm – 6cm, average 5mm) silty mudstone drapes and thin laminae, very slightly calcareous, reddish-brown siderite streaks, sharp lower bedding contact

4078.15m – 4082.30m (MS-lb)
Mudstone/Sandstone: dark grey to brownish black, planar laminated (2mm – 1cm, average 3mm), carbonaceous mudstone, interlaminated with light greyish-brown, fine-grained, poorly to moderately sorted, sub-angular to sub-rounded, planar laminated (1mm – 1cm, average 3mm) sandstone, common lenticular bedding, a light greyish-brown, fine-grained, poorly sorted, sub-angular to sub-rounded, bioturbated silty sandstone unit occurs between 4078.80m – 4079.30m, bioturbated between 4079.30m and 4079.80m, <1cm by <1.8cm horizontal burrows *(Chondrites)*, very slightly calcareous, abundant slickensides, sharp lower bedding contact

4082.30m – 4083.50m (SM-c)
Sandstone/Mudstone: light greyish-brown, fine- to medium-grained, poorly sorted, sub-angular to sub-rounded, bioturbated sandstone interbedded with dark grey, bioturbated, silty mudstone, clay-lined <1.5cm by <2cm horizontal burrows infilled with coarse clean sand and <1cm by <4cm sub-vertical and horizontal burrows *(Ophiomorpha* and *Teichichnus)*

4083.50m – 4085.10m (SM-c)
Sandstone/Mudstone: light greyish-brown, medium-grained, moderately sorted, sub-angular to sub-rounded, ripple bedded (1cm – 15cm, average 5cm) sandstone interbedded with dark grey, well-bedded, wavy laminated (2mm – 1.8cm) silty mudstone, mudstone beds increase in size and frequency upwards, common load structures, common mudstone intraclasts (<1cm by <1.5cm), clay-lined <1.5cm by <2cm sub-vertical burrow at c.4086.30 infilled with clean coarse sand *(Ophiomorpha)*, sideritic nodules occur at c.4084.50m, sharp lower bedding contact

4085.10m – 4086.57m (Ss-c)
Sandstone: light pinkish-grey, medium- to coarse-grained, moderately-well to well sorted, sub-angular to sub-rounded, normal graded bedded (1cm to 15cm, average 10cm) sandstone, with rare brownish-black, faint to well-bedded, wavy-laminated (<3mm) silty and carbonaceous mudstone drapes (2mm – 1.5m, average 7mm), clay-lined <1.5cm by <2cm sub-vertical burrow at c.4086.30 infilled with clean coarse sand *(Ophiomorpha)*, slightly to moderately calcareous, common disseminated pyrite grains

Core 6: 4086.57m – 4100.21m

4086.57m – 4092.50m (Ss-c)
Sandstone: light pinkish-grey, medium- to coarse-grained, moderately-well to well sorted, sub-angular to sub-rounded, normal graded bedded (10cm to 20cm, average 15cm) sandstone with rare brownish-black, faint to well-bedded, wavy-laminated (<3mm) silty and carbonaceous mudstone drapes, slightly to moderately calcareous, common disseminated pyrite grains, gradual lower bedding contact

4092.50m – 4097.15m (SM-c)
Sandstone/Mudstone: light greyish-brown to light pinkish-brown, medium- to coarse-grained, moderately-well sorted, sub-angular to sub-rounded, ripple bedded (10cm to 30cm, average 10cm) and planar cross-bedded (1cm to 10cm, average 5cm) at c.4093.50m and c.4094.62m sandstone interbedded with light to dark grey, well-bedded, planar to wavy laminated (2mm – 9.5cm, average 3cm) silty mudstone, common lenticular bedding within mudstone beds, flaser bedding occurs between 4095.10m and 4095.56m, load structures occur between 4095.60m and 4095.82m, convolute bedding occurs at c.4095.80m, moderately calcareous, lower bedding contact not observed

4097.15m – 4100.21m (Ss-mb)
Sandstone: light grey, fine- to medium-grained, moderately-well sorted, sub-angular to sub-rounded, massive bedded, sandstone, common mudstone intraclasts (<2mm by <3cm), rubble from 4097.10m to 4098.30 m and 4099.50m to 4100.20m

Core 7: 4100.21m – 4128.15m

4100.21m – 4111.96m (Ss-mb)
Sandstone: light pinkish-grey to light grey, fine- to medium-grained, moderately-well sorted, sub-angular to sub-rounded, massive bedded, sandstone, black, dull, hard, dense, blocky, brittle, fracture, planar-bedded coal seams (2cm – 8cm) containing inclusions of amber occur at c.4107.20m, c.4107.50m and c.4107.58m and c.4107.80m, common mudstone intraclasts (<2mm by <3cm), well-cemented calcareous intervals occur at c.4100.30m, c.4101.06m, c.4101.85m and c.4104.35m, vertical fracture infilled with carbonate occurs at 4107.70m, siderite bed (30cm thick) occurs at c.4107.60m, common disseminated mica flakes, scoured lower bedding contact

4111.96m – 4116.95m (SM-f)
Sandstone/Mudstone: moderate grey, fine- to medium-grained, angular to sub-rounded, moderately-sorted, wavy laminated (2mm – 2cm, average 2mm) and subordinate planar cross-bedding (1cm – 2cm average 3mm) at c.4113.00m, c.4113.20m and c.4115.25m) sandstone interbedded with light to dark grey, planar to wavy laminated (2mm – 1.5cm, average 5mm) and ripple-laminated (2mm – 2cm, average 5mm) at c.4112.60, mudstone, common carbonaceous mudstone intraclasts (<2mm by <1.5cm), moderately to strongly bioturbated, common pyrite nodules, common disseminated mica flakes, scoured lower bedding contact

4116.95m – 4122.20m (Ss-rc)
Sandstone: light greyish-brown to greyish-brown, medium- to coarse-grained, moderately-sorted, sub-angular to sub-rounded, massive bedded (5cm – 25cm, average 8cm) and planar cross-bedded (5cm - 10cm, average 7cm) at 4117.40m, 4120.70m and 4121.70m sandstone abundant dark-grey to brownish-black, well-bedded, coaly and carbonaceous mudstone laminations (< 6mm thick), moderate brown siderite laminae (< 10mm thick), vertical burrows 1.5cm by 15cm *(Ophiomorpha)* at c.4117.8m, scoured lower bedding contact

4122.20m – 4128.15m (Ss-rc)
Sandstone: greyish-brown, medium- to coarse-grained, moderately-sorted, sub-angular to sub-rounded, well defined normal graded bedding (5cm – 25cm, average 8cm) with brownish-black, discontinuous wavy silty mudstone laminae (2mm – 5mm, average 2mm), minor brownish-black mudstone intraclasts (<2mm by 2cm), , moderately calcareous, common pyrite nodules, lower bedding contact not observed

KAPUNI-15

Core 1: 4700.00m – 4718.60m

4700.00m – 4702.00m (Ss-p)
Sandstone: light greyish-white, medium-grained, moderately sorted, sub-rounded, planar bedded (1cm – 15cm, average 5cm) sandstone with grey, faint, planar and wavy silty mudstone drapes (2mm – 1cm), scoured lower bedding contact

4702.00m – 4703.65m (Ss-p)
Sandstone: greyish-white, medium-grained, moderately sorted, sub-rounded, massive bedded sandstone, gradual lower bedding contact

4703.65m – 4705.20m (Ss-p)
Sandstone: light greyish-white, medium-grained, moderately sorted, sub-rounded, planar bedded (1cm – 15cm, average 8cm) sandstone with grey, faint, planar and wavy silty mudstone drapes (2mm – 1cm), dark grey intraclasts (<5mm – <3cm) occur at c.4705.10m, scoured lower bedding contact

4705.20m – 4705.85m (Ss-p)
Sandstone: greyish-white, medium-grained, moderately sorted, sub-rounded, massive bedded sandstone, gradual lower bedding contact

4705.85m – 4709.90m (Ss-p)
Sandstone: light greyish-white, medium- to coarse-grained, moderately sorted, sub-rounded, planar bedded (1cm – 18cm, average 10cm) sandstone with grey, faint, planar and wavy silty mudstone drapes (2mm – 1cm), dark brown thin coal beds on some foresets, common dark-grey mudstone intraclasts (<5mm – <3cm), 1.5cm by 10cm horizontal burrow occurs in a silty mudstone drape at c.4706.30m infilled with coarse clean sand *(Thalassinoides)*, small fracture occurs at 4707.20m (vertical offset = 2cm), calcareous, scoured lower bedding contact

4709.90 – 4710.10m (Mc)
Mudstone: brownish-black, massive bedded, carbonaceous mudstone with dark brown, dull, brittle fracture, resinous coal bed (3 cm) at c.4710.00m, lower bedding contact not observed

4710.10m – 4710.70m (C)
Coal: dark brown, dull, brittle fracture, argillaceous coal, conchoidal fracture, lower bedding contact not observed

4710.70m – 4712.00m (Ss-p)
Sandstone: light grey-white, fine- to medium-grained, poorly sorted, sub-rounded, bioturbated sandstone, with grey to dark-grey, bioturbated carbonaceous mudstone, common load structures, 8mm by 3cm sub-vertical clay lined burrows infilled with coarse clean sand *(Ophiomorpha)*, gradual lower bedding contact

4712.00m – 4713.30m (Ss-p)
Sandstone: light greyish-white, medium-grained, moderately sorted, sub-rounded, massive bedded, sandstone, mudstone intraclasts (<2mm by <3cm), <2cm by <2.5cm sub-vertical <2cm by <15cm and vertical clay-lined burrows infilled with coarse clean sand *(Ophiomorpha)*, sharp lower bedding contact

4713.30m – 4714.80m (Ss-p)
Sandstone: light greyish-white, medium- to coarse-grained, moderately sorted, sub-angular to sub-rounded, planar cross-bedded (3cm – 15cm, average 7cm) sandstone with grey, planar and wavy silty mudstone drapes, gradual lower bedding contact

4714.80m – 4718.60m (Ss-p)
Sandstone: light greyish-white, medium-grained to very fine pebbles (3mm – 4mm), moderately to poorly sorted, sub-rounded, planar bedded (1cm – 18cm , average 15cm) sandstone, very fine pebble horizons occur below c.4717.00m, dark grey mudstone intraclasts (<1cm by <5cm) occur at c.4715.30m, lower bedding contact not observed

Appendix 4

XRD, DTA, IR ANALYSIS METHODOLOGY

4.1 SAMPLE PREPARATION

XRD, DTA and IR analysis studies were carried out using the technique described by Whitton and Churchman (1987). The rock was first crushed and finely ground with an agate pestle and mortar. For each of the 54 samples 10 grams of the sediment was weighed out and put into a 400ml beaker with distilled water. Pretreatment involved the removal of calcium carbonate, organic matter and iron and aluminium oxides and oxyhydroxides, before the clay could be separated from the silt and sand fraction of the rock.

i. Calcium Removal

To remove calcium carbonate 5ml of 1:1 HCL was added into each beaker with the samples, and then placed into a boiling water bath, until the reaction ceased. The samples were transferred into a 90ml centrifuge tube and centrifuged at 1,500 rpm for 10 minutes. The bottles were then removed and the clear supernatant water poured off. Distilled water was then added to cover the samples, and mechanically stirred until all the sediment was suspended. The samples were centrifuged again at 1,500 rpm for 10 minutes and the supernatant liquid poured off, and refilled with water.

ii. Organic Matter Removal

To remove organic matter 10ml of H_2O_2 was added to the tubes containing the samples. The samples were stirred and left overnight. The following day, the samples were centrifuged at 1,500 rpm for 15 minutes. The tubes were then removed and the clear supernatant liquid poured off. Distilled water was added to cover the samples, and stirred until all the sediment was suspended. The samples were centrifuged again at 1,500 rpm for 15 minutes and the supernatant liquid poured off.

iii. Removal of Iron and Aluminium Oxides and Oxyydroxides

Lastly, iron and aluminium oxides were removed. The tubes were placed into a water bath at 90 - 100°C. 30ml of citrate reagent (0.26M) and 5ml of 1M sodium bicarbonate were added to each tube and stirred. When the solutions in the tubes were hot 1 gram of solid sodium dithionite was added to each tube and stirred. The tubes were left in the bath for a further 15 minutes, stirring intermittently. The tubes were then removed from the bath and centrifuged at 1,500 rpm for 15 minutes and the clear supernatant liquid pored off. Distilled water was then added to cover the sample, and mechanically stirred until all the sediment was suspended. The samples were the repeatedly centrifuged and the supernatant liquid poured off until the brownish colouration disappeared and the water was clear.

iv. Clay Separation

To separate the clay minerals from sand and silt sized particles, distilled water was added to the tubes and the sediment stirred thoroughly with a motorised stirrer. The tubes were centrifuged at 800rpm for five minutes. The supernatant clay suspension was then poured into a beaker of 1000ml capacity and the separation was repeated 5 times until the supernatant water remained clear. 10ml aliquots of clay suspension were transferred to 15ml centrifuge tubes for orientated XRD analysis. The remaining clay suspension was air-dried in petri dishes, ground again with an agate pestle and mortar and stored in vials for XRD, DTA and IR analysis.

4.2 XRD ANALYSIS

4.2.1 Orientated Clay Samples

i. Saturation with cations

3ml of KCL (1 M) was added to the clay suspension and stirred. The clay was then allowed to flocculate overnight. The next day, the clear supernatant liquid was sucked off, and a further 10ml of KCl was added to each sample, the tubes were shaken and clay again allowed too flocculate overnight. The clear supernatant liquid was sucked off and the K^+- saturated clay suspension was washed with distilled water and centrifuged at 15000 rpm for 15 minutes, the clear supernatant fluid being discarded. Washing and centrifuging were repeated until the clay began to disperse. The clear

supernatant liquid was sucked off and the washed K^+-saturated clay retained for x-ray slide preparation.

To the remaining clay suspension, 10ml of saturated $MgCl_2$ was added, followed by 1drop of bromophenol blue indicator and then 1:1 HCl dropwise, until the colour turned yellow. The beakers were filled with distilled water and the clay suspension allowed too flocculate overnight. The clear supernatant liquid was then sucked off, the beaker refilled with distilled water and the clay again allowed too flocculate overnight. The next day, the clear supernatant liquid was sucked off and the washed Mg^{++}-saturated clay retained for x-ray slide preparation.

ii. Preparation of X-Ray Slides

Clean dry glass slides (25mm x 25mm) were covered with clay suspension (approximately 1 - 2ml) from one each of the Mg^{++}- and K^+-saturated clay samples and allowed to dry in air. The x-ray slides were then loaded into sample holders, stacked in the sample magazine and loaded into the sample changer and an x-ray diffractogram obtained using a Philips PW 1710 instrument (cobalt tube).

The Mg^{++}-saturated slides were then sprayed with a 10% glycerol in water solution, using an aerosol spray bottle. Each slide was allowed to dry overnight, giving time for the glycerol to react. After the diffractograms for the Mg^{++}-glycerol samples were obtained Mg^{++}-saturated slides were heated to 550°C for 2hrs, cooled and another diffractogram obtained.

iii. Semi-Quantitative Analysis

X-ray peaks for the clay minerals in each sample were identified using standard reference books of XRD data and/or the ATM index and data file, and the information present in Table 1. The amounts of each clay mineral were then estimated from peak height intensities (counts/sec) for characteristic XRD peaks for each of the clay minerals present in the K^+-saturated clay x-ray difractograms.

Clay minerals basal (001) spacings (Å) after various treatments

I Discrete minerals

Mineral	Treatments				
	Mg^{++}-air	Mg^{++}-glycerol	K^+	Heated 550°C	Formamide
(a) Mica*	10	10	10	10	–
(b) Chlorite	14	14	14	14	–
(c) Vermiculite	14–10	14	10	10	–
(d) HIV**	14	14	14	10	–
(e) Smectites	15–10	18	10	10	–
Kaolinite	7.2	7.2	7.2	No peak	7.2
Halloysite	7.2	10–11 (not all)	7.2	No peak	10.4

II Regularly interstratified minerals. *Note*: the key to their identification is the presence of high spacing (i.e. 24, 28 and 32 Å) 001 peaks and 002 spacings.

Mineral	Treatments			
	Mg^{++}-air	Mg^{++}-glycerol	K^+	Heated 550°C
(f) Mica-vermiculite	12 + 24	12 + 24	10	10
(g) Mica-HIV	12 + 24	12 + 24	12	10
(h) Mica-chlorite	12 + 24	12 + 24	12	12
(i) Chlorite-vermiculite	14 + 28	14 + 28	12	12
(j) Mica-smectite	12 + 24	14 + 28	10	10
(k) Chlorite-smectite	14 + 28	32	12	12

III Irregularly interstratified minerals

Mineral	Treatments			
	Mg^{++}-air	Mg^{++}-glycerol	K^+	Heated 550°C
Interlayered hydrous mica	20–14	10–14	10–14	10–12

*Mica is generally indistinguishable from illite and the two terms are considered synonymous, with mica being the preferred term.

**HIV = Hydroxy interlayered vermiculite

Table 1: Clay minerals basal (001) spacings (Å) after various treatments (Whitton and Churchman, 1987)

4.2.2 Non-Orientated Powder Samples

Dried powder clay from each sample were loaded into samples holders using the Philips PW 1981/80 back-loading powder sample holder and the Philips PW 1770 holder mounting clamp. Once packed, the powder holders were stacked in the magazine, loaded into the sample changer and an x-ray diffractogram obtained.

X-ray peaks for the clay minerals in each sample were identified using standard reference books of XRD data and/or the ATM index and data file. The amounts of each clay mineral were then estimated from peak height intensities (counts/sec) for characteristic XRD peaks for each of the clay minerals present. This was done by using graphs of peak height intensity against concentration, which have been prepared for each of the common minerals using pure mineral standards diluted with alumina and volcanic glass.

4.3 DTA ANALYSIS

The kandite (kaolinite) clay minerals were measured by a Differential Thermal Analysis (DTA) instrument. 1g of each dry clay sample material was packed into the platinum liner of the macro cup and 1g of Al_2O_3 was packed into the second platinum liner of the macro cup (as reference material) in the DuPont 99 micro-processor controlled DTA. The temperature was set at 550°C and the thermogram run.

Thermograms for each sample were then compared with thermograms run using standard pure mineral specimens. A quantitative estimate of kaolinite was made by measuring peak heights and obtaining the concentration of kaolinite minerals present from standard graphs.

4.4 IR ANALYSIS

Kandite minerals were measured by infrared analysis to cross-reference with XRD and DTA results. 1mg of each clay sample was mixed thoroughly with 200mg of pure KBr by grinding with an agate pestle and mortar. This KBr and clay was then made into a 13mm diameter disc by pressing at 6000kg cm-2 for 2 min in a SPECAC vacuum die. A fresh disc was prepared for each set of samples analysed. Sample discs are scanned relative to the pure KBr disc using a double beam PyeUnicam SP2000 spectrophotometer over the wavelength range from 200 - 4000cm-1 with a scan time of 12min.

Quantitative estimates of kaolinite were estimated from standard graphs in which the ratio of absorbance B/T is plotted against % mineral concentration, where B is the absorbance of the background and T is the absorbance of the characteristic peak for the particular mineral

Appendix 5

POROSITY PARAMETERS

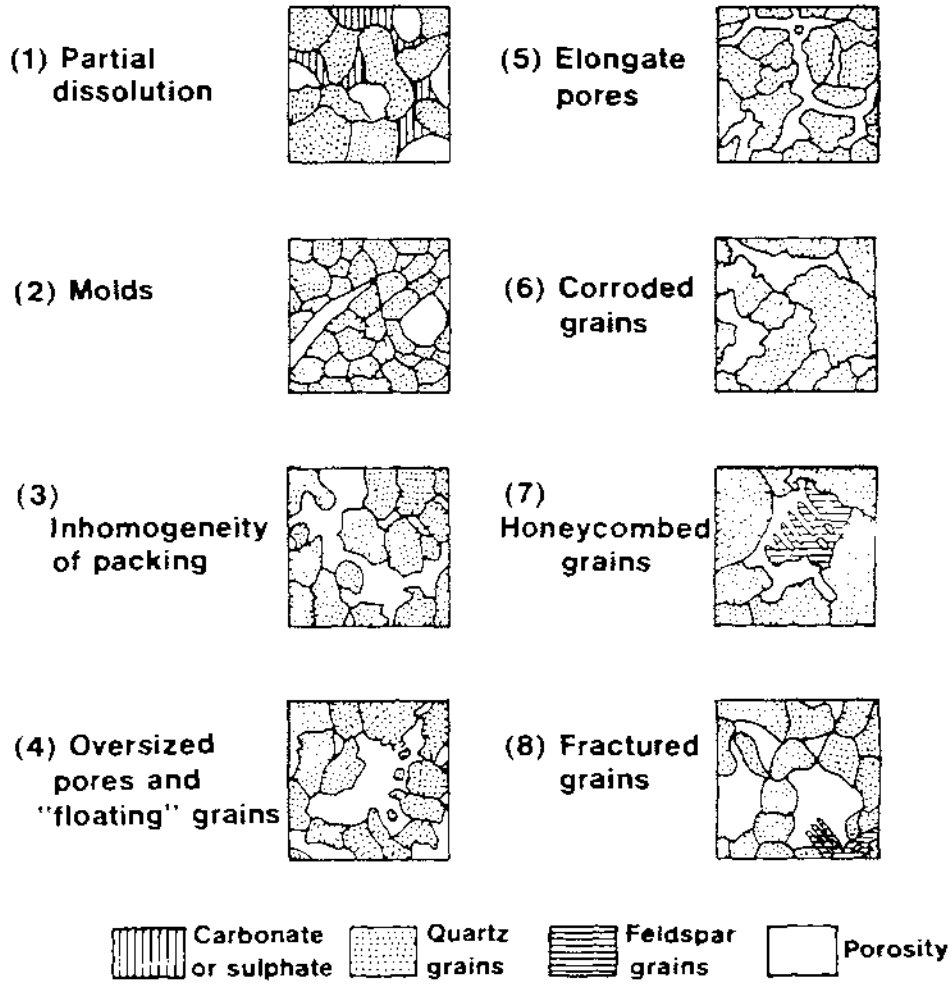

Petrographic criteria for secondary porosity (Schmidt, McDonald and Platt, 1977)

Appendix 6

TEXTURAL PARAMETERS

GRAIN SIZE

See Appendix 2

GRAIN ROUNDNESS AND SPHERICITY

See Appendix 2

GRAIN SORTING

See Appendix 2

GRAIN CONTACTS

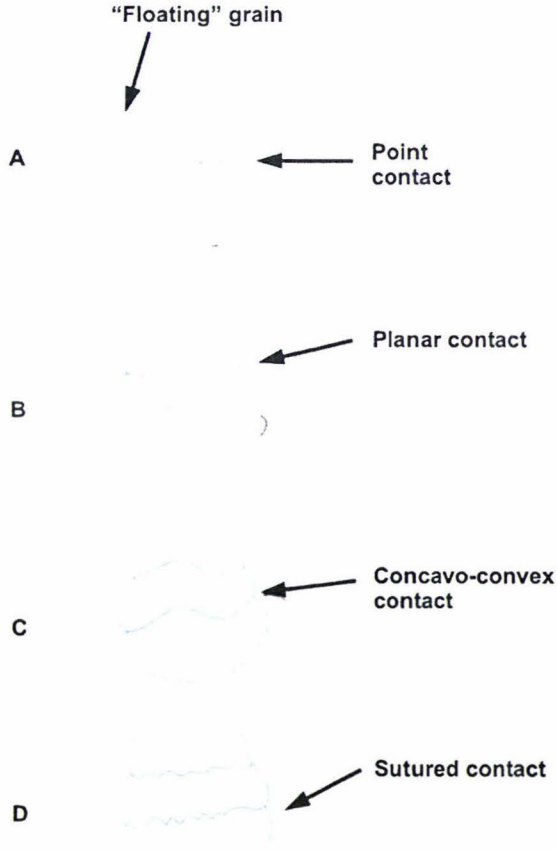

Diagrammatic illustration of principal kinds of grain contacts: A) point, B) planar, C) concavo-convex, D) sutured (Adapted from Taylor, 1950)

ENCLOSURE 1: CORRELATION OF MANGAHEWA FORMATION LOG MOTIFS IN THE KAPUNI FIELD

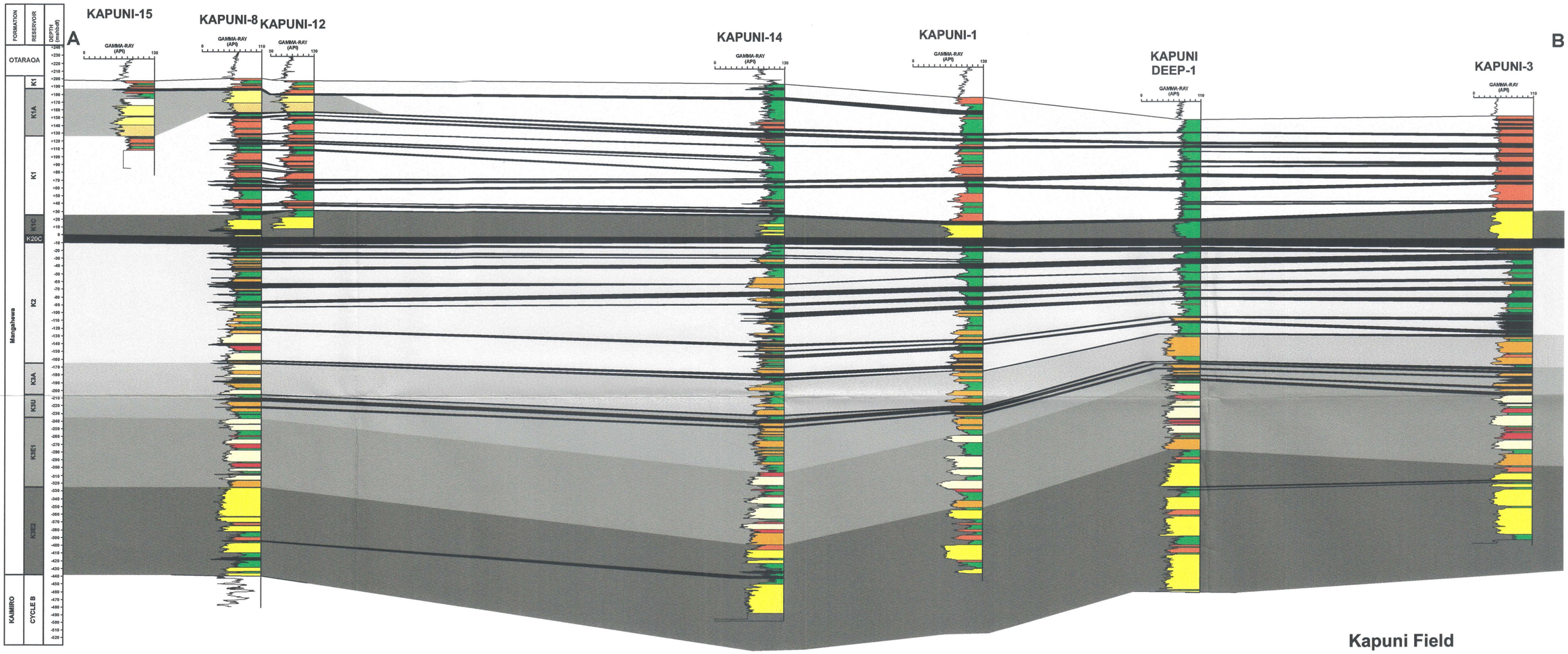

RESERVOIR POTENTIAL	MAJOR LITHOLOGICAL GROUPS		LITHOLOGICAL FACIES DESCRIPTIVE TERMINOLOGY	LITHOFACIES GROUP	LITHOFACIES	ENVIRONMENTAL INTERPRETATION
Reservoir or Reservoir Potential	Sandstone	Heterogeneous	Not Identified in core	Ss	N/A	Flood-Tidal Delta
			Coarse sandstone		Ss-c	Tidal Sand Bar
			Pebbly sandstone		Ss-p	Tidal-Inlet Channel
			Rafted coal sandstone		Ss-r	Fluvial-Tidal Channel
			Cross-bedded sandstone	Ss	Ss-cb	Spit Platform
			Massive bedded sandstone		Ss-mb	Sand Flat
			Speckled sandstone		Ss-s	Shallow Marine
	Heterolithic	Sand-dom.	Fine sandstone/mudstone	SM	SM-f	Meandering Tidal Channel
			Coarse sandstone/mudstone		SM-c	Tidal Channel
Non-Reservoir		Mud-dom.	Lenticular bedded mudstone/sandstone	M	MS-lb	Mud Flat
	Mudstone		Carbonacous mudstone		Mc	Swamp
	Coal		Coal	C	C	Marsh/ Swamp

1 0 1 Kilometres

Kapuni Field